Functional analysis of MarvelD3, a novel transmembrane protein of the tight junction

Emily Steed

This Thesis is submitted to University College London for the Degree of Doctor of Philosophy

September 2011

Department of Cell Biology

UCL Institute of Ophthalmology

11-43 Bath Street

London

EC1V 9EL

Declaration

I, Emily Steed, confirm that the work presented in this thesis is my own. Where information has been derived from other sources, I confirm that this has been indicated in the thesis.

This thesis is dedicated in loving memory to my Nanna and Grandad

Abstract

Tight junctions are an intercellular adhesion complex of epithelial and endothelial cells. They form a paracellular diffusion barrier and interact with a network of intracellular signalling mechanisms that control junction function, gene expression and cell behaviour. Tight junctions are formed by multiprotein complexes containing cytosolic and transmembrane proteins. In this thesis I have identified a novel four-pass transmembrane protein of the tight junction called MarvelD3 and begun to analyse its function in the regulation of intracellular signalling pathways from the junction. There are two isoforms of MarvelD3, both of which show a broad tissue distribution and are expressed in different types of epithelial and endothelial cells. MarvelD3 co-localises with occludin at the tight junction in epithelial cells. I have found that MarvelD3 is not necessary for junction formation, but may have a role in the regulation of ion conductance properties of the tight junction. Functional analyses combining loss- and gain-of-function approaches in epithelial cell lines have further identified a role for MarvelD3 in the regulation of cell proliferation, migration and the cellular response to hyperosmotic shock. MarvelD3 expression regulates levels of active c-Jun N-terminal kinase (JNK) and AP1 signalling, possibly via an interaction between its N-terminus and the MAP kinase kinase kinase MEKK1. I have also shown MarvelD3 to be implicated in regulation of the actin cytoskeleton, affecting leading edge formation in migrating cells and cytoskeletal rearrangements in response to hyperosmotic shock. I will also describe some initial studies conducted in *Xenopus laevis* embryos in which depletion of *Xenopus* MarvelD3 by morpholino injection results in curvature of the anterioposterior axis and reduced pigmentation, possibly resulting from a defect in neural crest cell migration.

Table of Contents

List of Figures 11

List of Tables 15

List of Abbreviations 16

Chapter 1: Introduction **19**

The apical junctional complex 21

Adherens junctions 22

Composition of adherens junctions 22

Adherens junctions and intracellular signalling 23

Desmosomes 24

Composition of desmosomes 24

Desmosomes and regulation of intracellular signalling pathways 25

Tight junctions 26

Composition of the tight junction 28

Four-pass integral membrane proteins of the tight junction 30

Claudins and the barrier function 30

Occludin 33

Tricellulin 34

Mutations of tight junction transmembrane proteins and disease 35

Tight junction-associated cytoplasmic proteins 36

Zonula occludens proteins 37

Polarity proteins 37

Cytoskeletal proteins 39

Actin cytoskeleton and junction assembly 39

Regulation of the cytoskeleton by the tight junction 40

Cell migration 41

Mechanisms of cell migration 42

Regulation of cell migration 43

Tight junctions and migration 44

Transitions between single and collective cell migration states 46
Tight junctions and epithelial-to-mesenchymal transition 47
Intracellular signalling pathways 47
Tight junction regulation of gene expression 48
Signalling by Rho GTPases 49
Activation of GTPase signalling 51
Regulation of gene expression by Rho GTPases 51
AP1 signalling 53
The mitogen-activated protein kinase pathway 53
Regulation of gene expression 56
Introduction to the current study 59
Identification of the Marvel domain 59
The Marvel domain and the tight junction 61
Summary of Aims 62
Chapter 2: Materials and Methods 63
2.1 Cell culture 64
2.1.1 Cell storage 65
2.2 Transfection methods 66
2.2.1. Lipofectamine 2000 66
2.2.2 JetPEI 67
2.2.3 Ca^{2+}-phosphate precipitation 67
2.2.4 Interferin 68
2.3 Generation of stable cell lines 69
2.3.1 Generation of MiaPaCa expressing MarvelD3_1:VSV 69
2.4 DNA methods 70
2.4.1 cDNA 70
2.4.2 Purification of PCR products with silica beads 73
2.4.3 Restriction digests 73
2.4.4 Agarose ligations 74

2.4.5 Preparation of competent cells 74

2.4.6 Transformation of competent cells 75

2.4.7 Preparation of plasmid DNA 75

2.4.8 Agarose gel electrophoresis 76

2.5 RNA methods 76

2.5.1 RNA extraction and reverse transcription PCR (RT-PCR) 76

2.5.2 RNA extraction and microarray analysis 77

2.6 Protein methods 78

2.6.1 Generation and purification of anti-MarvelD3 peptide antibody 78

2.6.2 Generation and purification of antibody against the entire N-terminus and two isoform-specific C-termini of MarvelD3 79

2.6.3 Production of GST-fusion proteins 80

2.6.4 Purification of GST-fusion proteins 81

2.6.5 Sodium dodecyl sulfate polyacrylamide gel electrophoresis (SDS-PAGE) 81

2.6.6 Immunoblotting 82

2.6.7 Methanol fixation 83

2.6.8 Paraformaldehyde fixation 83

2.6.9 Immunofluorescence 83

2.6.10 Primary antibodies 84

2.7 Experimental assays 86

2.7.1 Ca^{2+}-switch, paracellular permeability and transepithelial resistance (TER) measurements 86

2.7.2 Proliferation assay 87

2.7.3 Flow cytometry 87

2.7.4 Migration assay 88

2.7.5 Reporter assay 89

2.7.6 Hyperosmotic shock 90

2.7.7 Pulldowns 91

2.7.8 GTPase activation assay (G-LISA™) 91

2.7.9 Impedance analysis 92

2.7.10 Statistics 92

2.8 *Xenopus laevis* methods 93

2.8.1 Egg collection and fertilisation 93

2.8.2 De-jellying 93

2.8.3 RNA extraction from embryos and RT-PCR 94

2.8.4 *in vitro* transcription of mRNA 95

2.8.5 Phenol/chloroform extraction of RNA 95

2.8.6 Microinjection 96

2.8.7 Fixation 96

2.8.8 β-galactosidase staining 97

2.8.9 *In situ* hybridisation 97

2.8.10 Depigmentation of embryos after *in situ* hybridisation 99

2.8.11 Imaging 99

2.8.12 Preparation of samples for immunoblotting 99

2.8.13 Additional solutions for *Xenopus laevis* experiments 100

Chapter 3: Identification of MarvelD3 at the Tight Junction 101

Introduction 102

Results 103

Identification of two human isoforms of MarvelD3 by bioinformatic analysis 103

Generation of antibodies against MarvelD3 109

Expression pattern of MarvelD3 isoforms 112

Localisation of MarvelD3 to the epithelial cell tight junction 113

Functional characterisation of MarvelD3 at the tight junction 121

MarvelD3 and the regulation of ion conductance and paracellular permeability 124

Discussion 129

Chapter 4: Role of MarvelD3 in the regulation of proliferation and migration in epithelial cells 136

Introduction 137

Results 140

MarvelD3 expression is reduced or absent from metastatic tumour cell lines 140

Expression of MarvelD3 in MiaPaCa cells results in the formation of cell-cell contact sites and a more epithelial-like phenotype 141

MarvelD3 expression regulates epithelial cell proliferation and migration 147

MarvelD3 expression regulates the expression of genes involved in cell proliferation and migration 154

Regulation of transcription factor-specific promoter activity by MarvelD3 expression 157

Regulation of the AP1 promoter by MarvelD3 159

MarvelD3 regulates cytoskeletal rearrangements during cell migration 164

Discussion 168

Chapter 5: Regulation of AP1 signalling by MarvelD3 176

Introduction 177

Results 178

Levels of active JNK are reduced in MarvelD3-expressing MiaPaCa cells 178

JNK activity is necessary for MiaPaCa cell migration and proliferation 179

The N-terminus of MarvelD3 can interact with MEKK1 183

Regulation of AP1 promoter activity by the N-terminus of MarvelD3 184

Discussion 189

Chapter 6: Regulation of the cellular response to hyperosmotic shock by MarvelD3 194

Introduction 195

Results 198

Effect of hyperosmotic shock on MarvelD3 localisation 198

Regulation of MAPK signalling by MarvelD3 in response to hyperosmotic shock 202

Regulation of MarvelD3 internalisation in response to hyperosmotic shock 207

MarvelD3 depletion affects cytoskeletal reorganisation in response to hyperosmotic shock 209

Discussion 226

Chapter 7: Analysis of MarvelD3 function during development in *Xenopus laevis* **238**

Introduction 239

Results 243

Expression of MarvelD3 during *Xenopus laevis* development 243

Loss-of-function studies 244

Discussion 254

Chapter 8: Final Discussion **261**

Identification of MarvelD3 and regulation of tight junction properties 262

Regulation of cell proliferation and migration by MarvelD3 264

Regulation of the actin cytoskeleton by MarvelD3 272

Relevance of MarvelD3 function at the tight junction 275

Final conclusion 278

Acknowledgements **279**

References **281**

List of Figures

Introduction

Figure 1.1 – Schematic representation of the epithelial junctional complex 22

Figure 1.2 – Morphological features of the tight junction 27

Figure 1.3 – Schematic representation of the tight junction and its protein constituents 29

Figure 1.4 – Proposed model for regulation of paracellular permeability by a series of dynamic tight junction strands 32

Figure 1.5 – Regulation of Rho GTPase activity 50

Figure 1.6 – Representation of the major MAP kinase signalling cascades found in mammalian cells 55

Figure 1.7 – Regulation of the AP1 transcription factor by the MAPK signalling pathway 58

Chapter 3: Identification of MarvelD3 at the Tight Junction

Figure 3.1 – Identification and alignment of the two human MarvelD3 isoforms 104

Figure 3.2 – Membrane topology analysis of human MarvelD3 isoforms 1 and 2 105

Figure 3.3 – Analysis of vertebrate MarvelD3 sequences 107

Figure 3.4 – Detection of endogenous MarvelD3 in a Caco-2 and HCE cells 110

Figure 3.5 – Deconvolution of MarvelD3 siRNA pool 110

Figure 3.6 – Antibodies directed against the isoform-specific C-termini of MarvelD3 isoforms can only detect over-expressed MarvelD3 protein 111

Figure 3.7 – Expression of MarvelD3 in epithelial and endothelial cells 112

Figure 3.8 – Expression of MarvelD3 in mouse tissue 113

Figure 3.9 – MarvelD3 localises to cell-cell contacts in Caco-2 and HCE cells 114

Figure 3.10 – MarvelD3 colocalises with occludin in the apical junctional complex 115

Figure 3.11 – MarvelD3 localises apically to E-cadherin in the apical junctional complex 116

Figure 3.12 – Expression of full-length MarvelD3 constructs in MDCK cells 117

Figure 3.13 – MarvelD3 constructs localise to the cell periphery in MDCK and Caco-2 cells 118

Figure 3.14 – HA-tagged constructs of MarvelD3 localise to the cell periphery in MDCK and Caco-2 cells 119

Figure 3.15 – Pulldown assays suggest an interaction between MarvelD3 and occludin, but not ZO-1, -2 or -3 in Caco-2 cells 120

Figure 3.16 – Knockdown of MarvelD3 depletes the junctional pools of MarvelD3 in Caco-2 cells 121

Figure 3.17 – Depletion of MarvelD3 does not affect expression of tight junction proteins occludin, claudin-1, GEFH1, ZO-1, ZO-2, ZO-3 or tricellulin 122

Figure 3.18 – Depletion of MarvelD3 does not affect expression of adherens junction proteins β-catenin and E-cadherin 123

Figure 3.19 – Depletion of MarvelD3 does not affect occludin localisation 123

Figure 3.20 – Depletion of MarvelD3 and tight junction assembly 125

Figure 3.21 - Depletion of MarvelD3 and epithelial barrier properties 127

Figure 3.22 – Effect of MarvelD3 depletion on expression levels of claudin-1 and claudin-4 128

Chapter 4: Role of MarvelD3 in the regulation of proliferation and migration in epithelial cells

Figure 4.1 – Expression of MarvelD3 in tumour cell lines 140

Figure 4.2 – Expression of MarvelD3 in MiaPaCa cell lines 142

Figure 4.3 – MD3_1:VSV localises to cell-cell contact sites when constitutively expressed in MiaPaCa cells 143

Figure 4.4 – Expression of MarvelD3 results in a more epithelial-like phenotype in MiaPaCa cells 144

Figure 4.5 – Effect of MarvelD3 expression on occludin, ZO-1 and E-cadherin in MiaPaCa cells 146

Figure 4.6 – Effect of MarvelD3 expression on cell number increases in MiaPaCa cells 148

Figure 4.7 – MarvelD3 depletion results in increased proliferation of Caco-2 cells 149

Figure 4.8 – MarvelD3 expression reduces migration in MiaPaCa cells 151

Figure 4.9 – Depletion of endogenous MarvelD3 increases migration in Caco-2 cells 153

Figure 4.10 – Genes regulated by expression of MarvelD3 in MiaPaCa cells 156

Figure 4.11 – Regulation of transcription factor-specific promoters by MarvelD3 isoforms and occludin 158

Figure 4.12 – MarvelD3 regulates AP1 promoter activity in Caco-2 and MiaPaCa cells 160

Figure 4.13 – Effect of MarvelD3 depletion on EGFR expression and AP1 promoter activity in response to EGF 162

Figure 4.14 – Effect of MarvelD3 on cyclinD1 expression 163

Figure 4.15 – Effect of MarvelD3 depletion on the actin cytoskeleton in migrating Caco-2 cells 165

Figure 4.16 – Effect of MarvelD3 expression on the actin cytoskeleton in migrating MiaPaCa cells 166

Chapter 5: Regulation of AP1 signalling by MarvelD3

Figure 5.1 – Expression of MarvelD3 results in reduced levels of active JNK in MiaPaCa cells 179

Figure 5.2 – Inhibition of JNK activity reduces proliferation and migration in MiaPaCa cells 181

Figure 5.3 – JNK activity is necessary for increased cell migration following MarvelD3 depletion 182

Figure 5.4 – MEKK1 interacts with the N-terminus of MarvelD3 and localizes to cell-cell contacts in a MarvelD3-dependent manner 184

Figure 5.5 – Regulation of the AP-1 promoter by the N-terminus of MarvelD3 186

Figure 5.6 – Effect of MarvelD3 expression on RhoA-mediated cytoskeletal rearrangements 188

Chapter 6: Regulation of the cellular response to hyperosmotic shock by MarvelD3

Figure 6.1 – MarvelD3 is internalized in response to hyperosmotic shock in Caco-2 cells 199

Figure 6.2 – Redistribution of MarvelD3 to the cytoplasm in HCE cells exposed to hyperosmotic conditions 201

Figure 6.3 – Regulation of MEKK1 and JNK phosphorylation by MarvelD3 in response to hyperosmotic shock 204

Figure 6.4 – MarvelD3 depletion does not affect activation of p38 or ERK, or nuclear accumulation of p38, in response to hyperosmotic shock 206

Figure 6.5 – Regulation of MarvelD3 internalisation in response to hyperosmotic shock 208

Figure 6.6 – Effect of MarvelD3 on rearrangements of the actin cytoskeleton in response to hyperosmotic shock 210

Figure 6.7 – MarvelD3-depletion results greater disruption to the tight junctions in response to hyperosmotic shock 211

Figure 6.8 – Effect of MarvelD3 depletion and MAPK inhibition on hyperosmotic shock-induced reduction in apical cell area 213

Figure 6.9 – Effect of MarvelD3 depletion on hyperosmotic shock-induced changes in cortactin, cofilin and MLC 215

Figure 6.10 – Cellular localization of phospho-cofilin in response to hyperosmotic shock 217

Figure 6.11 – Cellular localisation of phospho-cofilin remains in MarvelD3-depleted cells in response to hyperosmotic shock 219

Figure 6.12 – Effect of hyperosmotic shock on phospho-MLC localisation in control Caco-2 cells 221

Figure 6.13 – Effect of hyperosmotic shock on phospho-MLC localization in MarvelD3-depleted Caco-2 cells 223

Figure 6.14 – Effect of MarvelD3 depletion on nuclei fragmentation in response to hyperosmotic shock 225

Figure 6.15 – Hypothetical model for the regulation of the hyperosmotic shock response by MarvelD3 233

Chapter 7: Analysis of MarvelD3 function during development in *Xenopus laevis*

Figure 7.1 – Representation of *Xenopus laevis* development 242

Figure 7.2 – Expression of xMD3 during *X. laevis* embryonic development 243

Figure 7.3 – Effect of bilateral xMarvelD3 morpholino injection during early stages of *Xenopus* development 245

Figure 7.4 – xMarvelD3 morpholino injection results in curvature of the neural fold in stage 20 embryos 246

Figure 7.5 – Injection of xMD3-MO results in shortening and curvature of the anterioposterior body axis 248

Figure 7.6 – Unilateral injection of xMD3-MO perturbs eye and melanophore development 249

Figure 7.7 – Expression of human MarvelD3 isoform 2 and GFP following mRNA injection in *Xenopus laevis* embryos 250

Figure 7.8 – Effect of xMD3-MO injection on *Twist* expression 252

Figure 7.9 – Effect of xMD3-MO injection on *myosin heavy chain* and *neural β-tubulin* expression 253

Chapter 8: Final Discussion

Figure 8.1 – Hypothetical model for the regulation of migration and proliferation by MarvelD3 in epithelial cells 267

Figure 8.2 – Preliminary observations suggest the MarvelD3 may exist in a complex with p120-catenin and p190RhoGAP at the tight junction 271

List of Tables

Chapter 2: Materials and Methods

Table 2.1 – Details of cell lines used in the current study 65

Table 2.2 – Lipofectamine transfection quantities 66

Table 2.3 – JetPEI transfection quantities 67

Table 2.4 – Interferin transfection quantities 69

Table 2.5 – Primers used to clone MarvelD3 constructs 72

Table 2.6 – Primary antibodies 85

Table 2.7 – Inhibitors used in hyperosmotic shock experiments 90

Chapter 3: Identification of MarvelD3 at the Tight Junction

Table 3.1 – Alignment scores of MarvelD3 sequences from different vertebrates 108

List of Abbreviations

Abbreviation used	Description
A-P	Anterior-posterior (body axis)
aa	amino acids
AJ	Adherens junction
AP	Alkaline phosphatase
AP1	Activating protein 1
APC	Adenomatous polyposis coli
aPKC	atypical protein kinase C
AR	Aldose reductase
β-gal	β-galactosidase
BGT1	Betaine transporter
BMP	Bone morphogenetic protein
BSA	Bovine serum albumin
CAR	Coxsackie and adenovirus-associated receptor
CDK4	Cyclin-dependent kinase 4
CDK6	Cyclin-dependent kinase 6
con-siRNA	control siRNA
Crb	Crumbs
CTD	C-terminal domain
cycD1	CyclinD1
DIG	Digoxigenin
DMEM	Dulbecco's Modified Eagle Medium
DMSO	Dimethyl Sulfoxide
DTT	Dithiothreitol
ECL	Enhanced chemiluminescence
EDTA	Ethylenediaminetetraacetic acid
EGF	Epidermal growth factor
EGFR	Epidermal growth factor receptor
EM	Electron microscopy
EMT	Epithelial-to-mesenchymal transition
ERK	Extracellular signal-regulated kinase
FACS	Fluorescence-activated cell sorting
GAP	GTPase-activating protein
GDP	Guanosine diphosphate
GEF	Guanine-nucleotide exchange factor
GFP	Green fluorescent protein
GSK3β	Glycogen synthase kinase 3β
GST	Glutathione S-transferase
GTP	Guanosine triphosphate
GTPase	Guanosine triphosphatase
GUK	Guanylate kinase-like domain
HA	Hemagglutinin (tag)
HCG	Human chorionic gonadotropin

HRP	Horseradish peroxidase
IFNγ	Interferon gamma
ILK	Integrin linked kinase
IPTG	Isopropyl β-D-1-thiogalactopyranoside
JAM	Junction adhesion molecule
JNK	cJun N-terminal kinase
LIMK	LIM kinase
MAB	Maleic acid buffer
MAGUK	Membrane-associated guanylate kinase-like homologue
MAL	Myelin and lymphocyte (protein)
MAPK	mitogen-activated protein kinase
MAPKK	mitogen-activated protein kinase kinase
MAPKKK	mitogen-activated protein kinase kinase kinase
MARVEL	MAL and related proteins for vesicle traffic and membrane link (domain)
MarvelD3	Marvel domain-containing protein 3
MBS	Modified Barth's Solution
MD3	MarvelD3
MD3_1	MarvelD3 isoform 1
MD3_2	MarvelD3 isoform 2
MD3p-siRNA	pool of MarvelD3 siRNAs
MDCK	Madin-Darby canine kidney
MEKK1	MAPK/ERK kinase kinase 1
MHC	Myosin heavy chain
MLC	Myosin light chain
MLK3	Mixed lineage kinase 3
MMP	Matrix metalloproteinase
MO	Morpholino
mRNA	messenger ribonucleic acid
n.s.	not significant
NBT	Neural β-tubulin
NEB	New England Biolabs
NTD	N-terminal domain
OD	Optical density
ODC	Ornithine decarboxylase
OSM	Osmo-sensing scaffold for MEKK3
P/S	Penicillin/Streptomycin
Par	Partitioning defective protein
PATJ	Pals1-associated tight junction protein
PBS	Phosphate-buffered saline
PCNA	proliferating cell nuclear antigen
PCR	Polymerase chain reaction
PDZ	post-synaptic density, discs large ZO-1 (domain)
PFA	Paraformaldehyde
PHD	Plant homeo domain

PI3K	phosphoinositide 3-kinase
PKC	Protein kinase C
PMSF	Phenylmethylsulfonyl fluoride
PMSG	Pregnant mare serum gonadotropin
PTB	Phosphorylated tyrosine binding (domain)
Rb	Retinoblastoma protein
ROCK	Rho-associated protein kinase
RT-PCR	Reverse transcription polymerase chain reaction
SAF-B	Scaffold-attachment factor B
SDS-PAGE	Sodium dodecyl sulfate polyacrylamide gel electrophoresis
SH2	Src homology 2 (domain)
SH3	Src homology 3 (domain)
siRNA	short interfering ribonucleic acid
Smad3	Mothers against decapentaplegic homolog 3
SRE	Serum response element
SRF	Serum response factor
SSC	Saline sodium citrate
Stat3	Signal transducer and activator of transcription 3
TAE	Tris-Acetate-EDTA
TBE	Tris-Borate-EDTA
TBS	Tris-buffered saline
TCF	Ternary complex factor
TEA	Triethanolamine
TEMED	Tetramethylethylenediamine
TER	Transepithelial electrical resistance
TGFβ	Transforming growth factor beta
TGFβR1/2	Transforming growth factor beta receptor 1/2
TJ	Tight junction
TNFα	Tumour necrosis factor alpha
TonEBP/OREBP	Tonicity-responsive enhancer/osmotic response element-binding protein
VSV	Vesicular stomatitis virus (tag)
xMD3	*Xenopus* MarvelD3
ZO	Zonula occludens
ZONAB	ZO-1-associated nucleic acid binding protein

Chapter 1:

Introduction

Chapter 1 - Introduction

Parts of this introduction were published as a review entitled “Dynamics and functions of tight junctions” (Steed et al., 2010).

Epithelial cells line the internal cavities and external surfaces of multicellular organisms, and are imperative for the maintenance of organ homeostasis. The polarised nature of epithelial cells, which have an apical membrane domain exposed to the internal cavity or external environment and a basolateral membrane domain interacting with neighbouring cells and the underlying extracellular matrix, enables them to regulate the necessary behaviours at the interface between external and internal milieu. Further specializations equip epithelia for specific functions, like microvilli enhancing absorption by cells of the intestine, and cilia on the apical surface of cells lining the respiratory tract facilitating the directional movement of mucous out of the body.

Many diseases are associated with aberrant behaviour of epithelial cells marking them as an important focus for scientific research. The majority of cancers, for example, are epithelial in origin and are associated with disintegrated junctional structures, which facilitates disease progression. Understanding epithelial cells and their properties, therefore, is important to our ability to get a handle such pathological conditions. It is the aim of this thesis to analyse the function of a novel component of the tight junction in epithelial cells, in the hope that advancing our understanding of epithelial tight junction architecture, will contribute to our future understanding of the mechanisms they control and the roles they may play in pathological processes.

First I will introduce the tight junction and its presence within the epithelial junctional complex, and describe some of the proteins from which it is made up. Then I will describe how this composition enables a variety of functions to be performed by the tight junction before introducing the novel transmembrane component, and focus of this thesis, MarvelD3. Cellular behaviours and signalling pathways required for the understanding of this thesis are also introduced as appropriate.

The apical junctional complex

In order to perform their functions and maintain the integrity of the epithelium, epithelial cells need to adhere tightly to their neighbours. Indeed, epithelial monolayers comprise densely packed cells connected by complex junctional structures; adherens junctions, tight junctions and desmosomes, which together form the epithelial junctional complex (Figure 1.1). Adherens junctions and desmosomes are adhesive junctions within the junctional complex enabling the epithelium to form a physical barrier between tissues, while tight junctions regulate the movement of ions and solutes through the paracellular pathway in an ion- and size-selective manner. In addition, gap junctions provide another type of intercellular junction. These small connexin-based channels allow small molecules and ions to move between neighbouring cells, affording epithelial cells the ability to propagate signals between their neighbours (Koval, 2002).

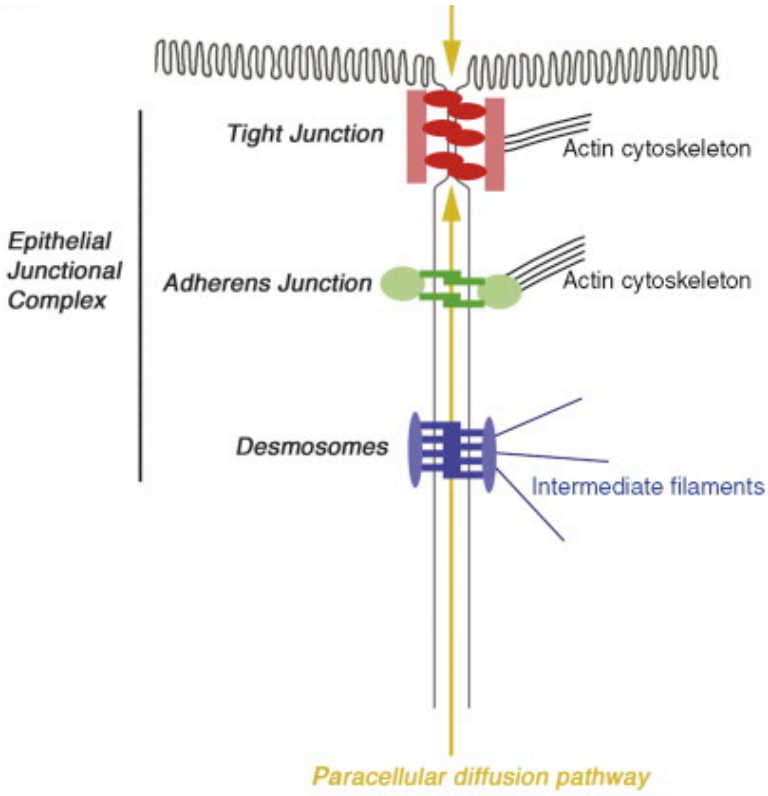

Figure 1.1 – Schematic representation of the epithelial junctional complex. The apical localisation of the tight junctions (red) to the adhesive epithelial junctions adherens junctions (green) and desmosomes (blue), is shown. The yellow arrows indicate the paracellular route for the diffusion of ions and hydrophilic solutes, and suggest how diffusion is restricted at the level of the tight junction. This figure was taken from (Steed et al., 2010).

Adherens junctions

Composition of adherens junctions

The adherens junctions and desmosomes (described below) provide important adhesive contacts between neighbouring epithelial cells. The adherens junction is composed of integral membrane proteins, E-cadherin and nectin, and underlying cytoplasmic proteins affording association with the actin cytoskeleton and an input to intracellular signalling pathways. E-cadherin is a type I classical cadherin primarily

expressed in epithelial cells. It has an extracellular N-terminus, a single transmembrane region, and a C-terminus extending in to the cytoplasm. Adherens junction assembly is thought to proceed via initial nectin-based contacts, followed by lamellipodia formation and subsequent binding between cadherins on the membranes of adjacent cells. In the extracellular space, cis-dimers are formed between two E-cadherin molecules from the same cell, which then interact with cis-dimers on the adjacent cell to form trans-dimers and provide adhesive activity (Takai and Nakanishi, 2003). In the cytoplasm, the C-terminus of E-cadherin interacts with β-catenin and p120-catenin via their armadillo repeats (Ozawa et al., 1989). The site where p120-catenin interacts with E-cadherin is also the target of ubiquitination and implicated in clathrin-mediated endocytosis, thus implicating p120-catenin binding in the stabilization of cadherin-catenin contacts between adjacent cells (Ishiyama et al., 2010). β-catenin binding mediates the interaction between E-cadherin and α-catenin, which also binds actin in a mutually exclusive manner (Yamada et al., 2005). Interactions between E-cadherin, β-catenin and α-catenin thus provide a dynamic link between the junction and the underlying actin cytoskeleton. Adherens junctions are also linked to the cytoskeleton via l-afadin-mediated binding of nectin and F-actin (Mandai et al., 1997). Perturbations in actin cytoskeleton organization following loss of adherens junction contacts suggest the importance of these cell-cell adhesion structures in maintaining epithelial integrity.

Adherens junctions and intracellular signalling

In addition to a role in cadherin-catenin adhesions, β-catenin also functions in the regulation of intracellular signalling pathways. Under basal conditions, any non-junctional, cytosolic β-catenin forms a complex with the tumour suppressor

adenomatous polyposis coli (APC), axin and glycogen synthase kinase 3β (GSK3β), in which β-catenin becomes phosphorylated by the latter and is degraded by the proteosome (Kikuchi, 2000). In the presence of Wnt signalling, however, β-catenin phosphorylation is inhibited, allowing cytosolic β-catenin to accumulate and interact with TCF/LEF family of DNA-binding proteins that go on to activate Wnt responsive genes (Behrens et al., 1996; Huber et al., 1996). By regulating the ratio of junctional or cytosolic β-catenin, therefore, the adherens junction can impact upon intracellular signalling and gene expression via the Wnt signalling pathway. Deregulation of β-catenin signalling is seen in many cancers (Morin, 1999).

Desmosomes

Composition of Desmosomes

Desmosomes are localised sites of cell-cell contact at which cells are held together very tightly. Desmosomal adhesion proteins desmocollin and desmoglein belong to the cadherin superfamily of adhesion molecules and, like E-cadherin, bind cytoplasmic proteins at their intracellular C-termini, while the N-terminus interacts with desmosomes on adjacent cells providing adhesion (Garrod et al., 2002). Armadillo protein family members plakoglobin and plakophilin are found in the desmosomal cytoplasmic domain and demonstrate a dual junctional and nuclear localisation. Linked to the desmosomal cadherins by plakoglobin, desmoplakin associates with intermediate filaments, thus completing the desmosome structure and linking intermediate filaments to the plasma membrane (Kouklis et al., 1994; Stappenbeck and Green, 1992). Plakophilin also mediates association with the intermediate filaments and has been shown to interact with plakoglobin, the

desmosomal cadherins as well as keratin (Hofmann et al., 2000). This interaction between desmosomal proteins in the plasma membrane and the intermediate filaments equips the cell with the ability to resist mechanical stress (Garrod and Chidgey, 2008; Getsios et al., 2004). Cells of the skin and heart, which are particularly exposed to mechanical stress, express high levels of desmosomal proteins. In the absence of correct desmosomal function, tissue integrity becomes severely compromised (Kottke et al., 2006).

Desmosomes and regulation of intracellular signalling pathways

In addition to providing significant adhesive strength between adjacent cells, desmosomes are also implicated in the regulation of intracellular signalling pathways (Thomason et al., 2010). As mentioned, desmosomal proteins plakoglobin and plakophilin demonstrate nuclear and junction localisation, indicating their potential as signalling molecules. Like β-catenin, plakoglobin complexes with APC/GSK3β which targets it for degradation by the proteasome. Plakoglobin has also been shown to be able to interact with TCF/LEF transcription factors indicating its potential to regulate Wnt signalling (Maeda et al., 2004; Miravet et al., 2002; Zhurinsky et al., 2000). Furthermore, plakoglobin has been shown to both promote and suppress the expression of c-myc (Kolligs et al., 2000; Williamson et al., 2006). The contribution of desmosomal regulation of these pathways, however, to physiological and pathological events has yet to be fully understood.

Tight junctions

The tight junctions, or zonula occludens, are the most apical of the epithelial junctional complexes and continuously circumvent the cell bringing the plasma membranes of neighbouring cells into close apposition (Farquhar and Palade, 1963). This is evident on electron micrographs in which the so-called "kissing points" of the outer leaflets of the plasma membrane and the consequent loss of intercellular space can be seen (Figure 1.2A). Underlying the membrane domain is the cytoplasmic plaque, which consists of a meshwork of densely packed cytoplasmic proteins. These morphological features enable tight junctions to perform three fundamental functions. First, to form a semi-permeable barrier capable of finely regulating the movement of ions, solutes and cells across the paracellular space (Tsukita et al., 2001). Second, to participate in establishing and maintaining apico-basal polarity (Shin et al., 2006). Third, to serve as a site for both the integration and divergence of various signalling pathways controlling gene expression, cell differentiation and proliferation (Guillemot et al., 2008; Matter et al., 2005).

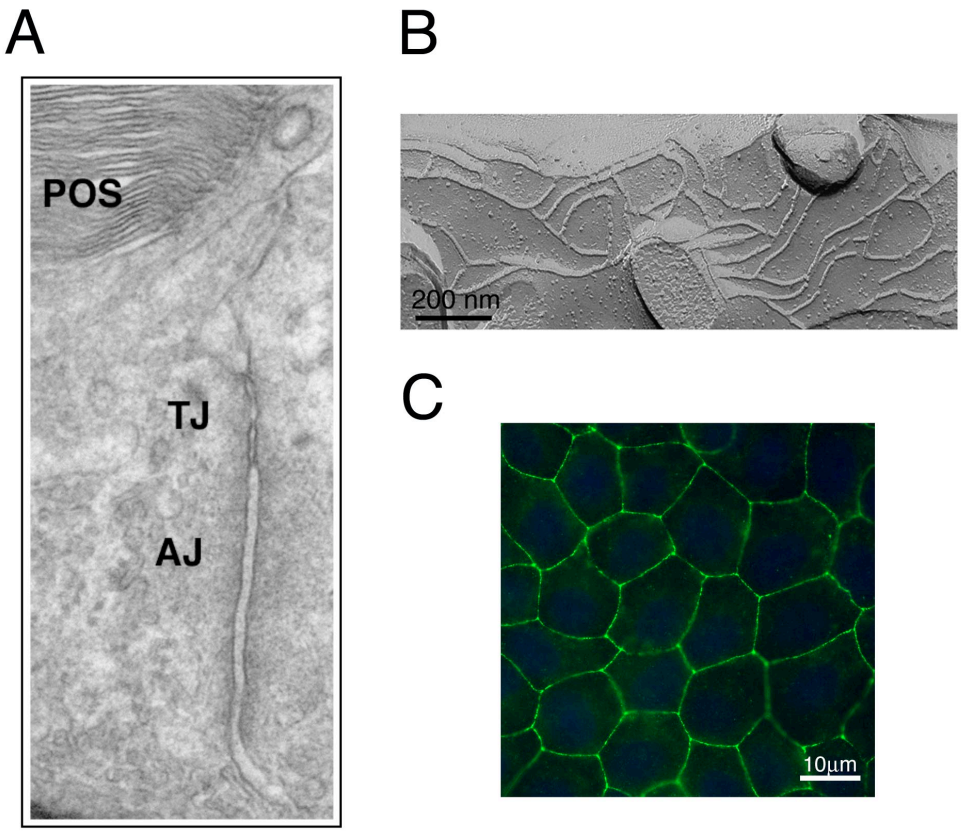

Figure 1.2 – Morphological features of the tight junction. (A) Electron micrograph sections of retinal pigment epithelial cells (POS; photoreceptor outer segments) clearly demonstrates the bringing together of plasma membranes at the level of the tight junction (TJ), but not at the level of the adherens junction (AJ). (B) Preparation of cells for freeze-fracture microscopy demonstrates the tight junctions as a series of strands. (C) Epifluorescence analysis of occludin localisation in an epithelial cell monolayer shows the tight junction to completely encircle the cell. Combined these observations of tight junction morphology enable one to imagine how the tight junction encircles the cell generating a barrier and effectively sealing the epithelium to free-moving molecular traffic. EM image in (A) was kindly provided by Professor Claire Futter, UCL Institute of Ophthalmology. Image in (B) was taken from (Steed et al., 2010).

Composition of the tight junction

The characteristic morphology of tight junctions is attributable to the protein complement from which they are composed. Integral membrane proteins of the tight junction are generally classified into two main classes depending upon the number of transmembrane domains they contain: the four-pass transmembrane proteins, like occludin, tricellulin and the claudin family; and single-span transmembrane proteins, like junctional adhesion molecule (JAM) and coxsackie and adenovirus-associated receptor (CAR). Underlying the plasma membrane domain of the tight junction are a variety of cytoplasmic proteins which together with the transmembrane proteins form a highly dynamic multiprotein complex enabling the tight junction to perform both a structural and a signalling role within the cell (Figure 1.3). While both single and four-pass transmembrane domain proteins participate in mediating cell-cell adhesion and facilitating various signalling processes, only the polytopic proteins form the diffusion barrier and regulate paracellular permeability (Matter and Balda, 2007).

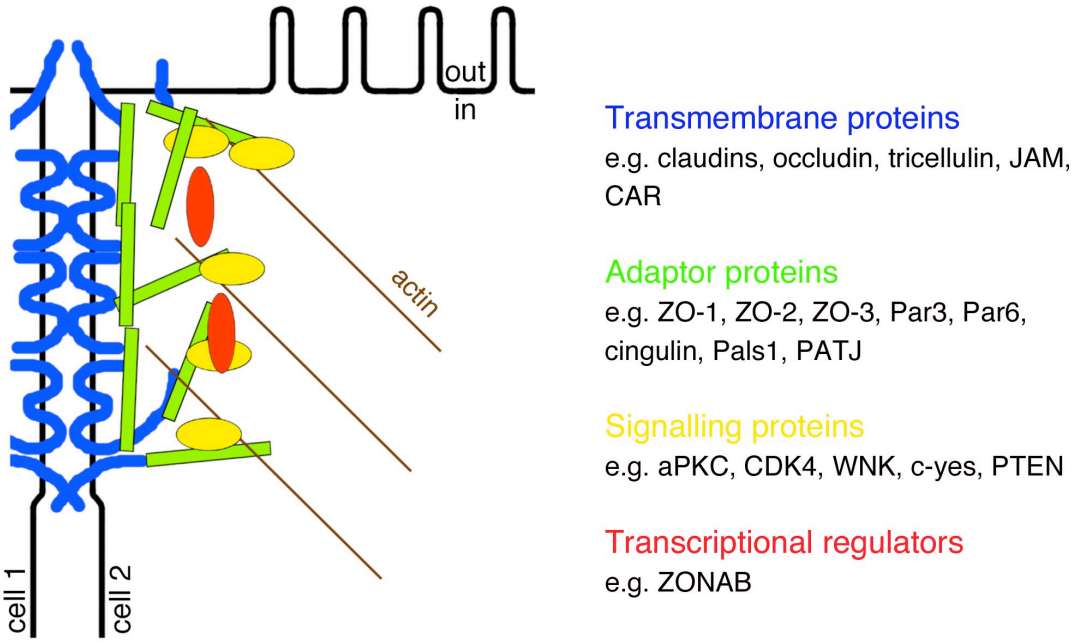

Figure 1.3 – Schematic representation of the tight junction and its protein constituents. Tight junctions are composed of a variety of different types of proteins. The transmembrane proteins are shown in blue. These include four-pass transmembrane proteins like claudins, occludin and tricellulin, and single-pass transmembrane proteins like JAM and CAR. Underlying the membrane proteins, adaptor/complex-forming proteins (green) regulate interaction between the membrane proteins and signalling molecules or the actin cytoskeleton. They also include cell polarity proteins like the Par polarity complex that localise at the tight junction. Signalling proteins (yellow) and transcriptional regulators (red) are also found at the tight junction. Some of these proteins, like ZONAB, show dual localisation at the junction and in the nucleus. For details of individual proteins, see the text below.

Four-pass integral membrane proteins of the tight junction

Claudins and the barrier function

Freeze-fracture electron microscopy shows tight junctions as a series of anastomosing membrane strands found at close contact sites between the outer leaflets of the plasma membrane of neighbouring cells, demonstrating the effective occlusion of the intercellular space between adjacent cells. Claudins have been identified as the major component of these tight junction strands (Furuse et al., 1998a; Furuse et al., 1998b). Lateral association between claudin molecules within the plasma membrane combined with homotypic adhesive interactions between claudin molecules on adjacent cells is thought to underlie the characteristic structure of the tight junction strands (Furuse et al., 1999). The number and distribution of charged residues in the first extracellular loop domain varies between claudin family members and enables the selective permeability of ions through the paracellular pathway based on charge. Claudin-2, for example, allows cations, but excludes the passage of anions through the paracellular space (Amasheh et al., 2002). Furthermore, alterations to specific charged residues in the first extracellular loop of claudin-15 has been shown to be sufficient to alter the preference from cations to anions through the paracellular space (Colegio et al., 2002). The ability of specific claudins to bestow distinct permeability properties is further demonstrated by the differential expression of claudin-1 and claudin-2 to tighter and more leaky segments of kidney tubules, indicating that variations to the complement of claudins expressed is one mechanism by which cells and tissues may organize their ionic permeability properties (Reyes et al., 2002).

The mechanism by which tight junctions regulate size-selective diffusion is not yet clear. When GFP-tagged claudin-1 was expressed in L cells, the network of intramembrane paired strands formed at plains of adhesion between adjacent cells were seen to be highly dynamic, constantly remodeling through rounds of breaking and annealing (Sasaki et al., 2003). Since the high density of endogenous strands and their orientation parallel to the observation axis makes visualization of strand behaviour in live cells difficult, it remains to be confirmed whether tight junctions *in situ* display the same dynamic properties. Visualizing tight junctions as a flexible network of strands, however, provides an attractive model of how tight junctions achieve size-selective diffusion, without compromising overall integrity (Figure 1.3) (Sasaki et al., 2003; Steed et al., 2010). It is likely, however, that interactions with the underlying cytoskeleton or cytoplasmic proteins would influence strand organization and their dynamic behaviour, and this is not yet fully understood.

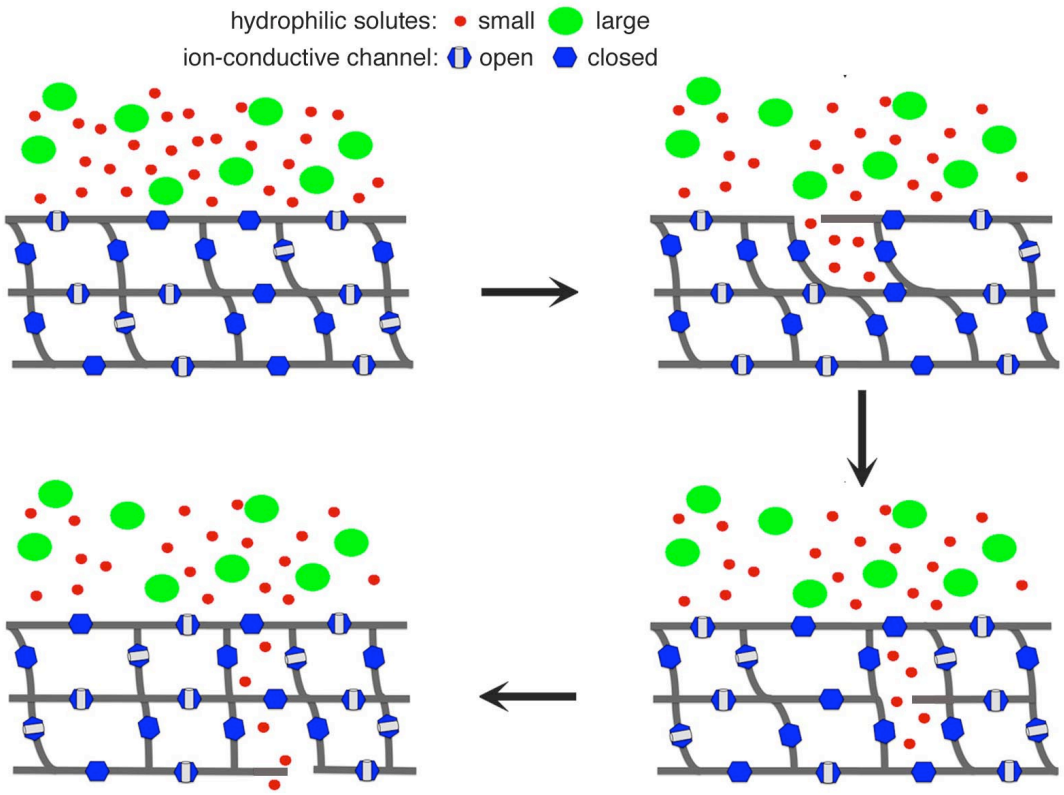

Figure 1.4 – Proposed model for regulation of paracellular permeability by a series of dynamic tight junction strands. Tight junctions are shown as grey lines that represent the intramembrane strands. The strands contain ion-selective channels that are thought to be formed by claudins and can be in an open or a closed state. Because claudins have characteristic ion-conductive properties, the types of claudin expressed determine the ion-selectivity of the paracellular pathway. The intramembrane strands are dynamic; hence, the network of strands is reshaping itself continuously, resulting in occasionally open network compartments that allow small solutes to enter and slowly diffuse across the junction (broken grey lines represent strand opening, while the integrity of the overall network is maintained). The size selectivity is determined by the functional distance of the two neighbouring plasma membranes at the level of tight junctions. Size-selective paracellular diffusion is also regulated by various signalling pathways and could involve interactions with the actin cytoskeleton and additional protein components of the strands. It is not yet known how ions are restricted from passing through the open strands, but perhaps the strand state could influence the state of opening of the channel. Taken from (Steed et al., 2010).

Occludin

Integration of additional transmembrane proteins in to the claudin-based strands provides additional complexity to the tight junction structure. Occludin was the first transmembrane component of the tight junction to be identified and localizes to the strands by electron microscopy (Furuse et al., 1993). The specific primary role for occludin at the tight junction is still unclear. Initial i*n vitro* assays suggested that occludin might function in the regulation of permeability properties of the tight junction since expression of occludin constructs in MDCK cells resulted in increased transepithelial resistance (TER) and increased paracellular flux (Balda et al., 1996). Later observations made in the occludin knockout mouse, however, demonstrated that, despite the lack of occludin expression, physiologically and structurally normal tight junctions were present in these animals (Saitou et al., 2000; Schulzke et al., 2005). In addition, cells arising from occludin-deficient embryonic stem cells demonstrated a comprehensive network of tight junction strands, further suggesting that occludin is dispensible for strand formation (Saitou et al., 1998). The reported discrepancies between over-expression studies *in vitro* and observations following loss of occludin *in vivo* could be due to interruption of endogenous complexes following the expression of occludin or occludin domain constructs *in vitro*. Studies utilizing RNA interference to deplete cells of occludin support the hypothesis that occludin influences barrier properties by demonstrating that occludin depletion resulted in reduced barrier disruption in response to cytokines (Van Itallie et al., 2010). Addition of Interferon gamma (IFNγ) and tumour necrosis factor alpha (TNFα) increased TER and paracellular flux across control cell monolayers, but these increases were attenuated in occludin knockdown monolayers, suggesting occludin is important for regulating the barrier properties of the tight junction in response to

cytokines (Van Itallie et al., 2010). Taken together, these studies suggest loss of occludin may not affect basal barrier properties, but may instead be important for the regulation of tight junction function in response to specific stimuli, like inflammatory cytokine signalling. Indeed, cytokine-induced cytoskeletal reorganization in endothelial cells required activation of the small GTPase RhoA (Campos et al., 2009), the activity levels of which are significantly reduced in epithelial cells depleted of occludin by RNA interference (Yu et al., 2005). Since the organization of the actin cytoskeleton appears to influence permeability properties of the tight junction (Nusrat et al., 1995), the ability to regulate F-actin organization at the tight junction via RhoA may be one mechanism in which occludin regulates barrier properties of the tight junction. More recently, it has been demonstrated that phosphorylation of occludin at serine residue 408 affected paracellular permeability by regulating the dynamic behaviour of other tight junction proteins (Raleigh et al., 2011). Therefore, perhaps the regulation of tight junction properties by individual constituents is more subtle than over-expression or siRNA-mediated depletion studies enable to be seen. Post-translational modifications in response to specific stimuli may be the significant factor in enabling occludin, and other tight junction components, to regulate the properties of the tight junction.

Tricellulin

Tricellulin is also a four-pass transmembrane protein of the tight junction, aptly named for its concentration at tricellular contact sites between three adjacent cells (Ikenouchi et al., 2005), as opposed to localization along the bicellular junction between two adjacent cells illustrated by the claudins and occludin. Tricellulin expression is thought to be instrumental in maintaining the integrity of the monolayer

since in its absence, both the tricellular and bicellular contact sites appeared to be compromised (Ikenouchi et al., 2005). Given the vulnerable nature of tricellular contacts as points of potential leakage it seems intuitive that these specialized points of cell contact may require some kind of reinforced structure that may not be necessary along the bicellular junctions. Indeed, exogenous expression of tricellulin caused increased cross-linking of claudin-1-based tight junction strands in L cells, suggesting tricellulin expression may mediate tricellular-specific organization of the tight junction (Ikenouchi et al., 2008).

Mutations of tight junction transmembrane proteins and disease

In addition to their altered expression in cancer, identification of specific mutations has implicated the transmembrane proteins of the tight junction in additional pathological conditions, further highlighting the importance of their physiological functions. Mutations in claudin-14 have been shown to cause hearing loss in humans (Wilcox et al., 2001) and loss of claudin-14 in knockout mouse studies causes alterations in ionic permeability within the inner ear resulting in significant loss of outer hair cells (Ben-Yosef et al., 2003). Mutations in tricellulin have also been associated with hearing loss (Riazuddin et al., 2006). These results suggest the importance of tight junction proteins in maintaining the correct compartmentalization of the inner ear, without which hearing becomes significantly impaired. Studies in knockout mice have also demonstrated the importance of claudin-11 expression in central nervous system (CNS) function and reproduction. Loss of tight junctions in CNS myelin and Sertoli cells in the absence of claudin-11 rendered mice with neurological deficits and left males sterile (Gow et al., 1999). Mutations in claudin-16 cause familial hypomagnesemia as renal Mg^{2+} resorption is perturbed (Simon et

al., 1999). Mutations in cytoplasmic components of the tight junction can also have pathological consequences. Mutations in the first PDZ domain of ZO-2, for example, have been linked to familial hypercholanemia (Carlton et al., 2003). Identification of such pathologies caused by loss of tight junction protein function demonstrates that tight junction function is important in a range of tissues. The tissue-specific phenotypes also allude to the ability of tight junctions to perform specific roles in different tissue types.

Tight junction-associated cytoplasmic proteins

The presence of protein-protein interaction domains in the cytoplasmic regions of the tight junction transmembrane proteins enables interaction with a number of scaffolding proteins in the underlying cytoplasm. The PDZ domain (an acronym of post-synaptic density protein 95, PSD-95; discs large, Dlg; and ZO-1, in which the common domain was first recognised) is a frequently occurring region of sequence homology eliciting protein-protein interactions between a variety of signalling proteins. Implicated in the organisation of functional plasma membrane domains, PDZ domain-containing scaffolding proteins serve to cluster together transmembrane proteins and recruit signalling molecules in larger protein complexes from which intracellular signalling pathways may be regulated. The Src homology 3 (SH3) domain facilitates protein-protein interaction by binding proline-rich sequences and is also found in many proteins of the tight junction.

Zonula Occludens proteins

Zonula occludens (ZO)-1, ZO-2 and ZO-3 are tight junction-associated members of the membrane-associated guanylate kinase-like homologue (MAGUKs) family. MAGUKs possess multiple PDZ domains, one SH3 domain and one guanylate kinase-like (GUK) domain. The PDZ domains of the ZO proteins facilitate interaction with PDZ domains found in the C-termini of tight junction transmembrane proteins. ZO-1, -2 and -3 have been shown to interact with claudins (Itoh et al., 1999a) and occludin (Furuse et al., 1994; Haskins et al., 1998; Itoh et al., 1999b). The interaction between ZO-1 and tricellulin however is not yet clear (Ikenouchi et al., 2008; Riazuddin et al., 2006). The PDZ domain also mediates interactions between the ZO proteins themselves, with ZO-2 and ZO-3 both being able to associate with ZO-1, but not with each other (Haskins et al., 1998). Since ZO proteins are increasingly implicated in the regulation of intracellular signalling pathways (discussed below), the identity of their membrane-binding partners is important in understanding how transmembrane proteins function in their regulation and subsequent effect on downstream signalling pathways.

Polarity proteins

The epithelial tight junction is also important in the establishment and maintenance of apicobasal polarity. Two important complexes in the regulation of cell polarity are found to concentrate at the tight junctions; the Par polarity complex, composed of Par3, Par6 and atypical protein kinase C (aPKC), and the Crumbs (Crb) polarity complex, made up of Crb, PatJ and Pals1. The recruitment of these complexes in the establishment of apicobasal polarity occurs after the formation of initial cell-cell

contacts and is necessary for the establishment of a distinct tight junction complex, apical to the adherens junction. Recruitment of JAMs to the plasma membrane following the initial formation of nectin and E-cadherin-based contacts is followed by recruitment of Par3 (Ebnet et al., 2001; Itoh et al., 2001). This is followed by the recruitment of Par6 and aPKC and establishment of the apical membrane domain (Horikoshi et al., 2009). Depletion of Par3 prevented Par6-aPKC recruitment and the formation of the apical domain is perturbed, indicating the importance of Par complex assembly in establishment of epithelial polarity (Horikoshi et al., 2009). Cdc42 activation after initial adherens junction contacts also promotes polarisation around the young contact sites by interacting with Par6 and subsequently activating its binding partner aPKC. Active aPKC is necessary for tight junction formation and establishment of cell polarity in epithelial cells. Par3 also promotes tight junction assembly via TIAM1-mediated activation of Rac1 (Chen and Macara, 2005). Depletion of Par3 by RNA interference results in constitutive activation of Rac1 and disruption of tight junction assembly in MDCK cells (Chen and Macara, 2005).

In the Crb complex, Pals1 links Crb and PATJ, which localises to the tight junction[30]. Inhibition of PATJ and Pals1 by RNA interference has been shown to impede tight junction formation and disrupt cell polarity (Roh et al., 2003; Straight et al., 2004). Interestingly, Par6 and Pals1 also directly interact providing a link between the two polarity complexes (Hurd et al., 2003). It is becoming increasingly apparent that in addition to regulating apicobasal polarity, interactions between tight junction proteins and polarity proteins may also play a significant role in migration. This will be discussed below.

Cytoskeletal proteins

Preparation of cells for freeze-fracture electron microscopy demonstrated the presence of an actin filament network underlying the tight junction membrane domain, alluding to a potential association between the actin cytoskeleton and the tight junction (Hirokawa and Tilney, 1982). Subsequent studies utilising cytochalasin D treatment to disrupt the polymerization state of actin in intestinal cells caused reductions in the extent of cross-linking and number of tight junction strands and perturbations in both paracellular permeability and TER, generating the hypothesis that interactions between the tight junction and the underlying actin cytoskeleton may be of functional relevance (Madara et al., 1986). Now, many proteins associated with the cytoskeleton and capable of interacting with actin have been identified, and the actin cytoskeleton is integral to the formation of tight junctions and the regulation of their behaviour therein.

Actin cytoskeleton and junction assembly

During junction assembly, actin filaments associate with E-cadherin contact sites and remodel as E-cadherin complexes associate to form a continuous band of cell-cell contact. This is facilitated by actin regulatory proteins recruited to the initial E-cadherin contact sites. Arp2/3, for example, is recruited to early contact sites by binding to E-cadherin (Kovacs et al., 2002) and subsequently promotes actin filament branching and lamellipodial extension necessary for the extension and assembly of cadherin-based cell-cell contacts (Verma et al., 2004). Arp2/3 activity in the apical junctional complex is, at least in part, regulated by α-catenin which, in its dimeric form, is thought to compete with Arp2/3 for actin binding and, in so doing, suppresses

Arp2/3-mediated actin polymerization and stabilizes actin at the junction (Drees et al., 2005). Recruitment of tight junction proteins to the E-cadherin-based cell contact sites and stabilization of the initial contacts is followed by the apical segregation of the tight junction away from the adherens junction to form two distinct junctional complexes. This segregation is prompted by integrin-mediated adhesion to the underlying extracellular matrix, which enables cells to recognize their apical-basal polarity (Drubin and Nelson, 1996) and involves reorganization of actin filaments to elongate the cell into a cuboidal morphology and generate the circumferential actin ring typical of polarized epithelial cells. This process appears to rely on the ability of Myosin II to activate contraction of the thin actin bundles peripherally located to initial junctional actin, to generate mature junctional actin and a polarized cell shape (Zhang et al., 2005a). Contraction of the perijunctional actin ring is believed to regulate paracellular permeability properties by opening the tight junction, thus the actin cytoskeleton plays a role in moderating the properties of the mature tight junction, in addition to mediating its assembly.

Regulation of the cytoskeleton by the tight junction

In addition to the requirement for actin cytoskeleton dynamics in the initiation and maturation of tight junctions, the tight junctions themselves appear to regulate the actin cytoskeleton in various cellular processes. Occludin, for example, has been implicated in the regulation of actin cytoskeleton reorganization via a signalling pathway involving RhoA (Yu et al., 2005). Occludin knockdown cells failed to activate RhoA in response to cholesterol addition and thus did not elicit the cytoskeletal rearrangements observed in control cells (Yu et al., 2005). In addition, apoptotic cells were not extruded from occludin-knockdown monolayers (Yu et al.,

2005). While loss of occludin could simply mean the healthy cells can no longer detect their dying neighbour, since occludin depletion does not affect other modes of cell-cell contact, it is also possible that in the absence of occludin cells are unable to initiate the Rho-mediated cytoskeletal rearrangements shown to be necessary for apical extrusion (Rosenblatt et al., 2001). In consideration, it seems logical that a junction protein be able to coordinate such a process, thus enabling dead cells to be extruded from the epithelium without compromising the integrity of the monolayer. Indeed, epithelial barrier function was maintained despite the extrusion of large numbers of apoptotic cells (Rosenblatt et al., 2001).

In addition to stabilizing the tight junction complex, interactions between the actin cytoskeleton and transmembrane proteins of the tight junction provide a scaffold for the recruitment of intracellular signalling proteins, from which signalling pathways can be regulated in response to external cues. In the next section I will discuss what is known about the regulation of migration and intracellular signalling pathways by proteins of the tight junction. I will also introduce signalling pathways not yet associated with the tight junction, but that are of significance to this thesis.

Cell migration

Cell migration describes the movement of a single cell or group of cells (collective migration) relative to the underlying substrate. Both single cell and collective cell migration are relevant to a number of physiological and pathological processes. During development, for example, cells migrate both singularly and collectively to generate tissues and organs within the embryo. Carefully regulated epithelial-to-mesenchymal transitions (EMT) generate mesenchymal cells, which migrate

individually or as loosely associated groups of cells, with increased cell migration often correlating with weaker cell-cell interactions. Neural crest cells are a highly migratory cell population, which demonstrate dynamic cell-cell contacts enabling them to migrate as a cohort through the embryo to their site of differentiation. Cell-cell contacts between neural crest cells are important for directional migration (Carmona-Fontaine et al., 2008). Single cell migration also occurs during the immune response and during cancer progression, where the induction of single cell migration can play an important role in the promotion of metastasis (Giampieri et al., 2009). Collective cell migration is also significant in tumour cell metastasis, as well as in the physiological wound healing response. Given its importance in development and physiology, understanding the mechanisms behind epithelial cell migration is likely to be of great biological and therapeutic significance.

Mechanisms of cell migration

Single cell migration can be further subdivided into amoeboid migration and mesenchymal migration. Both describe the movement of individual cells, but the mechanisms by which this movement is achieved differ considerably. During amoeboid migration, cells move with a rounded morphology and in a protease-independent manner. Amoeboid migration may proceed via membrane blebbing or through the extension of filopodia at the leading edge. In both cases however, and in contrast to mesenchymal migration, amoeboid cells show little or weak engagement with the substrate, lacking mature focal adhesions and stress fibres (Fackler and Grosse, 2008; Friedl and Wolf, 2010; Lammermann and Sixt, 2009). In mesenchymal migration, cells extend lamellipodia and filopodia at the leading edge, driven by polymerisation of the actin cytoskeleton. Attachment of these protrusions to the

underlying substrate followed by contraction of the actinomyosin cytoskeleton generates tension across the length of the cell and provides a driving force to propel the cell forwards. Detachment of the cell rear followed by continuing rounds of leading edge extension and substrate adhesion serves to coordinate the forward migration of the cell. Mesenchymal cell migration also utilises proteolysis to degrade the extracellular matrix. Production of matrix metalloproteinases (MMPs) by migrating cells results in degradation of the surrounding extracellular matrix and can promote cell migration and tumour cell invasion (Basbaum and Werb, 1996; Bjorklund and Koivunen, 2005; Giannelli et al., 1997; Koshikawa et al., 2000). In some cell types, inhibition of proteases has been shown to induce cells to change from a mesenchymal to an amoeboid, protease-independent mode of migration (Wolf et al., 2003).

During collective cell migration, cell-cell contacts between neighbouring cells are maintained and cells progress along the substrate as a group (Ilina and Friedl, 2009). Cells become polarised in a coordinated manner with cells at the front of the migrating sheet extending protrusions from which the sheet moves forwards. Interactions and coordinated cytoskeletal changes in cells behind those at the leading edge then enable forward migration of the sheet. Epithelial cells display collective migration as a sheet, which is important during the wound healing response.

Regulation of cell migration

Effective cell migration requires coordinated regulation of the actin cytoskeleton, which is achieved by the balance of activity of the RhoGTPases; RhoA at the rear of the cell and Rac and Cdc42 at the cell front. The activity of RhoGTPases plays an

important role in establishing polarity in the migrating cells. Extension of lamellipodia and filopodia from the leading edge cells relies on activity of the small GTPases Rac and Cdc42, respectively (Nobes and Hall, 1995). RhoA activity at the rear of single cells or in adjacent rear cells during collective migration allows forward movement by controlling actinomyosin contractility. Thus GTPases help to define the front-rear polarity axis required for directional migration.

Polarity proteins are also important regulators of epithelial cell migration. As discussed, localisation of polarity proteins to the tight junctions is important in the ability of the tight junctions to define the apicobasal membrane domains, establishing and maintaining apicobasal polarity in epithelial cells. During cell migration, cells lose their apicobasal polarity and assume front-rear polarity instead, observed by the redistribution of polarity proteins. Just as is involved in junction formation, cross-talk between Par polarity proteins and the RhoGTPases is involved in regulating cell migration. Cdc42 recruitment and activation at the leading edge of cells following wounding, results in an interaction with Par6 and subsequent activation of aPKC (Etienne-Manneville and Hall, 2001). Localised activation of aPKC is necessary for localised activation of cJun N-terminal kinase (JNK), which phosphorylates Paxillin, promoting migration by increasing focal adhesion dynamics (Rosse et al., 2009). By retaining polarity proteins at cell-cell junctions, therefore, tight junctions may function in perturbing the migration of epithelial cells.

Tight junctions and migration

Alterations to the localisation of tight junction proteins in migrating cells has lead to the hypothesis that tight junction proteins may function directly in the regulation of

cell migration. Occludin has been seen to localise to the leading edge of migrating MDCK cells and in its absence their migration was significantly reduced (Du et al., 2010). Without occludin, aPKC-Par3 and PATJ failed to recruit to the leading edge resulting in disorganisation of the microtubule network previously been shown to be mediated by PATJ (Shin et al., 2007). In addition to regulating the localisation of polarity proteins and subsequent directional migration, occludin was also implicated in the regulation of lamellipodia formation by regulating leading edge activation of PI3K and Rac1 (Du et al., 2010). Thus interactions between tight junction proteins and polarity proteins are important for both tight junction formation and regulation of migration.

ZO-1 is also implicated in the regulation of directional cell migration. At the tight junction, ZO-1 maintains epithelial integrity by binding transmembrane proteins occludin and claudins and the underlying actin cytoskeleton. At the onset of migration, ZO-1 resdistributes from the tight junction to the leading edge in response to phosphorylation by PKCε and interacts with α5-integrin (Tuomi et al., 2009). While the significance of this interaction is not yet known, depletion of ZO-1 resulted in elevated Rac activity and randomised migration, while loss of α5-integrin inhibited migration, indicating a role for ZO-1 in regulating directional cell migration from integrin-mediated contact points in the lamellipodia (Tuomi et al., 2009). In addition, ZO-1 has also been shown to interact with the Cdc42 effector kinase MRCKβ at the leading edge, activity of which is involved in the generation of cellular protrusions (Tan et al., 2008). Furthermore, expression of the N-terminal half of ZO-3 in MDCK cells resulted in reduced RhoA activity, reduced amounts of stress fibres and increased migration in a wound healing assay (Wittchen et al., 2003), further indicating a role for tight junctions in the regulation of cell migration, by impacting

on the cytoskeleton. While many studies, such as those mentioned above examining the role of ZO-1 in migration, have been performed in single cells, they also generate interesting information for our understanding of collective cell migration. During collective cell migration, the presence of cell contacts likely means some of the upstream signals affecting leading edge localisation of junction proteins may be different from those occurring in single cells. Nevertheless, understanding the capabilities of individual junctional constituents may shed light on the mechanisms governing both single and collective cell migration.

Transitions between single and collective cell migration states

As discussed, both single and collective cell migration have important roles in physiological and pathological processes. In addition to the mechanisms behind each type of migration, however, those processes defining the migration type also need to be understood. The arrangement of epithelial cells in to monolayers is necessary for organ homeostasis. During epithelial-to-mesenchymal transition (EMT) cells undergo a series of biochemical and morphological changes taking them from a polarised epithelial cell to a motile, individual, mesenchymal cell. Sometimes this process is advantageous, for example during development, and sometimes it is detrimental, for example during metastasis of cancer cells. Various signalling pathways are involved in triggering EMT in different biological contexts, including epidermal growth factor (EGF), Wnt, hepatocyte growth factor (HGF) and members of the transforming growth factor β (TGFβ) family, like TGFβ and bone morphogenetic protein (BMP) (Kalluri and Weinberg, 2009; Yang and Weinberg, 2008). Expression of transcription factors in response to these signalling pathways results in downregulation of epithelial

markers, like E-cadherin, occludin and claudins, and increased mesenchymal markers, like vimentin and smooth muscle actin (for review see (Kalluri and Weinberg, 2009)).

Tight junctions and Epithelial-to-Mesenchymal transition

The functional importance of the link between tight junctions and cell polarity is exemplified by the dissolution of tight junctions and polarity during epithelial-to-mesenchymal transition induced by TGFβ. The TGFβ receptor 1 (TGFβR1) has been shown to localize to the tight junction via an interaction with the second extracellular loop of occludin (Barrios-Rodiles et al., 2005). Interaction between TGFβR1 and TGFβ receptor 2 (TGFβR2) in response to TGFβ serves to recruit TGFβR2 to the tight junction, where it can then phosphorylate Par6, which in turn inhibits RhoA leading to disassembly of the tight junctions. Cells expressing mutant constructs of occludin lacking the second extracellular loop domain or phosphorylation mutants of Par6, display reduced tight junction loss in response to TGFβ than control cells indicating the importance of the interaction between occludin and TGFβR1 in TGFβ-induced tight junction loss (Barrios-Rodiles et al., 2005; Ozdamar et al., 2005). These data demonstrate a functional collaboration between tight junctions and polarity proteins in the regulation of epithelial-to-mesenchymal transition in response to TGFβ. Furthermore, the dissolution of junctions during EMT facilitates a transition from collective to single cell migration.

Intracellular signalling pathways

The regulation of intracellular signalling pathways is an important mechanism by which cells can transduce signals from the exterior to the interior of the cell, leading to necessary changes in gene expression and behaviour. Some of these pathways

involved in the regulation of epithelial cell proliferation and migration will now be discussed. It is also apparent that in addition to their structural role, tight junctions serve an important function in the integration and transmission of intracellular signals to regulate junction function and overall cell behaviour. Thus tight junctions not only receive and respond to signals to alter their own behaviour (for example, paracellular permeability properties), but also transmit signals to the interior of the cell to regulate gene transcription and control cell proliferation and differentiation (Matter and Balda, 2003b). Thus signalling at the tight junction occurs in a bidirectional manner (Matter and Balda, 2003b). Signalling pathways involved in tight junction assembly and function have been discussed above, so I will now focus on those signalling pathways emanating from the tight junction and their ultimate effects on gene expression.

Tight junction regulation of gene expression

There is increasing evidence of a role for tight junctions in the regulation of gene expression involved in cell proliferation and differentiation. Observations of ZO-1 downregulation in breast (Hoover et al., 1998) and colorectal cancer (Kaihara et al., 2003) combined with *in vitro* studies demonstrating reduced proliferation following ZO-1 overexpression (Balda et al., 2003) have implicated this cytosolic tight junction protein in the regulation of cell proliferation and differentiation. Identification of an interaction between the SH3 domain of ZO-1 and the transcription factor ZONAB (ZO-1-associated nucleic acid binding protein) provided a potential mechanism through which this regulation may take place (Balda and Matter, 2000). Gel shift assays showed ZONAB to be capable of interacting with the promoters of a number of cell cycle regulatory proteins and facilitators of cellular differentiation, like ErbB2 (Balda and Matter, 2000). When cells are at low confluence and ZO-1 levels are low,

ZONAB demonstrates dual localisation to both the tight junction and the nucleus where it promotes G1 to S phase transition by increasing transcription of cyclinD1 and proliferating cell nuclear antigen (PCNA) gene products. When cells become confluent and ZO-1 levels increase, interaction between ZO-1 and ZONAB serves to sequester ZONAB at the tight junction, reducing its nuclear activity and therefore inhibiting proliferation. ZONAB also complexes with CDK4, a regulator of G1 to S phase transition. Sequestration of ZONAB in the cytoplasm by ZO-1 also prevents nuclear localization of CDK4, further impairing proliferation (Balda et al., 2003). Regulation of the transcriptional activity of ZONAB has also been shown to be mediated by RhoA (Nie et al., 2009). By regulating Rho GTPase signalling, therefore, tight junctions may be able to further influence intracellular signalling pathways and gene expression.

Signalling by Rho GTPases

The Rho family of GTPases are small GTP-binding proteins of the Ras superfamily. RhoA, Rac and Cdc42 are the best-characterised members of the Rho GTPase family in mammalian cells. The Rho GTPases function as molecular switches by cycling between a GDP-bound inactive state and a GTP-bound active state. Rho GTPases have intrinsic GTPase activity converting GTP to GDP and resuming an inactive state. This cycling is additionally regulated by guanine-nucleotide exchange factors (GEFs), which catalyse the exchange of GDP for GTP, and by GTPase-activating proteins (GAPs), which promote GTP hydolysis to GDP (Figure 1.4). Therefore GEFs serve to activate RhoGTPase signalling pathways while GAPs serve to inhibit them. By acting on numerous downstream effector molecules Rho GTPases regulate an array of cellular processes including actin reorganisation, cell adhesion and signal

transduction (Etienne-Manneville and Hall, 2002; Ridley, 2001). In doing so Rho GTPases help coordinate diverse cellular processes like cell migration, proliferation and differentiation.

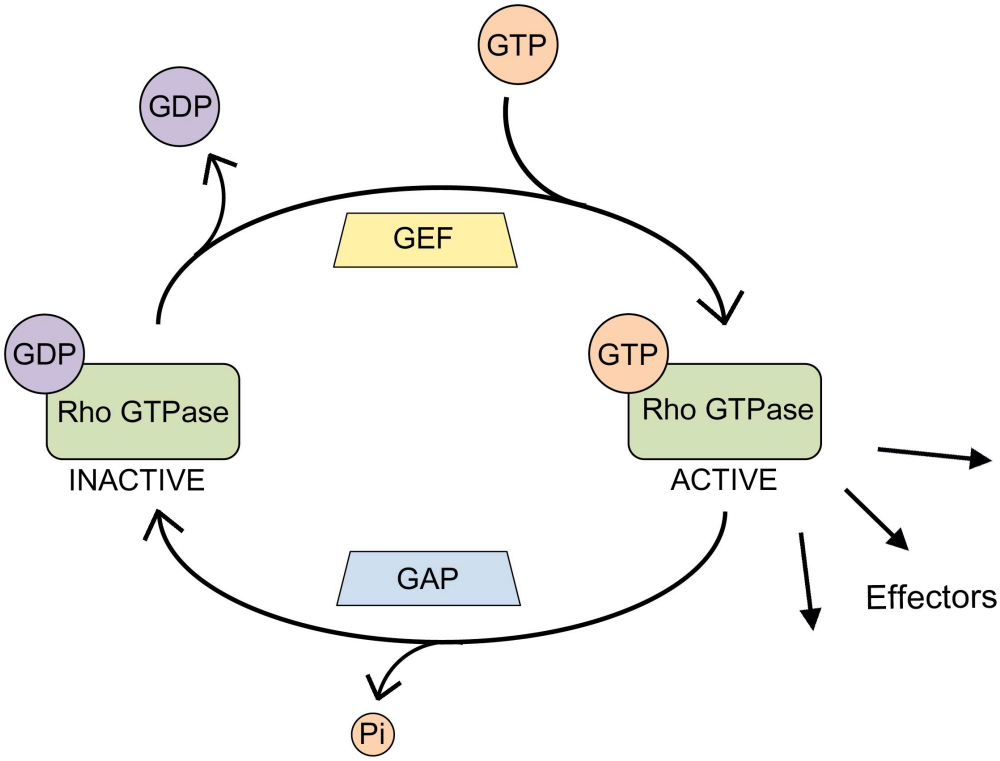

Figure 1.5 – Regulation of Rho GTPase activity. Rho GTPase signalling is regulated by their binding to GTP (active) or GDP (inactive). Rho GTPases display intrinsic GTPase activity, switching off their signalling by hydrolysing GTP to GDP. Switching between active and inactive states is further regulated by guanine nucleotide exchange factors (GEFs) and GTPase activating proteins (GAPs). As shown, GEFs promote the exchange of GDP for GTP, so increase GEF activity results in increased levels of active GTPase and increased activation of downstream effectors. GAPs promote intrinsic GTPase activity and therefore serve to switch off GTPase signalling by promoting hydrolysis of GTP to GDP. Rho GTPases are also regulated by guanine nucleotide dissociation inhibitors (GDIs), which can bind GDP-bound GTPases and prevent nucleotide dissociation, thus negatively regulating Rho GTPase signalling (not shown).

Activation of GTPase signalling

GEF activity is regulated by a number of different extracellular signals. Activation of growth factor receptors, cytokine receptors and receptors mediating adhesion have all been shown to activate GEFs and, in turn, downstream GTPases. Activation of RhoA in response to EGF and TNFα-induced activation of the EGFR, for example, is mediated by GEFH1 activation (Kakiashvili et al., 2011). Furthermore, phosphorylation of GEFH1 by ERK enhances the GEF activity of GEFH1 towards RhoA (Fujishiro et al., 2008). As ERK can be activated in response to EGFR signalling, this affords a mechanism through which growth factor signalling can activate the GTPase RhoA. Activated Rho GTPases then activate a number of effector molecules to elicit their effects. By activating effectors involved in both cytoskeletal reorganisation and intracellular signalling, active Rho GTPases may facilitate changes to both the actin cytoskeleton and gene expression in response to growth factor signalling. The direct mechanisms behind Rho GTPase-mediated regulation of gene transcription, however, are only beginning to be realised.

Regulation of gene expression by Rho GTPases

Rho GTPases have demonstrated the potential to impact on gene expression by a number of different mechanisms. By regulating actin dynamics, Rho GTPase activity affects the ratio of G-actin to F-actin within the cell. MAL, a coactivator of the serum response factor (SRF), binds to G-actin in the cytoplasm, which prevents its nuclear activity. In response to Rho-induced actin polymerisation, and subsequent reduction in the cytoplasmic G-actin pool, MAL redistributes to the nucleus where it

can regulate SRF (Miralles et al., 2003). Thus regulating actin cytoskeletal dynamics may be one mechanism by which Rho GTPases can mediate gene transcription.

In addition, as mentioned above, RhoA activation of ZONAB transcriptional activity enables RhoA to mediate cyclinD1 expression (Nie et al., 2009). RhoA is also attributed with restricting the induction of cyclinD1 to mid-G1 phase (Welsh et al., 2001). Binding of cyclinD1 to cyclin-dependent kinases (CDKs) 4 and 6 and subsequent CDK activation results in phosphorylation of the retinoblastoma protein (Rb), relieving the Rb-mediated inhibition of E2F-regulated genes. E2F-mediated expression of cyclins E and A facilitates entry in to S-phase (Kowalik et al., 1995). Thus by regulating cyclinD1 expression, Rho GTPases play a pivotal role in G1 phase cell cycle progression. These studies demonstrate how Rho GTPases can regulate gene expression by eliciting cytoskeletal changes or by feeding in to intracellular signalling pathways. By signalling through Rho GTPases, therefore, cells can regulate both cytoskeletal changes and intracellular signalling pathways, which may both lead to changes in gene transcription.

In addition to GTPases, other mechanisms that regulate gene expression have also been associated with the tight junction (Balda and Matter, 2009), like the interaction between ZO-2 and scaffold-attachment factor B (SAF-B) (Traweger et al., 2003), a regulator of chromatin structure. In addition, symplekin, which is implicated in the regulation of polyadenylation (Takagaki and Manley, 2000), demonstrates dual localisation within the nucleus and at the tight junction (Keon et al., 1996). Furthermore, transcription factors AP1 (activator protein-1) and Myc have been shown to interact with ZO-2 (Betanzos et al., 2004; Huerta et al., 2007). By interacting with Myc, ZO-2 mediates the down regulation of cyclinD1 (Huerta et al.,

2007). Overexpression of ZO-2 down regulates AP1 activity in reporter assays indicating a role for tight junction proteins in the regulation of this signalling pathway. For the purposes of this thesis, I will now discuss AP1 signalling and its regulation in the cell.

AP1 signalling

The AP1 transcription factor is composed of hetero- or homo-dimers of Jun and Fos family proteins. Activation of mitogen-activated protein kinase (MAPK) signalling by growth factors, stress signals and cytokines results in activation of AP1 transcription factors and changes in gene expression (Karin et al., 2001). AP1 transcription factors recognise and bind the DNA consensus sequence TGAGTCA found in the promoters of numerous genes involved in cell proliferation, survival, cell differentiation, migration and cell death (Shaulian and Karin, 2002), and their activity can be regulated transcriptionally and post-translationally by components of the MAPK pathway (Minden et al., 1994; Tanos et al., 2005).

The mitogen-activated protein kinase pathway

The MAPKs are serine/threonine-specific protein kinases that regulate cellular events in response to various extracellular signals. There are three main groups of MAPKs; extracellular signal-related kinases (ERKs), cJun N-terminal kinase (JNK) and p38 MAPKs. The MAPKs are activated in response to activation of an intracellular phospho-relay in which a specific stimulus activates a MAPK kinase kinase (MAPKKK) at the top of the pathway followed by the sequential activation of a

MAPK kinase (MAPKK) and then the MAPK. MAPKs regulate many cellular activities by regulating transcription factor activity affecting the expression of genes involved in proliferation and cell cycle progression, migration and apoptosis, and cell differentiation. In addition to nuclear substrates, MAPKs can also phosphorylate target proteins in the cytoplasm, such as the phosphorylation of paxillin by JNK during cell migration (Rosse et al., 2009).

A number of studies have reported a role for MAPK signalling in regulating the paracellular permeability properties of the tight junction. For example, in endothelial cells, oxidative stress induced by addition of H_2O_2 disrupts the tight junction barrier by activating ERK (Kevil et al., 2000). In epithelial cells, H_2O_2-induced barrier disruption is reduced following concomitant addition of EGF and this protection is mediated by an interaction between ERK and the C-terminus of occludin (Basuroy et al., 2006). In addition, JNK activation in response to osmotic stress mediates tight junction disruption induced by osmotic stress, which is reduced following JNK inhibition (Samak et al., 2010). These results suggest a role for the MAPK pathway in the regulation of paracellular permeability properties of the tight junction and places the tight junction downstream of MAPK activation. An upstream role for tight junctions in regulating and mediating the nuclear output of MAPK signalling, however, has not yet been shown.

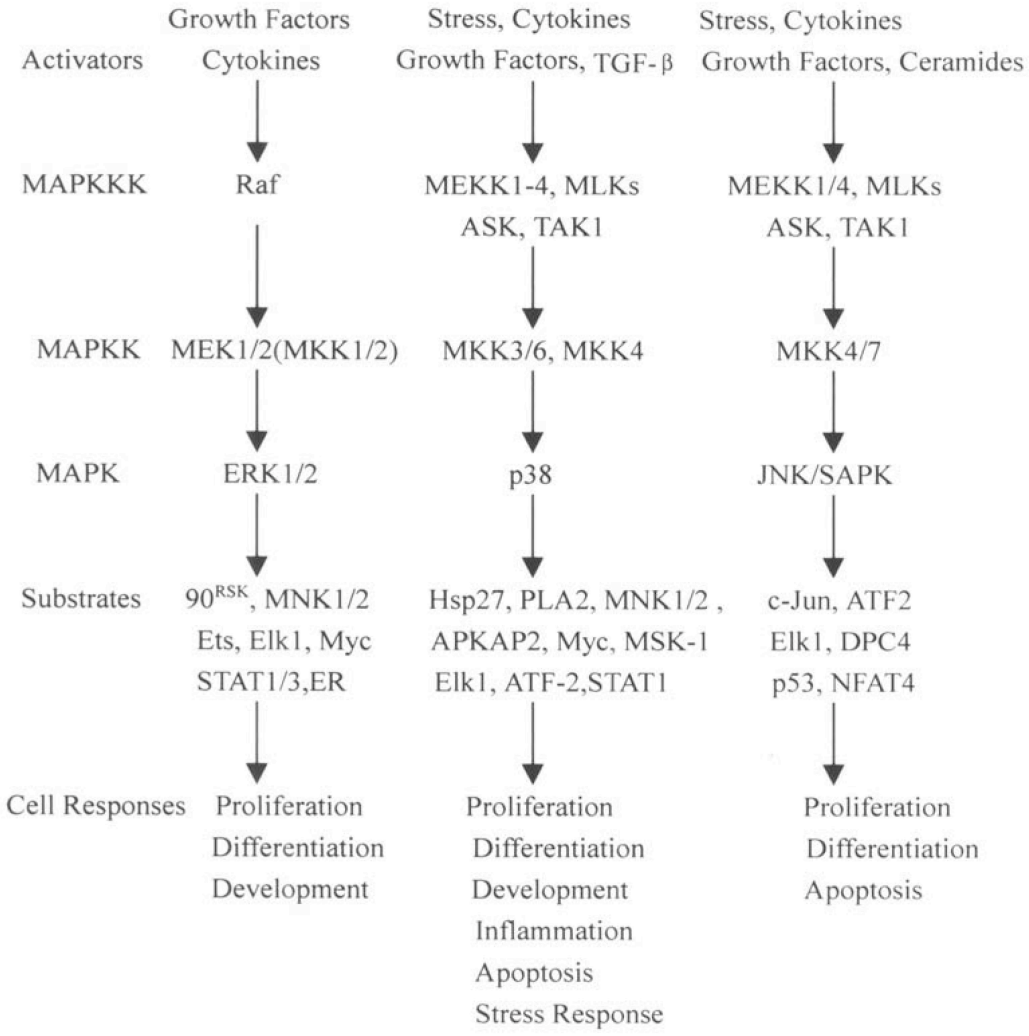

Figure 1.6 – Representation of the major MAP kinase signalling cascades found in mammalian cells. Care should be taken to remember that MAPK signalling involves a degree of cross-talk between the branches of the pathway shown above. Taken from (Zhang and Liu, 2002).

As figure 1.5 shows, MAPK signalling is activated in response to a diverse range of stimuli. By relaying, amplifying and integrating information from extracellular signals, the MAPK cascade enables an appropriate cellular response to be initiated. The regulation of proliferation by the MAPK pathway involves signalling by growth factors, which interact with and activate their receptors on the plasma membrane.

Binding of epidermal growth factor (EGF), for example, induces dimerisation and enzymatic activation of the EGF receptor (EGFR). Subsequent autophosphorylation of the cytoplasmic domain generates multiple docking sites for an array of signalling molecules. In response to EGF, this leads to activation of the small GTPase Ras followed by activation of the MAPKKK Raf and then the activation of ERK via MAPKK MEK. EGF can also lead to the activation of JNK and p38 MAPK branches of the MAPK pathway resulting in phosphorylation of Jun family transcription factors and AP1 signalling.

MAPK activation may also occur via ligand-independent mechanisms in response to various cellular stresses. Activation of JNK in response to UV light and osmotic shock is thought to involve the same receptors mediating activation in response to ligands. Alterations in receptor conformation caused by changes to the plasma membrane is thought to trigger receptor clustering and internalisation as would normally occur in response to ligand-binding, thus activating the same downstream pathways (Rosette and Karin, 1996). Interestingly, JNK activation is both pro-survival and pro-apoptotic depending on activator, cell type or duration of its active state. Prolonged activation of JNK in response to UV light exposure mediates cell death (Liu and Lin, 2005).

Regulation of gene expression

By translocating to the nucleus, activated MAPKs regulate the activity of a number of transcription factor targets leading to changes in gene expression. MAPK-mediated phosphorylation of ternary complex factor (TCF) Elk-1 enables its interaction with serum response factor (SRF). In complex with SRF, Elk-1, and other TCFs, promote

the expression of immediate early genes like *c-fos* (Buchwalter et al., 2004) (Figure 1.6). Expression of *c-fos* and its binding partner *c-jun* results in the formation of AP1 transcription factor dimers and facilitates the expression of AP1 responsive genes involved in differentiation, proliferation and apoptosis. MAPKs can further enhance or impair AP1 transcription factor activity by phosphorylation, which regulates their DNA-binding activity (Minden et al., 1994; Tanos et al., 2005). Genes containing AP1 sites within their promoters include EGFR, cyclinD1 and matrix metalloproteinases (MMPs), enabling MAPK signalling to regulate cell proliferation and migration through its regulation of AP1 signalling.

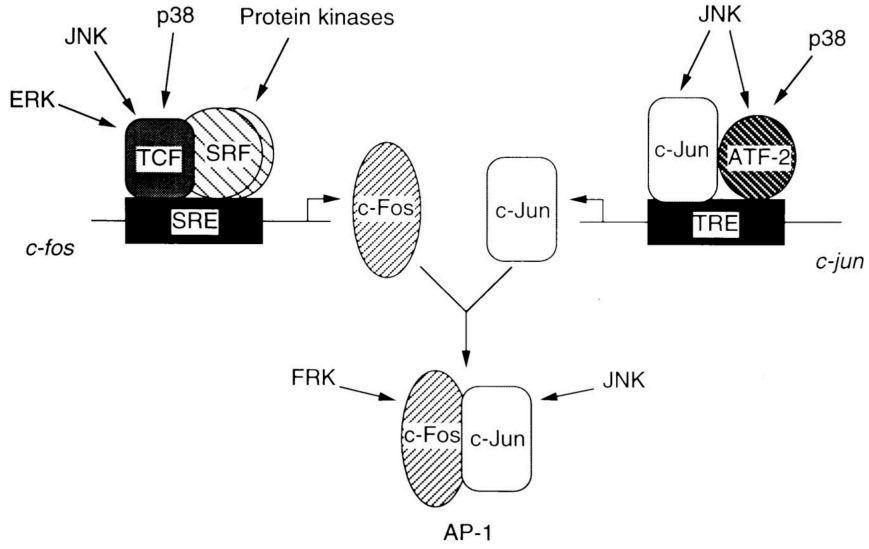

Figure 1.7 – Regulation of the AP1 transcription factor by the MAPK signalling pathway. ERK, JNK and p38 activate Elk-1 by phosphorylation. Binding of Elk-1, or other TCFs, to SRF results in binding to the serum response element (SRE) in the *c-fos* promoter and increased *c-fos* expression. Expression of *c-jun* is regulated by JNK and p38 MAPK signalling as shown. Increased levels of cFos and cJun results in increased AP-1 transcription factors, being composed of hetero- or homo-dimers of the jun and fos family proteins, and increased expression of genes with AP1 responsive elements in their promoters. The image in this figure was taken from (Whitmarsh and Davis, 1996).

Introduction to the current study

As the literature describes, tight junctions perform an array of functions in the cell, which are each attributable to the protein complement from which they are composed. Association of integral membrane proteins to the claudin-based strands and their interactions with cytosolic proteins beneath enables tight junctions to mediate paracellular permeability, cell polarity and intracellular signalling pathways, all of which are integral to the functioning of the epithelial monolayer as a whole. In order to understand how tight junctions perform these functions a comprehensive understanding of their constituents is required. In 2002, a novel transmembrane domain called the Marvel domain (MAL and related proteins for vesicle trafficking and membrane link) was identified and found to be present in tight junction proteins occludin and (though it had yet to be described) tricellulin (Sanchez-Pulido et al., 2002). Intriguingly, this study also highlighted two additional occludin-like proteins that were otherwise unknown. These sequences correspond to two isoforms of a protein called MarvelD3 (Sanchez-Pulido et al., 2002). Given the apparent importance of this domain at sites of membrane apposition and its presence in two known tight junction proteins, the aim of this thesis was to identify and characterise MarvelD3 and determine its relevance to the biology of the tight junction.

Identification of the Marvel domain

The Marvel domain is a novel domain with a four transmembrane-helix architecture first identified in proteins of the myelin and lymphocyte (MAL), physins, gyrins and occludin families, shown to be evolutionarily conserved between species (Sanchez-

Pulido et al., 2002). All currently described Marvel domain-containing proteins demonstrate an M-shaped topology, with four transmembrane helices weaving through the membrane between cytoplasmic N- and C-terminal regions. While putative functions for the Marvel domain have been proposed, its prevalence and significance within the cell is not yet fully understood. Interestingly, overexpression of occludin, MAL and synaptophysin results in the formation of intracellular vesicles, just as occurs following the overexpression of caveolin, a protein considered necessary for the organisation of membrane microdomains during caveolae formation (Razani and Lisanti, 2001; Smart et al., 1999). Though caveolin does not possess a Marvel domain itself, these similar phenotypes prompted the hypothesis that the Marvel domain may also be involved in organisation of cholesterol-rich membrane domains (Sanchez-Pulido et al., 2002). Indeed, during synaptic vesicle biogenesis, interaction between Marvel domain-containing synaptophysin and cholesterol has been implicated in facilitating the correct isolation of vesicular from plasma membrane constituents, as well as in the induction of vesicular curvature (Thiele et al., 2000). Though no direct interaction has been established, occludin and MAL family proteins have also been identified in membrane regions with high cholesterol content (Millan et al., 1997; Nusrat et al., 2000), supporting the notion that Marvel domains could perhaps function in the organisation of membrane domains during apposition events, such as those that occur during vesicular fusion, and at the tight junction.

The Marvel domain and the tight junction

Given the implication in events where membrane apposition occurs and its presence in two recognized tight junction proteins occludin and tricellulin, it seems clear that the Marvel domain may play a significant role in the physiology of tight junctions. Interestingly, tricellulin has been shown to redistribute along the bicellular tight junctions in cells depleted of occludin (Ikenouchi et al., 2008). This suggests that tricellulin may be able to compensate for some functions of occludin in occludin knockdown cells, and perhaps alludes to the importance of the presence of a Marvel domain at the tight junction. Indeed studies conducted during this thesis and by other labs have suggested that Marvel domain-containing proteins of the tight junction perform parallel, but not redundant, functions.

Aims

In consideration of reports in the literature implicating Marvel domain-containing proteins in membrane apposition events and the fact that two known tight junction proteins, occludin and tricellulin, contain a Marvel domain, MarvelD3 is thought to be a particularly interesting and appropriate candidate as a novel constituent of the tight junction. In light of this the aims of the current study were;

1. To initially characterise the Marvel domain-containing protein MarvelD3 by determining the extent of its expression in epithelial and endothelial cells and tissues, its localisation within the cell and, specifically to see if it localises within the epithelial junctional complex.

2. To validate MarvelD3 as a functional and significant component of epithelial cell tight junctions through analyses of junction formation and maintenance when MarvelD3 is stably over-expressed and suppressed via siRNA-mediated knockdown.

3. To investigate the role of MarvelD3 in the regulation of intracellular signalling pathways, which are becoming ever more associated with tight junctions and may provide additional insight in to how tight junction proteins can impact upon intracellular signalling involved in pathological conditions, like tumour progression.

Chapter 2:

Materials and Methods

2. Materials and Methods

All chemicals are from Sigma unless otherwise stated.

2.1 Cell Culture

The following cell types were cultured (Table 2.1): Caco-2, colon adenocarcinoma cells; HCE, immortalised corneal epithelial cells; MDCK, Madin-Darby canine kidney cells; PNT-1a and PNT2-C2, immortalised prostate epithelial cells; HepG2, hepatocellular carcinoma cells; HaCaT, spontaneously immortalised skin keratinocytes; MiaPaCa, human pancreatic tumour cells; ARPE-19, spontaneously immortalised retinal pigment epithelial cells; hCMEC/D3, immortalised brain endothelial cells; HCEC-B4G12, immortalised corneal endothelial cells. Caco-2, HCE, MDCK, HaCaT, MiaPaCa and HepG2 cells were grown in DMEM (Invitrogen, Paisley, UK) with 10% (HCE, MDCK, HaCaT, MiaPaca, HepG2) or 20% (Caco-2) foetal bovine serum (Invitrogen). PNT-1a and PNT2-C2 were cultured in RPMI 1640 (Invitrogen) supplemented with glutamine and 10% foetal bovine serum, ARPE-19 cells in a 1:1 mixture of DMEM and Nutrient Mixture F12 containing 10% foetal bovine serum and L-glutamine, hCMEC/D3 in EGM-2 medium (Cambrex BioScience, Wokingham, UK), and HCEC-B4G12 in human Endothelial-SFM containing 10 ng/ml FGF-2 (Invitrogen). MarvelD3-expressing MiaPaca cell lines (C2, C8 and P2) were cultured in DMEM with 10% foetal bovine serum and 30mg/ml G418 (PAA laboratories GmbH, Pasching, Austria). All cell lines were grown in the presence of penicillin (100U/ml) and streptomycin (100μg/ml; Invitrogen) at 37°C in a 5% CO_2 atmosphere.

Cell line	Tissue origin	Species	Metastatic phenotype
ARPE-19	retina	human	non-metastatic
Caco-2	gastrointestinal tract	human	non-metastatic
Caco-2 TC7	gastrointestinal tract	human	non-metastatic
HaCaT	skin	human	non-metastatic
HCE	cornea	human	non-metastatic
HCEC-B4G12	cornea (endothelial)	human	non-metastatic
hCMEC/D3	brain capillary (endothelial)	human	non-metastatic
HepG2	liver	human	metastatic
HUVEC	umbilical vein (endothelial)	human	non-metastatic
LnCaP	prostate	human	metastatic
MB231	breast	human	metastic
MCF10A	breast	human	non-metastatic
MCF7	breast	human	non-metastatic
MDCK	kidney	canine	non-metastatic
MiaPaCa	pancreas	human	metastatic
Muller cells	retina	human	non-metastatic
P4E6	prostate	human	non-metastatic
PC3	prostate	human	metastatic
PNT-1a	prostate	human	non-metastatic
PNT2-C2	prostate	human	non-metastatic
Schmac	prostate	human	metastatic

Table 2.1 – Details of cell lines used in the current study. The species and tissue of origin as well as the metastatic phenotype for all the cell lines used in the current study are shown. Those cells cultured were kept as described above. Cell lysates and cDNA from LnCaP, MB231, MCF10A, MCF7, Muller cells, P4E6, PC3 and Schmac cells were kindly provided by Professor Karl Matter, UCL Institute of Ophthalmology. HUVEC cDNA was kindly provided by Jay Stone, UCL Institute of Ophthalmology.

2.1.1 Cell storage

For long-term storage, cells at approximately 80% confluency were trypsinised completely in 1X Trypsin-EDTA (PAA laboratories GmbH) at 37°C. Fully trypsinised cells were resuspended in 6ml DMEM with 10% foetal bovine serum and centrifuged at 1000 rpm for 5 minutes at room temperature. The supernatant was removed and cell pellet gently resuspended in 3ml DMEM or RPMI 1640, each supplemented with 30% foetal bovine serum and 10% DMSO. Cell suspension was

separated into 1ml aliquots in cryovials and frozen at -80°C overnight. Samples were transferred to -150°C or liquid nitrogen for long-term storage.

2.2 Transfection Methods

2.2.1 Lipofectamine 2000

Plasmids were transfected into Caco-2 and MDCK cells using Lipofectamine 2000 reagent (Invitrogen). Cells were plated in DMEM containing 10% foetal bovine serum without antibiotics, 24 hours prior to transfection. For transfection, cDNA (Tube 1) and Lipofectamine 2000 (Tube 2) were diluted into OptiMEM, as shown in table 2.2, and incubated at room temperature for 5 minutes. Tubes 1 and 2 were combined and incubated at room temperature for a further 20 minutes. Finally, DNA-Lipofectamine complexes were added to each well containing DMEM with 10% foetal bovine serum without antibiotics in the final volumes shown (Table 2.2). Transfection medium was changed after overnight incubation at 37°C. Expression was analysed 48 hours after transfection.

	Tube 1		Tube 2		
Plate	DNA (μg)	OptiMEM (μl)	Lipofectamine 2000 (μl)	OptiMEM (μl)	DMEM w/out P/S (μl)
48-well	0.3	25	2	23	250
24-well	0.6	50	4	46	500

Table 2.2 – Lipofectamine transfection quantities. See text for details. Transfection was performed in DMEM without penicillin/streptomycin antibiotics (w/out P/S).

2.2.2 JetPEI

Plasmids were transfected into MiaPaCa cells using JetPEI reagent (Polyplus Transfection Inc., Illkirch, France). Cells were plated in DMEM containing 10% foetal bovine serum and antibiotics (complete medium), 16 hours before transfection. For transfection, cDNA (tube 1) and JetPEI (tube 2) were diluted into 150mM NaCl, as shown in table 2.3, and vortexed gently. The contents of tube 2 were then added to tube 1, vortexed gently, briefly spun and then incubated at room temperature for 30 minutes. The transfection mix was then added to each well containing complete medium in the final volumes shown (Table 2.3). Transfection medium was changed after 24 hours incubation at 37°C.

	Tube 1		Tube 2		
Plate	DNA (μg)	150mM NaCl (μl)	JetPEI (μl)	150mM NaCl (μl)	complete medium (μl)
48-well	0.5	25	1	24	250
24-well	1	50	2	48	500

Table 2.3 – JetPEI transfection quantities. See text for details.

2.2.3 Ca^{2+}-phosphate precipitation

Cells were plated in DMEM containing 10% foetal bovine serum with antibiotics, 24 hours prior to transfection. Plasmids were combined in an appropriate volume of 2X HEPES buffer (0.5M HEPES pH7.1, 3M NaCl, 1M $NaPO_4$ pH7.1). This was then shaken vigourously as an equal volume of 0.25M $CaCl_2$ was added drop-wise to the centre of the tube. The solution was left to precipitate for 30 minutes at room temperature. Medium was aspirated from cells and the precipitate added and

incubated for 20 minutes at 37°C. Finally, warm complete medium was added and the cells incubated overnight at 37°C. Transfection medium was replaced with fresh complete medium and cells returned to 37°C. For MDCK cells, a glycerol shock was performed after overnight incubation. MDCK cells were incubated with 12.5% glycerol (prepared in complete medium) for 2 minutes at room temperature, washed carefully with 1X PBS before adding back complete medium and returning to 37°C.

2.2.4 Interferin

For knockdown studies, Caco-2 and HCE cells were transfected with individual or a pool of siRNAs (MD3p-siRNA) specific for MarvelD3 (5' to 3' direction): siRNA13, GCGCAGGTGAACACGGAGT; siRNA14, GAGAGGAGGTGGAATATTA; siRNA15, CCGGAGAGAGACCAGGAGA; siRNA16, GCCGCAGACCCGAAAGTGA. All four target sequences are found in the N-terminus common to both isoforms of MarvelD3 (Thermo Scientific Dharmacon, Lafayette, CO). Used were On-Target plus siRNAs along with control On-Target plus siRNAs from the same provider. For transfections, Interferin transfection reagent (Polyplus Transfection Inc) was used according to the manufacturer's instructions. Briefly, cells were plated 16 hours prior to transfection. Interferin reagent was vortexed for 1 second and left to stand at room temperature for 10 minutes. Interferin was added to OptiMEM (Invitrogen) containing siRNA in the volumes detailed below (Table 2.4), pipetted up and down once to mix, and incubated at room temperature for 10 minutes. Complete medium was added to the Interferin-siRNA-OptiMEM mix, inverted 3 times and added to the cells. Transfection medium was changed after 24 hours and expression was analysed between two and four days after transfection.

Efficient knockdown of MarvelD3 was achieved with a final total siRNA concentration of 100nM. Other siRNAs were used in the volumes shown in Table 2.4.

Plate	20μM siRNA (μl)	OptiMEM (μl)	Interferin (μl)	complete medium (μl)
96-well	0.25	25	0.5	100
48-well	0.5	50	1	200
24-well	1	100	2	400

Table 2.4 – Interferin transfection quantities. See text for details.

2.3 Generation of stable cell lines

2.3.1 Generation of MiaPaCa expressing MarvelD3_1:VSV

VSV-tagged MarvelD3_1 was previously cloned into eukaryotic expression vector pCIN4 (kindly provided by Professor Karl Matter). MiaPaCa cells were plated at 50% confluence in complete medium with 2.5% horse serum (Invitrogen) the day before transfection. pCIN4-MD3_1:VSV (20μg) was transfected by Ca^{2+}-phosphate precipitation. After overnight incubation, the transfection medium was removed and cells incubated in 2ml complete medium for 8hours at 37°C. Medium was aspirated into a 15ml centrifuge tube. Cells were washed in 3ml PBS, which was added to the tube. Cells were fully trypsinised in 2ml Trypsin-EDTA, resuspended in 5ml complete medium and added to the 15ml tube. Cells were then centrifuged at 1000 rpm for 5 min and the supernatant discarded. The cell pellet was resuspended in 25ml complete medium with 2.5% horse serum and 0.6mg/ml G418, to select against

untransfected cells, and plated onto a 15 cm plate. Cells were incubated at 37°C for 17 days. After 17 days, 12 clones were picked by trypsinising until cell-cell contacts were lost, but cells remained adherent to the 15cm plate. Trypsin-EDTA was then aspirated completely and clones were picked using a 200µl pipette tip. Clones were plated onto a 24-well plate in complete medium with 2.5% horse serum and 0.6mg/ml G418. Remaining colonies were resuspended in 10ml complete medium with 2.5% horse serum and plated onto a 6-well plate to create a pool. Untransfected cells in the pool were selected against with 0.6mg/ml G418 or 3mg/ml G418. Clones and pools were then observed until 80%-90% confluent. Transfection efficiency was determined by immunoblotting and immunofluorescence. Expression of MD3_1:VSV was established in two independent clones (C2 and C8).

2.4 DNA Methods

2.4.1 cDNA

cDNAs coding for full length and truncated, tagged and untagged MarvelD3 isoforms were generated by PCR from reverse transcribed Caco-2 total RNA and from an EST clone obtained form Geneservice Source BioScience plc. The PCR reaction mix was composed of 5µl 10X buffer with $MgCl_2$, 8µl dNTPs (each 1.25mM), 1µl forward primer, 1µl reverse primer, 0.5µg template DNA, 5µl DMSO, 0.5µl Taq polymerase and brought to a final volume of 50µl with distilled water. The PCR was performed in a Thermocycler (Biometra GmbH, Germany) under the following conditions: 95°C for 2 minutes, a 2 hour 30 minute annealing-elongation cycle (30 seconds at 94°C – 30 seconds at 60-65°C – 1 minute at 72°C) and then incubated at 72°C for 10

minutes. Suitable annealing temperatures were determined for each pair of primers. Primers were designed to generate cDNAs containing the restriction sites necessary for cloning into a suitable expression vector, as shown in table 2.5. The resulting cDNA constructs were verified by sequencing.

Construct	Primers	Vector	Restriction sites
GST-fusion proteins			
GST:MD3_NTD	*forward:* AAAAAGGATCCATGGAAGATCCGTCGGGGGC *reverse:* AAAAAGAATTCTCTCCCAGTGCACAAGTATTTG	pGEX-4T-3	BamHI EcoRI
GST:MD3_CTD1	*forward:* AAAAAGGATCCGAACAGAAGCGCTACAAAGG *reverse:* AAAAAGAATTCTCAAAGAGTTCCAGACCACAG	pGEX-4T-3	BamHI EcoRI
GST:MD3_CTD2	*forward:* AAAAAGGATCCAAAGTTAGGAAGCTAAAAGAGAA *reverse:* AAAAAGAATTCTTAAAATTCAAACATTTCTGCTGG	pGEX-4T-3	BamHI EcoRI
VSV- and HA-tagged fusion proteins			
MD3_1:VSV	*reverse:* AAAAATCTAGATTACTTTCCAAGACGATTCATTTC GATGTCGGTGTAGCTAGCTCAAAGAGTTCCAGACCACAG	pcDNA4-TOmychisB	*NheI* XbaI
MD3_2:VSV	*forward:* AAAAACTTAAGATGGAAGATCCGTCGGGGGC *reverse:* AAAAAGCTAGCTTAAAATTCAAACATTTCTGCTGG	pcDNA4-TOmychisB	*NheI* XbaI
HA:MD3_1	GCAACGACAACAGCACCGCCGGCGCTAGCATGGAAGATCC GTCGGGGGC *reverse:* AAAAATCTAGATCAAAGAGTTCCAGACCACAG	pcDNA4-TOmychisB	HindIII *NheI* XbaI
HA:MD3_2	GCAACGACAACAGCACCGCCGGCGCTAGCATGGAAGATCC GTCGGGGGC *reverse:* AAAAATCTAGATTAAAATTCAAACATTTCTGCTGG	pcDNA4-TOmychisB	HindIII *NheI* XbaI
HA:ΔN-MD3_1	*forward:* AAAAAGCTAGCAAATACTTGTGCACTGGGAGAG *reverse:* AAAAATCTAGATCAAAGAGTTCCAGACCACAG	pcDNA4-TOmychisB	HindIII *NheI* XbaI
HA:ΔN-MD3_2*	*forward:* AAAAAGCTAGCAAATACTTGTGCACTGGGAGAG *reverse:* AAAAATCTAGATTAAAATTCAAACATTTCTGCTGG	pcDNA4-TOmychisB	HindIII *NheI* XbaI
ΔC-MD3_1:VSV	*forward:* AAAAACTTAAGATGGAAGATCCGTCGGGGGC *reverse:* AAAAAGCTAGCTCGGTAGCTACGCAGGGC	pcDNA4-TOmychisB	AflII *NheI* XbaI
ΔC-MD3_2:VSV*	*forward:* AAAAACTTAAGATGGAAGATCCGTCGGGGGC *reverse:* AAAAAGCTAGCTCGGTAGCCCTTTATGGCCA	pcDNA4-TOmychisB	AflII *NheI* XbaI
MD3_N:VSV	*forward:* AAAAACTTAAGATGGAAGATCCGTCGGGGGC *reverse:* AAAAAGCTAGCTCTCCCAGTGCACAAGTATTTG	pcDNA4-TOmychisB	AflII *NheI* XbaI
Full length, untagged constructs			
MD3_1	*forward:* AAAAACTTAAGATGGAAGATCCGTCGGGGGC *reverse:* AAAAATCTAGATCAAAGAGTTCCAGACCACAG	pcDNA4-TOmychisB	AflII XbaI
MD3_2	*forward:* AAAAACTTAAGATGGAAGATCCGTCGGGGGC *reverse:* AAAAATCTAGATTAAAATTCAAACATTTCTGCTGG	pcDNA4-TOmychisB	AflII XbaI
Constructs for use in *Xenopus laevis*			
pCS2-MD3_1*	cloned into pCS2+ from pcDNA4-TOmychisB-MD3_1	pCS2+	AflII XbaI
pCS2-MD3_2	cloned into pCS2+ from pcDNA4-TOmychisB-MD3_2	pCS2+	AflII XbaI
clone 7299735	predicted *xenopus* MarvelD3 sequence for *in situ* hybridisation probes	pBluescript SK-	-

Table 2.5 – Primers used to clone MarvelD3 constructs. The forward and reverse primers used to generate cDNA of each construct, and the restriction sites used to clone constructs into each vector, are shown. Internal restriction sites in VSV- and HA-tagged constructs are shown in italics. Constructs marked with an * were designed but have not yet been made.

2.4.2 Purification of PCR products with silica beads

PCR products were purified from a 1% low-melting agarose gel (AGTC Bioproducts, Hessle, UK) in 1X Tris-Acetate-EDTA (TAE) buffer (National Diagnostics, Atlanta, GA). Samples were run out at 50mV until they could be clearly resolved against the 1kb ladder. Bands were carefully cut from the gel, and melted in 1ml 6M NaI for 10 minutes at 70°C. Silica beads (40µl) were added to the melted agarose, inverted and incubated at room temperature for 10 minutes, inverting again after 5 minutes to mix. Samples were centrifuged at 2000 rpm for 1 minute, the supernatant removed and resuspended in 1ml wash buffer (50nM NaCl, 10mM TrisHCl pH7.5, 2.5mM EDTA, 50% v/v ethanol) and centrifuged again. This wash step was then repeated. After removing as much wash buffer as possible, beads were resuspended in 30µl water and incubated at 70°C for 10 minutes to elute the DNA. A 5µl sample of the eluate was run on a 1% agarose gel (Bioline Ltd, London, UK) to check for recovery.

2.4.3 Restriction digests

In order to clone the PCR products into the necessary expression vectors, both the PCR product insert and target vector were digested with the appropriate combination of restriction enzymes (Table 2.4). Restriction digests were set up on ice and contained 3µg vector DNA or 15µl PCR product, 3µl 10X buffer, 1µl enzyme 1, 1µl enzyme 2 and distilled water to give a final volume of 30µl, and then incubated at 37°C for 2 hours. All enzymes and buffers were supplied by New England Biolabs (NEB). Appropriate buffers for double digests were found by consulting the NEB Enzyme finder online (http://www.neb.com/nebecomm/enzymefinder.asp). To prevent self-ligation, 2µl Antarctic phosphatase (NEB) and 2µl Antarctic phosphatase

buffer (NEB) were added to the digested vector and incubated at 37°C for a further 30 minutes. This reaction was stopped by adding 2µl 0.5M EDTA and incubating at 70°C for 10 minutes.

2.4.4 Agarose ligations

The digested vectors and PCR product inserts were run out on a 1% low-melting agarose gel at 50mV for 1-2 hours. PCR product bands were carefully cut from the gel and purified with silica beads as described above (2.4.2). The linearised vector bands were cut from the gel and melted at 70°C for 10 minutes. Vectors and inserts were combined in appropriate ratios in a 10µl volume, and the ligation mix (containing 2µl 10X ligation buffer, 7µl distilled water and 1µl T4 DNA ligase (Roche Diagnostics, Mannheim, Germany)) was added. Ligations were incubated at room temperature for 2 hours and then left at 4°C overnight before being transformed into competent DH5α cells.

2.4.5 Preparation of competent cells

A single colony of the desired strain was inoculated into 5ml LB and incubated overnight at 37°C. The overnight culture was then diluted 1:100 in LB and incubated at 25°C until OD_{600}=0.4-0.5. Cells were then placed on ice, centrifuged at 4000 rpm for 10 minutes at 4°C and gently resuspended in 200ml ice-cold TB buffer (10mM Pipes-KOH, pH6.7, 15mM $CaCl_2$, 0.25M KCl, 55mM $MnCl_2$). Cells were centrifuged again and resuspended in 40ml ice-cold TB. DMSO (3ml) was added and

incubated on ice for 10 minutes before aliquoting cells and snap-freezing in liquid nitrogen. Efficiency was tested with the standard transformation protocol.

2.4.6 Transformation of competent cells

Competent DH5α (for preparation of cDNAs) and BL21 pLysS (for induction of GST-fusion proteins) were transformed according to the same standard protocol. First, cells were thawed slowly on ice. Once thawed, 1.4M β-mercaptoethanol was added, and incubated on ice for 10 minutes. Cells (100µl) were then incubated with the DNA to be transformed (1µl plasmid DNA, or 10µl for ligations) for a further 30 minutes. Samples were heat-shocked at 42°C for 45 seconds, returned to the ice for 3 minutes, before adding 1ml LB and incubating at 37°C for 1 hour. Samples were then plated as appropriate (100µl for cells transformed with plasmid DNA, while cells transformed with ligations were spun down, resuspended in 100µl and plated in full) onto LB agarose plates supplemented with 100µg/ml ampicillin or 50µg/ml kanamycin, as necessary. Plates for BL21 pLysS cells were further supplemented with 34µg/ml chloramphenicol to prevent protein expression. Plates were incubated at 37°C overnight to allow colony formation.

2.4.7 Preparation of plasmid DNA

To prepare plasmid DNA for transfection, colonies were picked from overnight plates and inoculated one colony per 5ml (for mini-prep) or 200ml (for midi-prep) LB containing the appropriate antibiotic. cDNAs were then prepared using a QIAGEN mini- or midi-prep kit according to the manufacturers instructions (QIAGEN, Hilden,

Germany). Presence of insert was determined by restriction digest and confirmed by sequencing (MWG Biotech). Concentrations were determined using a spectrophotometer (Eppendorf Biophotometer) and preparations were stored at -20°C until use.

2.4.8 Agarose gel electrophoresis

DNA gel electrophoresis was used to separate DNA samples according to size to assess the presence of inserts and prior to purification and agarose ligation. Gels were made from 1% agarose (Bioline, London, UK) in 1X Tris-Borate-EDTA (TBE) buffer (National Diagnostics) (for confirmation purposes), or 1% low-melting agarose in 1X TAE buffer (for purification and agarose ligations), containing 1:20000 SafeView nucleic acid stain for detection purposes (NBS Biologicals Ltd, Cambridgeshire). Gels were run at 100mV for 1-2 hours surrounded in 1X TBE or TAE buffer, as made. 1% low-melting agarose gels were run at 50mV for 1-2 hours. Gels were viewed in UV box (Syngene BioImaging system) or under UV lamp with wavelength 302nm (Upland, CA).

2.5 RNA Methods

2.5.1 RNA extraction and reverse transcription PCR (RT-PCR)

To assess the expression pattern of MarvelD3 in various cell and tissue types, total RNA was isolated from tissues and cultured cells using an miRNeasy Mini Kit (QIAGEN) according to the manufacturers instructions. Reverse transcription was performed at 45°C using AMV reverse transcriptase (Promega Corp, Madison, WI)

for 1 hour. A sample of HUVEC cDNA generated from total RNA was kindly provided by Jay Stone (UCL Institute of Ophthalmology, London, UK). The cDNAs were then amplified by PCR using FastStart Taq polymerase (Roche Diagnostics GmbH., Mannheim, Germany) at an annealing temperature of 63°C. The following primers were used (5' to 3' direction): human MarvelD3 AAAAATCTAGATCAAAGAG TTCCAGACCACAG and AAAAATCTAGATTAAAATTCAAACATTTCTGCTGG for reverse transcription, and AAAAAGCTAGCAAATACTTGTGCACTGGGAGAG, AAAAAGCTAGCTC GGTAGCTACGCAGGGC, AAAAAGCTAGCTCGGTAGCCCTTTATGGCCA for PCR amplification; mouse MarvelD3 CACAAATGCAGATACTTGTGCACAGG, CTAAAACTCAAGCATTTCTGTGGGC, TTAGAGCGTCCCGGACCACAGGTA ; GAPDH (human and mouse) ATCACTGCCACCCAGAAGAC and ATGAGGTCCACCACCCTGTT.

2.5.2 RNA extraction and microarray analysis

Wild-type and MarvelD3-expressing MiaPaCa clones C2 and P2 were plated into 6-well plates ($1.5x10^5$ cells/well) and grown at 37°C for 4 days, recreating the conditions under which the proliferation phenotype was first observed. Importantly, prior to RNA isolation, cells were not trypsinised thus avoiding any affects this may have on gene expression. Rather, medium was removed, cells quickly washed once in 1X PBS and QIAzol lysis reagent added to give a final volume of 700µl for each sample. RNA was then isolated according to the manufacturers instructions using an miRNeasy Mini Kit (QIAGEN). RNA from MarvelD3-expressing clones was combined. RNA from wild-type and MarvelD3-expressing MiaPaCa cells was

labelled using an Affymetrix WT labelling assay to create cDNA probes which were then hybridised to Human Affymetrix Gene 1.0 ST Arrays (Tony Brooks, UCL Institute of Child Health). Data was analysed using GeneSpring GX 11.0.1 software (Agilent Technologies, Santa Clara, CA) and the online bioinformatics resource DAVID (Huang da et al., 2009).

2.6 Protein Methods

2.6.1 Generation and purification of anti-MarvelD3 peptide antibody

To analyse MarvelD3 expression an antibody against a peptide of the N-terminal cytoplasmic domain (CAPDRGPRRDTHRDAG) was generated. To purify, the same peptide was coupled to epoxy-activated sepharose beads by incubating 2mg peptide with 2g swollen sepharose in a total volume of 50ml coupling buffer (0.1M sodium bicarbonate (pH11)), overnight on an end-over-end shaker at 4°C. Excess groups were then blocked with 1M ethanolamine, pH11, incubated overnight on an end-over-end shaker at 4°C. Peptide-conjugated beads were washed 3 times through a cycle of 50ml coupling buffer, 50ml distilled water, 50ml 0.1M acetate with 0.5M NaCl, pH4 and 50ml PBS, before being resuspended in PBS containing 0.1% NaN_3. The antibody-containing serum was diluted 1:5 with 10mM Tris (pH7.5), containing 150mM NaCl, 40μg/ml PMSF and 0.1% NaN_3, and centrifuged at 10,000 rpm for 15 minutes at 4°C. The supernatant was then added to the peptide-conjugated beads and incubated overnight on an end-over-end shaker at 4°C. To elute the antibody, samples were spun at 3000 rpm for 10 minutes and the beads resuspended in the 10mM Tris (pH7.5) described above. Resuspended beads were poured onto a Pierce column and washed with the Tris solution until the OD_{280} of the eluate was <0.01. To

elute the antibody, 15ml tubes containing 750µl 1M Tris (pH8) were prepared. The antibody was eluted into these tubes in 7ml aliquots first with 100mM glycine (pH2.8) and then with 100mM triethanolamine (pH11.5). Protein concentration was determined by measuring OD_{280} and the peak fractions were combined for each elution buffer. Pools were pH6-8.5. The antibody was then dialysed twice overnight against 1X PBS at 4°C. This antibody was used in results chapter 3.

2.6.2 Generation and purification of antibody against the entire N-terminus and two isoform-specific C-termini of MarvelD3

To improve detection of MarvelD3, an antibody was raised against the whole N-terminus (amino acids 1-198) and, since the sequence of the N-terminus is common to both MarvelD3 isoforms, against isoform-specific sequences at the C-termini (amino acids 384-411 isoform 1; amino acids 387-402 isoform 2). GST-fusion proteins were generated and injected into rabbits. Antibodies were purified by conjugating GST-fusion proteins of the relevant domain of MarvelD3 to hydrated CNBr-activated sepharose on an end-over-end shaker overnight, at 4°C. Antibody serum (10ml) was brought to a final volume of 50ml with 10mM Tris-HCl, pH7.5 containing 150mM NaCl, 40mg/ml PMSF and 0.1% NaN_3, and then centrifuges at 10,000 rpm for 15 minutes. Supernatant was added to the washed beads and incubated on an end-over-end shaker overnight, at 4°C. Beads were then centrifuged at 3000 rpm for 10 minutes, resuspended in 10mM Tris-HCl, pH7.5, 150mM NaCl and loaded onto a Pierce column with reservoir. The column was washed with 10mM Tris-HCl, pH7.5, 150mM NaCl until the OD_{280} of the eluate was below 0.01. Antibody was then eluted with 100mM Glycine, pH2.8, concentration was determined by measuring OD_{280}.

Peak fractions were combined and dialysed twice overnight against 1X PBS at 4°C. The antibody specific for the N-terminus of MarvelD3 purified in this way was used in results chapters 4 and 5.

2.6.3 Production of GST-fusion proteins

GST-fusion proteins were produced by transforming plasmids into competent BL21 pLysS cells as described above (Section 2.4.6). After overnight incubation at 37°C, colonies were picked, inoculated into 50ml LB containing ampicillin and chloramphenicol and grown overnight at 37°C on a shaker. Protein production was induced by adding 200ml LB, containing 100mg/ml ampicillin and 1mM Isopropyl β-D-1-thiogalactopyranoside (IPTG), to the overnight cultures and incubating at 25°C for 2 hours on a shaker. Cells were centrifuged at 4000 rpm for 15 minutes at 4°C and resuspended in 10ml PBS containing 0.5% Triton X-100 (PBSTx), a cocktail of protease and phosphatase inhibitors (50μg/ml bezamidine, 10μg/ml aprotinin, 10μg/ml leupeptin, 10μg/ml pepstatin A, 1mM PMSF) and 1mM DTT. Samples were sonicated, centrifuged at 10,000rpm at 4°C for 10 minutes and the supernatant stored at -80°C until use. Recovery of fusion protein was determined by adding a 300μl sample to 40μl 40% glutathione bead suspension and incubating for 1 hour on an end-over-end shaker at 4°C. Beads were washed 3 times with 1ml 0.5% PBSTx and once with 1X PBS before being resuspended in 30μl SDS sample buffer (see below, Section 2.6.5) and incubated at 70°C for 5 minutes. Presence of the fusion protein was assessed by sodium dodecyl sulfate polyacrylamide gel electrophoresis (SDS-PAGE). After running samples on a 12% gel, the gel was stained with coomassie blue (for 500ml; 1.25g coomassie blue, 450ml 1:1 methanol:H_2O, 50ml acetic acid)

for 30 minutes and then destained over night with destaining solution (20% methanol, 7.5% acetic acid) at room temperature with gentle agitation. GST-fusion proteins with an expected molecular weight could be identified with reference to the molecular weight marker.

2.6.4 Purification of GST-fusion proteins

For antibody production, GST-fusion proteins were purified from bacterial lysates. Lysates were thawed on ice and brought to 30ml with 0.5% PBSTx containing 1mM DTT and fresh protease and phosphatase inhibitors. Samples were centrifuged at 10000 rpm for 10 minutes at 4°C. The supernatant was incubated with 3ml 40% glutathione bead suspension for 2 hours on an end-over-end shaker at 4°C. Beads were then loaded on to Pierce columns (Thermo Scientific, Rockford, IL) and washed with 0.5% PBSTx until the OD_{280} of the eluate was <0.01. GST-fusion protein was eluted with 25mM reduced glutathione prepared in 1M Tris (pH8) and the concentration determined by measuring OD_{280}.

2.6.5 Sodium dodecyl sulfate polyacrylamide gel electrophoresis (SDS-PAGE)

Polyacrylamide gels were prepared using a MightySmall II gel electrophoresis system (Hoefer, Holliston, MA) and contained polyacrylamide, 0.1% ammonium persulphate, 0.1% SDS and TEMED. Stacking gels were prepared at 5% with Tris-HCl, pH6.8. Resolving gels were prepared at 12%, 10% or 8%, as necessary, with Tris-HCl, pH8.8. Whole cell lysates were collected by adding SDS sample buffer (3% SDS, 15% glycerol, 0.0015% bromophenol blue, 0.25M Tris HCl containing 150mM DTT

and 6M Urea) to samples pre-washed once in 1X PBS. The samples were incubated for 30 minutes at room temperature and then homogenised through a 25G needle before analysis by SDS-PAGE. Samples were transferred to nitrocellulose membrane (LI-COR Biosciences, Lincoln, NE) for western blotting at 100V, restricted to 450mA for 120-150 minutes depending on protein size. Transfer buffer contained 20% methanol and 1X SDS-Tris-Glycerol (National diagnostics, Atlanta, GA).

2.6.6 Immunoblotting

Nitrocellulose membranes were stained with 0.1% amido black for 30 seconds followed by agitated destaining in 20% methanol, 7.5% acetic acid for 15 minutes at room temperature. Nitrocellulose membranes were blocked in 5% milk prepared in TBST (1M Tris-HCl pH7.4, 3M NaCl, 0.5% Tween) and containing 0.1% NaN_3, for 30 minutes. Primary antibodies were incubated overnight in 5% milk-TBST with 0.1% NaN_3 at room temperature (see table 2.6 for primary antibody information). Secondary antibodies were incubated for 2 hours in TBST at room temperature without 0.1% NaN_3. MarvelD3 protein levels were detected with a horseradish peroxidase-conjugated donkey anti-rabbit antibody (1:5000) and enhanced chemiluminescence detection system (ECL; Amersham, Corp. Arlington Heights, IL). All other protein levels were detected using an Odyssey detector and IRDye-680- and IRDye-800CW-conjugated donkey anti-rabbit, donkey anti-mouse and donkey anti-goat secondary antibodies (LI-COR Biosciences; 1:5000).

2.6.7 Methanol Fixation

Cells grown on glass coverslips or filters (Fisher Scientific, Loughborough, UK), as specified, for at least 3 days were either fixed directly in methanol or first extracted on ice with 0.1% Triton X-100 in BB buffer (100mM KCl, 3mM $MgCl_2$, 1mM $CaCl_2$, 200mM sucrose, 1mM Hepes, pH7.1) for 1 minute and then fixed in methanol at -20°C for 10 minutes. Cells were rehydrated in PBS for 5 minutes and blocked for 15 minutes with 0.5% BSA in PBS (PBS-0.5%BSA).

2.6.8 Paraformaldehyde Fixation

Cells were grown on glass coverslips for at least 3 days prior to fixing. Cells were fixed in 4% PFA for 20 minutes at room temperature before being permeabilised in 0.1% Triton in PBS-0.5%BSA for 5 minutes at room temperature. Coverslips were washed twice in 1X PBS before blocking and quenching in PBS-0.5%BSA containing 20mM Glycine for 10 minutes at room temperature. Samples were kept in PBS-0.5%BSA until processed for immunofluorescence.

2.6.9 Immunofluorescence

Coverslips fixed in either methanol or PFA were incubated with primary antibodies (Table 2.6) for 2 hours at room temperature, washed three times with PBS-0.5%BSA and incubated with secondary antibody and Hoechst nuclear stain for 1 hour at room temperature. Filters were incubated in primary antibody overnight at room temperature in a moist atmosphere, washed three times with PBS-0.5%BSA and incubated in donkey Cy3- or FITC-, anti-rabbit, anti-rat or anti-mouse secondary

antibodies (1:300; Jackson Immunoresearch, West Grove, PA) with Hoechst (1:4000) for 1.5 hours at room temperature. Where necessary FITC- and Cy3-phalloidin (1:4000) were incubated with the secondary antibodies and nuclear stain. Coverslips and filters were then washed two times with PBS-0.5%BSA and once with PBS before being mounted onto glass microscope slides with ProLong Gold mounting medium (Invitrogen). Images were acquired using a Leica Image capture epifluorescent microscope and a Zeiss LSM510UV confocal microscope with 63x oil immersion lenses. Brightness and contrast were adjusted with Adobe Photoshop CS4 software.

2.6.10 Primary antibodies

Antibodies to detect MarvelD3 were generated as described above (2.6.1 and 2.6.2). Antibodies against all other proteins were previously described or were from commercial sources (Table 2.6).

Antibody	Source	Species	Dilution	
			IF	IB
α-tubulin	Kreis, T.E., 1987	Mouse	-	1:20
β-catenin	Sigma	Rabbit	-	1:1000
β-catenin	Santa Cruz	Goat	1:200	-
CDK6	Santa Cruz	Goat	-	1:500
claudin 1	Invitrogen	Rabbit	-	1:500
claudin 4	Invitrogen	Rabbit	-	1:500
cofilin	BD Biosciences	Mouse	-	1:1000
cyclinD1	Santa Cruz	Mouse	-	1:1000
E-cadherin	Sigma	Rat	1:400	-
E-cadherin	BD Biosciences	Mouse	-	1:1000
EGFR (ErbB1)	Santa Cruz	Rabbit	-	1:200
ERK	Cell Signalling	Rabbit	-	1:1000
ETS1	Santa Cruz	Mouse	-	1:2000
GEFH1	Benais-Pont et al., 2003	Mouse	-	1:10
GFP	Molecular Probes	Rabbit	-	1:2500
GST	Home-made	Rabbit	-	1:1000
HA	Daro et al., 1996	Mouse	1:10	-
ILK	Cell Signalling	Rabbit	-	1:1000
JNK	Cell Signalling	Rabbit	-	1:1000
MarvelD3	Steed et al., 2009	Rabbit	1:1000	1:4000
MarvelD3	Home-made	Rabbit	1:2000	1:4000
MD3_1	Home-made	Rabbit	-	1:2000 as shown
MD3_2	Home-made	Rabbit	-	1:5000 as shown
MEKK1	Santa Cruz	Rabbit	1:500	1:1000
MLC	Cell Signalling	Rabbit	-	1:1000
occludin	Invitrogen	Mouse	1:2000	1:2000
p120-catenin	BD Biosciences	Mouse	1:250	1:1000
p190RhoGAP	BD Biosciences	Mouse	1:250	1:1000
p38	Cell Signalling	Rabbit	-	1:1000
phospho-cJun	Cell Signalling	Rabbit	-	1:1000
phospho-cofilin	Cell Signalling	Rabbit	1:200	1:1000
phospho-ERK	Cell Signalling	Mouse	-	1:2000
phospho-JNK	Cell Signalling	Mouse	-	1:2000
phospho-MEKK1	E. Gallagher, Imperial College London	Rabbit	1:100	1:1000
phospho-MLC	Cell Signalling	Rabbit	1:200	1:1000
phospho-p38	Cell Signalling	Rabbit	-	1:1000
phospho-Smad3/1	Cell Signalling	Rabbit	-	1:1000
Smurf1	Santa Cruz	Rabbit	-	1:1000
Stat2	Transduction Labs	Mouse	-	1:1000
Stat3	Santa Cruz	Rabbit	-	1:1000
Tricellulin	ProteinTech Europe	Rabbit	-	1:1000
VSV	Kreis, T.E., 1987	Mouse	1:10	-
ZO-1	Benais-Pont et al., 2003	Rabbit	1:100	1:1000
ZO-2	Benais-Pont et al., 2003	Rabbit	-	1:2000
ZO-3	Benais-Pont et al., 2003	Rabbit	-	1:1000

Table 2.6 – Primary antibodies. Details of antibody, species of origin and dilutions used for immunofluorescence (IF) and immunoblotting (IB) are shown.

2.7 Experimental Assays

2.7.1 Ca^{2+}-switch, paracellular permeability and transepithelial resistance (TER) measurements

Caco-2 cells were transfected with control, pool or individual siRNAs against MarvelD3 in 6-well plates. The day after transfection, cells were trypsinised and plated at confluent density on Transwell filters (Corning Inc., Corning, NY) in quadruplicates, either in low calcium medium, for Ca^{2+} switch, or directly into DMEM++. After 24 hours, the medium was changed for fresh DMEM++ and cells were incubated at 37°C for 10 minutes before starting to measure TER. TER was recorded every 2 hours for the first 12 hours, then at 24, 36 and 48 hours by applying an AC square wave current of ± 20 μA at 12.5 Hz with a silver electrode and measuring the voltage deflection elicited with a silver/silver-chloride electrode using an EVOM (World Precision Instruments, Sarasota, FL), as previously described (Balda et al., 1996). To measure paracellular flux, 1 hour before the experiment, medium was replaced with 1000µl DMEM++ on the basolateral side and 250µl on the apical side and the cells returned to 37°C. Tracer solution containing 4kD FITC-dextran and 70kD Rhodamine-B-dextran was added to the apical side and incubated at 37°C for 4 hours (Matter and Balda, 2003a). 200µl samples were collected from the basolateral side and fluorescence was determined using a FLUOstar OPTIMA microplate reader (BMG LabTech, Offenburg, Germany). Fluorescence of the apical solutions was used to determine total values.

2.7.2 Proliferation assay

Wild-type and MarvelD3-expressing MiaPaCa cells were plated in triplicate onto 96-well plates at various cell densities and incubated at 37°C for 3 days. For knockdown experiments, Caco-2 cells were transfected with control, two individual siRNAs or a pool of siRNAs against MarvelD3 in 48-well plates and incubated at 37°C for 3 days. In both experiments, medium was removed after 3 days by inverting the plates onto paper towels and the samples immediately frozen at -80°C. Cell proliferation was determined the following day using a CyQUANT Cell Proliferation Assay Kit (Invitrogen). A 5X CyQUANT-GR solution, enabling a linear detection range extending to 250,000 cells, was prepared in nuclease-free distilled water containing 1X cell lysis buffer, and 200µl added to each well of the 96-well plate. Samples were gently pipetted up and down 3 times to mix and incubated for 5 minutes, protected from light. Fluorescence was determined using a microplate reader and converted into cell numbers against a reference standard curve for each cell type. In some experiments additional EGF (Peprotech) was prepared in water and added to complete medium at the concentrations described.

2.7.3 Flow cytometry

The effect of MarvelD3 on apoptosis was quantified by FACS analysis. First, $1.5x10^5$ cells were plated in a 6-well plate in complete medium and incubated at 37°C for 4 days. Cell culture medium was removed and collected in a 50ml tube. Cells were washed once in 1X PBS and the PBS added to the 50ml tube. Cells were then completely trypsinised with 1X Trypsin-EDTA. Trypsinisation was terminated with 2ml complete medium and cell suspensions transferred to the 50ml tube and

centrifuged at 1500 rpm for 5 minutes at room temperature. Medium was removed, cells gently resuspended in 2ml ice-cold 70% ethanol in PBS and incubated at 4°C for 30 minutes. Fixed cells were then pelleted at 1500 rpm for 5 minutes at 4°C and resuspended in 800µl PBS. A homogenous suspension was made by passing the cells through a 25G needle 10 times before adding 40µg/ml propidium iodide and 0.1mg/ml RNase and incubating at 37°C for 1 hour. Samples were then run through a FACSCalibur (Becton Dickinson) and analysed using CellQuest Pro.

2.7.4 Migration assay

To assess cell migration, MiaPaCa and Caco-2 cells were applied to both 0.22mm^2 chambers of a 9mm x 9mm x 5mm µ-Dish$^{35mm, high}$ culture-insert (Ibidi GmbH) in 70µl complete medium. The outer area of the dish was filled with 2ml complete medium to prevent drying out. Cells were plated in triplicate for each experiment. Cells were incubated at 37°C resulting in a confluent monolayer after 48 hours. For knockdown experiments, Caco-2 cells were transfected with control or two individual siRNAs against MarvelD3 in 24-well plates. Twenty-four hours after transfection, cells were trypsinised, added to the Ibidi culture inserts and incubated at 37°C until confluent (48 hours later). In all experiments, the culture insert was then gently removed generating a 500µm cell-free gap between monolayers, and the medium replaced with fresh complete medium containing mitomycin c to inhibit proliferation. When necessary, 20µM SP600125 or DMSO was added to the cells 3 hours before insert removal. Complete medium containing 20µM SP600125 or DMSO was then used for the duration of the experiment. Brightfield images were taken at regular time points (0, then every 2 hours up to 8 hours, and every 2 hours from 20 hours until the most

rapidly migrating cells showed approximately 80% wound closure) using an epifluorescent microscope to observe the migration of cells in to the cell-free space. ImageJ software was used to determine the area of cell-free space and subsequently enable % wound closure to be calculated at each time point (% wound closure = 100 – [(cell-free area at end-point)/(cell-free area at time 0)*100].

2.7.5 Reporter assay

Caco-2, MDCK and wild-type MiaPaCa cells were plated in triplicate or quadruplicate into 96-well plates in complete medium the day before transfection. After 24 hours, MDCK cells were transfected by Ca^{2+}-precipitation and Caco-2 and MiaPaCa cells were transfected with JetPEI reagent. In both cases, transfection mix was changed for fresh complete medium 24 hours after transfection. Luciferase luminescent signals were determined 24 hours later using a Dual luciferase reporter assay kit (Promega). Medium was removed from all cells and MDCK and Caco-2 cells were washed once with 1X PBS. MiaPaCa cells were not washed with PBS to prevent cell loss. Cells were lysed with 20µl lysis buffer (stock provided) and incubated at room temperature on a shaker for 20 minutes. Cell extract (12µl) was transferred to a white 96-well plate and the luciferase and renila luminescence signals measured sequentially using OPTIMAFluorostar microplate reader (BMG Labtech). Relative promoter activity was calculated by making a ratio between luciferase and renila luminescent signals, and then normalizing to the control.

2.7.6 Hyperosmotic shock

HCE and Caco-2 cells were plated into 24-well plate or on to glass coverslips and grown for 3 days at 37°C. For knockdown experiments, HCE cells were reverse transfected using Interferin reagent. Caco-2 cells were transfected 16 hours after plating, also with Interferin reagent. Three days after transfection, cells were incubated in the presence of hyperosmotic DMEM (containing 600mosM NaCl) or hypo-osmotic DMEM (containing 150mosM NaCl) for 15 minutes, 30 minutes, 1 hour or 2 hours. Cells incubated in isotonic DMEM (300mosM NaCl) were used as a control. After treatment, cells were fixed for immunofluorescence or harvested for analysis of protein levels by SDS-PAGE. Where necessary, cells were incubated with inhibitors, or diluent for controls, overnight prior to hyperosmotic shock (Table 2.7). Inhibitors/diluent were also present throughout the subsequent incubation with hyperosmotic medium.

Target	Inhibitor	Supplier	Diluent	Concentration
Src family kinases	PP1	BioMol EI-275	DMSO	10μM
Src family kinases	PP2	Calbiochem 529576	DMSO	10μM
Src family kinases	PP3	Calbiochem 529574	DMSO	10μM
p38	SB202190	Tocris 1264	DMSO	20μM
JNK	SP600125	Tocris 1496	DMSO	20μM
MEK	UO126	Tocris 1144	DMSO	20μM
EGFR tyrosine kinase	Gefitinib	Selleck Chemicals S1025	DMSO	10μM

Table 2.7 – Inhibitors used in hyperosmotic shock experiments. Final concentration refers to the concentration of the inhibitor present in the experiment. Controls were made by adding equal volume of the diluent to control cells.

2.7.7 Pulldowns

To identify potential interaction partners of MarvelD3 and the domains responsible, pulldown experiments were performed with GST-fusion proteins of the N-terminus and the isoform specific C-termini of MarvelD3. Caco-2 cells were grown on 15cm cell culture dishes at 37°C for 5 days. Pulldown beads were prepared by incubating purified GST-fusion proteins with 40µl glutathione beads on an end-over-end shaker, at 4°C for 2 hours. Beads were washed 3 times with 0.5% PBSTx and once with 1X PBS. Cell lysates were prepared quickly, on ice, in 0.1% PBSTx. Non-specific binding was reduced by incubating lysates with negative glutathione beads. Cell lysates were incubated with fusion protein-conjugated beads for 1.5 hours at 4°C. 0.1% PBSTx-harvested samples were either washed with 0.1% PBSTx followed by 1X PBS, or twice with 1X PBS. GB buffer-harvested samples were washed twice with 1X PBS. After the final wash, 50µl sample buffer was added to the beads and boiled at 70°C for 5 minutes before separating on by SDS-PAGE.

2.7.8 GTPase activation assay (G-LISA™)

To assess the effect of MarvelD3 on RhoA GTPase activity, control and MarvelD3-expressing MiaPaCa cells were in triplicate on 12-well plates and left to grow until 70% confluent. A G-LISA was performed to assess the relative levels of active RhoA in each sample according to the manufacturers protocol (Cytoskeleton). Briefly, samples were washed on ice with cold 1X PBS and lysed. The protein concentration of each sample was determined and equalised by addition of lysis buffer. Cell lysate was then added to wells of a 96-well plate containing a Rho-GTP-binding protein and incubated at 4°C for 30 minutes with gentle agitation. Samples were washed twice

with wash buffer to remove inactive, unbound RhoA. Bound RhoA was detected with an anti-RhoA primary antibody (1:250) and HRP-conjugated secondary antibody (1:62.5; both provided). Adding HRP detection reagent and measuring absorbance at 490nm determined the degree of RhoA activity. Subtracting background absorbance from all absorbance values and then normalising mean absorbance values to the control calculated relative RhoA activity.

2.7.9 Impedance analysis

Impedance was measured in response to hyperosmotic shock using Electric Cell-Substrate Impedence Sensing (ECIS) Model 1600R (Applied BioPhysics). Control and MD3p-siRNA transfected Caco-2 cells were plated in to ECIS electrode array containing 10 electrodes per well (8W10E; Applied BioPhysics). Array plates were prepared by addition of 200µl 10mM cysteine for 10 minutes and then washed three times with 1X PBS. Cells were plated in quadruplicate and grown at 37°C for 48 hours until confluent. Basal impedance across the monolayer was measure at 37°C for 1 hour. Complete medium was then replaced with DMEM containing 600mosM NaCl and measurements of impedance was taken at 2 minute intervals for a further 9 hours. Impedance values for each group (control or MD3p-siRNA) were normalised to readings taken before exposure to hyperosmotic shock.

2.7.10 Statistics

All statistical analyses were performed using Microsoft Excel. Statistical significance was calculated with a two-tailed Student's t-test.

2.8 *Xenopus laevis* Methods

2.8.1 Egg collection and fertilisation

Xenopus were injected with 500 units human chorionic gonadotropin (HCG) 5 days after injection with 50 units pregnant mare serum gonadotropin (PMSG). After 24 hours, *Xenopus* were placed in 1X egg laying solution (ELS; pH7.6). For fertilization, freshly laid eggs were collected using a Pasteur pipette and placed in a 7cm dish. ELS was removed and eggs were washed 3 times in 1X Modified Barth's solution (MBS), removing as much MBS as possible following the final wash. Eggs were fertilized by direct application of isolated testes extract prepared in 1X MBS. After 5 minutes, 0.1X MBS was added to facilitate sperm entry. Fertilised eggs were placed at 14°C to develop. Embryos were staged according to Niewkoop and Faber (1994). All embryo manipulations were in accordance with the UK Home Office regulations and guidelines.

2.8.2 De-jellying

The jelly coat was removed 1 hour after fertilization by addition of 2% cysteine solution, pH7.6-7.8, for 5 minutes at 14°C. Embryos were then washed 3 times in 0.1X MBS to remove all traces of cysteine and allowed to develop at 14°C in 0.1X MBS until required.

2.8.3 RNA extraction from embryos and RT-PCR

To determine the expression pattern of MarvelD3 during *Xenopus* development, total RNA was extracted from whole embryos at representative stages of development and subjected to semi-quantitative RT-PCR analysis. Embryos from the same fertilization were collected (20 embryos per developmental stage), snap-frozen in dry-ice and stored at -80°C until RNA extraction. Immediately before RNA extraction, embryos were thawed on ice and lysed in 1200µl RLT lysis buffer (provided in RNeasy kit detailed below) supplemented with 140mM β-mercaptoethanol. Embryos were homogenised mechanically by passing through a 23G needle 10 times, then centrifuged for 3 minutes at 13200rpm to clear the lysate. RNA extraction was then performed using an RNeasy mini-kit (QIAGEN) according to the manufacturers instructions. Reverse transcription was performed at 45°C using AMV reverse transcriptase (Promega) for 1 hour. The cDNAs were then amplified by PCR using FastStart Taq polymerase (Roche Diagnostics Gmb.) at an annealing temperature of 62°C (*Xenopus* MarvelD3; xMD3) and 58°C (*Xenopus* ornithine decarboxylase; xODC). Primers used for this study were as follows (5' to 3' direction): xMarvelD3 CGGAGCAGCAGATCAGGATCAG for reverse transcription and ACAAACCCCATAATAGAAATTTGCC and TTCAACATATTCCATATTCGAGCC for PCR amplification; ODC forward CAGCTAGCTGTGGTGTGG and reverse CAACATGGAAACTCACACC as previously described (Daniels et al., 2004).

2.8.4 *in vitro* transcription of mRNA

mRNA of the human MD3 isoform 2 was generated for microinjection, to both attempt to rescue the phenotype observed following morpholino injection, and to perform gain of function studies. Human MarvelD3 isoform 2 is most similar to the xenopus sequence. GFP and β-galactosidase mRNA for control injections and identification of injection sites, respectively, were synthesized in the same way. First, pCS2 vector containing the relevant cDNA was linearised by digestion with NotI restriction enzyme for 3 hours at 37°C. DNA was then purified from a 1% low-melting agarose gel. The *in vitro* transcription reaction was assembled at room temperature containing 1μg linearised DNA in a total volume of 20μl, using reagents from Ambion Message Machine kit (Ambion). The reaction was allowed to run for 2 hours at 37°C. Template DNA was removed by 15 minute incubation with TURBO DNase at 37°C and stopped by addition of ammonium acetate stop solution (Ambion). RNA was recovered by phenol/chloroform extraction and stored at -80°C until use.

2.8.5 Phenol/chloroform extraction of RNA

An equal volume of phenol/chloroform/isoamyl alcohol (25:24:1) was added to the *in vitro* transcription mix, vortexed and centrifuged at 13200 rpm for 2 minutes at 4°C. The aqueous phase was collected and 80μl RNase-free water added to the phenol/chloroform layer, vortexed and centrifuged again, and as much aqueous phase collected as possible. An equal volume of ice-cold isopropanol was then added, vortexed and left at -20°C overnight. RNA was pelleted by centrifugation at 13200

rpm for 30 minutes at 4°C and washed in 70% ethanol. Finally, RNA was resuspended in RNase-free water and stored at -80°C until use.

2.8.6 Microinjection

Morpholinos (MO) and mRNAs were injected into embryos at the 2-cell stage according to the same protocol. Borosilicate glass capilleries (1.2mm OD x 0.94mm ID; Harvard Apparatus, Kent, UK) were pulled into needles using a P-97 Flaming/Brown micropipette puller (Sutter Instrument Co., USA). Eggs were fertilised and de-jellied prior to injection. Embryos at the 2-cell stage were placed in injection dishes with 4% Ficoll solution (4% Ficoll with 50μg/ml Gentomicin in 0.2X MBS). Morpholinos and mRNAs were diluted to the necessary concentrations in RNase-free water and injected with 200pg β-galactosidase. A standard control morpholino was injected with 200pg β-galactosidase as a control in loss of function experiments. GFP mRNA was injected with 200pg β-galactosidase as a control in gain of function experiments. The xMD3 morpholino (AGACCCAAATCTTCCTTTTGTTCCC) and control morpholino were obtained from Gene Tools LLC (Philomath, OR). After injection embryos were placed at 14°C overnight. Ficoll solution was replaced with 0.1X MBS the following morning, and embryos returned to 14°C to monitor development.

2.8.7 Fixation

Embryos were fixed with MEMFA (3.7% formaldehyde (Fisher Scientific), 1X MEM; 0.1M MOPS, pH7.4, 2mM EGTA, 1mM $MgSO_4$) for 1 hour at room

temperature with gentle rocking. Embryos were then washed 3 times in 1X PBS and once with methanol. Fixed embryos were stored in methanol at -20°C.

2.8.8 β-galactosidase staining

Injection of β-gal mRNA alongside control and xMD3 morpholinos enabled us to identify successfully injected embryos by positive β-galactosidase staining. It also enabled us to identify the side of injection. Embryos were fixed in MEMFA for 1 hour at room temperature under gentle rotation. Embryos were washed 3 times in 1X PBS and pre-incubated in PBS containing 2mM $MgCl_2$ for 15 minutes at room temperature. β-galactosidase staining was then developed by placing embryos in X-Gal mixer solution (5.35mM $K_3Fe(CN)_6$, 5.35mM $K_4Fe(CN)_6.3H_2O$, 1.2mM $MgCl_2$, 0.01% sodium deoxycholate, 0.02% NP40 in 1X PBS) containing 1mg/ml X-Gal at 37°C for 30 minutes. Embryos were then washed twice in 1X PBS and stored in methanol at -20°C.

2.8.9 *In situ* hybridisation

To investigate the effect of MarvelD3 on neural crest cell migration, *in situ* hybridisation of whole embryos was performed on unilaterally xMD3-MO-injected embryos fixed at stages 20 and 23. Embryos were placed into baskets and the *in situ* hybridisation performed using a Biolane HTI automated incubation liquid handler (Holle and Huttner) at 22°C. Embryos were gradually rehydrated with 75% methanol for 10 minutes, and 50% and 25% methanol for 5 minutes each, before being washed 4 times in PBS containing 0.1% Tween-20 (PBST), for 5 minutes each. Embryos

were then incubated in 1.32μg/ml Proteinase K in PBST for 5 minutes. Incubation of embryos in 0.1M triethanolamine (TEA), pH7-8 and 0.1M TEA containing 0.5% acetic acid, for 5 and 10 minutes respectively was used to block reactive groups in the embryonic tissue by acetylation and therefore reduce background staining. Finally, embryos were refixed in 4% formaldehyde for 20 minutes and washed 6 times 5 minutes in PBST. Embryos were pre-hybridised at 60°C in hybridisation buffer (50% formamide, 5X (SSC), 1X Denhardts, 0.1% Tween-20, 0.1% CHAPS, 1mM EDTA, 1mg/ml torula RNA, 100μg/ml heparin) before being transferred to hybridisation buffer containing DIG-labelled RNA probes and incubated at 60°C overnight, with gentle rocking. Probes were previously synthesised and optimised in the Ohnuma lab and kindly donated for these experiments. Post-hybridisation, embryos were washed with 2X SSC pre-warmed to 65°C, incubated in 1μg/ml RNaseA in 2X SSC for 20 minutes at 37°C and washed in 0.2X SSC also pre-warmed to 65°C. Embryos were then washed in 1X MAB for 3 times 30 minutes before being blocked in 1X MAB containing 2% blocking solution (Roche) and 20% lamb serum (GIBCO) for 2 hours at 22°C. After blocking, embryos were incubated in the presence of anti-DIG AP Fab fragments (Roche) for 12 hours in 1X MAB containing 2% blocking solution and 20% lamb serum at 4°C. Embryos were then washed thoroughly in 1X MAB for 10 times 30 minutes before being transferred to glass vials. In glass vials, DIG probes were detected by adding BM Purple substrate in the presence of alkaline phosphatase (AP) buffer (0.1M Tris-HCL, pH9.5, 0.1M NaCl, 50mM $MgCl_2$, 0.1% Tween-20, supplemented with 2mM Levamisole). When the colour reaction was complete, embryos were washed in methanol for 30 minutes and fixed overnight in MEMFA at room temperature.

2.8.10 Depigmentation of embryos after *in situ* hybridisation

After development of *in situ* hybridisation probes, embryonic pigmentation was removed by bleaching to enable the staining pattern to be seen more clearly. Embryos were washed three times in PBST for 5 minutes each. They were then transferred to bleaching solution (5% Formamide, 1X SSC, 3% H_2O_2) and placed in a light box until bleached. Bleaching solution was then removed, embryos washed three times in PBST for 5 minutes each, and stored at room temperature in ME MFA.

2.8.11 Imaging

For imaging, embryos were handled in 1X PBS and photographed using a Leica M80 microscope and Leica DFC420C camera.

2.8.12 Preparation of samples for immunoblotting

Embryos were collected, snap-frozen in dry ice and stored at -80°C. Whole embryo lysates were prepared by adding lysis buffer (20mM Tris-HCl, pH8.0, 150mM NaCl, 2mM EDTA, 1% NP40 containing protease inhibitors) to embryos thawed on ice (10µl lysis buffer per embryo) and pipetting up and down to mix. Lysates were then centrifuged at 12000 rpm at 4°C for 5 minutes, and the clear middle layer removed and added to an equal volume of 3X sample buffer. Samples were then analysed by SDS-PAGE according to the standard protocol.

2.8.13 Additional solutions for *Xenopus laevis* experiments

For clarity, the recipes of some of the solutions used in *Xenopus laevis* experiments have not been included in the main body of text and are, instead, detailed below.

MBS: To prepare 4L of 10X MBS 205.2g NaCl, 3g KCl, 8g $NaHCO_3$, 95.2g Hepes, 8g $MgSO_4 \cdot 7H_2O$, 3.12g $Ca(NO_3)_2 \cdot 4H_2O$, 3.2g $CaCl_2 \cdot 6H_2O$ was dissolved in water. Adjusted to pH7.6 with NaOH. Solution was then autoclaved and stored at 4°C until use.

ELS: To prepare 4L of 8X ELS, 205.71g NaCl, 4.77g KCl, 2.72g $Na_2HPO_4 \cdot 2H_2O$, 5.815g Tris base, 5.38g $NaHCO_3$, 16.149 $MgSO_4 \cdot 7H_2O$ was dissolved in water. Adjusted to pH7.6 with glacial acetic acid. Stored at 4°C until use.

Denhardt's Solution: To prepare 100ml of 100X stock, 2g Ficoll 400, 2g polyvinylpyrrolidone, 2g BSA was dissolved in water and filter sterilised.

Chapter 3:

Identification of MarvelD3 at the Tight Junction

Chapter 3: Identification of MarvelD3 at the Tight Junction

Some results in this chapter have been published in reference (Steed et al., 2009)

Introduction

In their identification of the Marvel domain, Sanchez-Pulido and colleagues highlighted MarvelD3 as an as yet unknown Marvel domain-containing protein of the occludin family (Sanchez-Pulido et al., 2002). Since occludin and tricellulin are also MARVEL domain-containing proteins and both components of the tight junction, I wanted to determine whether MarvelD3 is also a component of the tight junction.

This chapter describes the identification of MarvelD3 at the tight junction using bioinformatics analysis and a range of cell and molecular biology techniques. Transepithelial resistance and paracellular permeability assays were also used to determine the role of MarvelD3 in the fundamental "barrier" properties of the tight junction.

These analyses showed that MarvelD3 is expressed in various epithelial and endothelial cells, and shows a broad tissue expression pattern. MarvelD3 colocalises with the tight junction protein occludin, apically to the adherens junction marker E-cadherin, suggesting a specific localisation to the tight junction within the apical junctional complex. Depletion of MarvelD3 does not affect the paracellular permeability properties of the tight junction, but does result in increased TER, suggesting MarvelD3 expression may have a role in regulating the ion conductance properties of the tight junction.

Results

Identification of two human isoforms of MarvelD3 by bioinformatic analysis

To begin these studies, a number of basic bioinformatic analyses were performed to gain further insight into the molecular properties of the MarvelD3 protein. Database searches were also conducted to see if and how it has been conserved through evolution.

Bioinformatics analysis revealed the existence of two human MarvelD3 isoforms: isoform 1 contains 410 amino acids [Genbank: NM_001017967] and isoform 2 401 amino acids [Genbank: NM_052858] (Figure 3.1). A membrane topology analysis with Phobius and TMpred confirmed that both isoforms are predicted to contain four transmembrane domains and to expose their N- and C-terminal domains to the cytosol (Figure 3.2). The two isoforms represent splice variants and share the predicted N-terminal cytoplasmic domain of 198 amino acids, but differ in their C-terminal halves that contain the transmembrane domains. Both MarvelD3 isoforms are predicted to possess only short C-terminal cytoplasmic domains (30aa isoform1; 18aa isoform 2) with no apparent similarities to the comparatively long C-terminal cytoplasmic domains of tricellulin and occludin that contain their ZO-1 binding sites (Riazuddin et al., 2006) (Fanning et al., 1998).

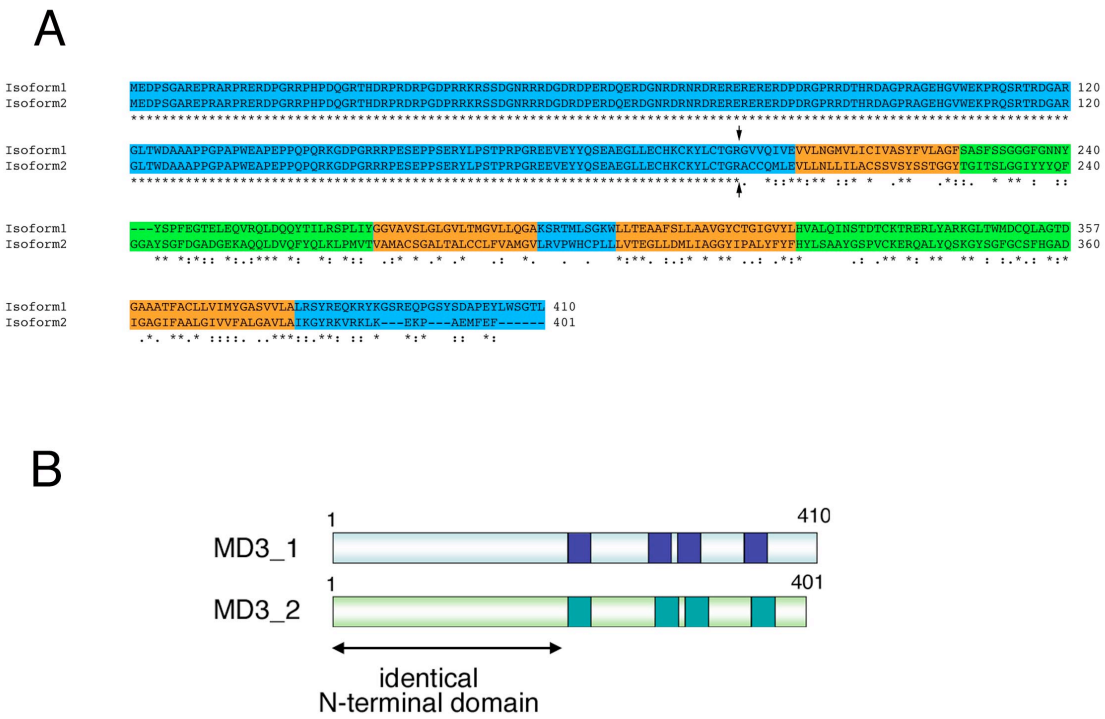

Figure 3.1 – Identification and alignment of the two human MarvelD3 isoforms (A) The cytosolic domains are highlighted in blue, the transmembrane domains in orange, and the extracellular domains in green. The splice junction between the N-terminal domain shared by both isoforms and the alternative domains is indicated by two arrows. (B) Representation of the two human isoforms of MarvelD3. The transmembrane (Marvel) domains are represented by dark blue (isoform 1; MD3_1) and dark green (isoform 2; MD3_2) shading. The presence of a common N-terminus is highlighted.

MarvelD3 isoform 1

A

Domain	Amino acids: Phobius prediction	Amino acids: TMpred prediction
Cytoplasmic	1-205	
Transmembrane	206-230	206-226
Non-cytoplasmic	231-265	
Transmembrane	266-287	266-286
Cytoplasmic	288-298	
Transmembrane	299-322	299-322
Non-cytoplasmic	323-357	
Transmembrane	358-379	360-379
Cytoplasmic	380-410	

B

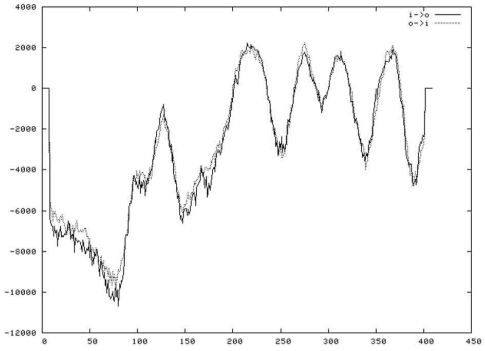

MarvelD3 isoform 2

C

Domain	Amino acids: Phobius prediction	Amino acids: TMpred prediction
Cytoplasmic		
Transmembrane		206-225
Non-cytoplasmic	1-266	
Transmembrane	267-289	274-293
Cytoplasmic	290-300	
Transmembrane	301-325	302-323
Non-cytoplasmic	326-360	
Transmembrane	361-382	361-380
Cytoplasmic	383-401	

D

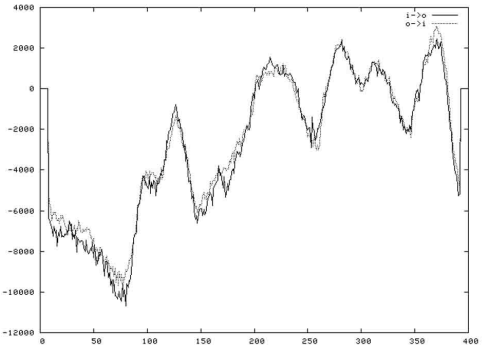

Figure 3.2 – Membrane topology analysis of human MarvelD3 isoforms 1 and 2. Amino acid sequences of each MarvelD3 isoform were entered into online membrane topology prediction programmes Phobius and TMpred. The predicted domains are summarised from each programme for each isoform (A, isoform 1; C, isoform 2). Hydrophobicity plots generated from the TMpred predictions are also shown (B, isoform 1; D, isoform 2).

Database searches revealed that MarvelD3 is expressed in chicken, *Xenopus* and various mammalian species, but not in any invertebrates, suggesting that it is expressed by vertebrates only (Figure 3.3 and Table 3.1). Alternatively spliced isoforms were only found in mammalian species. In contrast, the chicken genome contains two distinct MarvelD3 genes, variant A and B, which reside on different chromosomes. Variant A is more similar to mammalian isoform 2. Although variant

B is more similar to isoform 1 than 2, the two chicken proteins show a similar degree of conservation with mammalian isoform 1. It thus seems that mammalian isoform 2 and the variant A gene found in birds, fish and amphibians represent the MarvelD3 form common to all vertebrates.

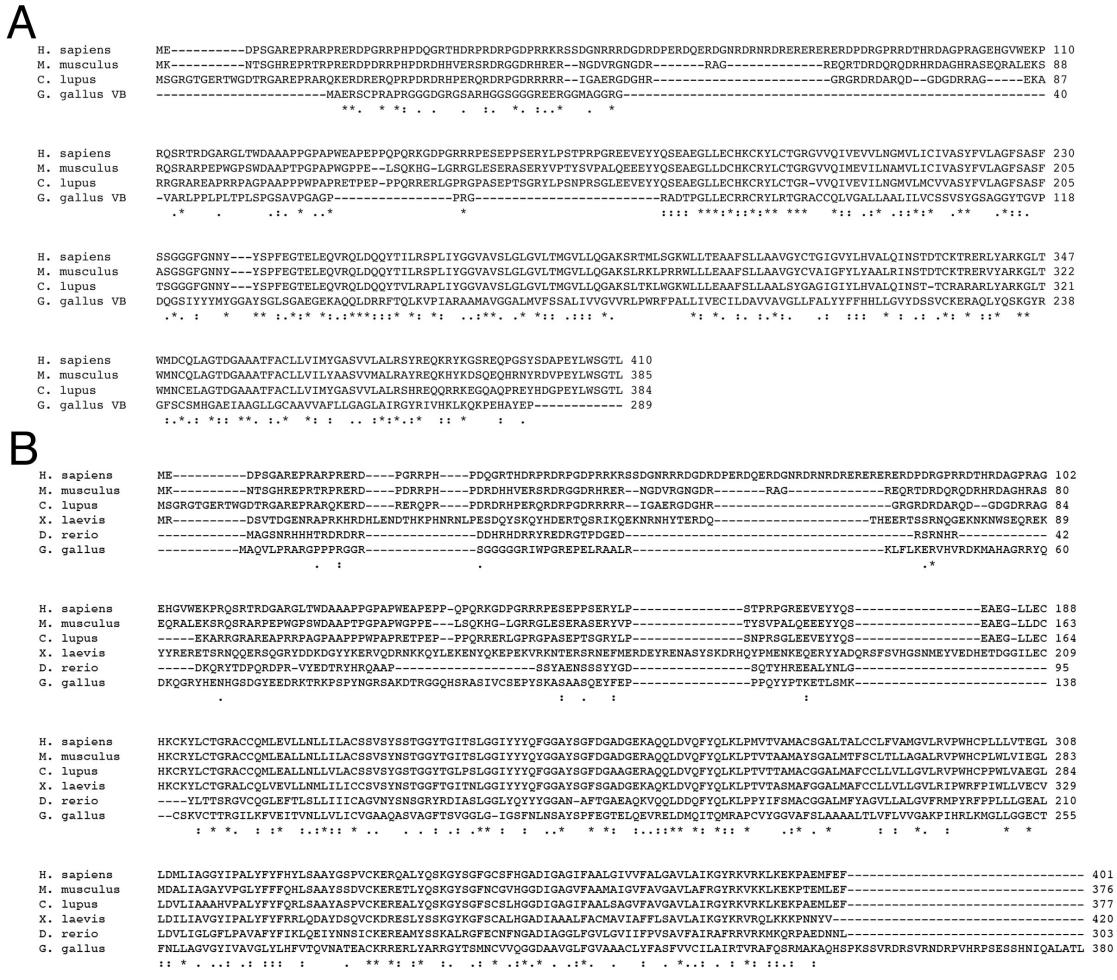

Figure 3.3 – Analysis of vertebrate MarvelD3 sequences. (A) Human, mouse and dog isoform 1 and chicken variant B; and (B) human, mouse and dog isoform 2 and chicken, *Xenopus laevis* and zebrafish variant A were aligned with ClustalW using default settings. The amino acid residues conserved in mammalian MarvelD3 sequences are highlighted in yellow. Conservation is labelled according to ClustalW definitions: identical residues (*); conserved substitutions (:); semi-conserved substitutions (.).

	H. sapiens isoform 1 NM_001017967	H. sapiens isoform 2 NM_052858	M. musculus isoform 1 NM_212447	M. musculus isoform 2 NM_028584	C. lupus familiaris Isoform 1 XM_848243	C. lupus familiaris Isoform 2 XM_546843	X. laevis Variant A BC_068841	G. gallus Variant A XM_418989	G. gallus Variant B XM_414239
H. sapiens isoform 1 NM_001017967	100								
H. sapiens isoform 2 NM_052858	63	100							
M. musculus isoform 1 NM_212447	72	40	100						
M. musculus isoform 2 NM_028584	43	68	61	100					
C. lupus familiaris Isoform 1 XM_848243	71	39	67	39	100				
C. lupus familiaris Isoform 2 XM_546843	40	69	38	68	61	100			
X. laevis Variant A BC_068841	25	43	24	42	23	44	100		
G. gallus Variant A XM_418989	30	51	28	48	28	50	44	100	
G. gallus Variant B XM_414239	30	24	30	21	28	22	23	24	100
D. rerio Variant A BC_055662	25	40	26	37	23	40	39	31	25

Table 3.1 – Alignment scores of MarvelD3 sequences from different vertebrates. MarvelD3 sequences were retrieved from Genbank and aligned using ClustalW (see Fig. 3.3 for a selection of the alignments). Indicated are all Genbank accession numbers. The scores reflect percent identity. For mammals, the two alternatively spliced isoforms were used. Two different MarvelD3 genes, variants A and B, exist in chicken. Only variant A was found in *X. laevis* and zebrafish.

Generation of antibodies against MarvelD3

To enable detection of MarvelD3 for analysis of protein expression, an antibody was generated against a peptide of the N-terminal cytoplasmic domain. Expression was analysed in two epithelial cell lines derived from different types of epithelia: Caco-2, a human colon adenocarcinoma cell line, and an immortalised human corneal epithelial cell line (HCE). Total cell extracts were generated from control cells as well as cells transfected with control siRNAs or a pool of four siRNAs targeting MarvelD3. All four targeted sequences are part of the common exon encoding the N-terminal cytoplasmic domain; hence, mRNAs encoding both isoforms should become degraded. Figure 3.4 shows that the antibody recognised a band of about 40 kD in both cell lines, as expected. The band became weaker with increasing concentrations of MarvelD3 siRNA, indicating that the band indeed corresponded to MarvelD3.

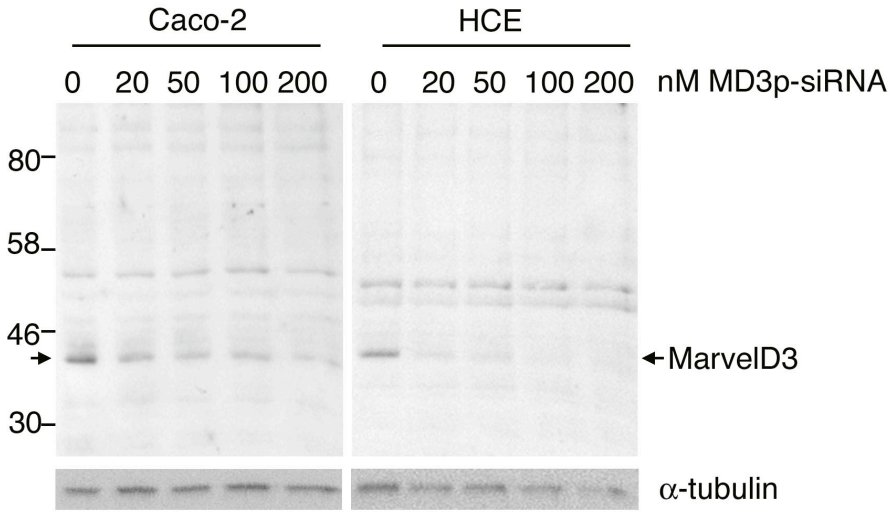

Figure 3.4 – Detection of endogenous MarvelD3 in a Caco-2 and HCE cells. Caco-2 and HCE cells were transfected with the indicated concentrations of siRNAs, using a pool of the four MarvelD3-directed siRNAs, or a control siRNA (lane 0). Three days after transfection, cell extracts were prepared and expression levels of MarvelD3 and α-tubulin were analysed by immunoblotting. Arrows indicate band corresponding to MarvelD3. An anti-α-tubulin antibody was used as loading control.

Deconvolution of the MarvelD3 siRNA pool revealed that siRNAs 14 and 16 were the most effective of the four sequences and were hence used individually, or together as a pool, for all subsequent analyses (Figure 3.5).

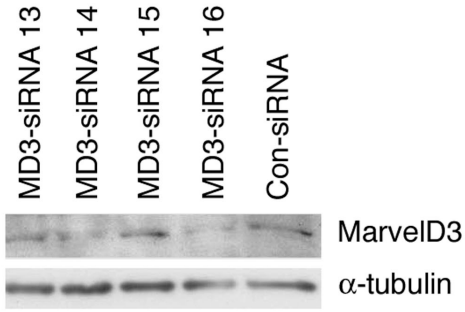

Figure 3.5 – Deconvolution of MarvelD3 siRNA pool. Caco-2 cells were transfected with 100nM control siRNA or each of the individual constituents of the MarvelD3-specific siRNA pool. Three days after transfection, cell extracts were prepared and analysed for effectiveness of MarvelD3 depletion by immunoblotting. An anti-α-tubulin antibody was used as loading control.

In an attempt to detect MarvelD3 in an isoform-specific manner antibodies were also raised against the complete C-terminal sequences of each isoform. Immunoblotting showed these antibodies were able to detect MarvelD3 when overexpressed in Caco-2 cells, but not the endogenous protein (Figure 3.6). Thus MarvelD3 protein was detected in a non-isoform-specific manner, using the antibody directed against the N-terminus, in all subsequent experiments in this thesis.

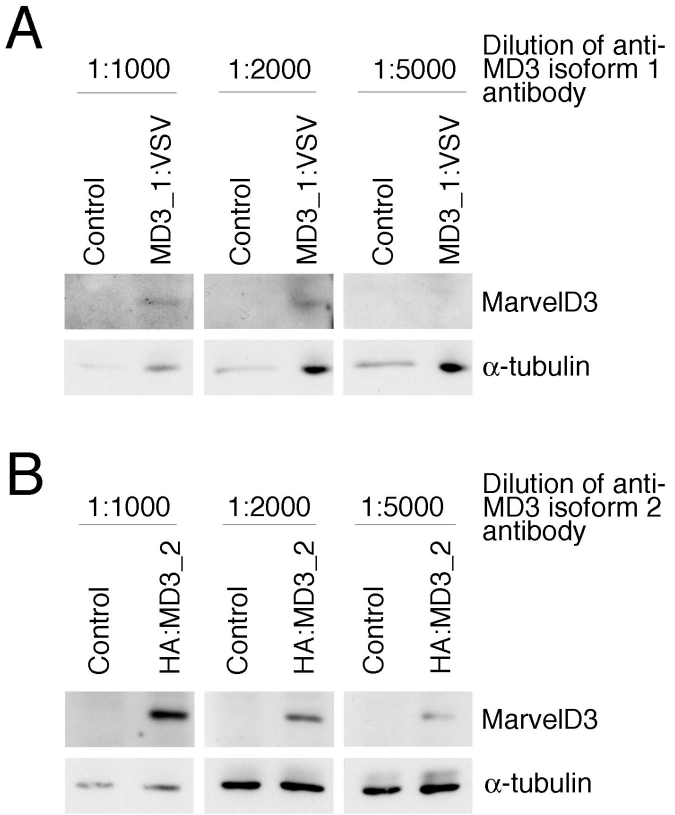

Figure 3.6 – Antibodies directed against the isoform-specific C-termini of MarvelD3 isoforms can only detect over-expressed MarvelD3 protein. Caco-2 cells were transfected with cDNAs encoding MarvelD3 isoform 1 (A) and isoform 2 (B). Three days after transfection, cell extracts were prepared and run on 10% SDS-PAGE gels. Immunoblotting was performed with antibodies against the C-terminus of MarvelD3 isoform 1 (A) and isoform 2 (B). Antibodies were able to detect the overexpressed protein, but not the endogenous protein, even after prolonged exposure. An anti-α-tubulin antibody was used as loading control.

Expression pattern of MarvelD3 isoforms

Since the MarvelD3 antibody was found to recognise both isoforms, reverse transcription PCR was used to determine the expression of MarvelD3 isoforms in different cultured epithelial and endothelial cell lines, as well as different tissues. Figure 3.7 shows that both isoforms are widely expressed by different epithelial and endothelial cells. Similarly, most tested adult mouse tissues expressed both isoforms (Figure 3.8). Both MarvelD3 isoforms are thus widely expressed and are found in different types of epithelial and endothelial cells. Nevertheless, apparent differences in isoform expression profiles were detected as, for example, both liver and the hepatocyte-derived cell line HepG2 only expressed isoform 1.

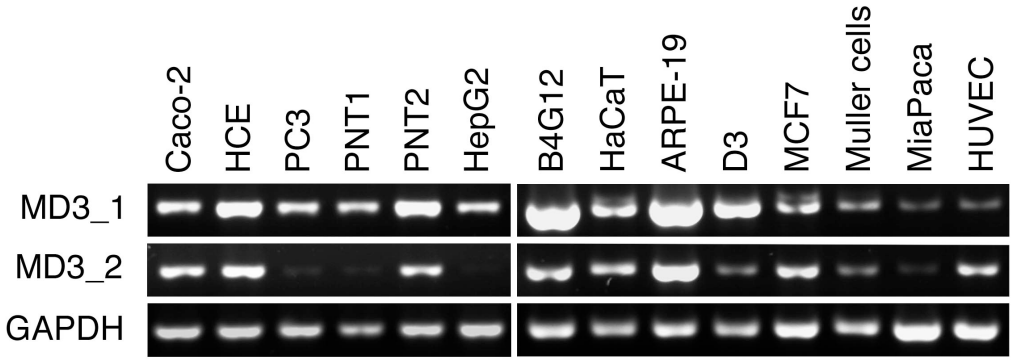

Figure 3.7 – Expression of MarvelD3 in epithelial and endothelial cells. Reverse transcription PCR was used to analyse the expression of MarvelD3 isoforms in cultured human epithelial and endothelial cells. HUVEC cDNA was kindly provided by Jay Stone, UCL Institute of Ophthalmology. Primers were used to specifically amplify human MarvelD3 isoforms or, as a control, GAPDH.

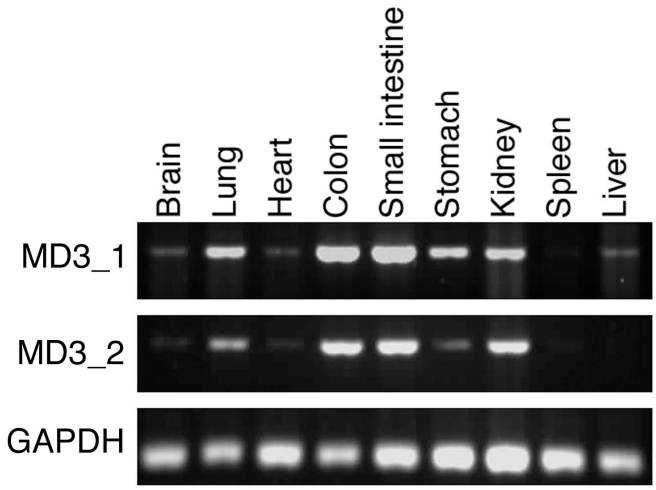

Figure 3.8 – Expression of MarvelD3 in mouse tissue. RT-PCR was performed on RNA extracted from adult mice (RNA was kindly provided by Prof. Maria Balda, UCL Institute of Ophthalmology) to analyse the expression of MarvelD3 in different tissue types. Primers were used to specifically amplify mouse MarvelD3 isoforms or GAPDH, as a control.

Localisation of MarvelD3 to the epithelial cell tight junction

Indirect immunofluorescence was used to determine the intracellular localisation of MarvelD3 in epithelial cells. As the antibody only recognises the human protein, we used Caco-2 and HCE cells for the localisation experiments as they form well-developed junctional complexes and are derived from two different types of epithelia. Confluent and semi-confluent cultures of the two cell lines were fixed in methanol and processed for double immunofluorescence using the rabbit anti-MarvelD3 antibody and a mouse monoclonal antibody against occludin. The samples were first analyzed by epifluorescence microscopy.

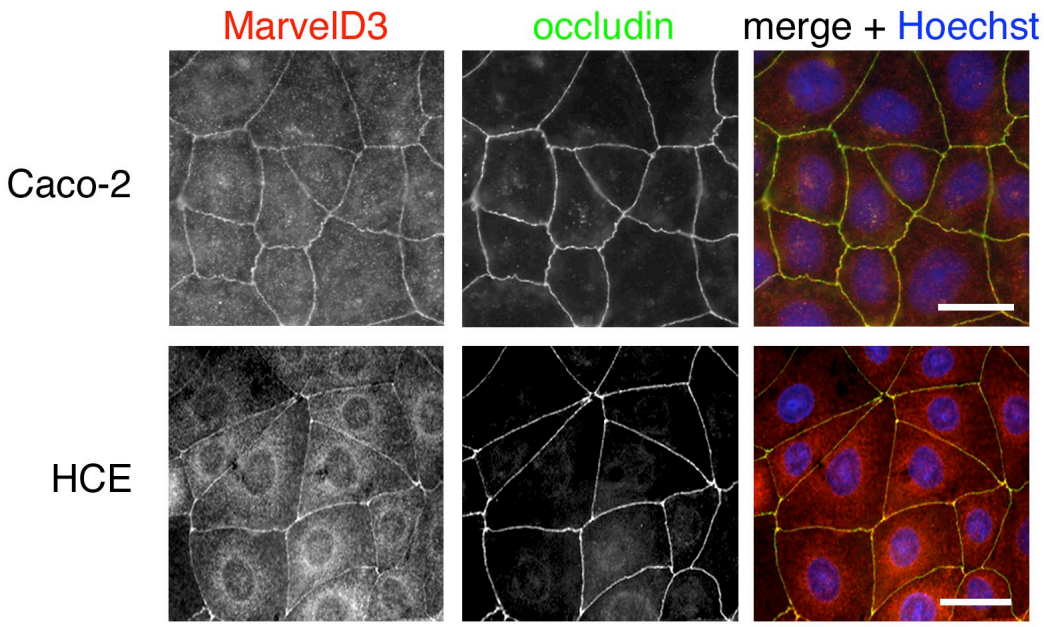

Figure 3.9 – MarvelD3 localises to cell-cell contacts in Caco-2 and HCE cells. Caco-2 and HCE cells were plated on to glass coverslips and grown at 37°C until cells were confluent (A). Cells were then fixed in methanol and immunofluorescence was performed with antibodies against MarvelD3 (red) and occludin (green). Hoechst (blue) was used as a nuclear stain. MarvelD3, like occludin, can be seen to localise to points of cell-cell contact in both cell types. Bars, 10μm.

Figure 3.9 shows that the anti-MarvelD3 antibody stained cell-cell contacts in Caco-2 and HCE cells. There was also some cytoplasmic and nuclear staining. However, the junctional staining was specific as it disappeared when MarvelD3 was depleted by RNA interference (see below). In both cell lines, MarvelD3 and occludin co-localised, suggesting that MarvelD3 is a component of the apical junctional complex. To analyse the specific junctional localisation of MarvelD3 samples were further analysed by confocal microscopy. Figures 3.10A and B show that MarvelD3 and occludin co-localised at cell junctions and in the same focal plane (note that the staining patterns of the two proteins enter and leave the focal plane at the same sites)

in Caco-2 cells. In contrast, MarvelD3 and the adherens junction marker E-cadherin localised in different focal planes (Figure 3.11). The concentration of MarvelD3 at the apical end of the lateral membrane together with occludin, apical to the lateral E-cadherin staining, was also observed in z-projections reconstituted from serial z line scans (Figure 3.10B and 3.11B). These data thus demonstrate that MarvelD3 co-localises with occludin, but not E-cadherin, at the junctional complex, indicating specific association with tight junctions.

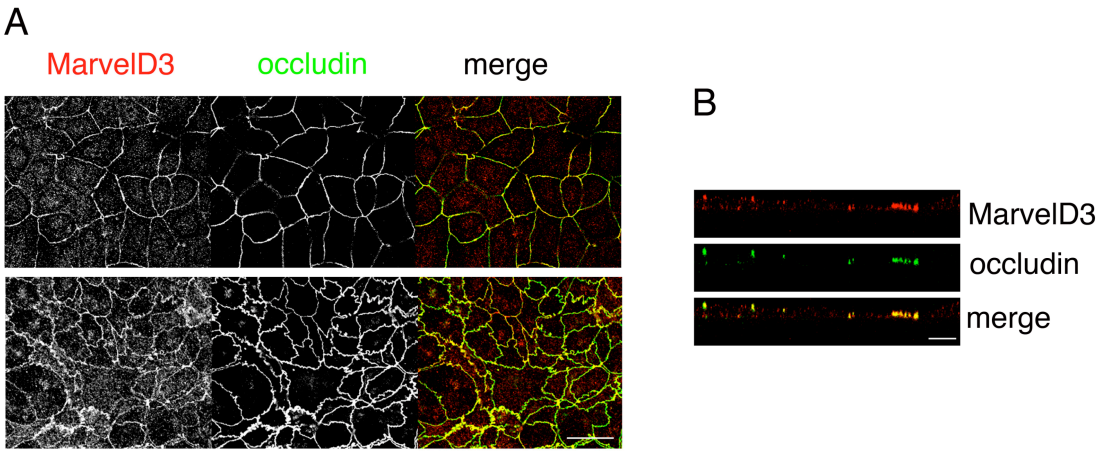

Figure 3.10 – MarvelD3 colocalises with occludin in the apical junctional complex. Caco-2 cells were grown on filters until confluent, fixed in methanol and processed for immunofluorescence with antibodies against MarvelD3 and occludin. The samples were then analyzed by confocal microscopy. (A) xy sections from different samples taken at the interface between the tight and adherens junctions. Occludin and MarvelD3 can be seen to follow each other in and out of the focal plane. (B) is a reconstitution of serial z line scans. Bars, 10μm.

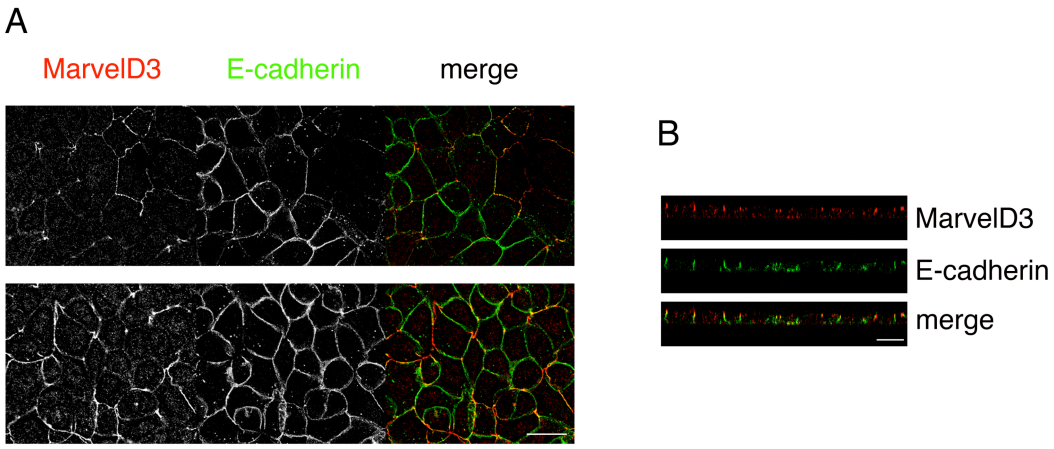

Figure 3.11 – MarvelD3 localises apically to E-cadherin in the apical junctional complex. Caco-2 cells were grown on filters until confluent, fixed in methanol and processed for immunofluorescence with antibodies against MarvelD3 and E-cadherin. The samples were then analyzed by confocal microscopy. (A) Shows two xy sections from different samples taken at the interface between the tight and adherens junctions. MarvelD3 and E-cadherin do not occupy the same focal plane (B) is a reconstitution of serial z line scans showing MarvelD3 to localise apically to E-cadherin in the apical junctional complex. Bars, 10μm.

Finally, to further confirm the localisation observed for the endogenous MarvelD3 protein, cDNAs encoding the two full-length isoforms untagged, as well as VSV- and HA-tagged full-length isoforms, were prepared and transfected into Caco-2 and MDCK cells. Figure 3.12 shows expression of all full-length MarvelD3 constructs in MDCK cells. Isoform 1 constructs were seen to run at a slightly higher molecular weight than isoform 2 constructs, which is in keeping with the slightly longer amino acid sequence of isoform 1 (410 amino acids) in comparison to isoform 2 (401 amino acids). HA-tagged constructs of both isoforms ran slightly higher than their untagged and VSV-tagged counterparts. The reason behind this is unknown, but has been observed for other HA-tagged constructs in the lab (K. Matter, personal

communication). Immunofluorescence analysis of transfected cells shows that both isoforms were enriched at cell-cell contacts (Figure 3.13), supporting the staining observed for endogenous protein in Caco-2 and HCE cells. Control MDCK cells did not reveal any staining for MarvelD3, possibly due to the species difference as the antibody was made against a sequence of the human protein that shows little conservation in the canine protein.

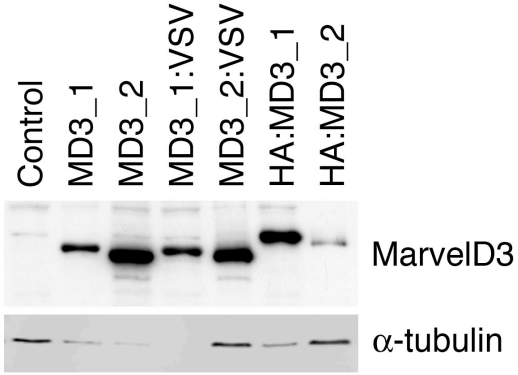

Figure 3.12 – Expression of full-length MarvelD3 constructs in MDCK cells. MDCK cells were transfected with cDNAs encoding the full-length isoforms of MarvelD3. Three days after transfection, cells were prepared for analysis by SDS-PAGE. Immunoblotting was performed with an antibody against MarvelD3 and anti-α-tubulin as a loading control. All constructs contain the full-length sequence of the specified MarvelD3 isoform and are shown as follows: MD3_1, untagged isoform 1; MD3_2, untagged isoform 2; MD3_1:VSV, C-terminally VSV-tagged isoform 1; MD3_2:VSV, C-terminally VSV-tagged isoform 2; HA:MD3_1, N-terminally HA-tagged isoform 1; HA:MD3_2, N-terminally HA-tagged isoform 2.

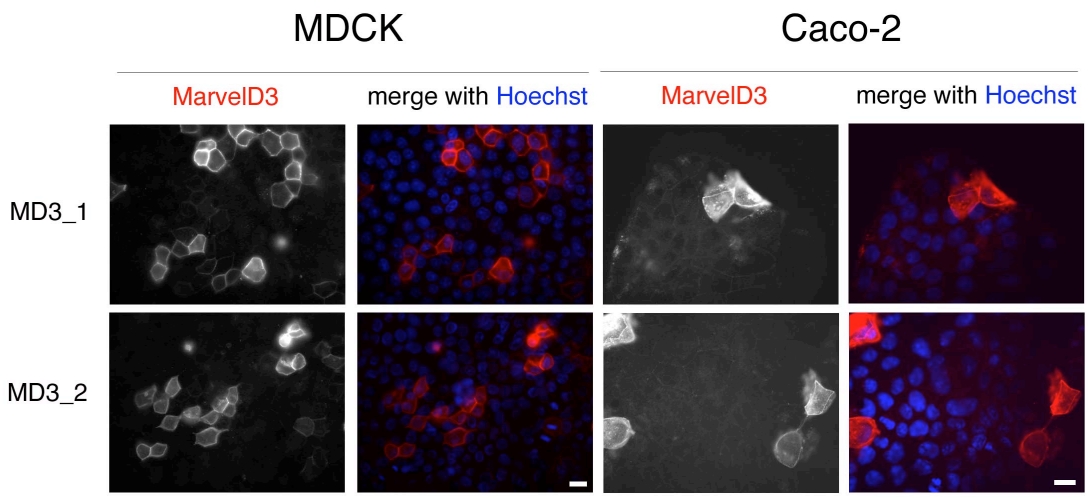

Figure 3.13 – MarvelD3 constructs localise to the cell periphery in MDCK and Caco-2 cells. Caco-2 and MDCK cells were transfected with cDNAs encoding the full-length, untagged isoforms of MarvelD3. Three days after transfection, cells were fixed in methanol and processed for immunofluorescence using antibody against MarvelD3 and Hoechst as a nuclear stain. Exogenously expressed MarvelD3 isoforms 1 and 2 can be seen to localise to the cell periphery in both MDCK and Caco-2 cells. Bars, 10μm.

Furthermore, expression of N-terminally HA-tagged MarvelD3 isoforms in Caco-2 and MDCK cells also resulted in staining of cell-cell contacts with anti-HA and anti-MarvelD3 antibodies (Figure 3.14). Unfortunately, C-terminally VSV-tagged constructs could not be detected by immunofluorescence with anti-VSV antibody, though the presence of the tag was confirmed by sequencing. These data indicate that both isoforms of MarvelD3 localise to cell-cell contacts in epithelial cells.

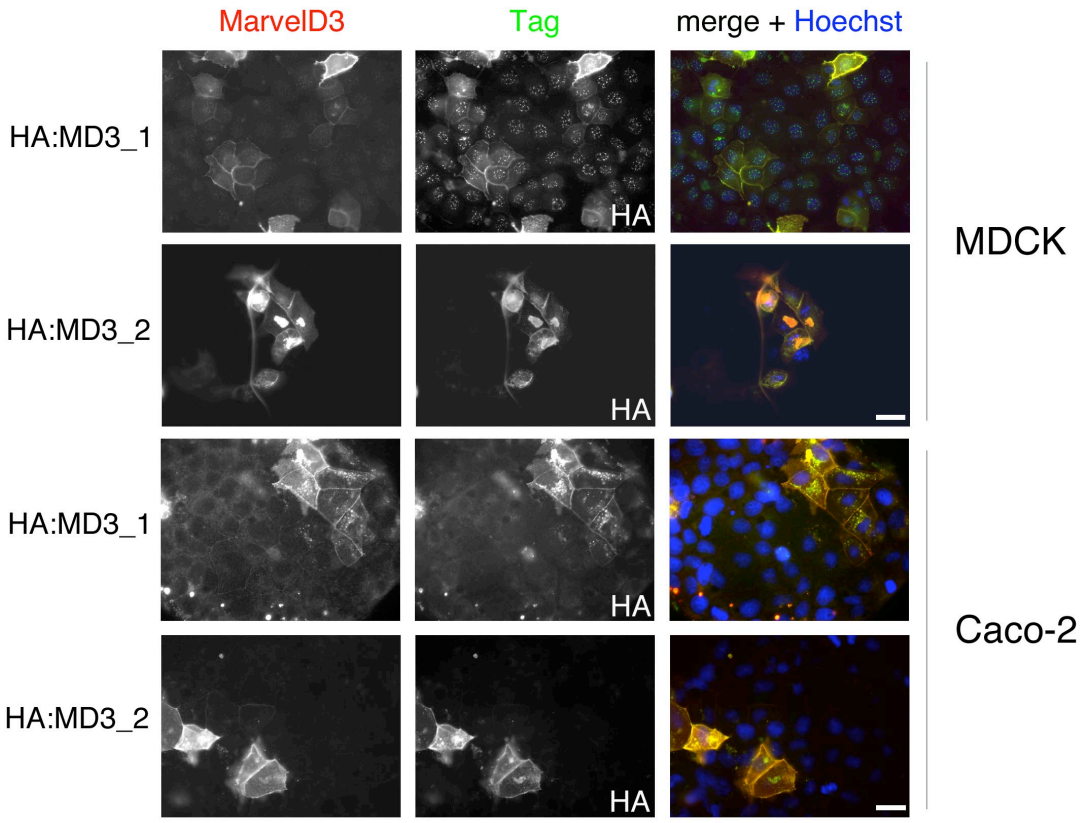

Figure 3.14 – HA-tagged constructs of MarvelD3 localise to the cell periphery in MDCK and Caco-2 cells. Caco-2 and MDCK cells were transfeted with cDNAs encoding full-length MarvelD3 isoforms tagged at the N-terminus with a HA tag. Three days after transfection, cells were fixed in methanol. Immunofluorescence was performed with antibodies against MarvelD3 and HA. Hoechst was used as a nuclear stain. HA-tagged constructs of each isoform localise to the cell periphery in both MDCK and Caco-2 cells. Bars, 10μm.

Occludin and tricellulin have both been shown to interact with ZO-1 via their cytoplasmic C-termini (Furuse et al., 1994; Riazuddin et al., 2006). In the case of occludin, this interaction has been implicated in its localisation to the tight junction (Furuse et al., 1994). To determine whether MarvelD3 may also interact with ZO-1, pulldown assays were performed with GST-fusion proteins of MarvelD3 N- and C-terminal domains from whole Caco-2 cell lysates. Immunoblotting with anti-ZO-1, -

ZO-2 and –ZO-3 showed no interaction between the cytoplasmic N- and C-termini of MarvelD3 isoforms and any of the ZO proteins (Figure 3.15). Immunoblotting with an anti-occludin antibody, however, showed a potential interaction between occludin and the N-terminus of MarvelD3. This suggests MarvelD3 and occludin may interact heterotypically within the tight junction.

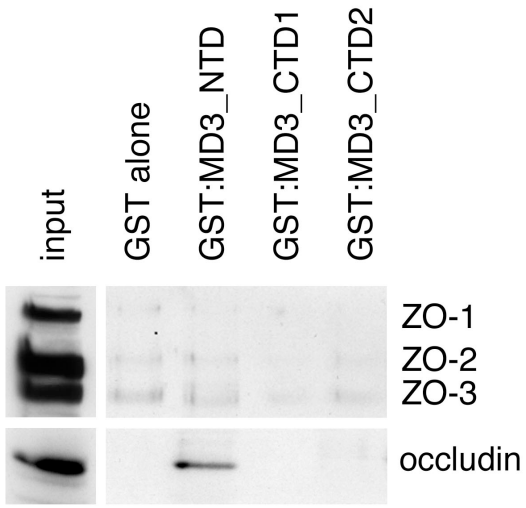

Figure 3.15 – Pulldown assays suggest an interaction between MarvelD3 and occludin, but not ZO-1, -2 or -3 in Caco-2 cells. Purified GST-fusion proteins of the N-terminus and two isoform-specific C-termini of MarvelD3 were loaded onto GST-agarose beads in equal quantities. Beads conjugated to the GST tag alone were used as a negative control. Pulldown assays using whole Caco-2 cell lysates demonstrated an interaction between the N-terminus of MarvelD3 and occludin, but not with any of the ZO proteins. The input lane shows all probed proteins were present in the original lysates.

Functional characterisation of MarvelD3 at the tight junction

To begin to address a functional role of MarvelD3 at the tight junction, the effect of siRNA-mediated depletion of MarvelD3 on the localisation and expression levels of other protein constituents of the apical junctional complex was assessed. Efficient knockdown of MarvelD3 was achieved with a pool of siRNAs as well as the two individual siRNAs identified above (Figure 3.16A). Depletion of MarvelD3 on immunoblots was mirrored by the absence of junctional staining by immunofluorescence (Figure 3.16B), indicating that knockdown of MarvelD3 was sufficient to efficiently deplete the junctional pools of MarvelD3. Transfection with MD3p-siRNA also caused reduced cytoplasmic staining suggesting some MarvelD3 may also exist in a cytoplasmic pool.

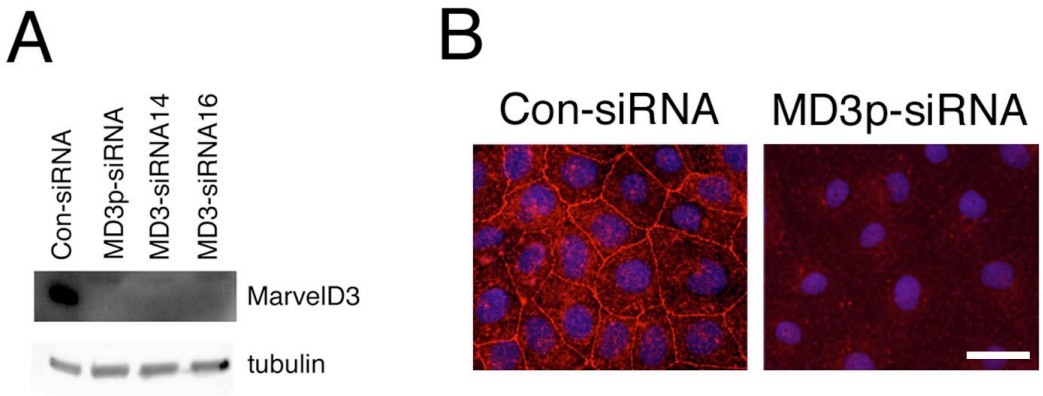

Figure 3.16 – Knockdown of MarvelD3 depletes the junctional pools of MarvelD3 in Caco-2 cells. Caco-2 cells were transfected with the indicated siRNAs and then processed for immunoblotting (A) or immunofluorescence. (A) Cells were immunoblotted with antibodies against MarvelD3 and α-tubulin. (B) Immunofluroescence was performed with an antibody against MarvelD3 and Hoechst was used as a nuclear stain. Depletion of MarvelD3 following siRNA transfection resulted in loss of junctional MarvelD3. Bar, 10μm.

The effect of MarvelD3 on the expression levels of other junctional proteins was then tested. Expression of the tight junction proteins occludin, tricellulin, claudin-1, GEF-H1, ZO-1, ZO-2 and ZO-3 (Figure 3.17), and the adherens junction proteins E-cadherin and β-catenin remained unchanged (Figure 3.18). Similarly, immunofluorescence analysis did not reveal any effects of MarvelD3 depletion on the distribution of the junctional proteins occludin, tricellular, GEF-H1, ZO-1, ZO-2, ZO-3, E-cadherin and β-catenin (Figure 3.19: shown is occludin). Although minor alterations cannot be excluded based on these data, depletion of MarvelD3 does not seem to affect the overall distribution of major junctional components.

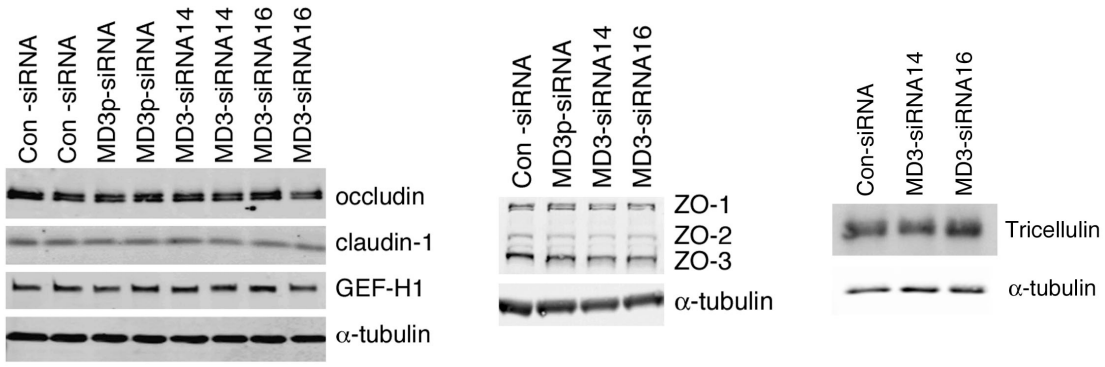

Figure 3.17 – Depletion of MarvelD3 does not affect expression of tight junction proteins occludin, claudin-1, GEFH1, ZO-1, ZO-2, ZO-3 or tricellulin. Cell extracts prepared from MarvelD3-depleted cells were separated by SDS-PAGE and probed with antibodies against various tight junction proteins. Extracts blotted for occludin, claudin-1 and GEFH1 were from cells grown on filters. Extracts blotted for ZO-1, ZO-2, ZO-3 and tricellulin were from cells grown on plastic. Note that the expression levels of none of the tight junction proteins were affected by MarvelD3 depletion, independent of whether filter- or plastic-grown samples were analysed. All blots are representative of at least three independent experiments.

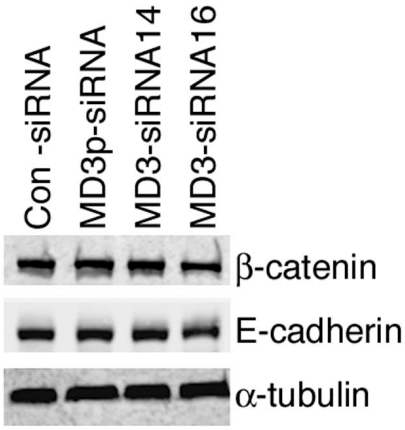

Figure 3.18 – Depletion of MarvelD3 does not affect expression of adherens junction proteins β-catenin and E-cadherin. Immunoblotting MarvelD3-depleted cell extracts for adherens junction proteins β-catenin and E-cadherin showed no effect of MarvelD3 depletion on expression of these proteins.

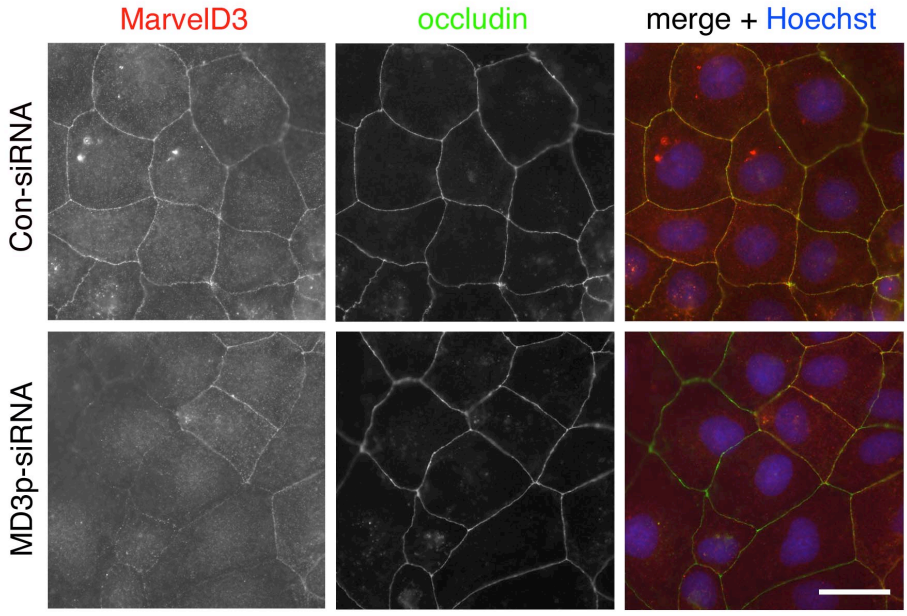

Figure 3.19 – Depletion of MarvelD3 does not affect occludin localisation. Caco-2 cells transfected with a pool of siRNAs against MarvelD3 (MD3p-siRNA) were fixed in methanol and processed for immunofluorescence with antibodies against MarvelD3 and occludin. Occludin distribution appears unaltered by MarvelD3 depletion. Bar, 10μm.

MarvelD3 and the regulation of ion conductance and paracellular permeability

An important function of tight junctions is the generation of a tight seal between neighbouring cells of the monolayer, which restricts the movement of ions and solutes through the paracellular pathway (Cereijido et al., 2004). To determine whether or not MarvelD3 plays a role in the assembly of the barrier or in the regulation of ion permeability, the TER of monolayers formed by control Caco-2 cells was compared to those formed by Caco-2 cells depleted of MarvelD3. To follow assembly and monolayer formation of the junction, cells were seeded first on plastic for transfection of the siRNA. 24 hours after transfection, the cells were re-plated onto permeable supports either in normal tissue culture medium (direct plating) or at low Ca^{2+} concentrations, which are insufficient to support junction formation. Junction assembly was then initiated 24 hours after plating by switching the cells to normal Ca^{2+} concentrations (Ca^{2+} switch) (Gonzalez-Mariscal et al., 1985), by which time depletion had already occurred. The monolayers were followed for a further 48 hours by measuring TER and then analysed for protein expression and paracellular tracer permeability. Figure 3.20A shows that MarvelD3 was still efficiently depleted at the end of the incubation period. Similarly, no effects on monolayer morphology and localisation of junctional proteins were observed (Figure 3.20B: shown are occludin and ZO-1).

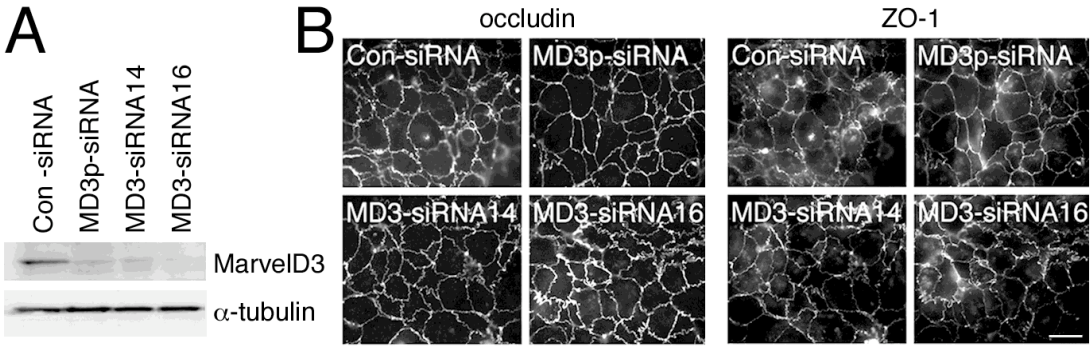

Figure 3.20 – Depletion of MarvelD3 and tight junction assembly. (A) Control and siRNA-transfected Caco-2 cells were plated on filters one day after transfection. The cells were lysed three days later and expression of MarvelD3 and α-tubulin was determined by immunoblotting. (B) Cells treated as those in panel A were fixed and processed for immunofluorescence at the end of the incubation period. Shown are epifluorescence images of samples labelled for the tight junction markers occludin and ZO-1. Note, depletion of MarvelD3 did not affect monolayer integrity and appearance. Bar, 10μm.

TER measurements revealed that formation of functional tight junctions still occurred at similar kinetics as in control cells (Figure 3.21A), suggesting MarvelD3 is not necessary for the formation of tight junctions. However, MarvelD3 depleted cells reached higher resistance values. Determination of tracer permeability using 4kD and 70kD fluorescent dextrans did not suggest any defects in barrier formation or significant alterations in tracer diffusion (Figure 3.21B). Cells that were directly plated in normal medium, and were hence 24 hours longer in normal Ca^{2+} medium, also formed functional tight junctions and reached stable TER values by the end of the incubation time (Figure 3.21C and D). As the Ca^{2+} switch cells, directly plated MarvelD3 depleted cells had reached 25% higher electrical resistance values than control cells. Taken together, these results indicate that MarvelD3 depletion does not

affect the formation of functional tight junctions, but that MarvelD3 levels are a determinant of paracellular ion conductivity.

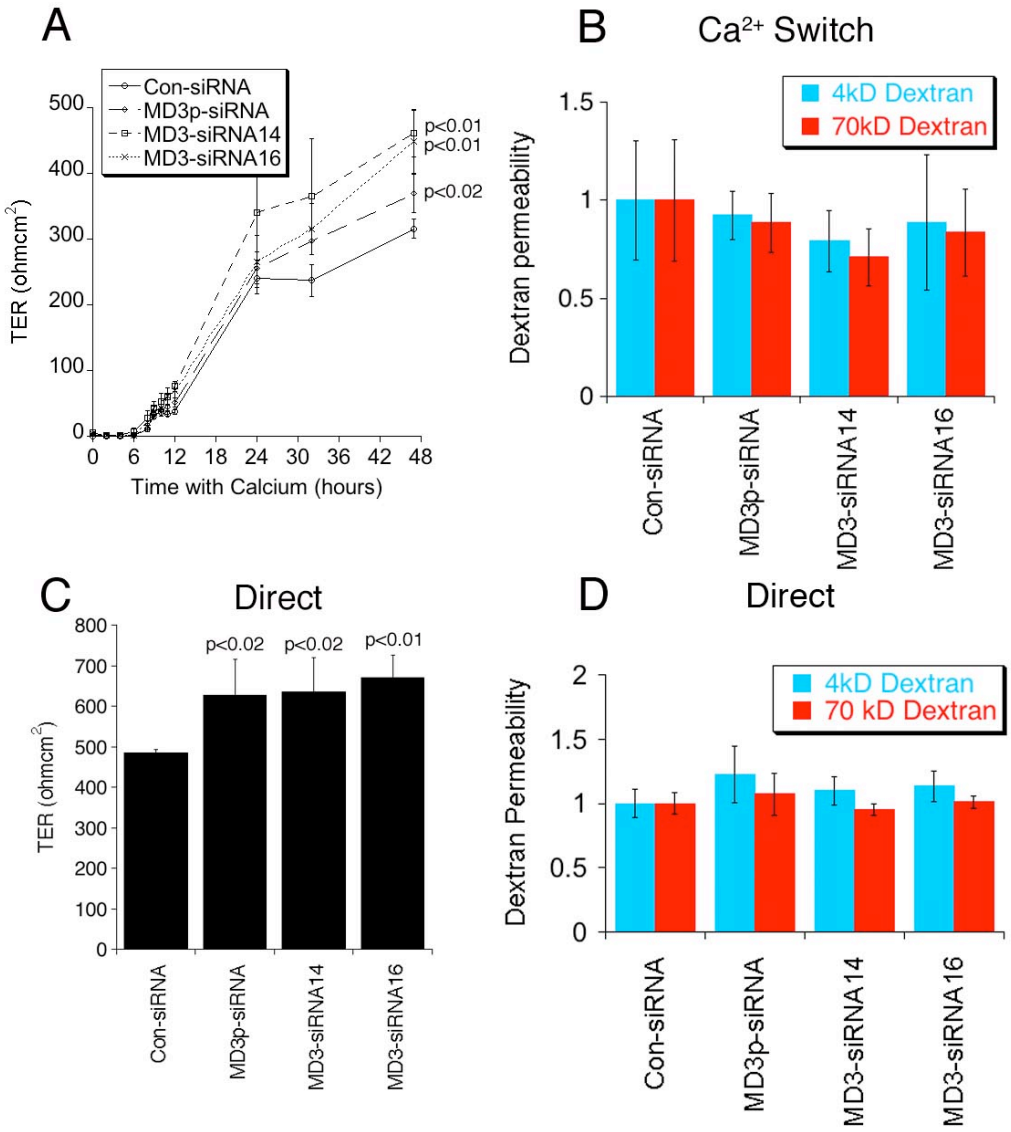

Figure 3.21 - Depletion of MarvelD3 and epithelial barrier properties. Caco-2 cells were cultured as in figure 3.20 either using the Ca^{2+} Switch (A, B) or Direct plating (C, D) protocol. TER and fluorescent dextran permeability using 4kD and 70kD dextran were measured as indicated. The amount of dextran diffused to the basolateral side of the monolayer was normalised against the average value obtained from control cells. Shown are averages ± 1 standard deviation of quadruplicate samples of a typical experiment. The indicated p values were obtained with a t-test comparing knockdown with control values; in panel A, the p values refer to the final TER values. Note, MarvelD3 knockdown had no significant effect on diffusion of either dextran tracer across monolayers in either the Ca^{2+} switch experiment (B) or those plated directly into complete culture medium (D).

Claudins are the main constituent of tight junction strands and thought to be the main regulators of ion conductance properties of the tight junction. Since MarvelD3 depletion caused an increase in TER, the effect of MarvelD3 depletion on claudin expressed was determined by immunoblotting. Figure 3.22 shows that MarvelD3 depletion does not effect expression levels of claudin-1, but may lead to increased expression of claudin-4, as detected by immunoblotting.

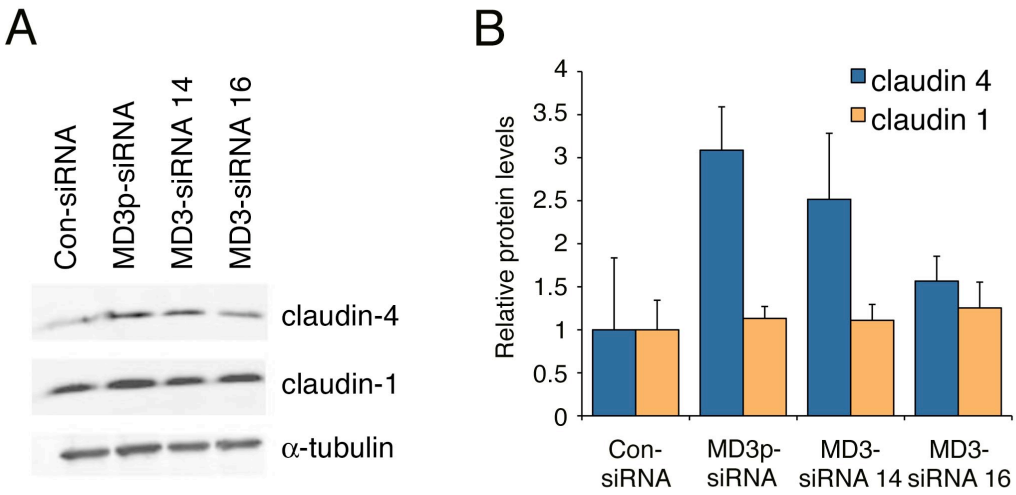

Figure 3.22 – Effect of MarvelD3 depletion on expression levels of claudin-1 and claudin-4. (A) Cell extracts prepared from control and MarvelD3-depleted cells grown on filters were separated by SDS-PAGE and probed with antibodies for claudin-4 and claudin-1. (B) Levels of claudin-4 were slightly, but not significantly, increased in MarvelD3-depleted cells, while there was no change in the expression levels of claudin-1, when compared to controls. Claudin-1 and claudin-4 levels were quantified relative to α-tubulin from three independent experiments. An anti-α-tubulin antibody was used as a loading control.

Discussion

MarvelD3 is a novel component of the epithelial cell tight junction

In the current chapter, MarvelD3 is identified as a novel component of the epithelial cell tight junction (Steed et al., 2009). MarvelD3, a four-pass transmembrane protein, co-localises with the tight junction protein occludin, apical to the adherens junction protein E-cadherin, indicating that MarvelD3 is a tight junction-associated Marvel domain protein. MarvelD3 has also been shown to localise to tight junctions in epithelial tissues from mouse (Raleigh et al., 2010) suggesting the presence of this protein at tight junctions may be of physiological relevance. Depletion of MarvelD3 using RNA-interference resulted in reduced junctional and cytoplasmic staining suggesting MarvelD3 exists in both a junctional and a cytoplasmic pool. A functional analysis using RNA interference-mediated depletion indicates that MarvelD3 is not essential for junction assembly or the formation of a functional paracellular diffusion barrier, but the observed increase in TER in depleted cells indicates that MarvelD3 is a determinant of paracellular ion permeability. The data presented demonstrate that MarvelD3 associates with the junctional complex of intestinal and corneal epithelial cells, and its expression was detected in multiple mouse tissues and cultured epithelial and endothelial cell lines. MarvelD3 thus seems to be a widely expressed protein and hence is likely to be a component of tight junctions with different functional properties.

MarvelD3 is expressed as two isoforms due to alternative splicing and translation of exon 4 (isoform 1) or exon 3 (isoform 2) (Raleigh et al., 2010). Both isoforms were recruited to the cell periphery when transfected into Caco-2 or MDCK cells in a

manner similar to the endogenous protein, suggesting that both isoforms associate with junctions. Attempts to generate isoform-specific antibodies, which are required to study endogenously expressed isoforms at the protein level, have so far failed. Based on reverse transcription PCR results, however, both isoforms seem to be widely expressed. The majority of epithelial and endothelial cell lines tested expressed both isoforms of MarvelD3, though some isoform-specific expression patterns were observed. The liver cell line HepG2, for example, expressed the transcript for MarvelD3 isoform 1, but not isoform 2. Interestingly, analysis of liver tissue from healthy mice also showed MarvelD3 isoform 1 to be expressed, but not isoform 2 (also observed in Raleigh et al., 2010), suggesting an expression preference for isoform 1 in the liver. In keeping with Raleigh *et al*., (2010), neither transcript of MarvelD3 was detected in the spleen, which contains little epithelial tissue. It would be interesting for future studies to be able to differentiate between MarvelD3 isoforms at the protein level and to determine whether there are any isoform-specific differences in expression, localisation and/or function, as has been suggested for occludin (Ghassemifar et al., 2002; Muresan et al., 2000). Intriguingly, the two MarvelD3 isoforms share a common N-terminal sequence and differ from their first transmembrane domain to the C-terminus, thus the sequences of their Marvel domains are not the same. In contrast, splice variants of occludin (occludin and occludin 1B) share the same Marvel domain, but differ at their N-terminus (Muresan et al., 2000). Tricellulin isoforms also share the same Marvel domain, but show differences in their cytosolic domains mediating interactions with potential signalling partners. This suggests the conservation of the N-terminal sequence between isoforms of MarvelD3 may be important in mediating the primary function of MarvelD3 at the tight junction, perhaps via interactions with cytoplasmic scaffolding or signalling proteins, while the

Marvel domain or differences at the C-terminus may be responsible for differential expression patterns. Perhaps the different Marvel domains of MarvelD3 isoforms 1 and 2 afford propensity for insertion into membranes with slightly different properties, or affect the stability/dynamics of the protein within the membrane. Indeed, analysis of the dynamic behaviour of MarvelD3 has shown isoform 1 to be more stable at tricellular junctions, while isoform 2 appears more stable along bicellular junctions (Raleigh et al., 2010). Under such a hypothesis, the existence of two isoforms would enable differential expression or cellular localisation based on membrane properties, without impairing the as yet unknown primary function regulated by the common N-terminal domain.

Occludin and tricellulin not only localise to tight junctions, but have been shown to associate with the junctional intramembrane strands observed in freeze fracture replicas (Fujimoto, 1995; Ikenouchi et al., 2005). The association of MarvelD3 with these structures and whether the Marvel domain, which is found in all three proteins, is important for strand association, has not been addressed here. It would be interesting for subsequent studies to use electron microscopy to see if MarvelD3 localises to the tight junction strands and, in combination with RNA interference, determine the effect it and other Marvel domain-containing proteins have on strand morphology.

The regulation of paracellular diffusion and ion conductance is an important property of the tight junction. Measurements of TER in MarvelD3-depleted monolayers revealed that formation of functional tight junctions occurred at similar kinetics as in

control cells. This is in contrast to Raleigh *et al*. (2010) who reported a delay in barrier formation following MarvelD3 depletion. Both of these studies were performed in Caco-2 cells, however unknown differences in the experimental set-ups make it difficult to comment on how the discrepancies between the two data sets may have arisen. More recently, MarvelD3 depletion has been shown to reduce TER and increase permeability to dextran tracers across pancreatic cell monolayers (Kojima et al., 2011), suggesting there could be cell type-specific differences in the response to MarvelD3 depletion. To further clarify the importance of MarvelD3 in junction formation it would be beneficial to generate an inducible MarvelD3 knockdown cell line which would enable more stable knockdown of MarvelD3 than is possible using siRNA. In their study, Raleigh *et al*. (2010) monitered TER for 9 days while the maximum knockdown in the system used in the current study is achieved at just 3 days, and could perhaps be the important difference between the two studies.

Since occludin overexpression was previously seen to increase TER (Balda et al., 1996), it was tested whether the increased TER observed in the present study could be attributable to elevated levels of occludin expression. Immunoblotting cell lysates from MarvelD3 knockdown cells however showed occludin levels, as well as levels of ZO-1, ZO-2 and ZO-3, to be unchanged. Neither were any significant changes in the distribution of these proteins observed by immunofluorescence. However, at this point it cannot be excluded that more subtle changes in occludin distribution might have caused the increase in TER. Given the importance of claudin family members for paracellular ion permeability (Van Itallie and Anderson, 2006; Krause et al., 2008; Angelow et al., 2008), it is possible that MarvelD3 depletion affected claudin

expression or function. Indeed, occludin knockdown has been shown to reduce expression levels of claudins 1 and 7 and increase levels of claudins 3 and 4 in MDCK cells (Yu et al., 2005) and, in the present study, depletion of MarvelD3 resulted in slightly elevated levels of claudin-4, which has been shown to cause increases in TER when overexpressed (Van Itallie et al., 2001). Aside from altering protein expression levels, depletion of MarvelD3 could also affect ion conductivity by altering the dynamics of other tight junction proteins, which would not have been seen with the approaches used here. In a recent study, the phosphorylation state of occludin at serine residue 408 (S408) has been shown to regulate paracellular permeability by affecting the dynamics of other tight junction proteins (Raleigh et al. 2010). Phosphorylation of occludin S408 weakened the interaction between occludin and ZO-1 and subsequently reduced the association between occludin and claudins 1 and 2. This promoted the assembly of claudin-1 and -2-based pores and subsequently promoted cation flux (Raleigh et al., 2011). When unphosphorylated at S408, occludin interaction with claudin molecules, mediated by ZO-1, impairs pore formation and reduced ion conductance. Thus by regulating the interactions and mobility of claudin-1, claudin-2 and ZO-1, the phosphorylation state of occludin can regulate paracellular permeability properties of the tight junctions (Raleigh et al., 2011). Pulldown assays showed the N-terminal domain of MarvelD3 was able to interact with occludin, supporting co-immunoprecipitation experiments, which have demonstrated an interaction between occludin and MarvelD3 (Raleigh et al., 2010), and extending them further by mapping the interaction to the N-terminal domain of MarvelD3. Perhaps interactions with MarvelD3 may also be able to influence the dynamic properties of occludin-based tight junction complexes, or additional complexes based on MarvelD3 alone. Identification of interactions between

MarvelD3, claudins and/or adaptor molecules other than ZO-1 may be needed to ascertain the mechanism behind MarvelD3 regulation of tight junction ion conductance.

Despite the lack of interaction between MarvelD3 and the ZO proteins in this and another independent study (Raleigh et al., 2010), it is possible that the fusion proteins used may prevent some interactions from occurring during the pulldown assay. Though generated independently, both experimental setups utilised a GST-fusion protein with the GST tag at the N-terminal end of the MarvelD3 N-terminal sequence. The presence of this tag may impair interactions occurring at distal regions of the N-terminus of MarvelD3, which would be freely exposed to the cytoplasm *in vivo*. To address this issue, efforts were made to generate a GST-fusion protein with the GST-tag at the C-terminal end of the N-terminus, but these unfortunately failed. It is important to note, however, that a different strategy may enable interactions between MarvelD3 and the ZO proteins, or other proteins, to be observed, despite no evidence of such interactions being reported here.

In conclusion, the experiments in this chapter identify MarvelD3 as a novel member of the occludin family, a subgroup of the Marvel domain proteins. MarvelD3 is expressed as two isoforms that each shows a broad tissue distribution. Similarly to occludin, normal MarvelD3 expression is not essential for tight junction formation. Nevertheless, knockdown of MarvelD3 affects the paracellular ion conductance properties of tight junctions by mechanisms that still have to be identified. The importance of MarvelD3 as an integral membrane component of the tight junction has

also been realised in additional studies performed during the preparation of this thesis (Kojima et al., 2011; Raleigh et al., 2011; Raleigh et al., 2010).

Chapter 4:

Role of MarvelD3 in the regulation of proliferation and migration in epithelial cells

Chapter 4: Role of MarvelD3 in the regulation of proliferation and migration in epithelial cells

Introduction

In the previous chapter, MarvelD3 was identified as a novel component of the tight junction. Since MarvelD3 appeared to have a relatively minor role in the regulation of ion conductance properties, and not in paracellular permeability, the work in this chapter aimed at determining what the primary function of MarvelD3 at the tight junction might be. In addition to providing a structural role to the cell and performing the well characterised barrier and fence functions, tight junctions are further appreciated for their role in the regulation of intracellular signalling pathways and gene transcription.

The work in this chapter addresses the idea that the primary function of MarvelD3 may be in the regulation of intracellular signalling pathways from the tight junction. Indeed, the majority of the work implicating tight junctions in intracellular signalling pathways considers cytoplasmic proteins of the tight junction and not the integral membrane proteins themselves (Balda et al., 2003; Huerta et al., 2007). Exposed to both the cell exterior and interior, the transmembrane proteins are ideally situated to elicit the transmission of signals from the extracellular space or neighbouring cell to the cell interior. That the cytoplasmic tails of these proteins interact with numerous cytoplasmic proteins implicated in intracellular signalling, further suggests the transmembrane proteins themselves could play an important role in the regulation of intracellular signalling pathways. Such a role has been touched on for occludin in the

sensing and extrusion of apoptotic cells from the monolayer (Rosenblatt et al., 2001), but remains relatively uninvestigated for other proteins and other processes.

This chapter demonstrates how expression of MarvelD3 protein is lost in a number of metastatic tumour cell lines and its exogenous expression in the metastatic pancreatic tumour cell line MiaPaCa results in a more epithelial-like phenotype and reductions in both cell proliferation and migration. In keeping, depletion of endogenous MarvelD3 in Caco-2 cells results in increased proliferative and migratory behaviours. Microarray analysis identified altered expression of epidermal growth factor receptor (EGFR) pathway components following MarvelD3 expression in MiaPaCa cells. Thus suggesting cross talk between MarvelD3 and the EGFR signalling pathway. Inhibition of AP1 promoter activity by MarvelD3 expression suggests MarvelD3 may regulate the EGFR via AP1. Taken together, data in this chapter implicates MarvelD3 in the regulation of epithelial proliferation and migration, suggesting its absence may contribute, at least in part, to the uncontrolled proliferation and propensity for migration observed in the tumourogenic process.

Results

To first address whether MarvelD3 may play a role in epithelial tumourigenesis, a number of benign and metastatic tumour cell lines were analysed for expression of MarvelD3 protein. Immunoblotting showed MarvelD3 to be expressed in immortalised and benign tumour cell lines, including human mammary epithelial cells MCF10A and MCF7. MarvelD3 protein was reduced or absent in metastatic cell lines, like MB231 cells and MiaPaCa cells (Figure 4.1). In prostate cell lines, reduction in MarvelD3 expression appeared to correspond with cells developing an invasive phenotype, just as reduced occludin levels have been shown to correspond with the progression of endometrial carcinoma (Tobioka et al., 2004) and breast cancer (Martin et al., 2010). This suggests that loss of MarvelD3 expression may play a role in tumour pathogenesis.

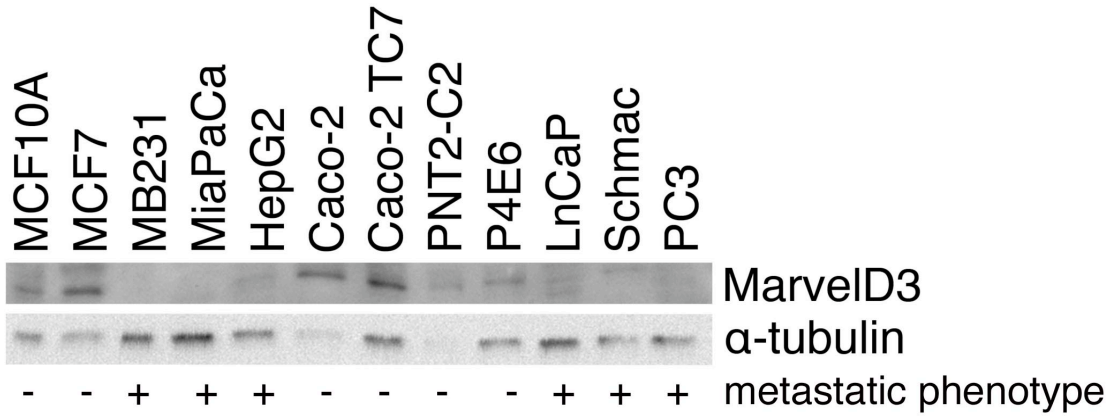

Figure 4.1 – Expression of MarvelD3 in tumour cell lines. Whole cell lysates prepared from a number of tumour cell lines were processed for immunoblotting with an antibody against the N-terminus of MarvelD3. MarvelD3 expression appears reduced in cells with a metastatic phenotype (-, non-metastatic; +, metastatic). α-tubulin was used as a loading control.

Expression of MarvelD3 in MiaPaCa cells results in the formation of cell-cell contact sites and a more epithelial-like phenotype

In order to begin to understand a possible function of MarvelD3 in tumourigenesis and in normal physiology, the human pancreatic carcinoma cell line MiaPaCa was used, in which endogenous MarvelD3 protein could not be detected. Semi-quantitative RT-PCR demonstrated that MarvelD3 transcript is greatly reduced in MiaPaCa cells in comparison to healthy pancreas (Figure 4.2A). As the pancreas expresses MarvelD3 isoform 1, but not isoform 2, MiaPaCa cell lines stably expressing a VSV-tagged construct of MarvelD3 isoform 1 (MD3_1:VSV) were generated. To compensate for possible clonal variations two independent clones were established (C2 and C8), both of which expressed MarvelD3 transcript and protein (Figure 4.2B).

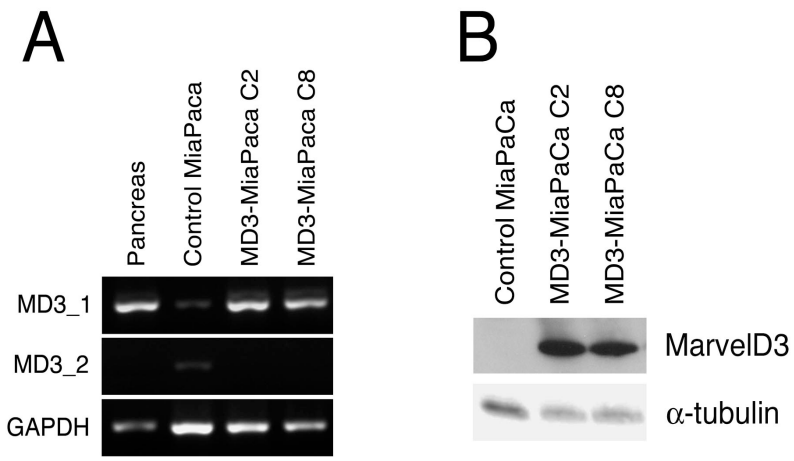

Figure 4.2 – Expression of MarvelD3 in MiaPaCa cell lines. (A) RT-PCR of RNA extracted from healthy pancreas and control MiaPaCa cells shows MarvelD3 isoform 1 (MD3_1) is expressed in healthy pancreas but not in MiaPaCa cells. MarvelD3 isoform 2 (MD3_2) is not expressed in healthy pancreas. RT-PCR (A) and immunoblotting (B) demonstrates that the MiaPaCa clones C2 and C8 express MarvelD3 isoform 1 at the transcript and protein level. Images are representative of three independent experiments. RNA from human pancreas was purchased from Clonetech.

Indirect immunofluorescence was used to determine the localisation of exogenously expressed MarvelD3 in MiaPaCa cells. Figure 4.3 shows that anti-MarvelD3 and anti-VSV antibodies detected the MarvelD3 construct at cell-cell contact sites in C2 and C8 MiaPaCa cells, at both low and high cell densities, consistent with the localisation pattern of the endogenous protein. Immunofluorescent staining also showed that MarvelD3-expressing MiaPaCa cells appeared more epithelial-like than control MiaPaCa cells.

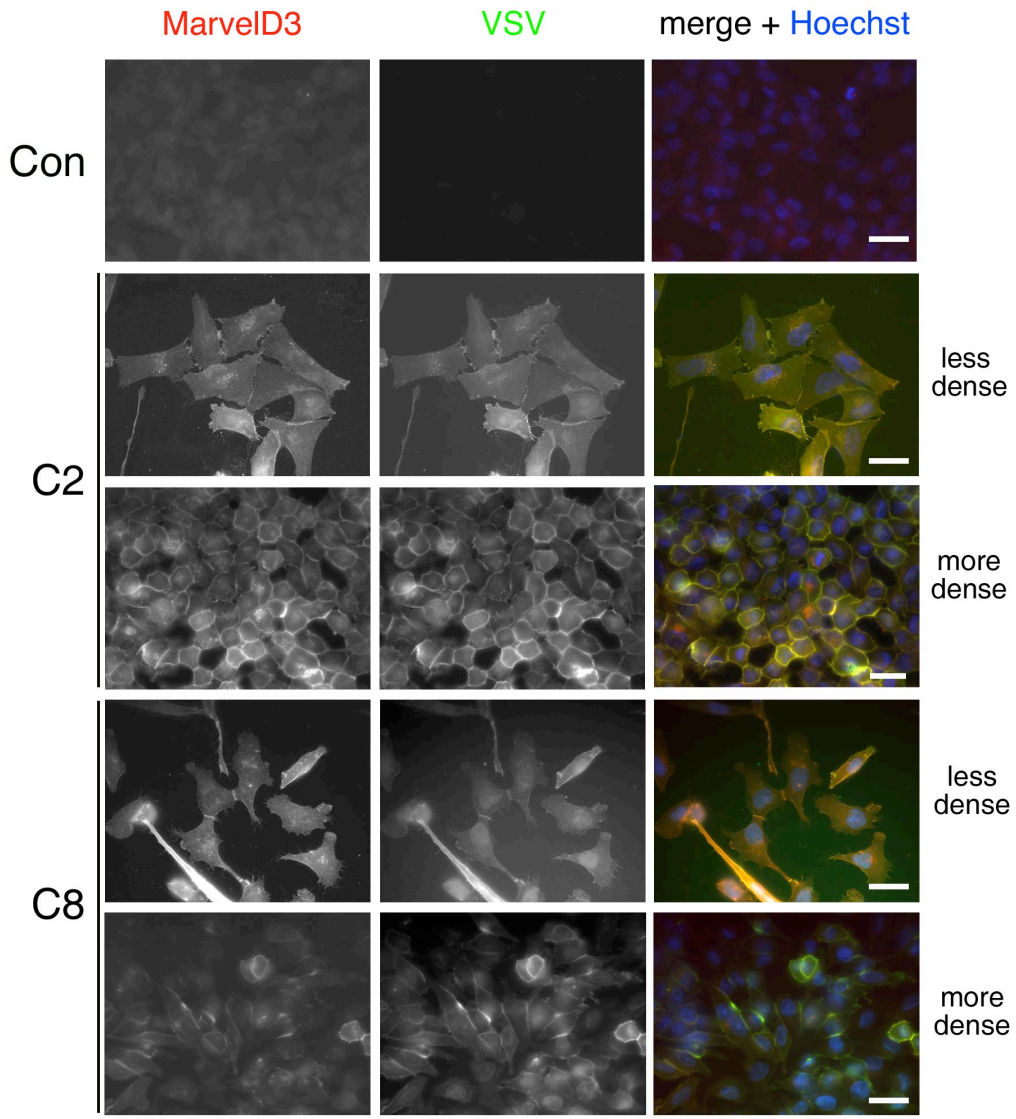

Figure 4.3 – MD3_1:VSV localises to cell-cell contact sites when constitutively expressed in MiaPaCa cells. Control and MarvelD3-expressing MiaPaCa cells were plated onto glass coverslips and grown for 3 days at 37°C. Cells were fixed in methanol and processed for immunofluorescence using anti-MarvelD3 and anti-VSV antibodies. Images were taken of cells at low density, to show early junctions, and high density, to show more mature junctions within the monolayer. Exogenously expressed MarvelD3 showed the same localisation pattern as that seen in cells expressing the endogenous protein (e.g. Caco-2 cells). Bars, 20μm.

Imaging by light microscopy confirmed that cells expressing MarvelD3 grew in defined colonies with an epithelial-like appearance in contrast to the fibroblast-like, migratory appearance of the control cells (Figure 4.4). Since endogenous MarvelD3 was not detectable in control MiaPaCa cells, expression of MarvelD3 may be responsible for the more epithelial-like phenotype observed.

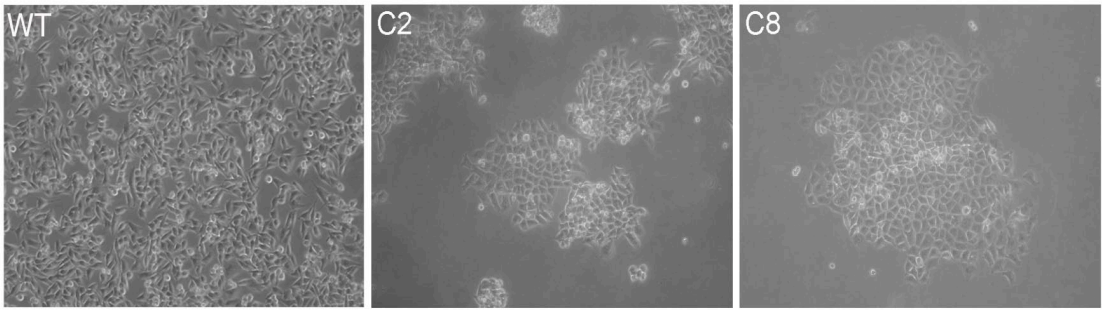

Figure 4.4 – Expression of MarvelD3 results in a more epithelial-like phenotype in MiaPaCa cells. Phase-contrast images were taken of control and MarvelD3-expressing MiaPaCa cells grown in complete medium for 48 hours. MarvelD3-expressing C2 and C8 cells grow in colonies characteristic of adhesive epithelial cells in comparison to the fibroblast-like appearance of control MiaPaCa cells.

In order to understand the nature of the cell-cell contact sites established following the expression of MarvelD3 in MiaPaCa cells, the effect of MarvelD3 expression on the expression and localisation of other junctional proteins was determined. As figure 4.5 shows, ZO-1 is recruited to early points of cell-cell contact following MarvelD3 expression while transmembrane components of the tight and adherens junctions, occludin and E-cadherin, were not. Both occludin and E-cadherin demonstrated an intracellular vesicular-like staining pattern in control MiaPaCa cells, which was still present following expression of MarvelD3. Immunoblotting showed expression

levels of occludin to be decreased in MarvelD3-expressing cells, while ZO-1 and E-cadherin levels were unchanged (Figure 4.5B). This suggests that exogenously expressed MarvelD3 can integrate into the membrane and partially restore the epithelial nature of MiaPaCa cells. The recruitment of ZO-1 (Figure 4.5C), but not occludin or E-cadherin, suggests these MarvelD3-based contact sites are simple points of cell-cell contact which may enable the specific functions of MarvelD3 to be looked at more closely, away from the complexity of the endogenous apical junctional complex. It will be important to combine such observations, however, with studies in epithelial cells expressing the endogenous protein, in case the presence or correct localisation of other junctional components are required for MarvelD3 functions.

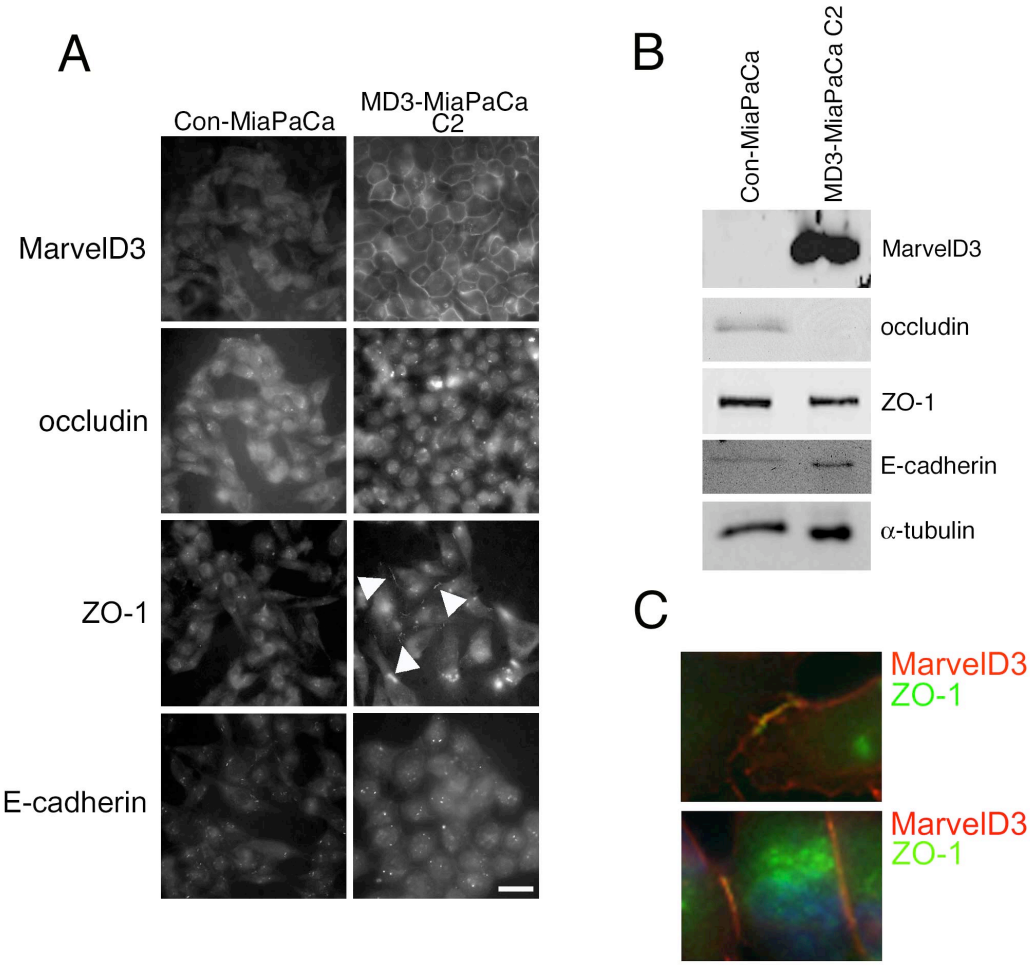

Figure 4.5 – Effect of MarvelD3 expression on occludin, ZO-1 and E-cadherin in MiaPaCa cells. (A) Control and MarvelD3-expressing MiaPaCa cells were processed for immunofluorescence with anti-MarvelD3, anti-occludin, anti-ZO-1 and anti-E-cadherin antibodies. ZO-1 can be seen to recruit to points of early cell-cell contact in MD3-expressing cells (arrowheads). E-cadherin and occludin retain the vesicular-like staining seen in control cells, following MarvelD3 expression. (B) Immunoblotting shows the effect of MarvelD3 on junctional protein expression levels. (C) Images taken at increased magnification show the colocalisation between MarvelD3 and ZO-1 at cell-cell contact points in MarvelD3-expressing C2 MiaPaCa cells. For clarity, only control and MarvelD3-expressing C2 MiaPaCa cells are shown. MarvelD3 expression had the same effect in C8 MiaPaCa cells (not shown). Bar, 20μm.

MarvelD3 expression regulates epithelial cell proliferation and migration

As tight junction formation inhibits proliferation, it was first asked whether MarvelD3 expression was sufficient to suppress proliferation of MiaPaCa cells. MiaPaCa cells were plated at a number of different cell densities and left to grow at 37°C for 4 days. The increase in cell number demonstrated by control MiaPaCa cells was greatly reduced in cells expressing MarvelD3 (Figure 4.6A). To determine whether this reduction was attributable to an increase in apoptosis, sub-confluent control and MarvelD3-expressing MiaPaCa were prepared for FACS analysis. Quantification of the numbers of fragmented nuclei, a sign of apoptosis, showed no significant increase in MarvelD3-expressing cultures than in control cells (Figure 4.6B). Furthermore, extensive immunofluorescent analyses, across a number of experiments, highlighted no observable increase in apoptotic nuclei following expression of MarvelD3 than in control cells. Taken together, this suggests the attenuation in cell number increases over time following expression of MarvelD3 in MiaPaCa cells may be due to an inhibition of cell proliferation, rather than an increase in apoptosis.

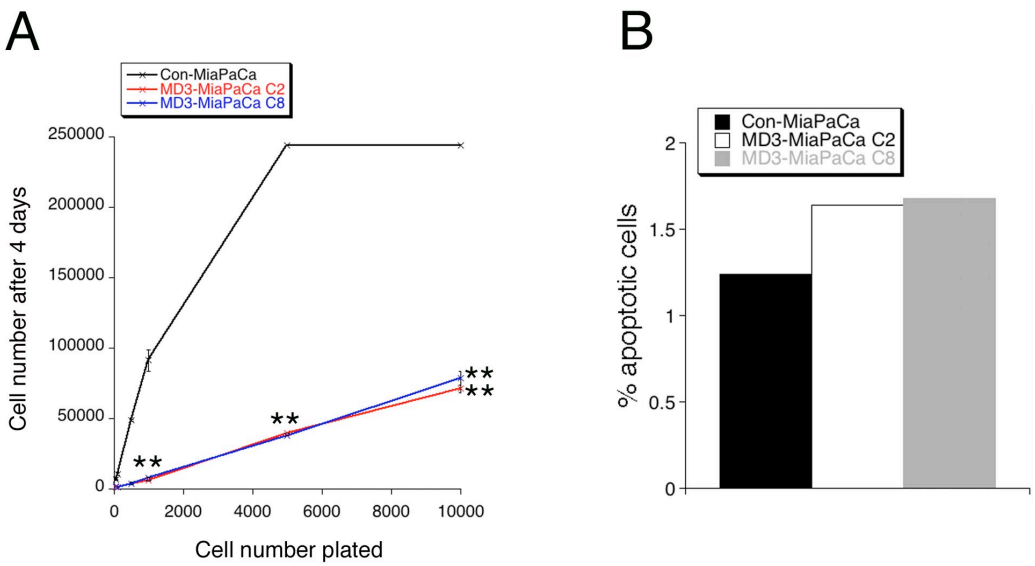

Figure 4.6 – Effect of MarvelD3 expression on cell number increases in MiaPaCa cells. MiaPaCa control cells and MarvelD3-expressing clones C2 and C8 were plated in quadruplicate at a number of different cell densities and a CyQUANT proliferation assay kit used to determine the cell number after 4 days. (A) The increase in cell number shown by control MiaPaCa cells is greatly reduced in cells expressing MarvelD3. Shown are mean cell numbers after 4 days (n=4) ± standard deviation (B) FACS analysis demonstrated there was no significant difference in the proportion of apoptotic cells following the expression of MarvelD3. 20,000 cells of each group were counted. **p<0.01 by Student's t-test.

To confirm this effect on proliferation was due to MarvelD3 expression and not a non-specific effect of overexpression or the presence of the VSV tag, Caco-2 cells, plated at the same cell density, were either transfected with a control siRNA, a pool of siRNAs, or two individual siRNAs to deplete the endogenous MarvelD3 protein. Quantification of cell numbers after 3 days at 37°C showed an approximately 20% increase in cell number following MarvelD3 depletion in comparison to control cells (Figure 4.7A). Immunoblotting confirmed good knockdown of the endogenous

MarvelD3 protein by all MarvelD3-siRNA treatments (Figure 4.7B). Work in the previous chapter demonstrated that tight junctions and adherens junctions are still present following siRNA-mediated knockdown of MarvelD3, ruling out the possibility that MarvelD3 depletion increases proliferation by breaking cell-cell contacts. Thus MarvelD3 may play a specific role in the regulation of proliferation in epithelial cells.

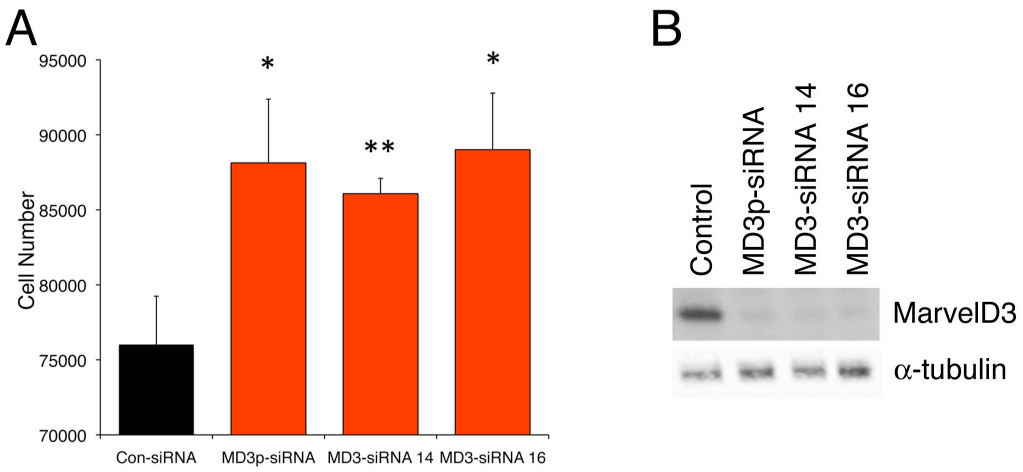

Figure 4.7 – MarvelD3 depletion results in increased proliferation of Caco-2 cells. Caco-2 cells were plated in quadruplicate at the same cell density and transfected with control or MarvelD3-specific siRNAs. Cell number was quantified after 3 days using a CyQUANT proliferation assay kit. (A) Caco-2 cells depleted of MarvelD3 show significantly increased cell numbers in comparison to control cells. Shown are mean cell numbers plus standard deviation (n=4) representative of 3 independent experiments. (B) Immunoblotting for MarvelD3 was used to confirm depletion of the endogenous protein. Significance was determined by Student's t-test *$p<0.05$, **$p<0.01$.

Since metastasis is also an important part of the tumourigenic process and given the recently reported role for occludin in regulating migration (Du et al., 2010), the effect of MarvelD3 expression on cell migration was also determined. This question was first addressed using the control and MarvelD3-expressing MiaPaCa cells under the assumption that an effect on migration would be most apparent in this highly migratory cell type. Cells were plated in to cell culture inserts, which, upon reaching confluency, were removed to reveal a 500μm cell-free space. Migration of the cells into the cell-free space was monitored at regular intervals by brightfield microscopy until the most migratory cells showed approximately 80% wound closure. Quantification of wound closure showed control MiaPaCa cells to migrate into the cell-free space more rapidly than MarvelD3-expressing cells (Figure 4.8). In the time it took control cells to close the wound by 80%, MarvelD3 expressing clones C2 and C8 demonstrated approximately 6% and 40% closure, respectively. Thus MarvelD3 expression appears to inhibit migration in MiaPaCa cells.

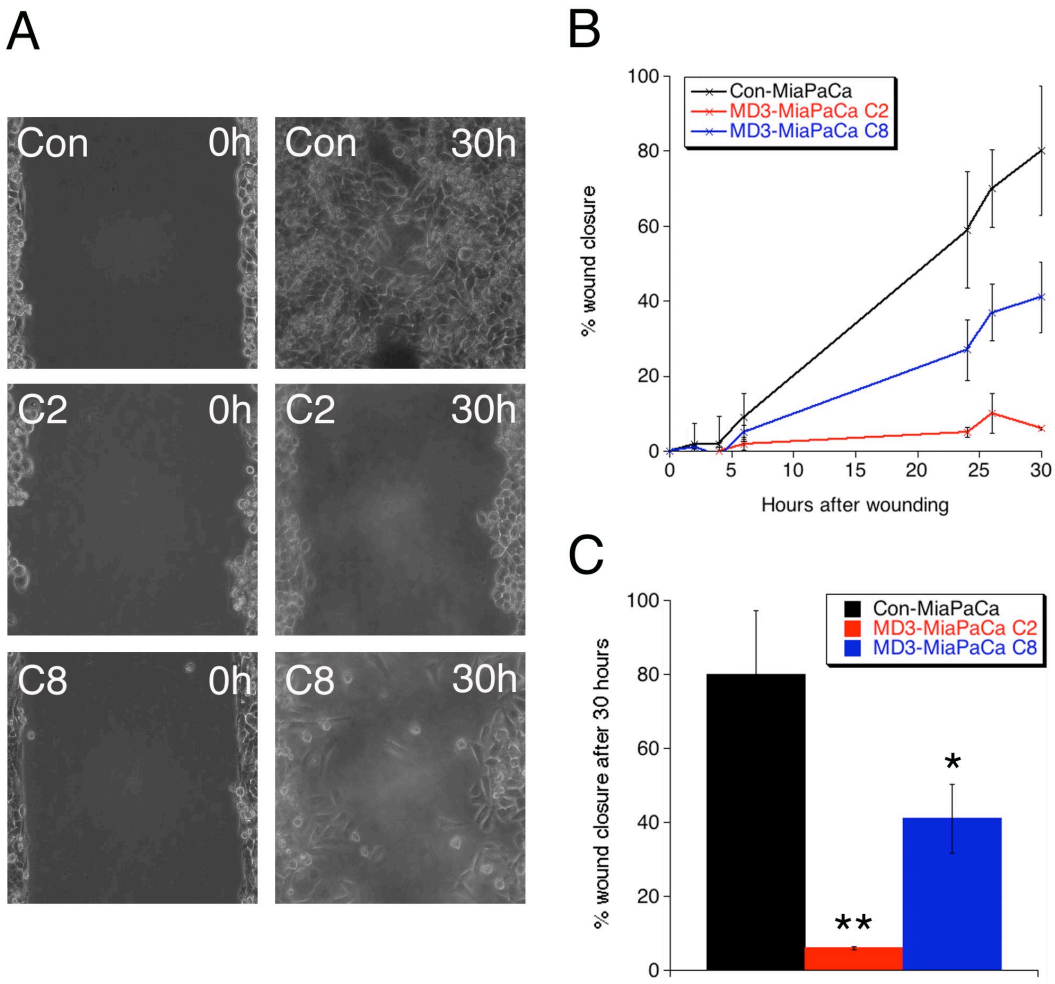

Figure 4.8 – MarvelD3 expression reduces migration in MiaPaCa cells. MiaPaCa cells (control and MarvelD3-expressing clones) were plated into cell culture inserts and grown until confluent. Inserts were then removed and cell migration monitored by light microscopy. (A) Phase-contrast images show reduced migration into the cell-free space by MarvelD3-expressing C2 and C8 cells in comparison to control MiaPaCa cells. (B) Quantification of migration shows control cells to begin migrating into the cell-free space more rapidly than MarvelD3-expressing cells, and result in significantly greater closure of the wound area, also represented in (C). Images were quantified using ImageJ software. Shown are mean values (n=3) from a single representative experiment. Error bars represent the standard deviation. Significance was calculated by Student's t-test; **p<0.01, *p<0.05.

It is important to note that control MiaPaCa cells do not form cell-cell contacts and migrate as single cells, while the cell-cell contacts formed following expression of MarvelD3 means C2 and C8 cells migrate collectively. The difference in migration speeds between these two groups, therefore, could be due to the transition from single to collective cell migration and not necessarily a MarvelD3-specific effect. To see if MarvelD3 may have a signalling role in the regulation of migration, the migration assay was repeated with Caco-2 cells depleted of MarvelD3, which retain cell-cell contact, but lack MarvelD3 at the tight junction. Migration in to the cell-free space following insert removal showed MarvelD3-depleted cells to migrate more rapidly than control cells (Figure 4.9). Migration assays were performed in the presence of 10μg/ml Mitomycin c to ensure the effect seen is due to increased migration, and not increased proliferation, which is also thought be regulated by MarvelD3. Brightfield imaging showed MarvelD3-depleted cells kept their sheet-like morphology like control cells, and knockdown of MarvelD3 did not result in cells breaking free from the monolayer and migrating in to the cell-free space. This suggests loss of MarvelD3 results in increased collective migration of Caco-2 cells.

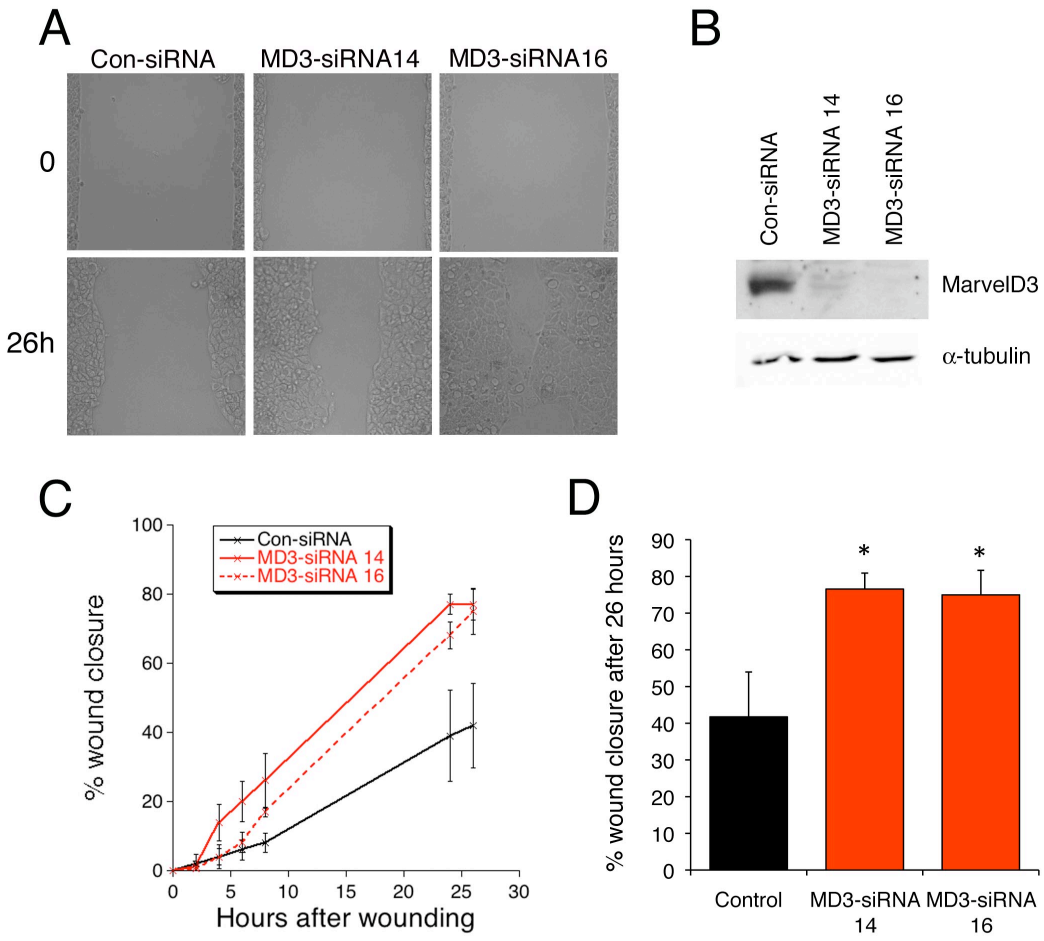

Figure 4.9 – Depletion of endogenous MarvelD3 increases migration in Caco-2 cells. Caco-2 cells transfected with control or two individual MarvelD3-specific siRNAs (14 and 16) were plated into cell culture inserts to reach confluency after 2 days. (A) Brightfield microscopy was used to track migration of cells into the cell-free space following insert removal. (B) Immunoblotting was used to confirm knockdown of the endogenous MarvelD3 protein, with α-tubulin as a loading control. (C) Cell migration was quantified by calculating the area of the cell-free space at each time point and represented as a % of the original area. MarvelD3-depleted cells can be seen to migrate more rapidly into the space than control cells, to cover a greater proportion of the original cell-free space by the end of the experiment, also represented in (D). Migration images were quantified using ImageJ software. Shown are the means (n=3) of a single representative experiment, plus the standard deviation. Significance was calculated with a Student's t-test; *$p<0.05$.

Since junctions are maintained in the absence of MarvelD3, these data together suggest that MarvelD3 may function in the regulation of intracellular signalling pathways in order to regulate epithelial cell proliferation and migration from the tight junction. The rest of this chapter is dedicated to elucidating a mechanism through which this may be achieved.

MarvelD3 expression regulates the expression of genes involved in cell proliferation and migration

To begin to address how MarvelD3 may be regulating epithelial cell proliferation and migration, a microarray was performed comparing changes in mRNA transcripts between control and MarvelD3-expressing MiaPaCa cells, to obtain a profile of the potential signalling pathways affected by expression of MarvelD3. The microarray was performed by Tony Brooks, UCL Institute of Child Health, and of a list of significant genes provided from this analysis, data was analysed further using GeneSpring and DAVID software. These analyses revealed that expression of MarvelD3 in MiaPaCa cells resulted in changes in the expression of a number of genes involved in proliferation and migration, among others. Focusing on genes involved in proliferation and migration, or otherwise relevant to the tight junction, figure 4.10 shows genes affected by MarvelD3 expression. Pathway analysis using GeneSpring software based on 170 genes that were at least 2-fold differentially regulated further revealed the importance of EGFR signalling and Wnt signalling, both heavily implicated in tumourigenesis. Potential hits of the microarray were validated by immunoblotting cell lysates using antibodies already available in the lab. MiaPaCa cells grown in the same way as those harvested for RNA prior to microarray

analysis were used for this validation. Figure 4.10B confirms EGFR, integrin-linked kinase (ILK), ETS1, Stat3, Smurf1, CDK6 and (phospho-)Smad3/1 are changed at the protein level, as well as at the level of the transcript. To confirm the functional importance of reduced EGFR expression following MarvelD3 expression the proliferation of control, MD3-MiaPaCa C2 and MD3-MiaPaCa C8 cells in response to EGF was quantified. MarvelD3-expressing MiaPaCa cells did not increase their proliferation in response to addition of EGF, but control cells did (Figure 4.10C). This suggests MarvelD3 expression reduces responsiveness to EGF, likely by reducing expression of the EGFR.

A

Gene symbol	Gene name	Function	Fold change
CDK6	cyclin-dependent kinase 6	Cell cycle	-5.74
DKK1	Dikkopf homolog 1	Wnt signalling	-3.25
FZD4	Frizzled homologue 4	Wnt signalling	-4.72
F2R	coagulation factor II (thrombin) receptor	Wnt signalling	+11.2
SFRP1	Secreted frizzled-related protein 1	Wnt signalling	-5.06
DLG1	Discs large homologie	Wnt signalling	-3.94
EGFR	Epidermal growth factor receptor	Proliferation	-1.98
Smad3	Smad family member 3	EGFR pathway, TGFbeta signalling	+1.39
Stat3	Signal transducer and activator of transcription 3	EGFR pathway	-1.7
EPS8	EGFR kinase substrate 8	EGFR pathway	-7.36
Pxn	Paxillin		-1.43
Usp6NL	USP6 N terminal-like 6	EGFR pathway	-2.1
FADD	Fas-associated receptor with death domain	TNFa/NFkB signalling, apoptosis	+1.97
RASAL2	Ras protein activator-like 2	TNFa/NFkB signalling	+3.25
TSPAN1	Tetraspanin 1	Cell motility	-5.82
TNFSF4	TNF ligand	TNFa signalling	+10.8
RTN1	Reticulon 1	DNA binding, apoptosis	+6.92
NPAS2	Neuronal PAS domain-containing protein 2	Transcription factor, cell cycle regulation	-8.51
CLDN11	Claudin 11	Tight junction	+8.4
MSX2	muscle segment homeobox 2	Repressor of transcription, cell survival, Ras signalling, epithelial-mesenchymal signalling	+4.63
ETS1	v-ets erythroblastosis virus E26 oncogene homolog 1	Invasion, angiogenesis, development	-2.23
CORO1C	Coronin 1C	signal transduction, cell cycle progression, apoptosis	-1.59
APC7	Anaphase promoting complex, subunit 7	Cell cycle	-1.67
APC5	Anaphase promoting complex, subunit 5	Cell cycle	-1.68
ARPC2	Actin related protein 2/3 complex, subunit 2	Cytoskeleton regulation	-1.44
ARPC3	Actin related protein 2/3 complex, subunit 3	Cytoskeleton regulation	-2.01
CAV1	Caveolin 1	Endocytosis	-2
Smurf1	SMAD specific E3 ubiquitin protein ligase 1	Smad (1 and 5) inactivation	-2.71
ILK	Integrin-linked kinase	migration, proliferation, differentiation	-2.13
CLDN1	Claudin 1	Tight junction	+2.35
CLDN12	Claudin 12	Tight junction	-1.67

B

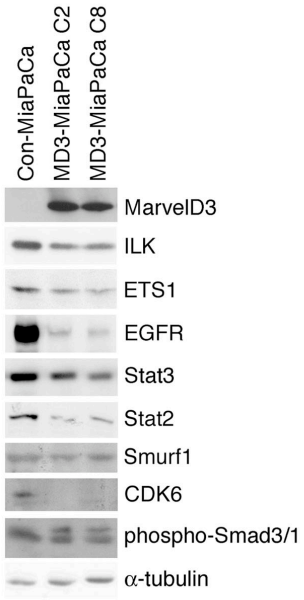

C

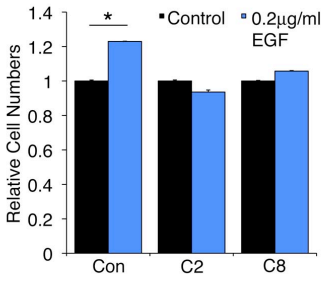

Figure 4.10 – Genes regulated by expression of MarvelD3 in MiaPaCa cells. (A) Shown is a list of genes involved in proliferation and migration affected by MarvelD3 expression in MiaPaCa cells. Fold changes are shown and colour-coded; green for increased expression, blue for reduced expression. (B) For validation purposes, MiaPaCa control and MarvelD3-expressing cell lysates were separated by SDS-PAGE and immunoblotted for differentially expressed proteins identified in the microarray. α-tubulin was used as a loading control. (C) Reduced EGFR expression leaves MD3-MiaPaCa C2 and C8 cells unresponsive to EGF in CyQuant proliferation assay. Only control cells increased cell number in response to EGF. Shown are mean cell numbers normalised to control for each MiaPaCa cell type (n=4) plus normalised standard deviation. Significance was calculated by Student's t-test; *$p<0.05$ compared to control (i.e. without EGF).

Regulation of transcription factor-specific promoter activity by MarvelD3 expression

The microarray analyses performed in MiaPaCa cells alluded to the ability of MarvelD3 expression to regulate the expression of genes involved in proliferation and migration. It was therefore reasoned that expression of MarvelD3 must somehow modulate the transcriptional activity of certain promoters in order to elicit these effects of gene expression. To test this hypothesis, transcription factor-specific reporter plasmids, consisting of transcription-factor-responsive promoter elements reading in to a firefly luciferase reporter gene and a separate, eBM2 mutant promoter upstream of a renilla luciferase reporter gene, were cotransfected into cells alongside a plasmid encoding MarvelD3 isoform 1 (MD3_1) or isoform 2 (MD3_2), occludin or a control plasmid. Occludin overexpression was used to determine the specificity of promoter regulation to MarvelD3. The ability of MarvelD3 and occludin expression to affect promoter activity was first assessed in MDCK cells due to their ease of transfection. Figure 4.11 shows the effect of expressing each isoform of MarvelD3 or occludin on the activity of a number of transcription-factor-specific promoters relative to the promoter activity in control MDCK cells. Expression of both MarvelD3 isoforms resulted in reduced activity of promoters regulated by the serum response element (SRE), AP1, myc, cyclinD1 and ZONAB, but not at the TCF promoter, suggesting some specificity in the effects of MarvelD3. Since ZONAB is a repressor of this promoter, the reduction in promoter activity illustrates an increase in ZONAB signalling following expression of MarvelD3. Interestingly, AP1 signalling, cyclinD1, SRE, ZONAB and myc all have previously reported roles in cell proliferation and/or cell migration. In addition, the presence of AP1-binding sites in the promoters of cyclinD1 and myc, and the ability of AP1 signalling to regulate the

activity of the SRE suggested regulation of the AP1 promoter could be the significant role of MarvelD3 in regulating gene expression. Furthermore, occludin expression significantly reduced activity of the SRE, cyclinD1 and myc promoters, but not of AP1, suggesting this regulation may be specific for MarvelD3.

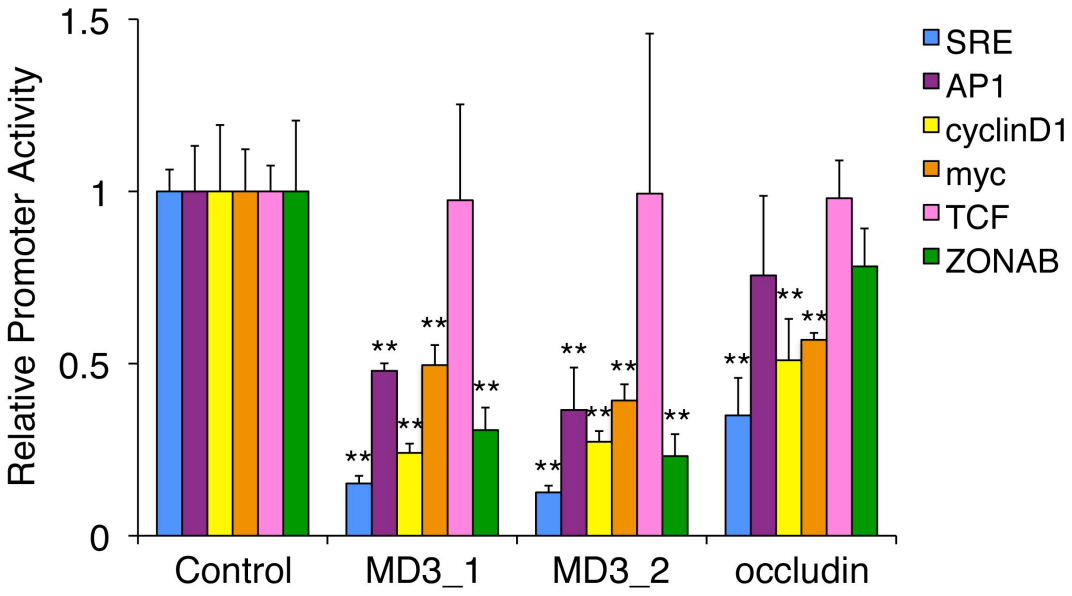

Figure 4.11 – Regulation of transcription factor-specific promoters by MarvelD3 isoforms and occludin. MDCK cells were plated on to 96 well plates and transfected with cDNAs encoding MarvelD3 isoform 1, isoform 2, occludin or a control plasmid, alongside a luficerase reporter construct and a renilla control plasmid. Promoter activity was detected using a Dual luciferase reporter assay kit and luminescence signals for firefly and renilla luciferase activity were measured sequentially on a microplate reader. Ratios of firefly luciferase to renilla luciferase activity were calculated, averaged (n=3) and normalised to control-transfected cells to give relative promoter activity values. Expression of both isoforms of MarvelD3 attenuated SRE, AP1, myc, and cyclinD1 promoter activity. TCF promoter activity is not affected by MarvelD3 expression in MDCK cells. Error bars represent the standard deviation. Significance was calculated by Student's t-test; **p<0.01 compared to promoter activity in control cells.

Regulation of the AP1 promoter by MarvelD3

To confirm regulation of the AP1 promoter by MarvelD3, the luciferase reporter assay was repeated in Caco-2 and MiaPaCa cells. Consistent with the observations made in MDCK cells, expression of either isoform of MarvelD3 caused a significant reduction in AP1 promoter activity when compared to control cells (Figure 4.12). AP1 promoter activity was not affected by expression of occludin. It is also notable that MD3_2 appeared to reduce AP1 promoter activity more than MD3_1 in all cell types tested. While isoform-specific differences have not been a focus of this thesis, it is interesting that the isoforms appear to display slightly different properties, especially when the differential tissue expression patterns are considered.

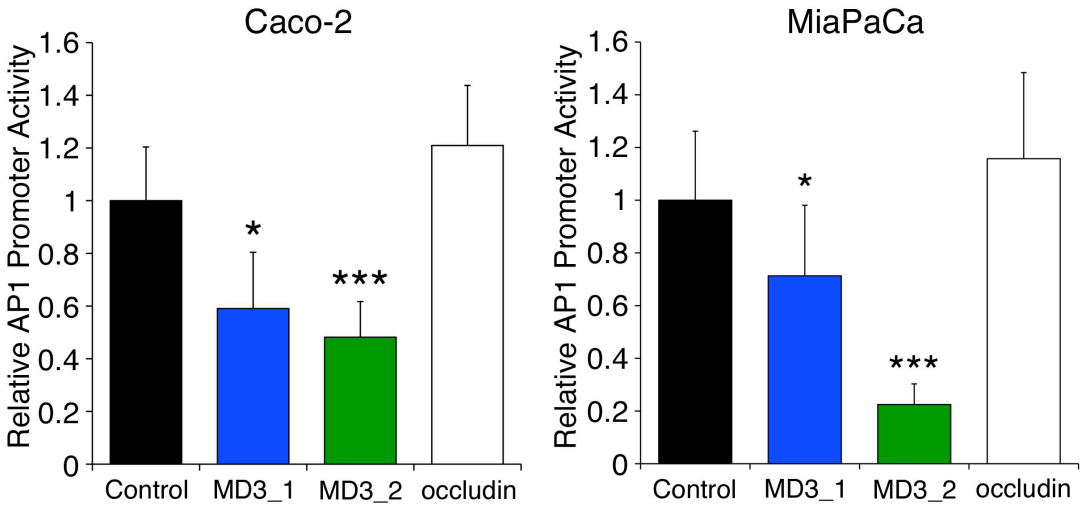

Figure 4.12 – MarvelD3 regulates AP1 promoter activity in Caco-2 and MiaPaCa cells. Caco-2 and MiaPaCa cells were transfected with control plasmid or that encoding MarvelD3 isoform 1 or isoform 2, alongside the AP1-firefly reporter plasmid and a Renilla control. Detection of firefly and Renilla luciferase luminescent signals showed AP1 promoter activity to be reduced in both cell types following expression of both isoforms of MarvelD3, but not occludin. Relative promoter activity was calculated as previously described (n=3) and error bars represent standard deviation. Significance was calculated by Student's t-test; *p<0.05, ***p<0.001.

Since the reporter assays performed so far have relied upon over-expressing MarvelD3, it was asked if depletion of MarvelD3 resulted in increased transcriptional activity. To address this question, Caco-2 cells were plated into 96-well plates and transfected with control or MarvelD3-specific siRNAs according to the standard transfection protocol. Reporter plasmids were then transfected 48 hours later. Medium was changed after overnight incubation in transfection mix, and promoter activity was assayed after a further 6 hours. Interestingly, depletion of MarvelD3 did not result in an increase in AP1 promoter activity (data not shown), despite the

consistent and substantial reductions following MarvelD3 overexpression. Since these studies were performed in unstimulated cells, it is possible that, if MarvelD3 acts as a brake on AP1 signalling, loss of MarvelD3 alone may not be enough to potentiate AP1 promoter activity. Perhaps, MarvelD3 depletion in combination with the addition of an inducer of AP1 activity is necessary in order to be able to observe the effect of loss of MarvelD3.

In addition to EGFR expression being transcriptionally regulated by AP1 signalling (Johnson et al., 2000), AP1 is also a major downstream target of signalling induced by EGF (Whitmarsh and Davis, 1996). The microarray analysis above implicated MarvelD3 expression in the regulation of the EGFR pathway and MiaPaCa cells expressing MarvelD3 failed to respond to EGF in a proliferation assay. Taken together with the observation that MarvelD3 expression reduces AP1 promoter activity and the presence of multiple AP1 sites in the EGFR promoter, it was hypothesised that MarvelD3 may function in regulating expression of the EGFR via regulation of AP1 signalling. Despite there being no potentiation in AP1 promoter activity in MarvelD3-depleted cells, however, immunoblotting cell lysates suggested increased levels of EGFR protein following loss of MarvelD3 and increased AP1 promoter activity in response to EGF (Figure 4.13). Therefore, MarvelD3 expression in Caco-2 and MiaPaCa cells appears to regulate expression of the EGFR and subsequently affects AP1 activity and proliferation in response to EGF. Furthermore, depletion of MarvelD3 resulted in increased levels of cyclinD1 protein and activity of the cyclinD1 promoter, a previously reported downstream target of the EGFR (Figure 4.14). While the mechanism behind the increased EGFR levels remains to be determined, these data allude to a function for MarvelD3 in the regulation of the EGFR pathway.

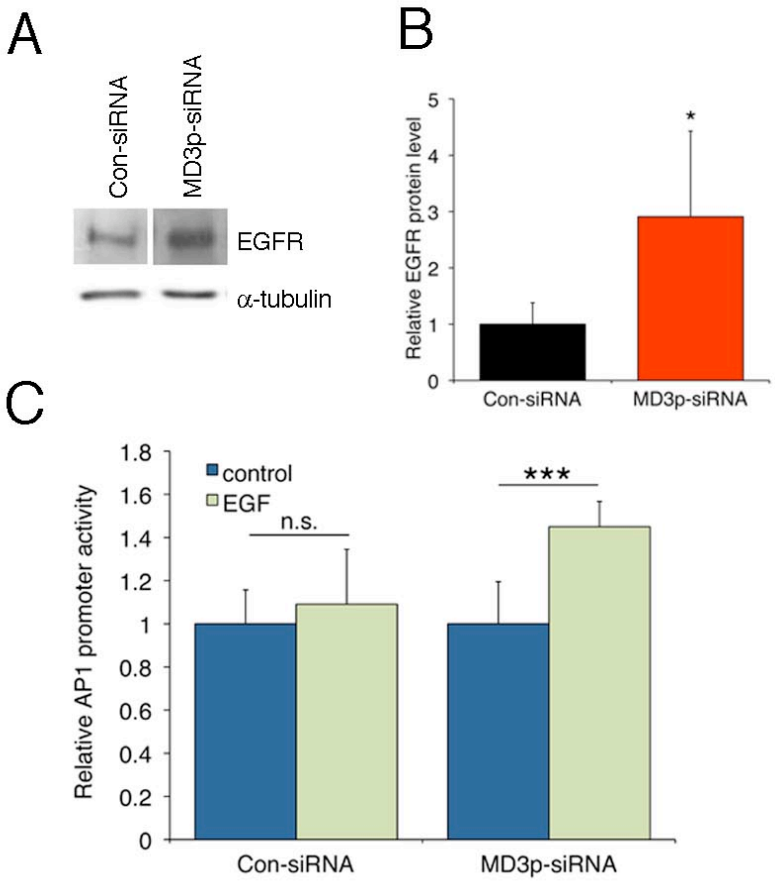

Figure 4.13 – Effect of MarvelD3 depletion on EGFR expression and AP1 promoter activity in response to EGF. (A) Immunoblotting MarvelD3-depleted Caco-2 cell lysates showed an increase in EGFR protein in comparison to controls. Con-siRNA and MD3p-siRNA samples were run on the same gel and are shown with α-tubulin as a loading control. (B) Quantification of band intensities from 3 independent experiments using ImageJ software confirmed increased EGFR protein in cells depleted of MarvelD3. (C) Control and MarvelD3-depleted Caco-2 cells expressing AP1-firefly luciferase and Renilla luciferase control reporter constructs were incubated with 0.2μg/ml EGF or the appropriate volume of water (control) for 24 hours at 37°C. Detection of firefly and Renilla luciferase luminescent signals showed AP1 promoter activity to be potentiated in response to 0.2μg/ml EGF in the absence of MarvelD3, but not in control cells. All treatments were performed in quadruplicate and shown are mean values of a representative experiment. Significance was calculated by Student's t-test, *** $p<0.01$, *$p<0.05$, n.s. = not significant.

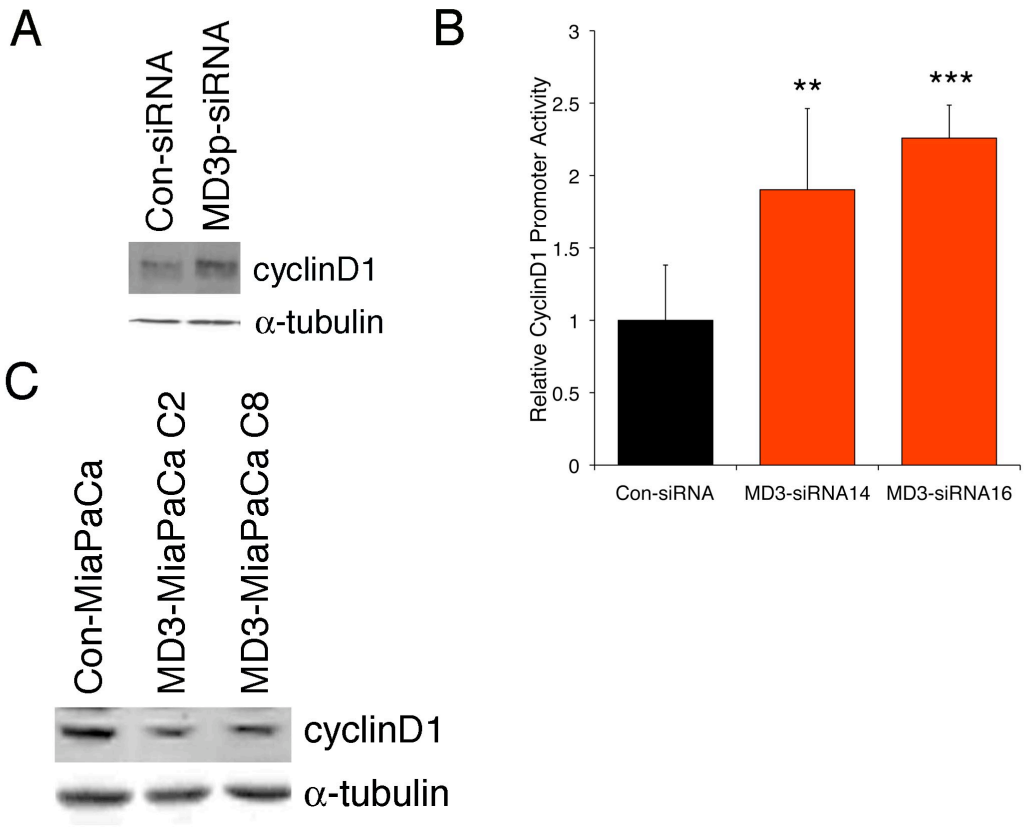

Figure 4.14 – Effect of MarvelD3 on cyclinD1 expression. (A) Caco-2 cells depleted of MarvelD3 show increased levels of cyclinD1 protein when compared to control transfected cells. (B) Activity of the cyclinD1 promoter is increased following depletion of MarvelD3 by two independent siRNAs. Shown are mean values representative of three independent experiments (n=4), plus the standard deviation. Significance was determined by Student's t-test. **p<0.01 (C) MarvelD3 expression reduces the level of cyclinD1 protein in MiaPaCa cells. α-tubulin is used as a loading control in both immunoblots.

MarvelD3 regulates cytoskeletal rearrangements during cell migration

Reorganisation of the actin cytoskeleton is a critical event involved in cell migration. Since MarvelD3 appears to play a role in migration of Caco-2 and MiaPaCa cells, it was hypothesised that alterations in MarvelD3 expression may affect rearrangements of the cytoskeleton conducive to migration. To address this, control and MarvelD3-depleted Caco-2 cells monitored during the migration assay on Ibidi cell culture inserts were fixed after 26 hours and stained with phalloidin to observe the effect of MarvelD3 depletion on arrangement of the actin cytoskeleton. Although 26 hours was the end point of the migration assay, the most migratory cells showed approximately 80% wound closure after this time (see above, Figure 4.9) and cells were therefore still considered to be migrating at the time of fixation. Depletion of MarvelD3 resulted in increased numbers of protrusions into the cell-free space from the monolayer (Figure 4.15), suggesting that MarvelD3 may regulate migration by regulating the formation of a constructive leading edge.

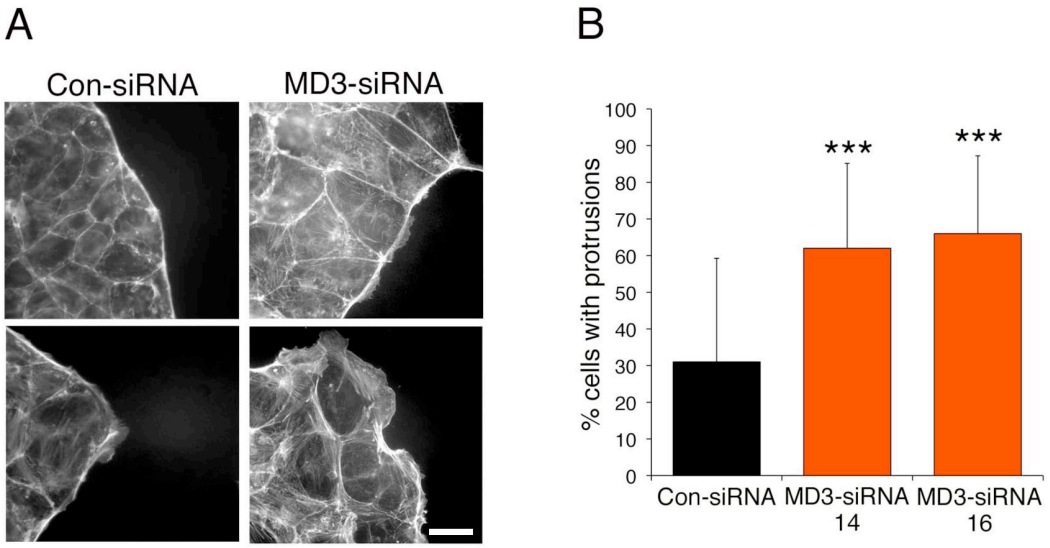

Figure 4.15 – Effect of MarvelD3 depletion on the actin cytoskeleton in migrating Caco-2 cells. Caco-2 cells transfected with control or MarvelD3-specific siRNA were fixed on Ibidi cell culture inserts 26 hours after the onset of migration. (A) Representative F-actin staining shows the actin cytoskeleton in control and MarvelD3-depleted cells. Cells transfected with MD3-siRNA appeared to have more protrusive structures than control cells. (B) Quantification of cell protrusions into the cell-free space shows an increase following depletion of MarvelD3. Counts were made by determining the ratio of cells with protrusions into the cell-free space compared to the total number of cells with an edge exposed to the cell-free space along the full length of the ibidi insert. Shown are the mean values plus the standard deviation from three different plates. ***, $p<0.001$ by Student's t-test. Bar, 10μm.

To further confirm a role in regulation of leading edge formation, migrating MiaPaCa cells were fixed and stained with Cy3-phalloidin to observe the arrangement of the actin cytoskeleton following expression of MarvelD3. Interestingly, while there were protrusive structures in both C2 and C8 MarvelD3-expressing cells, they did not resemble the actin-rich lamellipodia seen in the control cells (Figure 4.16A). Quantification confirmed a reduced number of cell protrusions in both MarvelD3-expressing cells when compared to the controls (Figure 4.16B). Since this

quantification was made of any structure that appeared to protrude from the migration front, they have been termed “protrusions” rather than “leading edges” and may not all be structures supportive of migration. Thus this quantification is likely to be an underestimate of the effect of MarvelD3 on the cytoskeletal rearrangements necessary for cell migration. The reduced number of leading edges in MarvelD3-expressing cells, however, supports the hypothesis that MarvelD3 may play a role in leading edge formation, which is an integral part of the cell migration process.

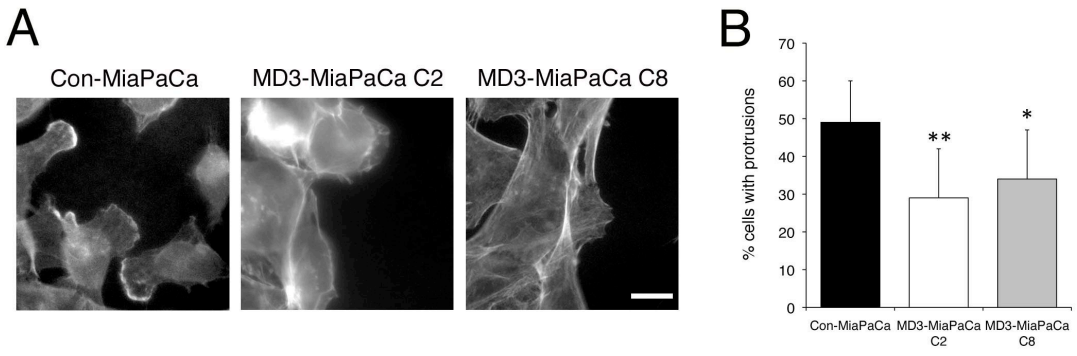

Figure 4.16 – Effect of MarvelD3 expression on the actin cytoskeleton in migrating MiaPaCa cells. (A) Migrating MiaPaCa cells were fixed and stained with phalloidin to observe the arrangement of the actin cytoskeleton following the expression of MarvelD3. Actin-rich lamellipodia can be seen in control MiaPaCa cells, but not in MarvelD3-expressing C2 or C8 clones. C2 and C8 cells show some protrusive structures at the migration front. (B) Quantification of immunofluorescence images shows a reduction in protrusive structures following expression of MarvelD3 in comparison to controls. n=112, 114 and 259 for control, C2 and C8 cells respectively. Bar, 5μm.

Taken together, the data presented suggests a role for MarvelD3 in the regulation of epithelial cell proliferation and migration by affecting the expression of genes

involved in these processes and regulating the cytoskeletal rearrangements involved in cell migration. To appreciate how this is achieved, the next step will be to elucidate the events upstream that link MarvelD3 at the cell membrane to events in the nucleus and underlying cytoplasm.

Discussion

The experiments described above suggest a role for MarvelD3 in the regulation of epithelial proliferation and migration. Loss of MarvelD3 from metastatic tumour cell lines and the increased proliferation and migration observed following siRNA-mediated depletion of MarvelD3 suggests MarvelD3 may function as a tumour suppressor at the tight junction. Consistently, expression of MarvelD3 in tumour cells lacking the endogenous protein resulted in the formation of a more epithelial, sheet-like morphology and cells became less migratory and less proliferative. As MarvelD3-depleted cells retain cell-cell contacts but lack MarvelD3 at the tight junction, it is proposed that MarvelD3 regulates these processes via intracellular signalling pathways and not indirectly by breaking cell-cell contacts. Reduced expression levels of the EGFR following MarvelD3 expression in MiaPaCa cells prompted the hypothesis that MarvelD3 may regulate both proliferation and migration by impacting on the activity of EGFR signalling. Reporter assays suggested inhibition of AP1 promoter activity following MarvelD3 expression. As the EGFR both regulates and is regulated by AP1 signalling, impacting upon AP1-mediated gene expression could be one mechanism by which MarvelD3 inhibits proliferation and migration.

Exogenous expression of MarvelD3 results in a partial restoration of epithelial morphology in MiaPaCa cells

The reduction or loss of MarvelD3 in a number of metastatic tumour cell lines tested suggested that MarvelD3 may play a role as a tumour suppressor. To investigate this further, exogenous MarvelD3 isoform 1 (MD3_1:VSV) was expressed in MiaPaCa

cells, which lack the endogenous protein expressed in the healthy pancreas. Strikingly, MarvelD3 expression induced an epithelial-like morphology with MarvelD3 expressing cells growing in distinct colonies and remaining in contact with their neighbours in contrast to the single cell behaviour of control MiaPaCa cells. MarvelD3 expression, however, did not lead to redistribution of other junctional proteins to contact sites, with occludin and E-cadherin retaining the cytoplasmic, vesicular-like staining observed in untransfected cells. Interestingly, despite there being no interaction between MarvelD3 and ZO-1 in pulldown assays, ZO-1 is recruited to early sites of cell contact in MarvelD3-expressing MiaPaCa cells. Thus expression of MarvelD3 appears to be sufficient for the formation of basic cell-cell contacts and maybe be capable of initiating the formation of simple protein complexes.

Regulation of proliferation and migration by MarvelD3

Analysis of proliferation and migration in response to MarvelD3 expression levels demonstrated that MarvelD3 inhibits proliferation and migration of both MiaPaCa and Caco-2 cells. Interestingly, depletion of MarvelD3 in Caco-2 cells resulted in increased proliferation and migration without disrupting cell-cell contacts, suggesting MarvelD3 may possess some signalling activity that enables this regulation rather than an indirect effect of breaking down cell-cell junctions.

Microarray analyses of RNA extracted from MarvelD3 expressing and control MiaPaCa cells demonstrated that many genes involved in proliferation and migration

were affected by MarvelD3 expression. The microarray was performed as an initial strategy to identify potential pathways that may be being regulated by MarvelD3. As described above, the protein assemblies formed at the cell-cell contact sites following MarvelD3 expression in MiaPaCa cells are less complex than those found at endogenous tight junctions. It is possible, therefore, that some signalling partners/modules may not be present and subsequently downstream signalling pathways that may normally be regulated by MarvelD3 may have been missed. In recognition of this, the microarray was used to initially highlight potential pathways of interest that could then be investigated further using additional protocols and in other cell types. The microarray data was also a useful resource to confirm results found by other approaches.

Initial pathway analysis of microarray data highlighted the EGFR signalling pathway as being significantly altered following MarvelD3 expression in MiaPaCa cells. Elevations in EGFR activation due to increased receptor expression levels or increased availability of its ligands, including EGF and TNFα, confers significant growth and survival advantages and is reported in numerous types of cancer, including pancreatic cancer (Korc et al., 1992). The high levels of EGFR displayed by MiaPaCa cells in the current study were greatly reduced upon expression of MarvelD3 at both the transcript and protein levels. This reduction in EGFR significantly diminished the responsiveness of MiaPaCa cells to EGF in a proliferation assay. The increase in EGFR levels following siRNA-mediated depletion of MarvelD3 further suggested that MarvelD3 might regulate EGFR signalling by regulating the expression of the EGFR itself. It would be interesting to

test this hypothesis by determining whether or not expression levels of MarvelD3 and EGFR correlate in tumour cell lines and primary tumour samples.

The promoter of the EGFR contains multiple AP1 response elements that ensure its expression in response to AP1 signalling (Johnson et al., 2000). Since EGFR activation itself activates AP1 signalling, this establishes a positive feedback loop that further amplifies the activity of the EGFR pathway in response to ligand binding (Grose, 2003). Inhibition of AP1 activity by MarvelD3 may therefore result in the attenuated expression of the EGFR gene and protein observed in MiaPaCa cells. This could be confirmed by performing reporter assays with the wild-type EGFR promoter and those with mutated AP1 binding sites and assaying the effect of MarvelD3 on promoter activity. If MarvelD3 regulates EGFR expression via AP1, only those constructs containing the responsive AP1 binding sites should be affected by MarvelD3 expression. AP1-mediated regulation of EGF signalling could be how MarvelD3 regulates epithelial cell proliferation and migration. The increased EGFR protein levels in unstimulated MarvelD3 knockdown cells without increased AP1 promoter activity, however, suggests there could be additional factors by which MarvelD3 regulates EGFR expression. Smad3 and Smad4 have been shown to cooperate with AP1 to mediate gene transcription induced by TGFβ (Zhang et al., 1998). Therefore, while overexpression of MarvelD3 may be sufficient to inhibit JNK activity and AP1 activity, loss of MarvelD3 and the proposed increase in JNK activity may not be sufficient to increase AP1 signalling if the activities of cooperation partners are not equally upregulated. Addition of AP1-promoting signals, like TGFβ, to control and MarvelD3-depleted cells may enable the identification of

potential signalling pathways that could converge with MarvelD3-regulated JNK-MAPK pathway at promoter sites regulated by AP1.

It has also been reported that inhibition of the EGFR in pancreatic cancer cells results in reduced nuclear localisation of ZO-1 (Takai et al., 2005). Interestingly, ZO-1 was recruited to cell-cell contact sites in MarvelD3-expressing MiaPaCa cells despite there being no interaction between MarvelD3 and ZO-1 in pulldown assays. Inhibition of EGFR signalling by MarvelD3, therefore, may also regulate proliferation by altering the localisation of ZO-1 and perhaps its binding partner and regulator of proliferation, ZONAB (Balda and Matter, 2000). Somewhat surprisingly, reporter assay data demonstrated an increase in ZONAB signalling following expression of MarvelD3 isoforms 1 and 2. Since increased ZONAB signalling is associated with increased proliferation, this was unexpected and suggests MarvelD3 does not mediate its inhibition of proliferation via ZONAB. The functional significance of MarvelD3-mediated increases in ZONAB transcriptional activity, however, requires further investigation. Immunoflourescent analysis of the nuclear to junctional ratios of ZO-1 and ZONAB with respect to MarvelD3 expression may help to determine how MarvelD3 impacts on the ZO-1-ZONAB signalling pathway.

Cell cycle regulators were also highlighted in the microarray. Immunoblotting cell lysates from unsynchronised MiaPaCa cell cultures demonstrated reductions in CDK6 and cyclinD1 protein levels in MarvelD3-expressing MiaPaCa cells. MarvelD3 expression also reduced cyclinD1 promoter activity in MDCK cells, thus regulation of cell cycle progression by reducing the availability/formation of cyclinD1/CDK6

complex could be another mechanism through which MarvelD3 regulates proliferation. In keeping with this hypothesis, depletion of MarvelD3 potentiated cyclinD1 promoter activity and increased the amount of cyclinD1 protein in Caco-2 cells. Since MarvelD3 depletion was not sufficient to increase AP1 promoter activity, however, it is possible that MarvelD3 regulates the cyclinD1 promoter by a mechanism other than AP1. Interestingly, activated Stat3 has previously been shown to correlate with elevations in cyclinD1 protein levels (Leslie et al., 2006). In the current study, MarvelD3 expression reduced the levels of Stat3 transcript and protein, and therefore could explain the reduced levels of cyclinD1 in MarvelD3-expressing MiaPaCa cells. Levels of Stat3 in MarvelD3-depleted cells should be assessed to determine if MarvelD3 could be regulating cyclinD1 promoter activity via Stat3. The effect of MarvelD3 expression on Stat3 localisation in response to EGFR activation should also be determined. Though further work is required to determine the underlying mechanism, the regulation of cyclinD1 and progression through the cell cycle is another mechanism by which MarvelD3 may regulate cell proliferation.

The inhibition of epithelial cell migration following MarvelD3 expression suggests MarvelD3 and occludin have opposite effects on the regulation of migration. Depletion of occludin reduced the rate of wound closure of MDCK cells (Du et al., 2010), while MarvelD3 knockdown in the current study increased Caco-2 cell migration. In addition, occludin depletion resulted in reduced numbers of cellular protrusions (Du et al., 2010), while MarvelD3 depletion appeared to promote protrusion formation, implicating both proteins in the regulation of the actin cytoskeleton during migration. The activation and localisation of Rac1 at the leading

edge, which regulates lamellipodia formation during cell migration, was attenuated in occludin-depleted cells, implicating occludin in the localised activation of this RhoGTPase (Du et al., 2010). Preliminary studies have suggested that Rac1 may be inhibited following the expression of MarvelD3 in MiaPaCa cells (data not shown), but this needs to be confirmed. It is also important to realise that the effects of occludin and MarvelD3 upon migration have been studied in different cell types and therefore require some standardisation before firm conclusions can be drawn. Based on current observations, however, it is interesting to speculate that occludin and MarvelD3 may serve opposing roles in regulation of the actin cytoskeleton during cell migration.

In conclusion, loss of MarvelD3 expression, which is observed in a number of metastatic tumour cell lines, resulted in increased proliferation and migration of Caco-2 cells. Microarray analysis suggested MarvelD3 expression might regulate these processes by impacting on, and inhibiting, the activity of the EGFR signalling pathway. In keeping, alterations in MarvelD3 expression levels appeared to affect signalling pathways downstream of the EGFR, with MarvelD3-expressing MiaPaCa cells being less responsive to EGF and MarvelD3-depleted cells displaying elevated AP1 promoter activity following addition of EGF. Furthermore, depletion of MarvelD3 resulted in elevation of cyclinD1 levels, which can also be regulated in response to EGFR signalling. The mechanism behind MarvelD3-mediated regulation of EGFR expression, however, is not yet known. In consideration of the results presented here, however, MarvelD3 may serve a function in maintaining homeostasis of the monolayer in response to growth factor signalling. Absence of this MarvelD3-

mediated inhibition in tumour cells may contribute to the exacerbation of the tumourogenic state. Understanding the timing of loss of MarvelD3 expression during tumour progression may also be useful to see if MarvelD3 is a potential therapeutic target.

Chapter 5:

Regulation of AP1 signalling by MarveID3

Chapter 5 – Regulation of AP1 signalling by MarvelD3

Introduction

The results described in the previous chapter suggested a role for MarvelD3 in the regulation of epithelial cell proliferation and migration. Further analyses suggested this could be mediated by changes in the levels of EGFR signalling components in response to MarvelD3 expression. Furthermore, reporter assays demonstrated that MarvelD3 expression inhibits AP1 promoter activity. As EGFR expression can be regulated by AP1 signalling (Johnson et al., 2000), this could be a potential mechanism through which MarvelD3 impacts upon the EGFR pathway. In addition, due to the presence of AP1 sites in the promoters of a large number of genes involved in a variety of cellular processes, the regulation of AP1 could be a significant cellular function of MarvelD3. To better appreciate this potential function, work in this chapter aimed to elucidate the events upstream of AP1, that link MarvelD3 at the cell membrane to events in the nucleus.

In this chapter, pulldown assays identified an interaction between the N-terminus of MarvelD3 and the MAP kinase kinase kinase MEKK1. The N-terminus of MarvelD3 is also shown to be sufficient for the inhibition of AP1 promoter activity alluding to the importance of this domain in the signalling properties of MarvelD3. In addition, MarvelD3 expression is shown to result in reduced levels of active JNK, which is necessary for proliferation and migration of MiaPaCa cells and suggests MarvelD3 preferentially regulates the JNK branch of the MAPK signalling pathway, over p38 or ERK.

Results

Levels of active JNK are reduced in MarvelD3-expressing MiaPaCa cells

To first determine whether MarvelD3 may regulate AP1 promoter activity via the MAPK pathway, cell lysates from control and MarvelD3-expressing MiaPaCa cells were immunoblotted for levels of phosphorylated (active) and total ERK1/2, JNK and p38 MAPKs. The levels of phospho-JNK were reduced in MiaPaCa cells expressing MarvelD3 in comparison to control cells, while total levels of JNK remained constant (Figure 5.1). Levels of phospho-p38 and phospho-ERK were unchanged in response to MarvelD3 expression (Figure 5.1). This suggests that, in unstimulated cells, increased MarvelD3 expression may inhibit signalling via the JNK branch of the MAPK pathway.

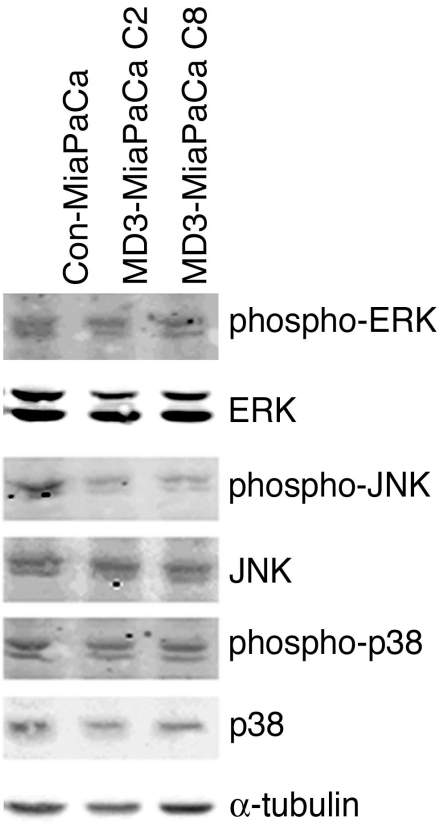

Figure 5.1 – Expression of MarvelD3 results in reduced levels of active JNK in MiaPaCa cells. Control and MarvelD3-expressing MiaPaCa cell lysates were immunoblotted for total and active forms of ERK1/2, JNK and p38 MAPKs. Levels of phospho-JNK are reduced in MarvelD3-expressing MiaPaCa clones C2 and C8 in comparison to control cells. Levels of active p38 and ERK do not change following expression of MarvelD3 in MiaPaCa cells. Immunoblotting is representative of at least 3 independent experiments. α-tubulin was used as a loading control.

JNK activity is necessary for MiaPaCa cell migration and proliferation

JNK activity is heavily implicated in the regulation of cell proliferation and survival and is known to be required for migration in a number of cell types (Huang et al., 2003; Kavurma and Khachigian, 2003). Before investigating whether JNK may be responsible for the proliferation and migration phenotypes observed following

manipulation of MarvelD3 expression levels, the importance of JNK activity for proliferation and migration in control MiaPaCa cells was first determined. First, MiaPaCa cells were incubated in the presence of the JNK inhibitor SP600125 for two hours to determine an appropriate inhibitor concentration in order to inhibit JNK activity. Immunoblotting whole cell lysates revealed 20μM SP600125 was sufficient to reduce levels of active cJun, a JNK substrate, without increasing apoptosis, as was apparent with the higher 50μM concentration (observation made visually). Thus 20μM SP600125 was used in the subsequent experiments (Figure 5.2A).

In order to determine the importance of JNK activity on MiaPaCa cell proliferation, cells were plated at an equal cell density on to a 96 well plate and allowed to adhere overnight. Cells were incubated with the JNK inhibitor SP600125 (20μM) or DMSO for 48 hours before quantifying cell number. As expected, inhibition of JNK activity resulted in reduced cell numbers in comparison to control-treated cells (Figure 5.2B). Verification that extended incubation with SP600125 did not result in cell death was made visually by labelling nuclei with Hoechst; no increase in fragmented nuclei was apparent between control cells and those incubated with 20μM SP600125. To further determine a role for JNK in MiaPaCa cell migration, control MiaPaCa cells were plated in to cell culture inserts and grown until confluent. They were then incubated with the JNK inhibitor SP600125 (20μM) or DMSO for two hours before insert removal to inhibit JNK activity prior to the onset of migration. As expected, MiaPaCa cell migration was significantly reduced following JNK inhibition in comparison to control treated cells. This suggests JNK activity is involved in the regulation of

MiaPaCa cell migration and proliferation, just as has been observed previously in other cell types.

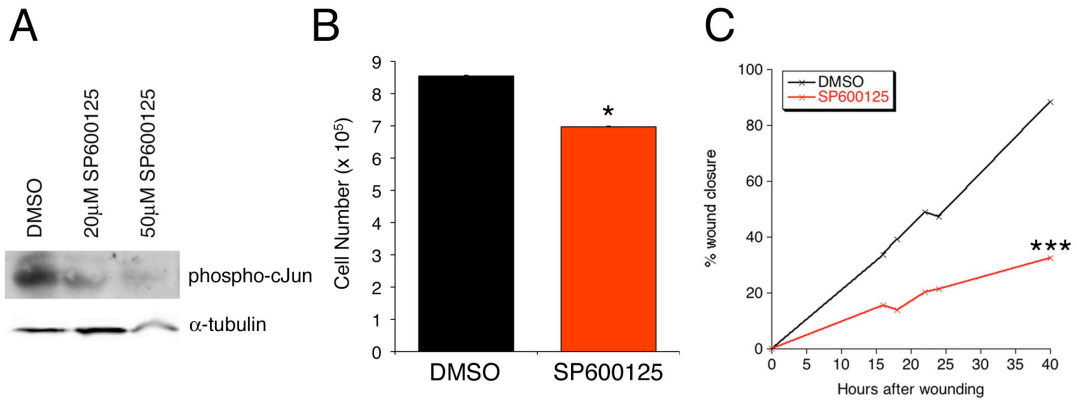

Figure 5.2 – Inhibition of JNK activity reduces proliferation and migration in MiaPaCa cells. (A) Immunoblotting cell lysates for phospho-cJun, a downstream target of JNK, shows reduced levels after 2 hours of SP600125 incubation, suggesting efficient inhibition of JNK. (B) SP600125 reduced increases in cell number of MiaPaCa cells (n=4). (C) MiaPaCa cells were plated onto cell culture inserts and grown until confluent. When confluent, cells were incubated with 20μM SP600125 for two hours prior to insert removal. SP600125 inhibited the migration of MiaPaCa cells following insert removal (n=3). Confirmation that the 20μM SP600125 dose did not cause apoptosis was made visually.

To determine whether JNK activity is important for the regulation of cell migration by MarvelD3, control and MarvelD3-depleted Caco-2 cells were allowed to migrate in the presence and absence of the JNK inhibitor SP600125. As figure 5.3 shows, inhibition of JNK inhibits the migration of control Caco-2 cells and prevents the increase in migration caused by depletion of MarvelD3. This suggests JNK activity is necessary for the increased migration caused by MarvelD3 depletion, and alludes further to the possibility that MarvelD3 may be regulating migration via JNK.

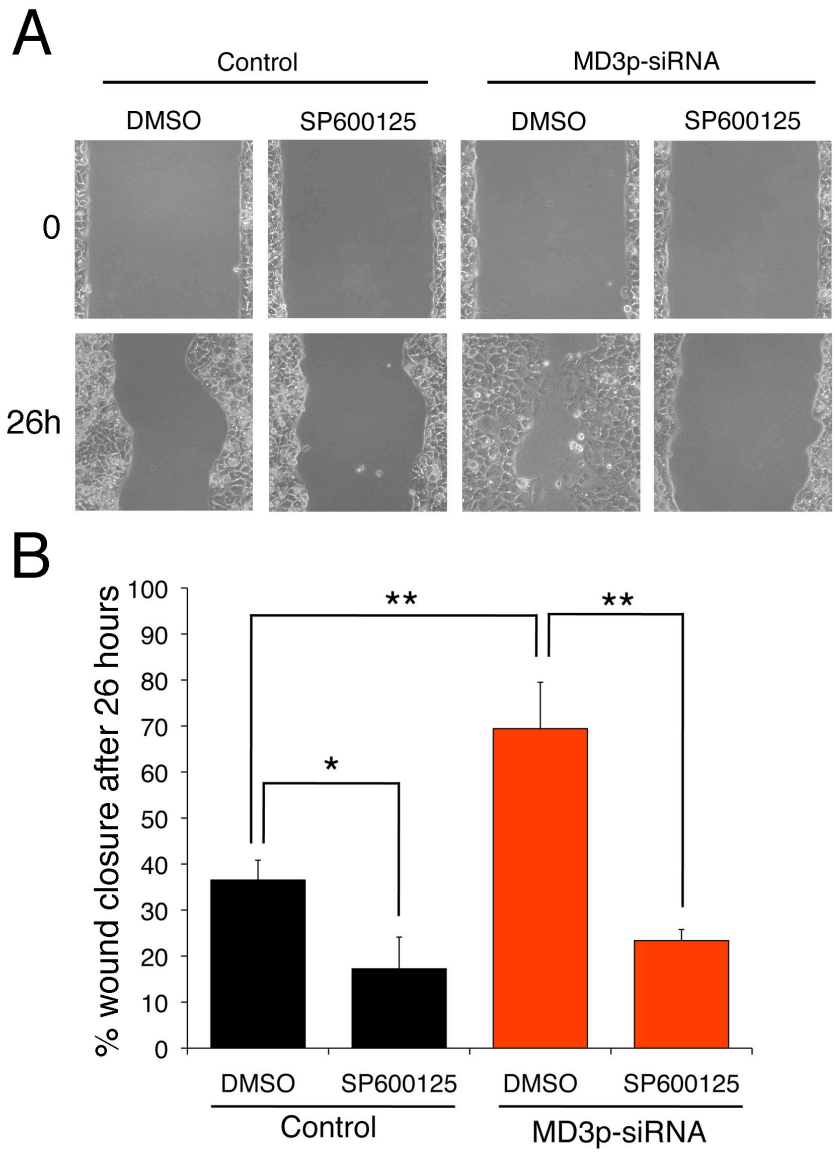

Figure 5.3 – JNK activity is necessary for increased cell migration following MarvelD3 depletion. Caco-2 cells transfected with control or MarvelD3-specific siRNAs were plated on to cell culture inserts, as previously described. Upon reaching confluency, cells were incubated with 20μM SP600125 for 2 hours before insert removal. Cell migration with or without SP600125 was then monitored for 26 hours using brightfield microscopy (A) and quantified with ImageJ software (B). Quantification shows mean values of wound closure (n=3) plus standard deviation. Inhibition of JNK prevented migration of control Caco-2 cells. Depletion of MarvelD3 was not able to increase migration in the absence of JNK activity. Significance was calculated by Student's t-test between groups as shown; *p<0.05, **p<0.01.

The N-terminus of MarvelD3 can interact with MEKK1

The data shown so far suggests MarvelD3 expression inhibits JNK activation and perturbs proliferation and migration in MiaPaCa cells. JNK inhibition also appears to prevent the increased migration resulting from depletion of MarvelD3, which further suggests MarvelD3 may function to inhibit migration by restricting JNK activity. To ascertain how MarvelD3 may achieve this, it was determined how MarvelD3 may feed in to the MAPK pathway. Pulldown assays were performed with GST-fusion proteins of N- and C-termini of MarvelD3 and identified a clear interaction between the N-terminus of MarvelD3 and MEKK1 from Caco-2 cell lysates, but not with other kinase kinase kinases MEKK3 or MLK3 (Figure 5.4A). Though some degradation of the N-terminal domain GST protein can be seen, this does not appear to affect the ability of the N-terminus of MarvelD3 to interact with MEKK1. To check the potential relevance of this interaction *in vivo*, Caco-2 cells were processed for immunofluorescence with antibodies against MEKK1 and occludin as a marker of the tight junction. In addition to the previously reported cytoplasmic localization of MEKK1, MEKK1 was seen to colocalize with occludin at points of cell-cell contact (Figure 5.4B). Immunostaining MarvelD3-depleted cells with anti-MEKK1 antibody showed the continuous peripheral MEKK1 staining to be disrupted or lost following depletion of MarvelD3 by siRNA, suggesting MEKK1 may require MarvelD3 for its localization to cell contacts and further supporting the hypothesis of an interaction between these two proteins (Figure 5.4C). Thus MarvelD3 may be able to regulate AP1 signalling and JNK activity via an interaction with MEKK1.

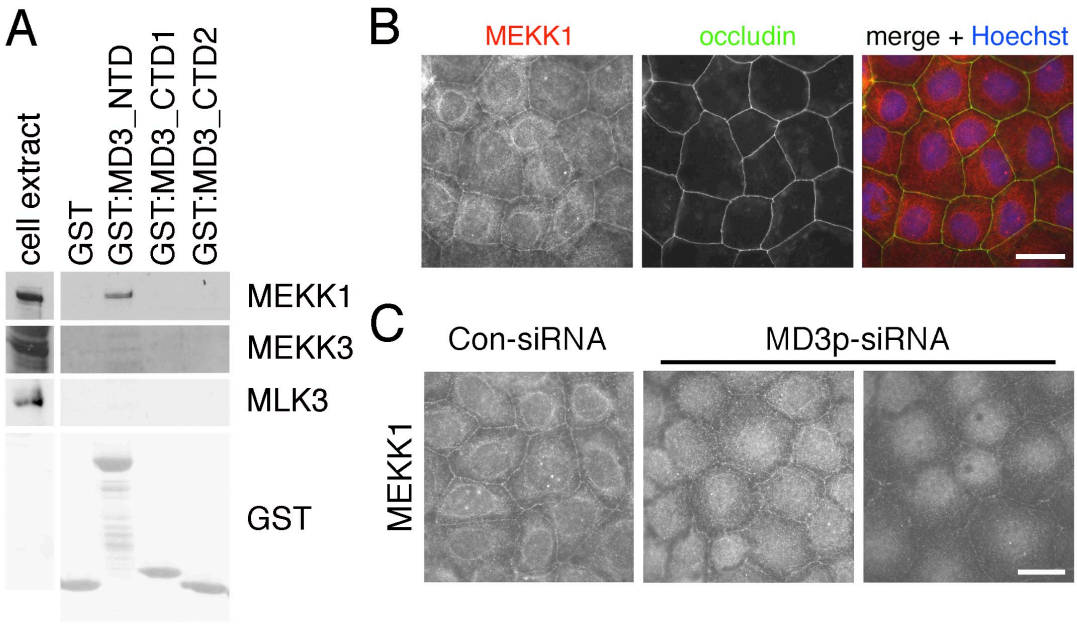

Figure 5.4 – MEKK1 interacts with the N-terminus of MarvelD3 and localizes to cell-cell contacts in a MarvelD3-dependent manner. (A) Caco-2 cell lysates were incubated with GST-fusion proteins attached to glutathione beads for 1.5 hours. Immunoblotting of pulldown samples shows a clear interaction between the N-terminus of MarvelD3 and MEKK1, but not MEKK3 or MLK3. An anti-GST antibody was used as a loading control. (B) MEKK1 can be seen to colocalise with occludin at the edge of the cell. (C) Localisation of MEKK1 to cell-cell contact sites seen in control cells is disrupted following siRNA-mediated depletion of MarvelD3. All are representative images of three independent experiments. Bars, 10μm.

Regulation of AP1 promoter activity by the N-terminus of MarvelD3

Since MEKK1 is an upstream regulator of AP1 signalling, and MarvelD3 has been shown to inhibit the activity of the AP1 promoter, the significance of the N-terminus in MarvelD3-mediated regulation of the AP1 promoter was assessed. First, Caco-2 cells were transfected with cDNAs encoding full-length MarvelD3 isoform 1

(MD3_1), full-length VSV-tagged MarvelD3 isoform 1 (MD3_1:VSV), a VSV-tagged N-terminal construct (NTD:VSV) or a VSV-tagged MarvelD3 isoform 1 construct lacking the N-terminus (ΔN_1:VSV), alongside the AP1 promoter firefly luciferase reporter plasmid and the Renilla luciferase control. Relative promoter activity was determined 3 days after transfection. Expression of the full length constructs reduced AP1 promoter activity consistent with previous observations (Chapter 4, Figure 4.12). Expression of the N-terminal domain of MarvelD3 was sufficient to reduce AP1 promoter activity. Interestingly, the ΔN_1:VSV construct reduced promoter activity, but this reduction did not reach significance. It is possible that the ΔN_1:VSV construct disrupts endogenous MarvelD3 signalling by integrating into the same complexes as the endogenous protein, but failing to regulate the same signalling pathways. To investigate this further, the N-terminal constructs (NTD:VSV and ΔN_1:VSV) were transfected in to MiaPaCa cells, which do not express endogenous MarvelD3 and presumably therefore do not assemble the same multi-protein junctional complexes found in Caco-2 cells. In the absence of endogenous junctions, expression of NTD:VSV significantly reduced AP-1 promoter activity, but ΔN_1:VSV did not (Figure 5.5), suggesting the N-terminal domain is responsible for the AP1-inhibitory activity of the full length MarvelD3 molecule. As the N-terminal region interacts with MEKK1, this further supports the hypothesis that the interaction with MEKK1 is significant in the signalling properties of MarvelD3.

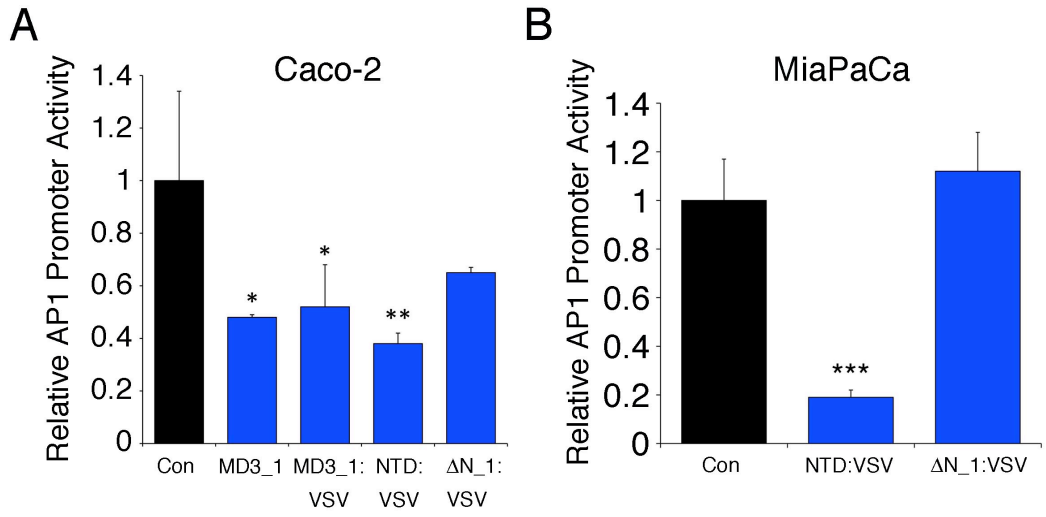

Figure 5.5 – Regulation of the AP-1 promoter by the N-terminus of MarvelD3. (A) Caco-2 cells were transfected with control plasmid, or plasmid encoding various constructs of MarvelD3 (as mentioned in main text), alongside the AP1 firefly luciferase reporter plasmid and a Renilla luciferase control. Detection of the luciferase and Renilla luminescent signals were made in triplicate and showed AP1 promoter activity to be significantly reduced by the full-length and N-terminal constructs, and less so in the absence of the N-terminal domain. (B) Transfection of N-terminal constructs in to MiaPaCa cells showed the N-terminus to be necessary and sufficient to reduce AP1 promoter activity. Results are presented as mean luminescent signals normalised to the control, ± standard deviation. Significance was calculated by Student's t-test.***$p<0.001$, ** $p<0.01$, * $p<0.05$, in comparison to control.

In addition to its role in regulating transcription, MEKK1 is necessary for transcription-independent stress fibre formation in migrating epithelial cells. Activation of RhoA in response to TGFβ induces stress fibre formation and requires MEKK1 (Zhang et al., 2005b). To further address the existence of a functional interaction between MarvelD3 and MEKK1, and since MarvelD3 expression appears to regulate the cytoskeleton during migration, the effect of MarvelD3 expression on

the arrangement of the cytoskeleton was analysed more closely. It was proposed that, if MarvelD3 reduces MEKK1 activity, there should be few or no stress fibres in MarvelD3-expressing cells. Indeed, immunofluorescence showed fewer stress fibres and more lateral actin in MD3-MiaPaCa C2 cells than in control MiaPaCa cells (Figure 5.6A). To see whether this was due to differences in RhoA activity, a GLISA was performed to ascertain the abundance of active RhoA in MiaPaCa cell extracts. As expected from the reduced stress fibres, there was less active RhoA in MarvelD3-expressing cells than control MiaPaCa (Figure 5.6B). Depletion of MarvelD3 in Caco-2 cells did not significantly increase the amount of stress fibres when compared to control cells (Figure 5.6C). Consistent with the suspected elevations in active RhoA, however, MarvelD3-depleted cells exhibited higher levels of phospho-MLC staining associated with the stress fibre structures. This data offers further support for a functional interaction between MarvelD3 and MEKK1, suggesting MarvelD3 may regulate cytoskeletal rearrangements coordinated by RhoA and MEKK1.

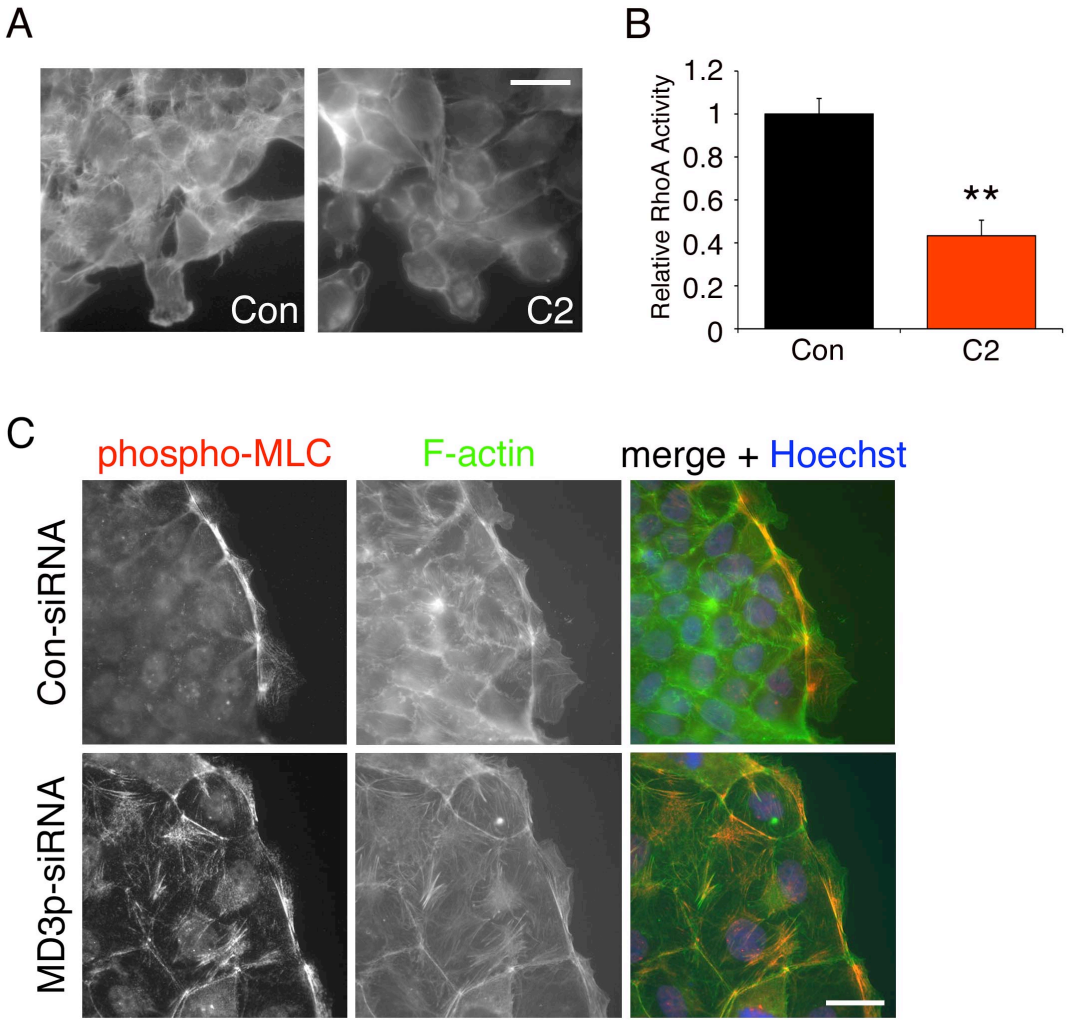

Figure 5.6 – Effect of MarvelD3 expression on RhoA-mediated cytoskeletal rearrangements. (A) Control and MarvelD3-expressing MiaPaCa clone C2 were fixed and processed for immunofluorescence during migration. Phalloidin staining shows more lateral actin and less stress fibre-like structures following MarvelD3 expression than in control cells. (B) RhoA activity levels were quantified in control and MarvelD3-expressing MiaPaCa clone 2. RhoA activity was significantly reduced following expression of MarvelD3. Shown are mean values (n=4) plus the standard deviation. (C) Stress fibres in MarvelD3-depleted Caco-2 cells stain positively for phospho-MLC, in contrast to controls. Significance was determined by Student's t-test; **p<0.01. Bars, 10μm.

Discussion

The aim of this chapter was to begin to understand the mechanism through which MarvelD3 elicits its inhibitory effects on the AP1 promoter, as observed in chapter 4. Results presented here suggest this could be mediated by an inhibitory interaction between the N-terminus of MarvelD3 and MEKK1, a promoter of AP1 signalling. For the first time, MEKK1 was shown to localize to cell-cell contacts and this localization was dependent on MarvelD3. The inhibition of AP1 promoter activity by the N-terminus of MarvelD3 and the reduced abundance of stress fibres following MarvelD3 expression in MiaPaCa cells, is consistent with an inhibitory role for MarvelD3 over MEKK1 activity. MarvelD3 expression also caused reductions in the levels of active JNK, which is downstream of MEKK1 in the MAPK pathway. Inhibition of JNK activity with the inhibitor SP600125 prevented MiaPaCa cell migration and proliferation, and migration increases caused by loss of MarvelD3. Thus a hypothetical model is proposed in which MarvelD3 regulates AP1 activity via an interaction with MEKK1. Furthermore, the subsequent regulation of the JNK MAPK pathway and the actin cytoskeleton may offer an additional influence of MarvelD3 over epithelial cell proliferation and migration.

The MAP kinase pathway functions in the transmission of extracellular stimuli, like growth factors or cellular stress, through the cytoplasm to the nucleus, and is known to regulate AP1 signalling. Pulldown assays identified an interaction between the N-terminus of MarvelD3 and the MAPKKK MEKK1, and levels of active JNK were reduced following the expression of MarvelD3 in MiaPaCa cells. Furthermore, the absence of any change in levels of active ERK or p38 suggested MarvelD3 might

specifically function in the regulation of the JNK branch of the MAPK pathway, a preference that is also shown by MEKK1 (Yujiri et al., 1999). Immunofluorescence analyses of Caco-2 cells showed a clear enrichment of MEKK1 at cell-cell contacts, which was perturbed or lost in MarvelD3-depleted cells. Thus MarvelD3 regulates the junctional localisation of MEKK1 and perhaps its activity. Impaired embryonic eyelid closure in MEKK1$^{-/-}$ mice implicated MEKK1 in the regulation of epithelial cell migration where it was shown to be necessary for phosphorylation of c-Jun in the migrating epithelium (Zhang et al., 2003). The interaction with MEKK1, the inhibition of JNK activation by MarvelD3 and the reduced cell migration phenotype, strongly suggests MarvelD3 could regulate migration by impacting on this pathway. Indeed, MEKK1 downregulation leads to reduced JNK activation and reduced wound healing by keratinocytes (Deng et al., 2006). Thus by reducing MEKK1 activity, MarvelD3 could function in the transmission of signals involved in cell migration.

In order to understand the significance of the interaction between the N-terminus of MarvelD3 and MEKK1, regulation of AP1 promoter activity by the N-terminus of MarvelD3 was examined. It was hypothesised that if MEKK1 is inhibited by interacting with the N-terminus of MarvelD3, AP1 promoter activity should be reduced when the N-terminus of MarvelD3 is present, but not in its absence. As expected, expression of a MarvelD3 N-terminal construct was sufficient to inhibit AP1 signalling in MiaPaCa and Caco-2 cells, suggesting the N-terminus alone is capable of interacting with MEKK1 and preventing its activation of AP1 signalling. Furthermore, in the absence of its N-terminus, MarvelD3 did not inhibit AP1 promoter activity in MiaPaCa cells, further demonstrating the importance of the N-

terminal domain in this signalling pathway. In contrast, however expression of the same MarvelD3 construct lacking the N-terminus (ΔN_1:VSV) caused partial, though not significant, reduction of AP1 promoter activity in Caco-2 cells. This discrepancy may have arisen due to the differences in junctional complexes present in these two cell types. The tight junction in Caco-2 cells is a complex structure involving many protein-protein interactions. Addition of an exogenous protein to such a system may interrupt endogenous protein complexes and subsequently affect their downstream signalling. For example, if ΔN_1:VSV were to replace endogenous MarvelD3 in a number of protein complexes, it may liberate the endogenous protein making more of it available to interact and inhibit MEKK1, which could be responsible for the partial reduction in AP1 promoter activity by ΔN_1:VSV in Caco-2 cells observed here. Such effects are difficult to confirm, but cannot occur in a system devoid of the endogenous protein, like in MiaPaCa cells, which do not possess endogenous cell-cell junctions and therefore provide a more simple system in which to address the functional properties of individual protein domains. Taken together, these results suggest the N-terminus of MarvelD3 is necessary for the inhibition of AP1 promoter activity. As the N-terminus interacts with MEKK1, an activator of AP1 signalling, it is proposed that this interaction serves to inhibit MEKK1 activity and ultimately its downstream signalling. Further work should focus on elucidating the mechanism of inhibition. Does MarvelD3 interact with MEKK1 in its inactive form and prevent its activation? Or does MarvelD3 sequester activated MEKK1 thus preventing activation of its downstream targets? This could be addressed by probing cell lysates from pulldown or co-immunoprecipitation assays with antibodies specific for various phosphorylated forms of MEKK1 to identify the nature of the MEKK1 molecules interacting with MarvelD3. In addition, kinase assays should be performed to

determine the effect of MarvelD3 on MEKK1 kinase activity in the presence and absence of the N-terminal domain.

The MEKK1/JNK pathway is also thought to regulate the actin cytoskeleton, with MEKK1 being required for actin stress fibre formation (Zhang et al., 2003). Interestingly, there are fewer stress fibres in MarvelD3-expressing MiaPaCa cells than control cells, perhaps due to reduced MEKK1 activity in the presence of MarvelD3. Stress fibre formation is regulated by activity of the small GTPase RhoA, the activity of which is greatly reduced following expression of MarvelD3 in MiaPaCa cells, and has previously been implicated in promoting tumour cell migration (Joshi et al., 2008; Kamai et al., 2003). In the absence of MarvelD3 the amount of stress fibres in Caco-2 cells does not appear to change, but increased phospho-MLC staining suggests they are more contractile than those in control cells. As RhoA-induced phosphorylation of MLC and subsequent contractility is thought to drive stress fibre formation, the increased phospho-MLC staining could be indicative of a more dynamic stress fibre cycle of assembly (and therefore disassembly) in MarvelD3-depleted in comparison to control cells. Increased stress fibre turnover is supportive of increased migration.

While the MEKK1/JNK cascade has not been implicated in the regulation of proliferation directly, demonstrations have been made of the cross-talk between RhoA and EGFR signalling pathways mediated by MEKK1 (Li et al., 2009; Zhang et al., 2003). In light of the observations made in chapter 4, therefore, it is possible that MarvelD3 regulates proliferation through the EGFR signalling pathway via its interaction with MEKK1. So far, changes in the levels of ERK activity have not been

seen in response to changes in MarvelD3 expression, despite an effect of MarvelD3 on EGFR signalling. While activation of ERK by EGFR may be stimulus specific and MEKK1-mediated activation of ERK doesn't occur in all cell types (Xu et al., 1995), it could be that MarvelD3 regulates ERK in response to specific stimuli that have not been identified here. Therefore, future studies could look more closely in to the potential role of MarvelD3 in regulating ERK, possibly via MEKK1-mediated cross-talk with the EGFR pathway.

In conclusion, the data presented in the last two chapters suggests MarvelD3 regulates proliferation and migration by affecting activity through the EGFR signalling pathway. By interacting with MEKK1, it is proposed that MarvelD3 prevents activation of JNK and, subsequently, restricts AP1 promoter activity. Reduced AP1 promoter activity may then be responsible for the reduced expression of EGFR in MarvelD3-expressing cells. Reduced AP1 activity and/or EGFR signalling may then attenuate cyclinD1 expression levels, which in turn perturbs cell cycle progression. Future studies should examine the effect of MarvelD3-MEKK1 on localized JNK activation, which has been shown to be necessary at the leading edge for migration (Rosse et al., 2009). Alongside analysis of the effects of MarvelD3 on Rac and Cdc42 activity, this may enable the mechanism behind MarvelD3-mediated protrusion formation to be better understood.

Chapter 6:

Regulation of the cellular response to hyperosmotic shock by MarveID3

Chapter 6 – Regulation of the cellular response to hyperosmotic shock by MarvelD3

Introduction

Results in this thesis have so far implicated MarvelD3 in the regulation of epithelial cell proliferation and migration via a proposed inhibitory interaction with MEKK1. In addition to a role in migration, MEKK1 has been shown to protect cells from apoptosis when activated by stresses that alter cell shape and the arrangement of the cytoskeleton (Yujiri et al., 1998). To see if MarvelD3 regulates MEKK1 in other contexts and to further examine the nature of this regulation, this chapter looks at the role of MarvelD3 in the cellular response to hyperosmotic shock, which is known to cause significant rearrangement of the actin cytoskeleton and involve activity of MEKK1 (Yujiri et al., 1998).

Hyperosmotic shock occurs when the solute concentration surrounding cells is suddenly increased, resulting in rapid cell shrinkage as water moves out of the cell in to the hypertonic surroundings. The cells of the kidney, for example, are frequently physiologically exposed to hyperosmotic conditions due to the accumulation of NaCl and urea during antidiuresis. Also, in dry-eye syndrome, increased evaporation of tears or abnormal tear composition results in cells of the cornea being exposed to hypertonic conditions. When cells are exposed to a level of hyperosmotic stress that is either too great or for too long, apoptosis may be induced and the integrity of the monolayer becomes compromised. It is important, therefore, that cells activate protective mechanisms in response to hyperosmotic exposure that enable restoration of cellular integrity and maintenance of monolayer homeostasis.

Epithelial cell responses to hyperosmotic shock can be classified into three main groups; the activation of ion transport systems, the rearrangement of the cytoskeleton and the changes in the expression of osmosensitive genes, such as aldose reductase (AR). Further, it has been proposed that changes to the cytoskeleton may be necessary for the facilitation of the other osmoadaptive processes, like recovery of osmotic balance by various ion transporters in the plasma membrane, which are thought to require an intact actin cytoskeleton in order to be able to function (Henson, 1999; Pedersen et al., 2001).

Cell shrinkage in response to hypersmotic conditions in mammalian cells results in activation of the small GTPases Rac and Cdc42 and their translocation to the cell periphery where they recruit cortactin and Arp2/3, resulting in localised actin polymerisation and the subsequent reinforcement of the cell cortex (Di Ciano et al., 2002). In addition, hypersomotic shock-induced activation of RhoA has been shown to induce myosin light chain (MLC) phosphorylation and the dephosphorylation of cofilin, leading to further reinforcement of the cytoskeletal reorganizations (Di Ciano-Oliveira et al., 2003; Miranda et al., 2010). The levels of F-actin increase in mammalian cells in response to hyperosmotic shock (Pedersen et al., 1999).

In addition to offering mechanical protection to the cell, the cytoskeleton may also participate in the hyperosmotic response by mediating intracellular signalling cascades. In response to hyperosmotic shock, Rac-positive actin ruffles are seen to recruit a signalling module consisting of Rac, OSM (osmosensing scaffold for MEKK3), MEKK3 and MKK3, which facilitates the activation of p38 (Uhlik et al.,

2003). p38 is thought to regulate the osmoprotective transcription factor TonEBP/OREBP, which in turn regulates expression of osmoprotective genes like AR and the betaine transporter (BGT1) (Nadkarni et al., 1999). Thus p38 is involved in re-establishing cellular volume and inhibition of p38 impairs the ability of cells to restore cell volume following hyperosmotic insult (Bustamante et al., 2003). In addition to p38, cell shrinkage has also been shown to stimulate the activation of JNK MAP kinases (Rosette and Karin, 1996). Expression of mammalian JNK in yeast rescues defects in growth of yeast grown on hyperosmotic media suggesting JNK may function in the regulation of the hyperosmotic response in mammalian cells too (Galcheva-Gargova et al., 1994). In the absence of MEKK1, JNK fails to be activated in response to hyperosmotic shock (Yujiri et al., 1998), but the consequence of this has not yet been realized.

Despite the physiological relevance of this process, relatively little is known about the mechanisms behind the mammalian cell response to hyperosmotic shock. In this chapter, I have identified a function for MarvelD3 in regulating activation of JNK MAPK signalling and the cytoskeletal response of epithelial cells to hyperosmotic conditions. This could provide a novel mechanism through which changes in the extracellular environment can be communicated to the cell interior, facilitating the changes necessary in order for the cell to adapt, and provides additional support to the hypothesis that regulation of MEKK1 and JNK by MarvelD3 is of functional significance.

Results

Effect of hyperosmotic shock on MarvelD3 localisation

To first assess if MarvelD3 may participate in the epithelial cell response to hyperosmotic shock, Caco-2 and HCE cells exposed to hyperosmotic conditions (600mosM NaCl) were processed for levels of MarvelD3 expression and localization. Immunofluorescent analysis revealed that both Caco-2 and HCE cells exposed to hyperosmotic conditions showed a redistribution of MarvelD3 from the junction to the cytoplasm within 15 minutes of exposure (Figure 6.1, Caco2; Figure 6.2, HCE). In Caco-2 cells, junctional staining of MarvelD3 began to return after 2 hours of hyperosmotic shock and, after 8 hours, demonstrated a linear staining pattern similar to that observed prior to hyperosmotic shock, indicating cells might have adapted to the increased osmotic conditions at this later time. In contrast to MarvelD3, occludin showed junctional disruption at the 30-minute, 1-hour and 2-hour time points, but remained at the cell-cell junction, and this was again corrected by 8 hours.

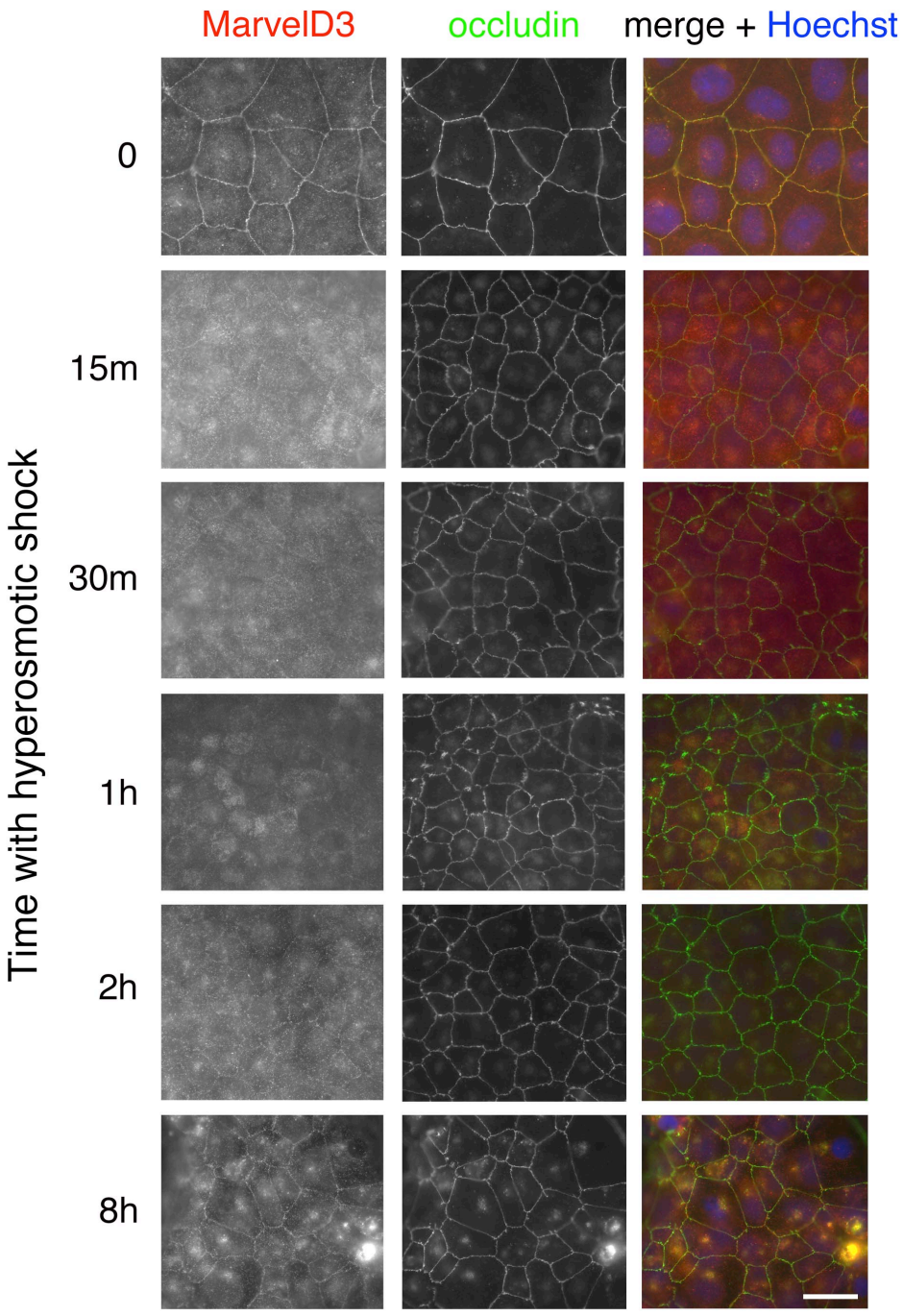

Figure 6.1 – MarvelD3 redistributes to the cytoplasm in response to hyperosmotic shock in Caco-2 cells. Caco-2 cells were plated on to glass coverslips and grown until confluent. Medium containing 600mosM NaCl was added for the times shown and then fixed in methanol. Staining with anti-MarvelD3 and anti-occludin antibodies shows redistribution of MarvelD3 to the cytoplasm, but not occludin, in response to hyperosmotic shock. Images are representative of at least 3 independent experiments. Bar, 10μm.

In HCE cells, junctional MarvelD3 could still be seen alongside the increased cytoplasmic signal (Figure 6.2). Figure 6.2 shows occludin staining is also less disrupted in HCE cells than in Caco-2 cells. What is more, both MarvelD3 and occludin staining appears normal again after just 2 hours of hyperosmotic exposure, suggesting the kinetics of the hyperosmotic response is quicker in HCE cells when compared to Caco-2 cells. Due to the more obvious phenotype in Caco-2 cells and the longer time course in which to dissect it, these cells were used for subsequent studies into the effects of hyperosmotic shock and the role of MarvelD3 therein.

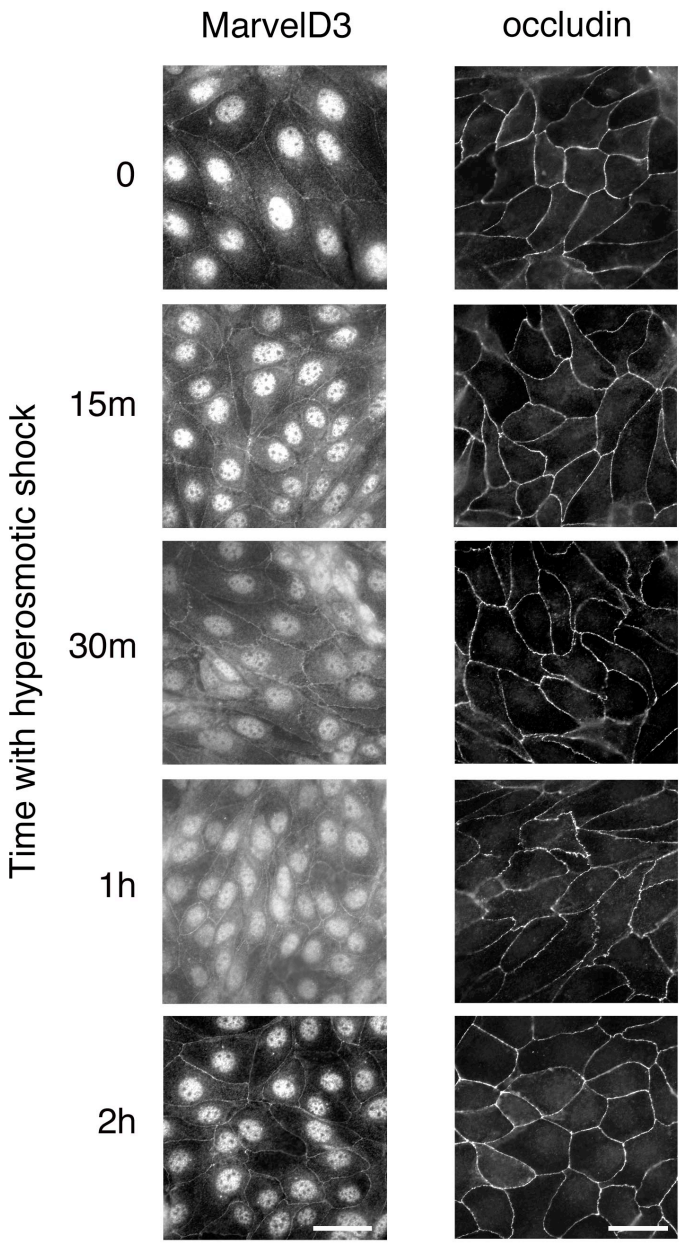

Figure 6.2 – Redistribution of MarvelD3 to the cytoplasm in HCE cells exposed to hyperosmotic conditions. HCE cells were plated on to glass coverslips and grown until confluent. Cells were incubated in medium containing 600mosM NaCl (hyperosmotic) for the times shown and then processed for immunofluorescence with anti-MarvelD3 and anti-occludin antibodies on separate coverslips. MarvelD3 staining gives an increased cytoplasmic signal following hyperosmotic exposure. Occludin remained in the cell membrane. Images are representative of 3 independent experiments. Bars, 10μm.

Regulation of MAPK signalling by MarvelD3 in response to hyperosmotic shock

The internalization of MarvelD3 in response to hyperosmotic shock, while occludin remained within the membrane, provoked the idea that MarvelD3 may have a function in the regulation of the hyperosmotic response. As an interaction between MarvelD3 and MEKK1 was identified in the previous chapter, and as MEKK1 has been shown by others to be involved in the response to hyperosmotic shock (Yujiri et al., 1998), I wanted to determine if MarvelD3 regulates MEKK1 in response to hyperosmotic shock. To address this, antibodies against phosphorylated forms of MEKK1 were kindly donated by Dr Ewen Gallagher, Imperial College London. The levels of total MEKK1 protein were unaffected by hyperosmotic shock or MarvelD3 depletion, but an antibody specific for MEKK1 phosphorylated at serine residue 1455 (Ser1455; now termed phospho-MEKK1) gave an increased signal 15 minutes after hyperosmotic shock in control and MarvelD3-depleted cells, suggesting MEKK1 is regulated in response to hyperosmotic shock (Figure 6.3A). Quantification of phospho-MEKK1 levels, compared to total MEKK1 levels, from three independent experiments demonstrated that levels of phospho-MEKK1 were elevated more greatly in the absence of MarvelD3 and, in addition, this elevation appeared to be more prolonged (Figure 6.3B). Immunofluorescence showed some junctional staining of phospho-MEKK1 in control cells (Figure 6.3C). MarvelD3 depletion also resulted in more rapid induction and prolonged activation of JNK in response to hyperosmotic shock (Figure 6.3D and E). In control cells, levels of active JNK peaked after 1 hour exposure to hyperosmotic shock. In contrast, JNK activation was more rapidly induced after 15 minutes hyperosmotic exposure of MarvelD3-depleted cells, peaking after 2 hours exposure and was still present after 8 hours. Thus MarvelD3 appears to

regulate the activity of MEKK1 and JNK in response to hyperosmotic shock induced by 600mosM NaCl.

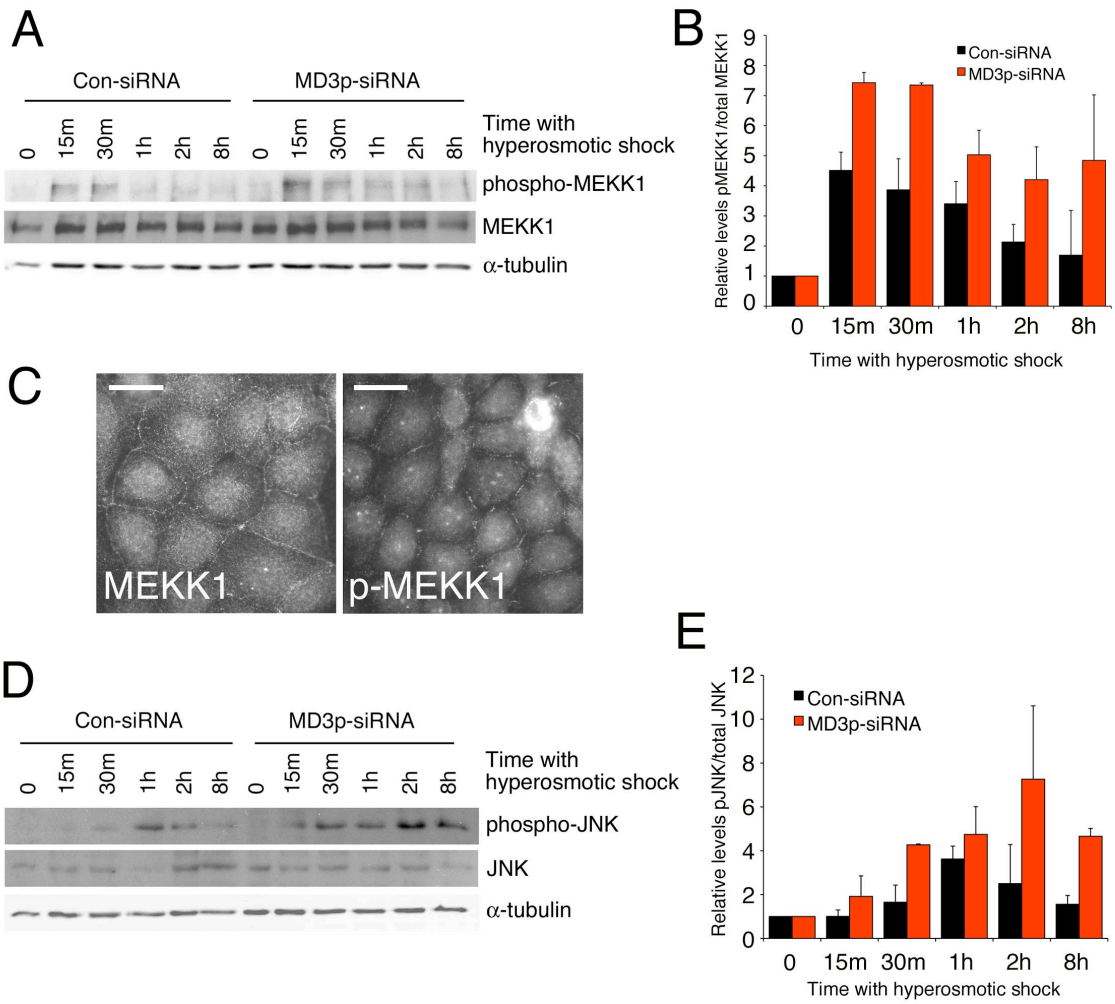

Figure 6.3 – Regulation of MEKK1 and JNK phosphorylation by MarvelD3 in response to hyperosmotic shock. (A) Control and MarvelD3-depleted Caco-2 cells were exposed to hyperosmotic shock for the times shown. Immunoblotting with an antibody specific for MEKK1 phosphorylated at S1455 showed increased phosphorylation in response to hyperosmotic shock in control and MarvelD3-depleted cells. This phosphorylated form persisted longer in MarvelD3-depleted cells. Hyperosmotic shock did not effect total levels of MEKK1. (B) Levels of phospho-MEKK1 in comparison to total MEKK1 levels were quantified using ImageJ software from 3 independent experiments. (C) Immunofluorescence of control (untreated) Caco-2 cells showed localization of MEKK1 and partial localization of phospho-MEKK1 (p-MEKK1) to cell-cell contacts. (D) MarvelD3 depletion affects the level and duration of JNK phosphorylation in response to hyperosmotic shock, without increasing total JNK. (E) Levels of phospho-JNK in comparison to total JNK levels were quantified using ImageJ software from 3 independent experiments.

The initiation of intracellular signalling pathways in response to hyperosmotic shock enables cells to activate adaptive programmes in order to be able to survive in hyperosmotic conditions. In yeast, activation of the Hog1 MAPK pathway is the primary mechanism through which the activation of osmoresponsive genes is thought to occur. In mammalian cells, the Hog1 homologue p38 is activated in response to sorbitol-induced hyperosmotic shock and facilitates long-term adaptation through regulation of cytoskeletal remodeling proteins and transcription of osmoprotective genes (Bell et al., 2000; Uhlik et al., 2003). Since this study utilizes NaCl to induce hyperosmotic shock, it was important to determine whether p38 was also activated and accumulated in the nucleus and whether MarvelD3 was involved in the regulation of this MAPK pathway. Prior to addition of hyperosmotic shock, p38 showed weak nuclear staining in Caco-2 cells. Figure 6.4 shows that addition of 600mosM NaCl to Caco-2 results in an increase in active, phosphorylated p38 and its increased accumulation in the nucleus. Immunofluorescence analysis suggested this nuclear accumulation may initially be slowed in MarvelD3-depleted cells (comparing 15 minute time points), but immunoblotting suggested no difference in the total levels of phospho-p38 between control and MarvelD3-depleted cells following exposure to hyperosmotic shock. Similarly, the activation of ERK, which is sometimes found downstream of MEKK1, was also unaffected by MarvelD3 depletion (Figure 6.4B). Taken together, these results suggest MarvelD3 is not involved in the hyperosmotic activation of p38 or ERK and thus shows preference for the JNK branch of the MAPK pathway.

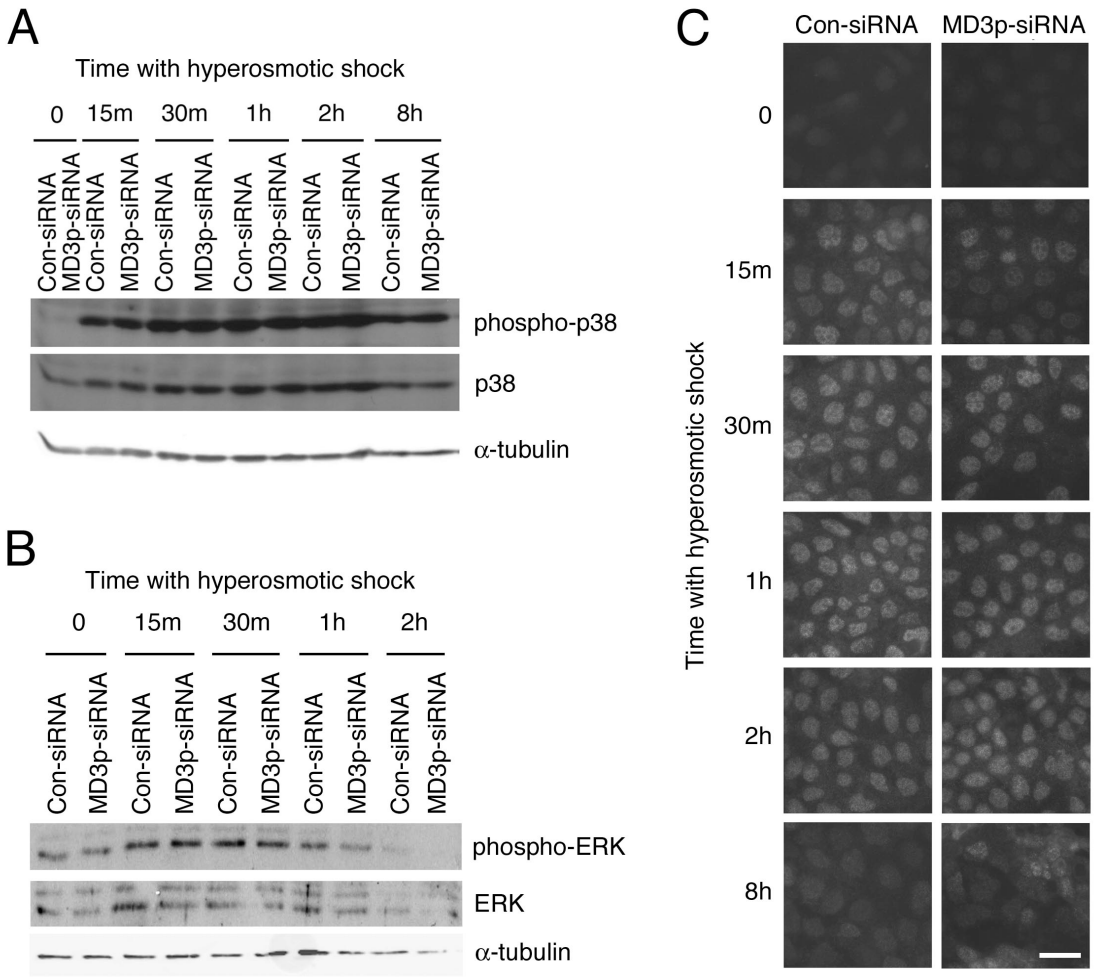

Figure 6.4 – MarvelD3 depletion does not affect activation of p38 or ERK, or nuclear accumulation of p38, in response to hyperosmotic shock. Hyperosmotic shock caused by 600mosM NaCl increases levels of (A) phospho-p38 and (B) phospho-ERK. These increases are not affected by loss of MarvelD3. (C) Control and MarvelD3-depleted cells exposed to hyperosmotic shock were processed for immunofluorescence with an anti-phospho-p38 antibody. Hyperosmotic shock caused increased nuclear phospho-p38. This is not affected by depletion of MarvelD3. All images are representative of three independent experiments. Bar, 10μm.

Regulation of MarvelD3 internalisation in response to hyperosmotic shock

Immunoblotting lysates of cells exposed to hyperosmotic shock demonstrated that levels of MarvelD3 and occludin were not reduced in response to hyperosmotic shock (Figure 6.5A). Thus the loss of junctional MarvelD3 may be due to a redistribution of MarvelD3, rather than loss of the total protein. The EGFR is internalized in response to hyperosmotic shock in a mechanism dependent on the Src kinase Yes (Rosette and Karin, 1996). Activation of EGFR in response to hyperosmotic shock requires p38 (Cheng et al., 2002). Caveolin internalization also occurs in response to hyperosmotic shock and requires active p38 and c-Src (Volonte et al., 2001). To determine the mechanism of MarvelD3 internalisation, Caco-2 cells were incubated in the presence of various inhibitors prior to addition of hyperosmotic shock. Cells were then fixed after 15 minutes hyperosmotic shock and the localization of MarvelD3 was observed. Incubation with inhibitors of the Src family of kinases PP1 and PP2, or the negative control inhibitor PP3, did not prevent the internalization of MarvelD3 in response to hyperosmotic shock (Figure 6.5B). Some junctional MarvelD3 could be observed following PP2 incubation suggesting this inhibitor may partially reduce MarvelD3 internalisation but junctional staining was much reduced compared to PP2-treated cells prior to hyperosmotic exposure. The specific p38 inhibitor SB202190 also failed to prevent internalization of MarvelD3 (Figure 6.5C). Following JNK or EGFR inhibition, however, MarvelD3 remained at the cell membrane in response to hyperosmotic shock (Figure 6.5C). Inhibition of ERK signalling with the MEK1/2 inhibitor UO126 appeared to partially reduce MarvelD3 internalisation, but significant cytoplasmic staining was still observed (Figure 6.5C). This suggests MarvelD3 internalisation may occur via an EGFR- and JNK-dependent mechanism. Also, though prior incubation with some inhibitors resulted in a reduction in cell size

when compared to control-treated cells (Figure 6.5B and C), further hyperosmotic shock-induced reductions failed to occur in cells pre-treated with PP2, SP600125 and Gefetinib, which also had the greatest effect on MarvelD3 internalisation.

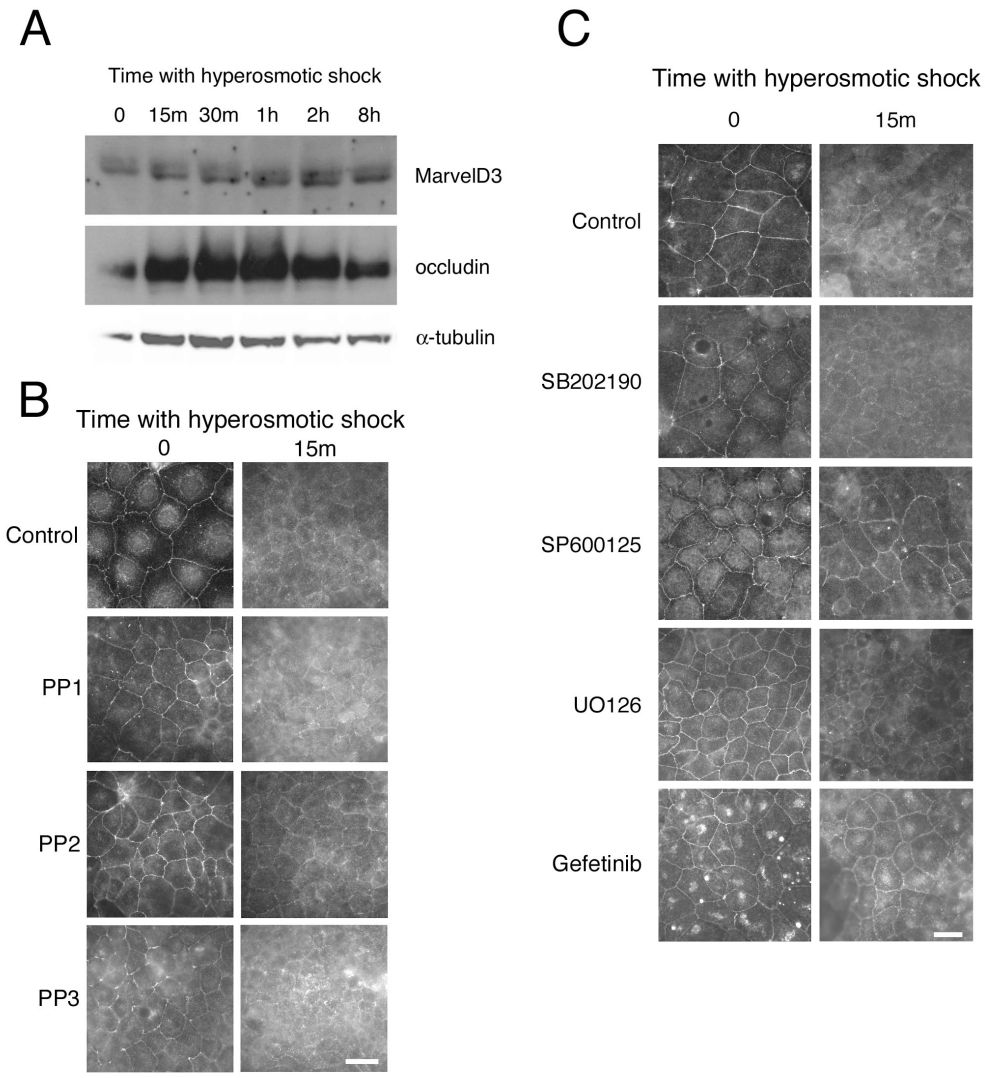

Figure 6.5 – Regulation of MarvelD3 internalisation in response to hyperosmotic shock. (A) Immunoblotting cell lysates confirms MarvelD3 and occludin protein levels are not lost in response to hyperosmotic shock. (B) MarvelD3 immunofluorescence showed inhibition of Src family kinases does not prevent redistribution of MarvelD3 following hyperosmotic shock. PP3 used as a negative control for PP1 and PP2 (C) MarvelD3 remained at the cell membrane after hyperosmotic shock following inhibition of JNK (SP600125) and EGFR (Gefitinib), but not p38 (SB202190) or ERK signalling (UO126). Images are representative of at least two independent experiments. Bars, 10μm.

MarvelD3 depletion affects cytoskeletal reorganisation in response to hyperosmotic shock

To determine the importance of MarvelD3 in the response to hyperosmotic shock, the effect of MarvelD3-depletion on the hyperosmotic response was assessed. Reorganisation of the actin cytoskeleton is an important osmoadaptive response, generating a rigid actin cortex to physically protect the cell from changes to the extracellular environment. The reinforced cortex is in turn believed to facilitate the inclusion of additional transmembrane transporters that function to resume the isotonic balance within the cell (Kwon and Handler, 1995). These cytoskeletal rearrangements are therefore considered to be critical to the successful response of a cell to hyperosmotic stress. Since MarvelD3 appears to function in cytoskeletal rearrangements during epithelial cell migration, it was wondered whether it may also play a role in organizing those involved in the hyperosmotic shock response. Caco-2 cells, both control and MarvelD3-depleted, were exposed to hyperosmotic stress before being stained with FITC-phalloidin to observe the arrangement of the actin cytoskeleton. Figure 6.6 shows that in control cells, hyperosmotic shock causes a dramatic loss of cortical actin within 15 minutes of exposure. After 1 hour in hyperosmotic conditions, F-actin can be seen at the cell periphery as well as additional enrichment in the underlying cytoplasm. Further F-actin enrichment at the cell cortex after 2 hours is accompanied by a change in cell shape, with cells having much more linear edges and appearing less round than at earlier time points. After 8 hours of hyperosmotic exposure, control cells demonstrate a highly organized F-actin network fortified along the cell periphery. MarvelD3 depletion perturbs these hyperosmotic shock-induced F-actin rearrangements. First, F-actin does not collapse from the cortex in response to hyperosmotic shock, with junctional F-actin still clearly

visible in MarvelD3-depleted cells at the 15 minutes time point. After 30 minutes exposure, junctional F-actin and the underlying enrichment resembles the control cells after 1 hour, suggesting MarvelD3-depleted cells are attempting to rearrange their cytoskeleton in response to hyperosmotic shock. These rearrangements are not able to be completed, however, as at later time points the cells begin to come away from each other and the actin cytoskeleton appears highly disorganized (Figure 6.6).

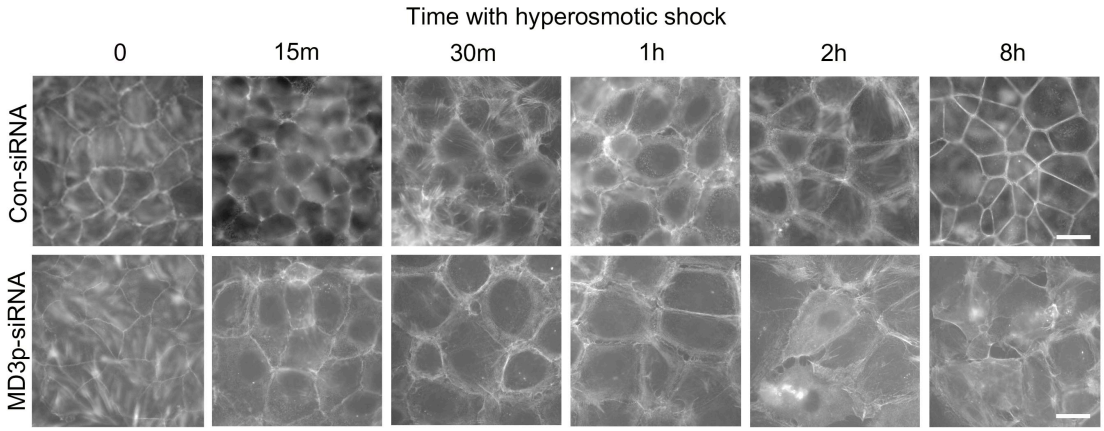

Figure 6.6 – Effect of MarvelD3 on rearrangements of the actin cytoskeleton in response to hyperosmotic shock. Control and MarvelD3-depleted Caco-2 cells were fixed in PFA after exposure to hyperosmotic shock for the durations shown. FITC-Phalloidin staining showed failure of MarvelD3-depleted cells to reorganize their actin cytoskeleton in response to hyperosmotic shock. Images are representative of three independent experiments. Bars, 10μm.

The cells appeared to retract away from each other more following MarvelD3 depletion than in control cells, prompting the analysis of the effect of hyperosmotic shock on the morphology of the tight junctions. MarvelD3-depleted and control cells were fixed after 2 hours of hyperosmotic shock as this was the time point at which the

retraction phenotype first became apparent by F-actin staining. Occludin and ZO-1 staining were more disrupted in MarvelD3-depleted cells than control cells (Figure 6.7). The disruption to ZO-1 staining was more severe than for occludin, which perhaps reflects the fact that it is a cytoplasmic protein and not integral to the membrane as occludin is. Impedance measurements were initially reduced in response to hyperosmotic shock in both control and MarvelD3-depleted cells. While control cells recovered their integrity, however, MarvelD3-depleted cells failed to do so (Figure 6.7B). In the absence of MarvelD3, therefore, it appears junctional integrity is more severely compromised following hyperosmotic insult. This could be due to the disruption of the actin cytoskeleton, which is known to be necessary for tight junction barrier function.

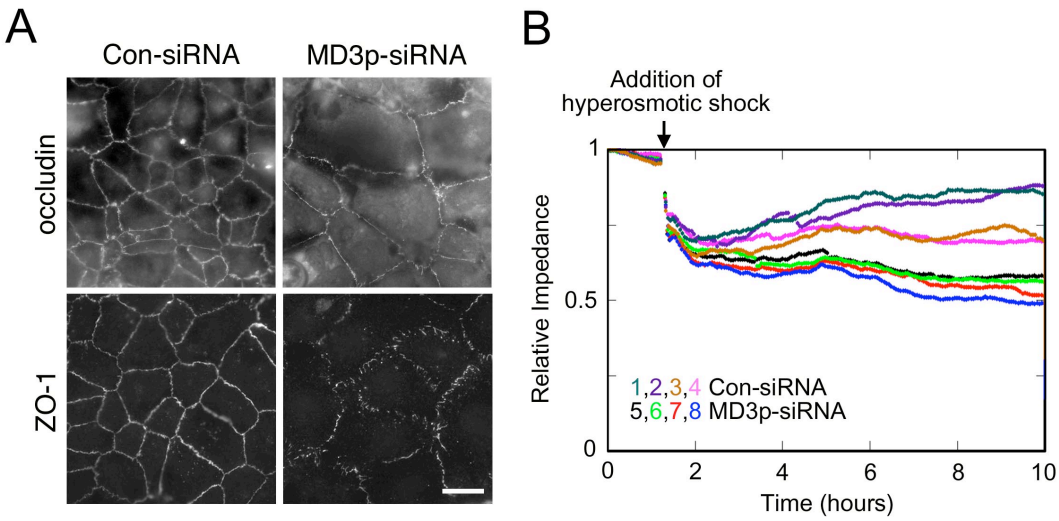

Figure 6.7 – MarvelD3-depletion results greater disruption to the tight junctions in response to hyperosmotic shock. (A) occludin and ZO-1 staining patterns appeared more disrupted in MarvelD3-depleted Caco-2 cells than control cells following exposure to hyperosmotic shock for 2 hours. Images are representative of at least three independent experiments. (B) Impedance analysis shows hyperosmotic shock-induced reduction in impedance values are recovered by control Caco-2 cells, but not in those depleted of MarvelD3. This experiment was performed in quadruplicate, but so far has just been performed once. Bar, 10μm.

Staining for F-actin and the tight junction proteins occludin and ZO-1 demonstrated a dramatic reduction in cell area, at the level of the tight junction, in control cells in response to hyperosmotic shock. This reduction, however, did not occur in the absence of MarvelD3. Quantification confirmed that MarvelD3-depleted cells have a greater apical cell area at the level of the tight junction in comparison to control cells, which rapidly contract in response to hyperosmotic shock (Figure 6.8A). Cell shrinkage is a characteristic response to hyperosmotic shock as water rushes out of the cell due to the altered osmotic balance. Cell shrinkage induces p38 activation in response to hyperosmotic shock. Since p38 activation is unaffected by loss of MarvelD3, this cell area phenotype is thought to be due to a failure in apical contraction of MarvelD3-depleted cells and not because they do not shrink. Confocal microscopy should be used to confirm the effect of MarvelD3 depletion on cell volume in response to hyperosmotic shock. The lack of apical contraction further implicates MarvelD3 in the regulation of the cytoskeletal response to hyperosmotic shock. Interestingly, quantification of cell area from MAPK inhibitor-treated cells demonstrated that cell area also failed to reduce following inhibition of JNK (Figure 6.8B). Since MarvelD3 internalisation is blocked by JNK inhibition, these data suggest signalling processes downstream of MarvelD3 internalisation may be responsible for constriction of apical cell area.

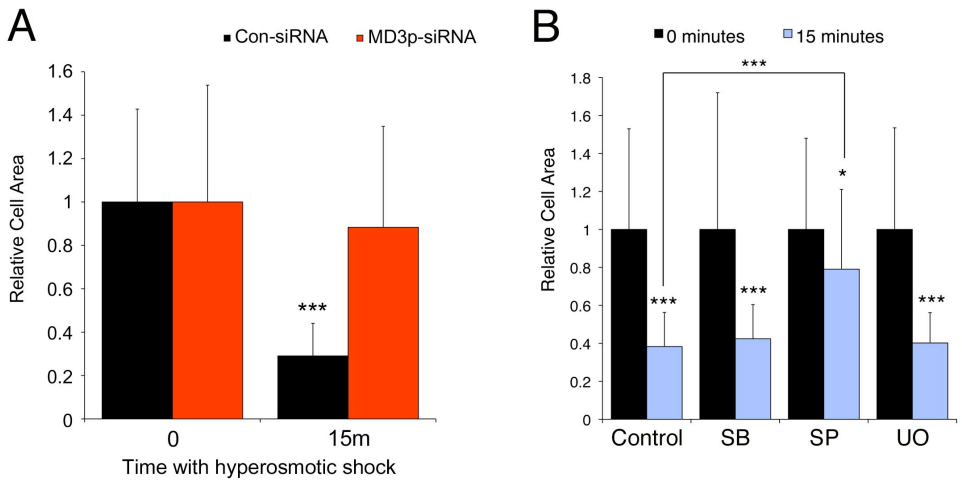

Figure 6.8 – Effect of MarvelD3 depletion and MAPK inhibition on hyperosmotic shock-induced reduction in apical cell area. Cell area at the level of the tight junction was quantified using ImageJ software from immunofluorescence images of cells exposed to hyperosmotic shock under the conditions shown and then stained with an anti-occludin antibody to enable to junction to be seen. (A) Comparison of apical cell area between control and MarvelD3-depleted Caco-2 cells before and after 15 minutes (15m) exposure to hyperosmotic shock. (B) Comparison of apical cell area after 15 minutes exposure to hyperosmotic shock in cells incubated overnight with DMSO (Control), SB202190 (SB), SP600125 (SP) or UO124 (UO). Shown are mean values for relative cell area averaged from three independent experiments counting 20-40 cells per experiment, plus the standard deviation. Significance was determined using Student's t-test. ***$p<0.001$, *$p<0.05$ compared to relevant controls, or as depicted.

Since the osmoresponsive cytoskeletal changes seem so perturbed in MarvelD3-depleted cells, attempts were made to determine the mechanism by which MarvelD3 may be regulating them. F-actin assembly in response to hyperosmotic shock has been shown to involve cortactin/Arp2/3 relocalisation to the cell membrane, phosphorylation of MLC and the dephosphorylation of cofilin (Di Ciano et al., 2002; Di Ciano-Oliveira et al., 2003; Miranda et al., 2010). The effect of hyperosmotic

shock on phosphorylation of MLC and cofilin in control and MarvelD3-depleted Caco-2 cells was subsequently assessed. Due to antibody difficulties, the effect of MarvelD3 on cortactin has not yet been addressed by immunoblotting or immunofluorescence. Levels of phospho-MLC were moderately increased in response to 15 minutes exposure to hyperosmotic shock in both control and MarvelD3-depleted cells (Figure 6.9A). Both phospho- and total cofilin appeared to reduce with increasing time spent in hyperosmotic conditions in both control and MarvelD3-depleted cells (Figure 6.9B).

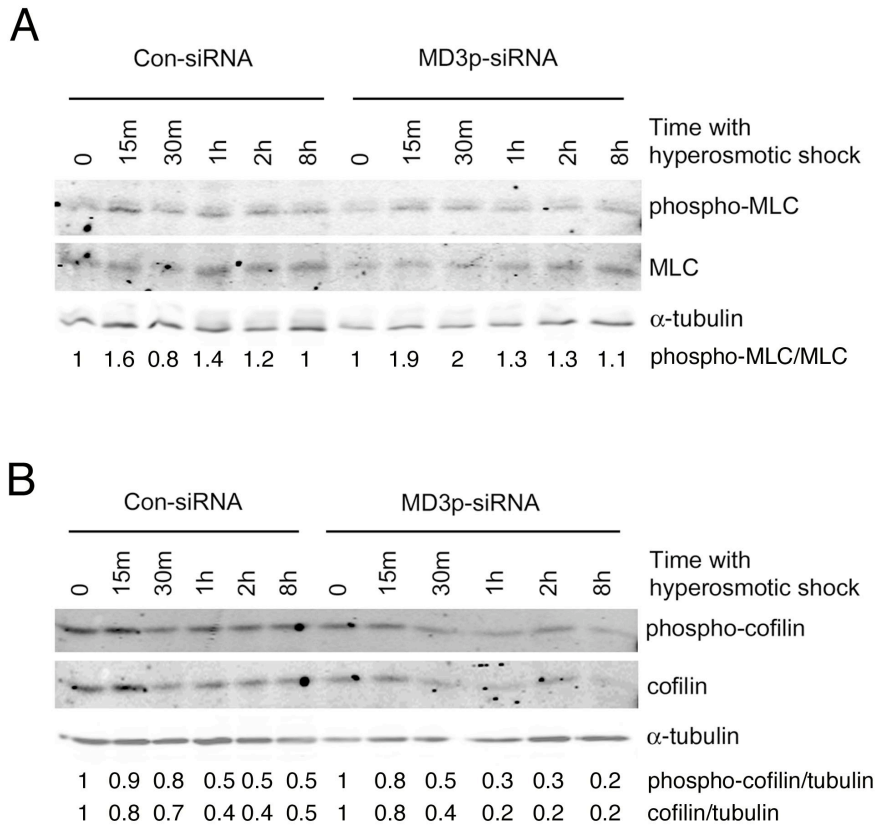

Figure 6.9 – Effect of MarvelD3 depletion on hyperosmotic shock-induced changes in cortactin, cofilin and MLC. Lysates prepared from control and MarvelD3-depleted Caco-2 cells exposed to hyperosmotic shock were immunoblotted for levels of (A) phospho- and total MLC and (B) phospho- and total cofilin. The increase in phospho-MLC relative to total MLC in response to hyperosmotic shock was quantified and values normalised to protein levels prior to hyperosmotic exposure are shown. Similarly, the decreases in phospho-cofilin and cofilin levels following hyperosmotic exposure were quantified relative to tubulin, as shown. Immunoblots are representative of 3 independent experiments.

To complement the studies of protein levels, the effect of MarvelD3 depletion on the localization of phospho-MLC and phospho-cofilin was also characterized. In untreated control cells, phospho-cofilin displays a predominantly nuclear localization, with some staining at cell-cell junctions (Figure 6.10, yellow arrows). It is not known

if the nuclear phospho-cofilin signal is specific for phospho-cofilin as phospho-cofilin has not been reported in the nucleus before. Specificity for phospho-cofilin should be tested before the importance of nuclear phospho-cofilin is addressed. Hyperosmotic shock induced an increase in cytoplasmic phospho-cofilin. Interestingly, the cytoplasmic phospho-cofilin signal was reduced after 1 hour exposure and increased in the cytoplasm again after 2 hours, suggesting there may be some biphasic regulation of the activity of phospho-cofilin in response to hyperosmotic shock. After 8 hours exposure, cytoplasmic phospho-cofilin was once again low shows a predominantly nuclear localization with additional staining at the cell-cell junctions. Co-staining for F-actin allows one to see the concomitant changes in the organization of the actin cytoskeleton.

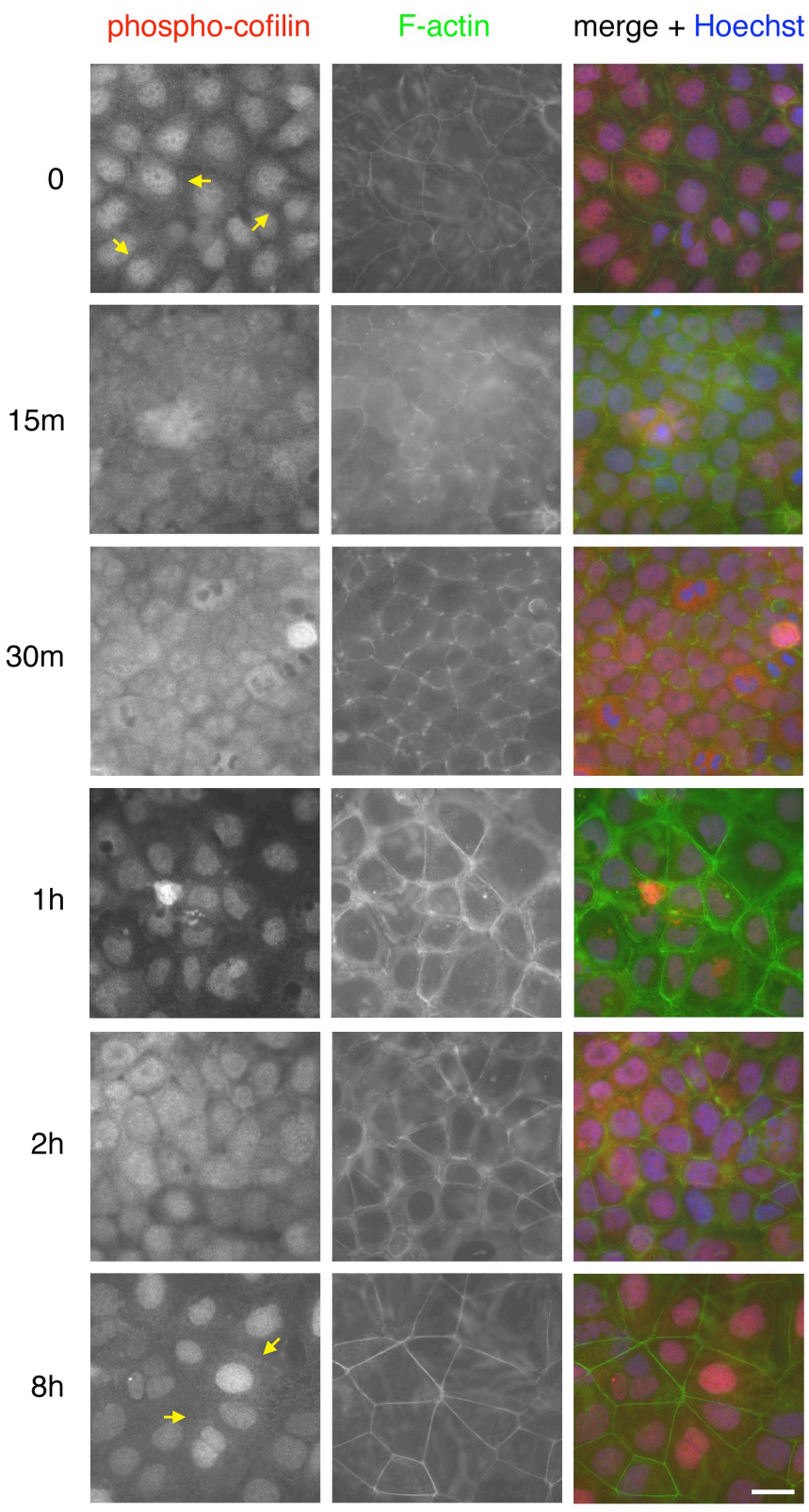

Figure 6.10 – See legend below

Figure 6.10 (above) – Cellular localization of phospho-cofilin in response to hyperosmotic shock. Control Caco-2 cells were plated on to glass coverslips and grown until confluent. Cells were then exposed to medium containing 600mosM NaCl for the times shown before being fixed and processed for immunofluorescence. Anti-phospho-cofilin antibody shows increased cytoplasmic staining after 15 and 30 minutes hyperosmotic shock exposure. After 1 hour phospho-cofilin localizes primarily in the nucleus, and again in the cytoplasm after 2 hours with hyperosmotic shock. Phospho-cofilin can be seen at the junctions at 0 and 8 hour time points (yellow arrows). Shown are representative images of at least 3 independent experiments. Bar, 10μm.

Depletion of MarvelD3 impairs the increase in cytoplasmic phospho-cofilin in response to hyperosmotic shock. Figure 6.11 shows a nuclear localization for phospho-cofilin at all time points and a clear lack of phospho-cofilin in the cytoplasm of MarvelD3-depleted cells. In kidney tubular cells, F-actin remodeling does not occur in the absence of phospho-cofilin (Thirone et al., 2009). Therefore, perhaps the reduced phospho-cofilin in MarvelD3-depleted cells prevents F-actin remodelling from occurring as it does in control cells in response to hyperosmotic shock.

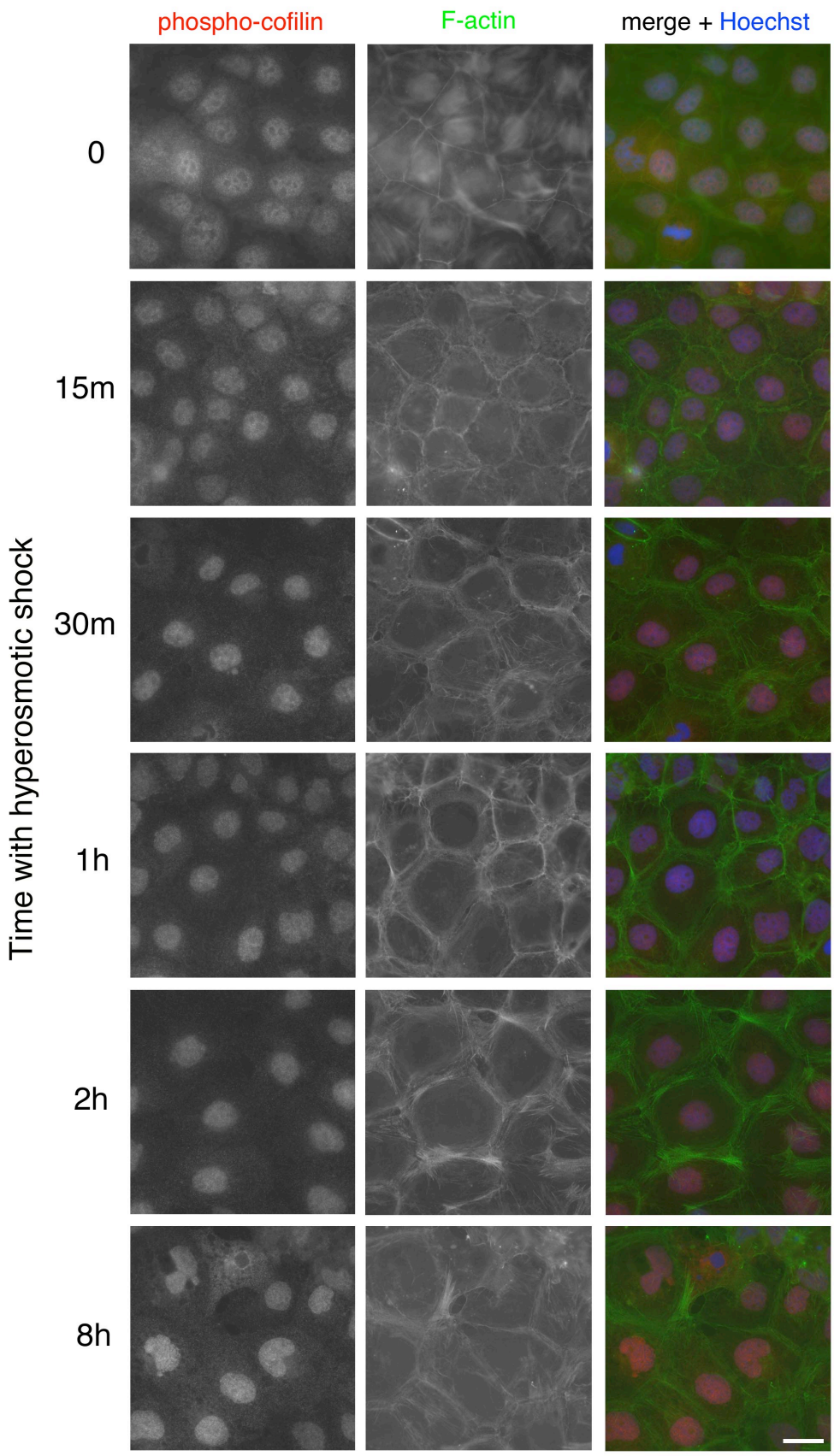

Figure 6.11 – See legend below

Figure 6.11 (above) – Cellular localisation of phospho-cofilin remains in MarvelD3-depleted cells in response to hyperosmotic shock. Once confluent, MarvelD3-depleted Caco-2 cells were exposed to medium containing 600mosM NaCl for the times shown and then fixed and processed for immunofluorescence. Phospho-cofilin localizes to the nucleus at all time points. Cytoplasmic phospho-cofilin staining does not increase in the absence of MarvelD3. Shown are representative images of at least 3 independent experiments. Bars, 10μm.

Phospho-MLC, like cofilin, is downstream of the GTPase RhoA. In control cells, phospho-MLC localizes to the cytoplasmic domain adjacent to the junctions, but not actually at the membrane, after 1 hour of exposure to hyperosmotic conditions (Figure 6.12). At this location it colocalises with the F-actin enriched adjacent to the plasma membrane. Phospho-MLC assumes a similar distrubution in MarvelD3-depleted cells at the 1 hour time point but, in contrast to the cells, the F-actin is very disorganized (Figure 6.13). Therefore, phospho-MLC appears to be able to localize correctly (as seen in controls), but between the 30 minutes and 1 hour time points something is missing that prevents F-actin from enriching in the sub-junctional cytoplasm. Subsequently, the sub-junctional phospho-MLC staining present in control cells at 2 hours is lost in the absence of MarvelD3 and the F-actin organization is further perturbed.

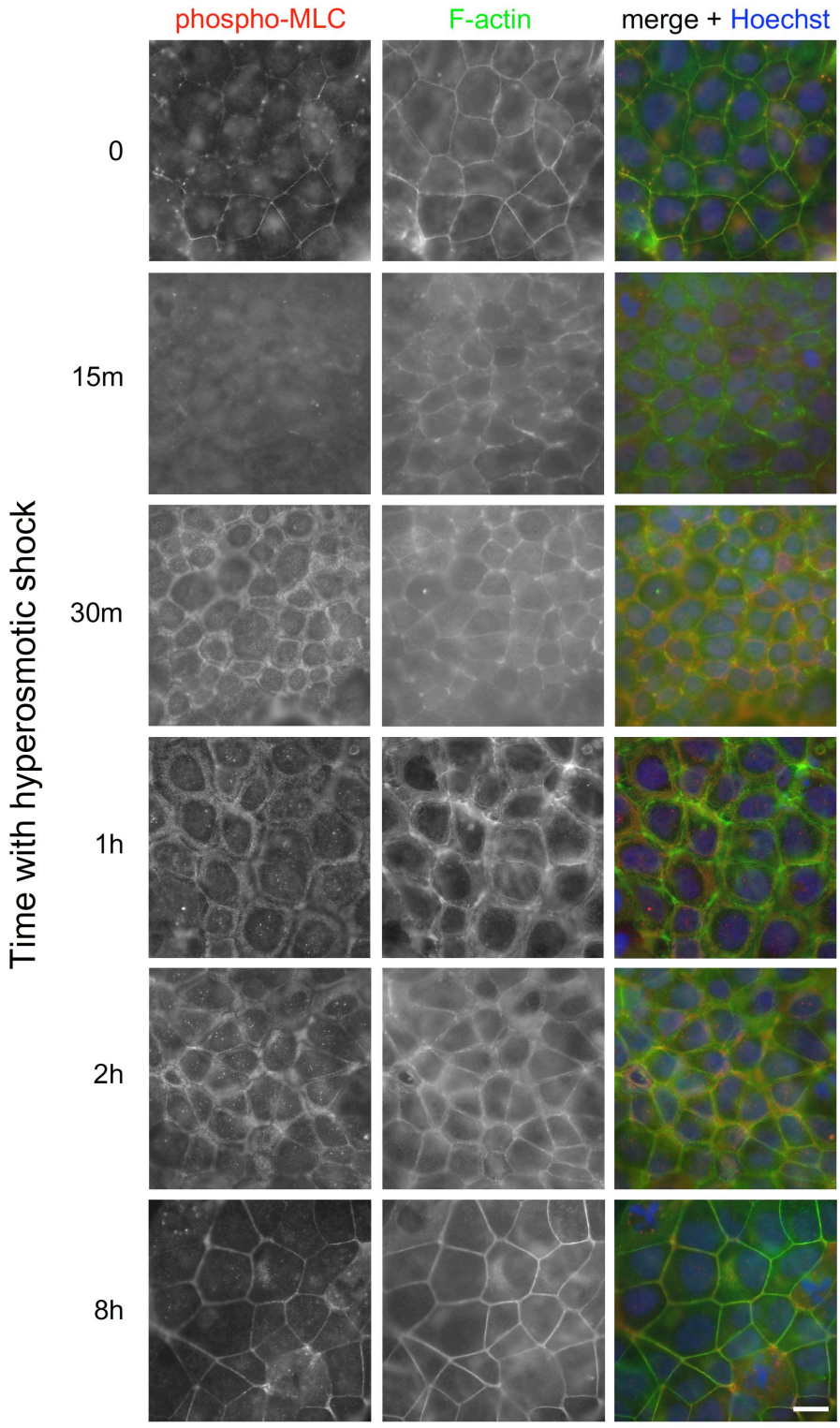

Figure 6.12 – See legend below

Figure 6.12 (above) – Effect of hyperosmotic shock on phospho-MLC localisation in control Caco-2 cells. Control Caco-2 cells exposed to hyperosmotic conditions were fixed and processed for immunofluorescence with an anti-phospho-MLC antibody and FITC-phalloidin to label F-actin. Phospho-MLC enriches in the cytoplasm adjacent to cell-cell contacts after 30 minutes exposure to hyperosmotic shock. Concentration of this signal towards junctional actin appears to begin at the 2 hour time point and junctional phospho-MLC staining is intense after 8 hours of hyperosmotic exposure. Shown are representative images of at least 3 independent experiments. Bar, 10μm.

Figure 6.13 (below) – Effect of hyperosmotic shock on phospho-MLC localization in MarvelD3-depleted Caco-2 cells. MarvelD3-depleted cells exposed to hyperosmotic shock for the times shown were fixed and processed for immunofluorescence with an anti-phospho-MLC antibody and FITC-phalloidin to label F-actin. Phospho-MLC enriches in the cytoplasm adjacent to cell-cell contacts after 30 minutes exposure to hyperosmotic shock. Subsequent concentration of this signal towards junctional actin at the 2 and 8 hour time points fails to occur. The concomitant disorganization of F-actin can be seen. Shown are representative images of at least 3 independent experiments. Bar, 10μm.

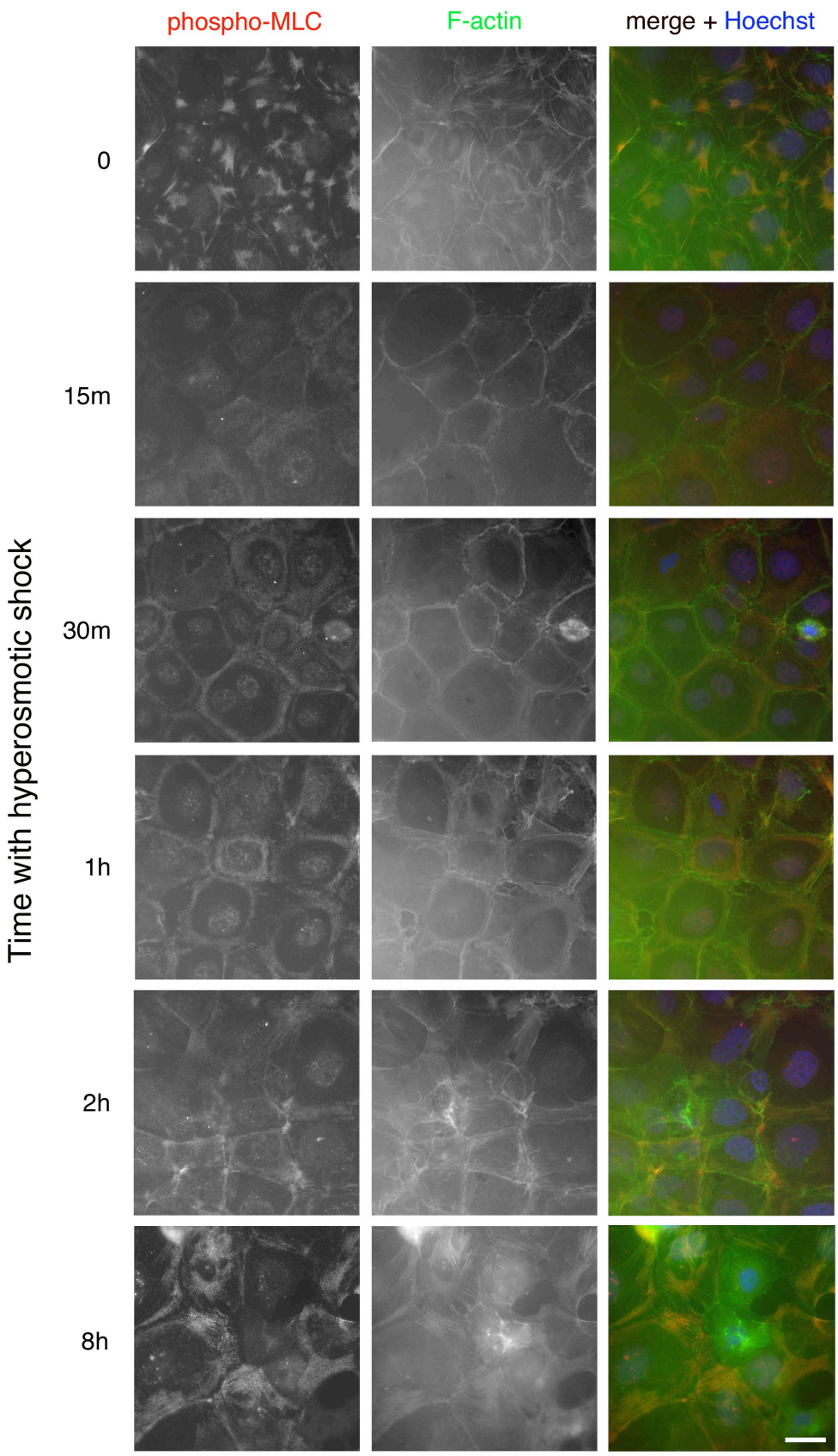

Figure 6.13 – See legend on previous page

In addition to altering the arrangement of the cytoskeleton, the hyperosmotic response also requires changes in gene transcription. Transcription of osmoresponsive genes in response to high NaCl is regulated by Tonicity-responsive enhancer/osmotic response element-binding protein (TonEBP/OREBP). TonEBP/OREBP target genes frequently display one or more AP1 binding sites, binding to which enhances TonEBP/OREBP-induced gene activation in response to high NaCl (Irarrazabal et al., 2008). In the previous chapter, MarvelD3 expression was seen to inhibit activation of the AP1 promoter in a reporter assay. Thus efforts were made to determine the effect of hyperosmotic shock on AP1 promoter activity and the regulation of this by MarvelD3. In preliminary experiments, AP1 promoter activity was increased in MarvelD3-depleted cells exposed to hyperosmotic conditions for 2 hours, but there is variability in the response of control cells, sometimes AP1 promoter activity appears unaffected by hyperosmotic shock, and sometimes it is increased (data not shown). This provides an early indication that MarvelD3 may regulate AP1 activity in response to hyperosmotic shock, but the extent of this regulation is unknown and will require further work.

Prolonged exposure or failure to adapt to hyperosmotic conditions results in apoptosis. Since MarvelD3-depleted cells display a defective cytoskeletal response to hyperosmotic shock, the effect of MarvelD3 on cell survival following hyperosmotic insult was assessed. Quantifying fragmented nuclei as a marker of apoptosis demonstrated that in the absence of MarvelD3, cells were more sensitive to apoptosis in response to hyperosmotic shock (Figure 6.14). During the time course tested, apoptosis was not increased in response to hyperosmotic shock in control cells. This

suggests events mediated by MarvelD3 may be important for survival in response to hyperosmotic shock.

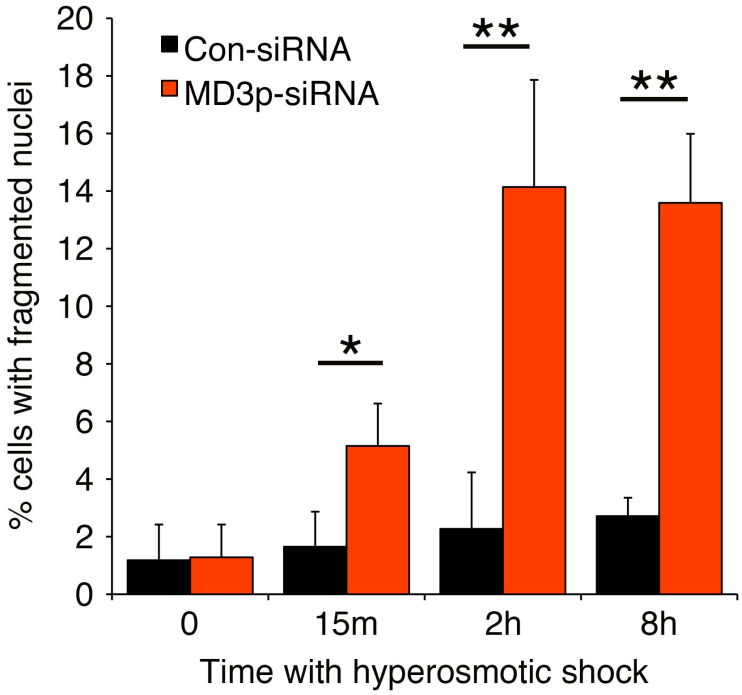

Figure 6.14 – Effect of MarvelD3 depletion on nuclei fragmentation in response to hyperosmotic shock. Caco-2 cells previously transfected with control or MarvelD3-specific siRNAs were exposed to hyperosmotic shock for the time points shown. Cells were fixed and stained with Hoechst to visualise the nucleus. The number of fragmented nuclei were then quantified across three coverslips for each time point. Shown is the mean % of cells with fragmented nuclei compared to the total number of cells plus the standard deviation across three coverslips. Image is representative of 3 independent experiments.

Discussion

The results shown above suggest a role for MarvelD3 in regulating JNK signalling and the actin cytoskeleton in response to hyperosmotic shock. Exposure of Caco-2 and HCE cells to hyperosmotic conditions induced by 600mosM NaCl resulted in a transient redistribution of MarvelD3, but not occludin, to the cytoplasm. This redistribution appears to be dependent on activity of the EGFR and JNK. MarvelD3 also appears to regulate the hyperosmotic shock-induced activation of MEKK1 and JNK, and the subsequent inactivation of their signalling. The most striking phenotype observed is the failure of MarvelD3-depleted cells to rearrange the actin cytoskeleton following hyperosmotic exposure, which may be due to aberrant regulation of MLC and cofilin in MarvelD3-depleted cells. Finally, loss of MarvelD3 predisposes cells to apoptosis by hyperosmotic shock. Taken together these data allude to a significant role for MarvelD3, and the tight junction, in coordinating the activation of MAPK signalling pathways and cytoskeletal rearrangements in response to hyperosmotic shock.

Localisation of MarvelD3 dramatically changes in response to hyperosmotic shock in Caco-2 and HCE cells. Interestingly, however, occludin remains in the cell membrane suggesting this is a MarvelD3-specific event. In an attempt to confirm the internalization of MarvelD3, cells were lysed in the presence of Triton-X to separate fractions from the plasma membrane (triton insoluble) and the cytoplasm (triton soluble). Immunoblotting these lysates suggested an increase in the cytoplasmic pool of MarvelD3 following hyperosmotic shock, but the signal was weak. Confocal microscopy could also be used to determine whether MarvelD3 is indeed internalised,

and not just redistributed over the apical membrane. In addition, immunofluorescence analyses of various intracellular trafficking pathways may help to identify the structures in which cytoplasmic MarvelD3 is found. Confirmation of MarvelD3 internalisation could be achieved by performing further extraction protocols appropriate to the mechanism of internalisation, once identified. The increased cytoplasmic staining could also be attributable to detection of an N-terminal cleavage product. As no additional bands are detected by immunoblotting lysates from cells exposed to MarvelD3 with the anti-MarvelD3 antibody, however, this is not thought to be the reason for increased cytoplasmic MarvelD3 signal. In addition to the junctional and cytoplasmic staining, a strong nuclear signal was also apparent in HCE cells stained with anti-MarvelD3 antibody, independent of hyperosmotic shock. Immunofluorescence should be performed on HCE cells depleted of MarvelD3 by siRNA to determine whether this nuclear signal is specific for MarvelD3.

Internalisation of cell surface receptors is a recognized mechanism for modulating receptor activity. Blocking TNF receptor internalisation, for example, prevents the activation of JNK and downstream signalling leading to TNF-induced apoptosis (Schutze et al., 1999). The mechanism behind MarvelD3 internalisation is not known, though it appears to require EGFR and JNK activity. The EGFR is activated and internalized in response to hyperosmotic shock in a mechanism that is dependent on the Src kinase Yes (Rosette and Karin, 1996). Inhibition of Src kinase family members with PP2 inhibitor however had only a minor effect on hyperosmotic shock-induced internalization of MarvelD3, and MarvelD3 internalisation occurred as in

controls following incubation with PP1 inhibitor, thus suggesting MarvelD3 may be internalized via a distinct mechanism to that of the EGFR.

Inhibition of JNK activity with the specific inhibitor SP600125 and of the EGFR with Gefitinib also impaired internalisation of MarvelD3 in response to hyperosmotic shock. EGFR has been shown to activate JNK in response to hyperosmotic shock (Fischer et al., 2004), alluding to the possibility that these events are upstream and necessary for MarvelD3 internalisation. Surprisingly, inhibition of p38, which is required for EGFR activation in response to hyperosmotic shock (Fischer et al., 2004), did not affect MarvelD3 internalisation, suggesting MarvelD3 internalisation in response to hyperosmotic shock may rely on another mode of EGFR activation. Despite reports of PP3-mediated EGFR inhibition (Klinger et al., 2002; Kong et al., 2011), redistribution of MarvelD3 was not affected by PP3 inhibitor but was inhibited by incubation with Gefetinib. This difference may be due to the efficiency of each of these inhibitors to inhibit the EGFR. PP3 demonstrates a moderate inhibition of EGFR (IC_{50}=2.7μM; (Klinger et al., 2002)) while Gefetinib is much more potent (IC_{50}=0.033μM; (Wakeling et al., 2002)). To confirm the effect of EGFR inhibition on MarvelD3 internalisation, the experiments described should be repeated with other commercially available EGFR inhibitors. In addition, the effect of hyperosmotic shock on MarvelD3 localisation in EGFR-depleted cells could also be examined.

Immunoblotting showed activation of JNK in response to hyperosmotic shock to occur after MarvelD3 internalisation. If MarvelD3 internalisation requires JNK activity and JNK activation requires MarvelD3 internalisation, this could provide a

positive feedback loop whereby MarvelD3 facilitates its own internalisation and further amplification of downstream signalling pathways. In their study, Schutze *et al*., (1999) utilised K^+ depletion to impair endocytosis and demonstrated the effects of blocking TNF receptor internalisation on the activation of downstream signalling pathways. It would be interesting to see if K^+ depletion prevents MarvelD3 internalisation and, if so, if this prevents activation of MEKK1 and JNK. This would avoid the use of small molecule inhibitors like SP600125, which may complicate interpretations as JNK is implicated in more than one stage of the pathway. Collecting cell lysates at earlier time points following addition of hyperosmotic conditions may also allow the transient nature of JNK activation to be seen and enable more detailed dissection of its role in regulating the localisation of MarvelD3.

To determine whether the loss and subsequent restoration of junctional MarvelD3 in response to hyperosmotic shock affected protein levels, cell lysates were immunoblotted for MarvelD3 and occludin, the localisation of which appears unaffected by hyperosmotic exposure. Interestingly, there was no loss of MarvelD3 protein compared to cells in isotonic medium. Thus, at earlier time points, hyperosmotic shock appears to cause a relocalisation of MarvelD3 away from the junction and in to the cytoplasm. At later time points, MarvelD3 returns to the junction and cytoplasmic staining is reduced. Total levels of MarvelD3 protein are unaffected in this process, but whether this relies on recycling of internalised MarvelD3, or its degradation followed by protein synthesis remains to be determined. Clathrin-mediated internalization of the EGFR commits it for degradation, while clathrin-independent mechanisms promote EGFR signalling by recycling the receptor

back to the cell surface (Sigismund et al., 2008). Identifying the mechanisms behind MarvelD3 internalisation could be a focus of future studies.

Regardless of the mechanism, the return of MarvelD3 to the membrane appears to be an important event in the response to hyperosmotic shock, as shown by the loss of junctional integrity in MarvelD3-depleted cells. After being exposed to hyperosmotic conditions for 2 hours, MarvelD3 begins to return to the junctions in control cells. This time course is coincident with the recovery of impedance readings in response to hyperosmotic shock. Control cells recover the initial loss of impedance values during the osmoadaptation process, but this does not occur in MarvelD3-depleted cells. Disruption of occludin and ZO-1 staining at the tight junction further suggests MarvelD3-depleted monolayers are more severely compromised following hyperosmotic insult than control monolayers.

The restoration of junctional MarvelD3 also appears to be significant in the regulation of JNK signalling in response to hyperosmotic shock. Both MEKK1 and JNK activation are prolonged in the absence of MarvelD3 suggesting failure of these cells to restrict MEKK1-JNK signalling and implicating MarvelD3 in the temporal regulation of this intracellular signalling pathway. Earlier in this thesis an interaction between MarvelD3 and MEKK1 was identified and it was hypothesised that this interaction inhibited the action of MEKK1. In response to hyperosmotic shock, MEKK1 becomes phosphorylated at Ser1455, which lies within the kinase domain of MEKK1, but is otherwise not annotated. Thus the significance of this residue and its phosphorylation state in the function of MEKK1 is not yet known. The coincidence of

MEKK1 phosphorylation at Ser1455 with MarvelD3 internalisation and JNK activation stimulated the hypothesis that internalisation of MarvelD3 functions to activate MAPK signalling in response to hyperosmotic shock (Figure 6.15). That is, at the tight junction, MarvelD3 interacts with MEKK1 inhibiting its signalling activity. Internalisation of MarvelD3 in response to hyperosmotic shock serves to liberate MEKK1 from this MarvelD3-mediated inhibition. This could be because the internalisation of the MarvelD3-MEKK1 complex brings MEKK1 into close proximity of an activator, or maybe because internalised MarvelD3 can no longer interact with MEKK1, thus releasing it in to the cytoplasm for activation. Performing co-immunoprecipitation experiments with cells exposed to hyperosmotic shock and those left in normal complete medium may help to identify whether phosphorylation of MEKK1 affects its interaction with MarvelD3. In addition, immunofluorescent analysis of phospho-MEKK1 and MEKK1 localisation in response to hyperosmotic shock may help to show the importance of this relocalisation away from the plasma membrane. By relieving its inhibition by MarvelD3, hyperosmotic shock results in the activation of MEKK1 and, subsequently, JNK. Loss of both MEKK1 and JNK phosphorylation in control cells concomitant with the return of MarvelD3 to the tight junction, suggests MarvelD3 switches off this signalling pathway by interacting again with MEKK1 at cell-cell contacts. Since MarvelD3 depleted cells are unable to restore MarvelD3 at the membrane, MEKK1 and JNK activity in response to hyperosmotic shock is prolonged. If MarvelD3 internalisation is necessary for MEKK1 phosphorylation, SP600125 and Gefitinib-mediated inhibition of MarvelD3 redistribution should subsequently prevent phosphorylation of MEKK1. Thus the effect of SP600125 and Gefitinib on MEKK1 phosphorylation may help determine the importance of MarvelD3 internalisation on activation of this signalling pathway in

response to hyperosmotic shock. This model also suggests a link between the findings of Samak and colleagues, that osmotic shock-induced activation of JNK is responsible for tight junction disruption (Samak et al., 2010), with the initial observation here that MarvelD3-depleted monolayers fail to recover alterations to impedance values following hyperosmotic exposure. In addition to inhibiting the effect of JNK on gene expression, restoration of junctional MarvelD3 may also serve to inhibit JNK activity towards the tight junction, perhaps attenuating junction disruption and allowing integrity of the tight junction to be recovered, which thus doesn't occur in MarvelD3-depleted cells.

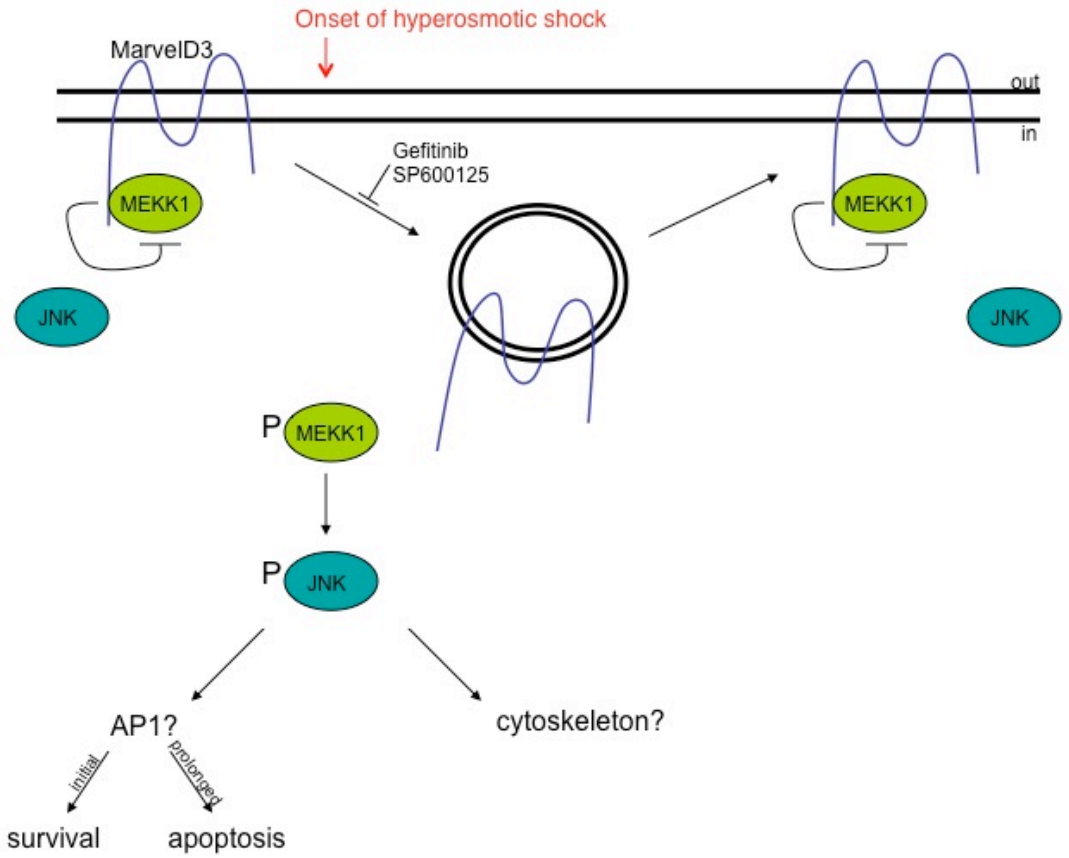

Figure 6.15 – Hypothetical model for the regulation of the hyperosmotic shock response by MarvelD3. Within the membrane domain of the tight junction, the N-terminus of MarvelD3 interacts with MEKK1 and inhibits its activity. Thus MEKK1 and JNK are inactive. Exposure to hyperosmotic shock results in redistribution of MarvelD3 to the cytoplasm and activation of MEKK1 and JNK. The consequence of JNK and MEKK1 activation are discussed in the text below. Following prolonged exposure to hyperosmotic shock, MarvelD3 returns to the membrane where it can interact with MEKK1, and inhibit its activity. JNK activity is also reduced. In MarvelD3 knockdown cells, therefore, MarvelD3 is not available to be returned to the membrane and therefore MEKK1 and JNK activity persist.

The most striking phenotype observed is the failure of MarvelD3-depleted cells to rearrange their cytoskeleton in response to hyperosmotic shock. Previously, the increase in F-actin in response to hyperosmotic shock has been shown to require phosphorylation of cofilin at Ser3 and inactivation of its actin severing activity (Thirone et al., 2009). In the current study, loss of MarvelD3 did not affect the level of phospho-cofilin in response to hyperosmotic shock when compared to control cells, but did affect its localization. Immunofluorescence analyses showed a biphasic increase in cytoplasmic phospho-cofilin in response to hyperosmotic shock at the 15 minute, 30 minute and 2 hour time points in control cells, but there was no such increase in cytoplasmic phospho-cofilin in MarvelD3-depleted cells, with phospho-cofilin only localizing to the nucleus. This may suggest that there is more active, unphosphorylated cofilin in the cytoplasm of MarvelD3-depleted cells which, according to the results of Thirone *et al*., (2009), may explain the failure of these cells to increase F-actin. Assaying the ratio of G- and F-actin in control and MarvelD3-depleted cells in response to hyperosmotic shock would help to confirm this. Immunofluorescence analysis should also be performed with anti-cofilin antibodies to determine the localization of the active protein in response to hyperosmotic shock and if MarvelD3 regulates this. In response to sucrose-induced hyperosmolarity, cofilin phosphorylation is regulated by the RhoA/ROCK/LIMK pathway (Thirone et al., 2009). Thus MarvelD3 may regulate cofilin activity in response to hyperosmotic shock via RhoA, which is thought to be elevated in MarvelD3-depleted cells, though there could also be differences in the GTPases affected by hyperosmotic shock induced by NaCl. Experiments to confirm the effect of MarvelD3 knockdown on RhoA activity levels need to be performed.

Interaction between MEKK1 and the actin cross-linker α-actinin affords a mechanism by which MEKK1 may impact on the cytoskeleton (Christerson et al., 1999). Interestingly, in the presence of a severing protein (like cofilin) and a cross-linker (like α-actinin), actin filaments aggregate into filament bundles (Maciver et al., 1991). Thus MarvelD3 may regulate actin bundling via MEKK1-α-actinin and by regulating the localization/activation of cofilin. The specific mechanism by which this is achieved, however, remains to be confirmed.

MLC phosphorylation is also important for bundling of actin filaments and is also activated downstream of RhoA (Etienne-Manneville and Hall, 2002). In response to hyperosmotic shock, increased phospho-MLC signal is observed in the cytoplasm adjacent to the membrane, but not at the membrane in both control and MarvelD3-depleted cells. The difference in pMLC staining between control and MarvelD3-depleted cells may be due to the prior failure of MarvelD3-depleted cells to generate actin filaments upon which pMLC and Myosin II can act. Thus at later time points, pMLC staining appears perturbed when compared to controls.

Cells depleted of MarvelD3 seemed to be more sensitive to apoptosis in response to hyperosmotic shock than control cells. This could be due to the prolonged JNK activation seen in MarvelD3-depleted cells. In response to TNFα, JNK activation initially promotes cell survival, but when prolonged enhances the expression of proapoptotic pathways (Ventura et al., 2006). Thus in response to hyperosmotic shock, JNK activation may initially stimulate the expression of genes promoting osmoadaptation and cell survival, like AR and Hsp70. Prolonged activation of JNK,

as observed in the absence of MarvelD3, may then lead to the activation of pro-apoptotic pathways, like the cytochrome c pathway (Tournier et al., 2000). Interestingly, AR and Hsp70, which both contain AP1 sites in their promoters, were both downregulated in response to MarvelD3 expression in the microarray performed in chapter 4. It would be interesting to examine the genetic profile of MarvelD3-regulated JNK signalling in response to hyperosmotic shock by performing the AP1 reporter assay in control and MarvelD3-depleted cells exposed to hyperosmotic shock for varying amounts of time. These studies would be complemented by immunoblotting for candidate target proteins, like Hsp70, AR or markers of apoptosis like caspase 3 activation, to elucidate the mechanism through which MarvelD3 expression may be promoting survival and preventing apoptosis after prolonged exposure to hyperosmotic shock.

The N-terminal region of MEKK1 contains a plant homeodomain (PHD), which is involved in protein-protein interactions and acts as an E3 ubiquitin ligase. The ubiquitination and degradation of cJun by MEKK1 in response to hyperosmotic shock has previously been shown to result in increased apoptosis (Xia et al., 2007). Assessing the effect of MarvelD3 depletion on levels of cJun in response to hyperosmotic shock may hint at whether MarvelD3 expression regulates the ligase activity of MEKK1. In addition, the kinase domain of MEKK1 has been shown to be necessary for the induction of apoptosis in response to cytoskeletal disruption (Tricker et al., 2011). Interestingly, phosphorylation of MEKK1 in response to hyperosmotic shock occurs within its kinase domain, but the function of this phosphorylation site has never before been addressed. Furthermore, RhoA binds to the PHD of MEKK1 in

a GTP-dependent manner and promotes its kinase activity (Gallagher et al., 2004). If, as hypothesised, RhoA activity levels are elevated in MarvelD3-depleted cells, the greater abundance of RhoA-GTP could lead to greater levels of active MEKK1, which may in turn promote apoptosis via ubiquitination of cJun or prolonged activation of JNK, or both. Identifying how phosphorylation at Ser1455 affects the activity of MEKK1 could be key to understanding this. These data implicate MarvelD3 in protecting cells from hyperosmotic shock-induced apoptosis.

The data presented suggests MarvelD3 may play more than one role in the hyperosmotic shock response. First, by enabling MEKK1 and JNK activation, MarvelD3 internalisation may be involved in promoting the expression of osmoadaptive genes. Restoration of junctional MarvelD3 then serves to switch off MEKK1 and JNK activity and prevents the induction of pro-apoptotic signalling pathways. Concomitant rearrangement of the cytoskeleton and recovery of junctional disruption ensures the integrity of the monolayer is maintained despite the hyperosmotic surroundings. In the absence of MarvelD3, regulation of these processes is impaired and monolayer integrity is subsequently compromised. Thus, by regulating JNK MAPK signalling, MarvelD3 plays a vital role in maintaining monolayer homeostasis in response hyperosmotic stress.

Chapter 7:

Analysis of MarveID3 function during development in *Xenopus laevis*

Chapter 7 – Analysis of MarvelD3 function during development in *Xenopus laevis*

Introduction

Studies performed so far in cell culture have identified a role for MarvelD3 in the regulation of epithelial cell proliferation and migration. As these processes are also fundamental to embryonic development, I asked if MarvelD3 might also regulate these processes *in vivo*. The African clawed frog *Xenopus laevis* provided an ideal system in which to perform these initial studies. Although the pseudotetraploid genome of *X. laevis* renders it unsuitable for genetic studies, the large size and relative robustness of the eggs (approx. 1.2-1.4mm diameter) and embryos means *X. laevis* is easy to manipulate *in vitro*. Simple hormone injections are used to induce females to lay large quantities of eggs, which can then be collected and fertilized *in vitro* to generate a synchronised population. The aim of this chapter therefore was to utilise this relatively simple, yet *in vivo*, system to examine the function of MarvelD3 during embryonic development, with particular attention to proliferation and migration.

The initial cleavage stages of *Xenopus laevis* development

Following fertilisation, the *Xenopus* embryo undergoes are series of synchronous cell divisions generating 2 (stage 2), 4 (stage 3), 8 (stage 4), 16 (stage 5) and 32 blastomeres (stage 6). At stage 6.5 the early embryo consists of a solid ball of approximately 48 cells and is termed the morula, which will go on to develop into the blastula. Interestingly, the first 12 divisions of *Xenopus* development do not require gene transcription and rely instead upon the expression of maternal RNAs, which are regulated through post-transcriptional modifications in the early *Xenopus* embryo.

These maternal transcripts are stable in the embryo until the mid-blastula transition (Paris et al., 1988), an important developmental transition involving the coordinated induction of both gene transcription and cell motility (Newport and Kirschner, 1982a, b).

Migration during *Xenopus laevis* development

Cell migration is crucial to embryonic development. During gastrulation, the precursors of the three distinct germ layers, the endoderm, mesoderm and ectoderm, assume their positions through a series of coordinated cell movements to give rise to the internal endoderm, the external ectoderm and the mesoderm in between. Directed cell migration is one mechanism through which this is achieved. The prechordal mesodermal cells migrate inside the embryo towards the animal pole as a group, relying on extracellular matrix secreted by the blastocoel roof (Winklbauer, 1990). Gastrulation also involves the process of convergent extension, which, in *Xenopus laevis*, is a cell sorting mechanism and does not involve migration. The combined effects of migration and convergent extension, however, result in closure of the blastopore lip by the end of gastrulation.

Neurulation is the next developmental stage after gastrulation. During neurulation, dorsal ectoderm cells assume a neural fate and involute at the dorsal midline to form the neural tube. The formation of the neural tube during neurulation relies on alterations in cell shape and cell packing causing the epithelium to role up in to a tubular structure. The border between the neural plate and non-neuronal ectoderm gives rise to the neural crest cells, which are induced at gastrulation and maintained through neurulation in response to Wnt and BMP signalling (Steventon et al., 2009).

The neural crest cells undergo an epithelial-to-mesenchymal transition and delaminate from the dorsal side of the neural tube. Neural crest cells then migrate through the embryo and differentiate in to a great number of cell types upon reaching their destinations, including neurons, skin pigment cells and a number of connective tissues in the head, including skull and jaw bones. Myoblasts, which are muscle precursor cells, are another migratory cell type. Myoblasts migrate from the somites positioned on either side of the notochord and later differentiate into muscle cells.

Tight junctions in *Xenopus laevis*

In *Xenopus laevis*, tight junctions are observed during the first cell division as the blastocoel forms during the early cleavage stages. Tight junction proteins occludin, cingulin and ZO-1 are maternally expressed indicating their importance from the earliest stages of development (Fesenko et al., 2000). By observing the degree of biotin penetration between blastomeres during development, tight junctions have been shown to initially form deep within the embryo before assuming their characteristic apical position, prior to the onset of gastrulation (Merzdorf et al., 1998). Functional tight junctions have been implicated in the establishment of left-right asymmetry, which becomes randomized following overexpression of *Xenopus* claudin (Brizuela et al., 2001). Loss of *Xenopus* claudin following morpholino injection appears to prevent convergent extension movements during gastrulation (Chang et al., 2010), further alluding to a role for tight junctions during *Xenopus* embryonic development. Importantly for this study, *Xenopus laevis* expresses a homologue of MarvelD3 (Chapter 3, Table3.1/Figure 3.3), buts its significance and role in development has not been addressed. Figure 7.1 shows the stages of *X. laevis* development and the events of relevance to the present study.

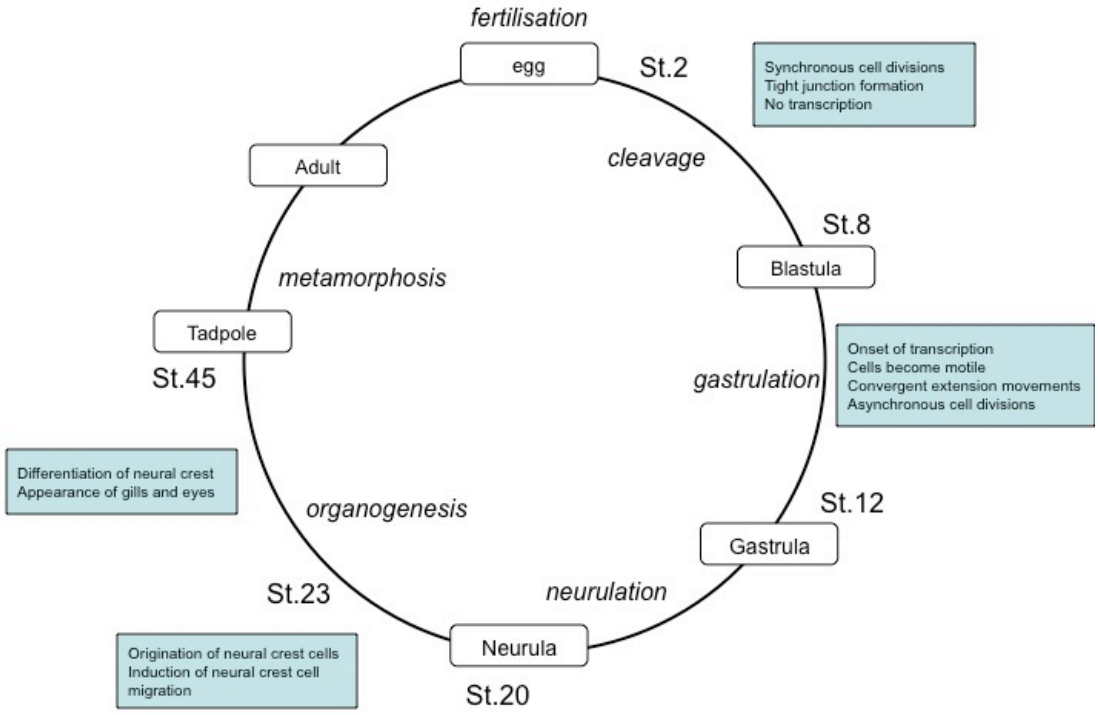

Figure 7.1 – Representation of *Xenopus laevis* development. The main stages of *X. laevis* development are shown. The experiments in this chapter utilize embryos from fertilization to stage 37/38, after the appearance of eyes and gills. Tight junctions are established and stabilized during the cleavage stages to enable the formation of the blastocoel. Cell migration is initiated during gastrulation. Migration of neural crest cells and myoblasts through the embryo is also an important developmental process requiring cell migration.

Using *Xenopus laevis* embryos as a tool in which to study migration *in vivo*, the results presented below provide evidence to suggest a role for MarvelD3 during *Xenopus laevis* development and, possibly, in the regulation of neural crest cell migration. Future work looking at the regulation of neural crest cells in the absence of MarvelD3 combined with work already conducted in cell culture systems may help to consolidate a function for MarvelD3 in the regulation of cell migration.

Results

Expression of MarvelD3 during *Xenopus laevis* development

To first confirm the expression of MarvelD3 in the *Xenopus* embryo (xMD3) and to determine its expression pattern during early embryogenesis, RT-PCR was performed on RNA extracted from embryos at representative stages of development. Transcripts of xMD3 were detected in the unfertilized egg suggesting xMD3, like occludin and cingulin (Fesenko et al., 2000), is supplied maternally to the *X. laevis* embryo (Figure 7.2). Expression of xMD3 mRNA persisted through the cleavage stages, in the blastula (stage 8) and at the onset of gastrulation (stage 10). At later stages xMD3 transcript could still be detected though levels were relatively low. A doublet also appeared in samples taken from stage 10 to stage 35 embryos, the identity of which is not yet known. To confirm the band(s) correspond to xMarvelD3, PCR products should be cloned into a TA-cloning vector and sequenced. This may also enable the identity of the second band to be identified, which may represent MarvelD3 variant B.

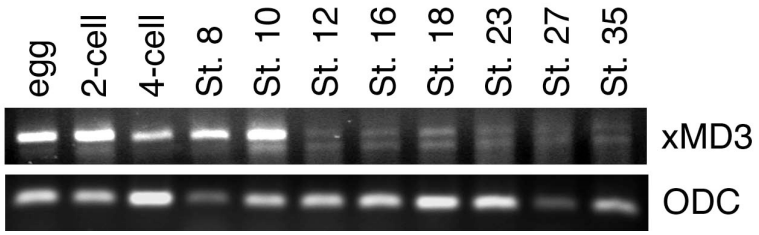

Figure 7.2 – Expression of xMD3 during *X. laevis* embryonic development. RNA extracted from *Xenopus* embryos collected at representative stages of development was subjected to RT-PCR to identify the temporal expression pattern of xMD3 during development. xMarvelD3 transcript was present in the maternal RNA in embryos and in stage 10 embryos after the mid-blastula transition. xMarvelD3 transcript persisted in later stage embryos, though levels were relatively low in comparison to earlier stages. Amplification of ornithine decarboxylase (ODC) was used as a control, due to its ubiquitous expression during early development.

Loss-of-function studies

In order to gain insight in to the functional relevance of MarvelD3 expression in *Xenopus* development, 30ng morpholino specific for the *Xenopus* sequence of MarvelD3 (xMD3-MO) or a control morpholino (Con-MO) was injected into the animal pole of both cells of the 2-cell embryo. Embryos injected with xMD3-MO appeared to develop normally and were indistinguishable from Con-MO-injected and uninjected embryos until stage 15 (Figure 7.3A). After stage 15, xMD3-MO-injected embryos began to develop more slowly than the Con-MO and uninjected embryos. Uninjected and Con-MO-injected embryos developed at the same rate (Figure 7.3A). The effect of xMD3-MO injection became even more apparent at later stages of development. The appearance of the eye and gills were delayed in xMD3-MO-injected embryos, although they did eventually appear. Eye pigmentation in the xMD3-MO embryos, however, did not darken in the same way as the controls. Embryos injected with xMD3-MO were incubated until they reached stage 37/38, staged by position of the proctoderm, but still the pigmentation of the eye did not darken to the level of the controls (Figure 7.3B). In addition, the number of melanophores and their degree of pigmentation along the lateral epidermis also appeared reduced following injection of xMD3-MO. Disruption of MarvelD3 function, therefore, appears to slow down development of *X. laevis* embryos after gastrulation.

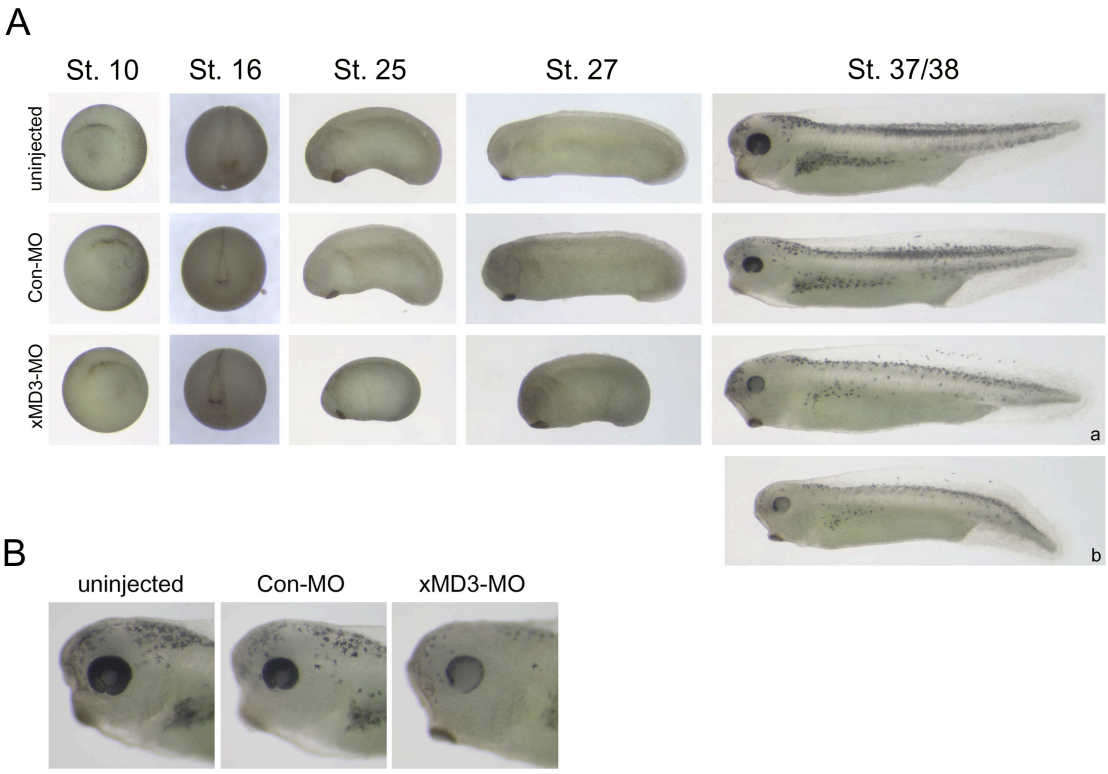

Figure 7.3 – Effect of bilateral xMD3 morpholino injection during early stages of *Xenopus* development. (A) Injection of 30ng xMD3-MO in to both cells at the 2-cell stage had no effect on embryonic development prior to stage 16. After stage 16, injection of xMD3-MO resulted in developmental delay. Images show time-matched representative development of each treatment group until uninjected embryos reached stage 37/38. (b) xMD3-MO injected embryos were left to develop to stage 37/38 to see if the eye and melanophore pigmentation reached that of the controls. (B) Increased magnification of the head shows reduced eye pigmentation following xMD3-MO injection. Injection of xMD3-MO also appears to reduce the number of pigmented cells on the head and sides of the embryo. Shown are representative images of stage 37/38 embryos from three independent experiments.

MarvelD3 MO was also injected into one cell of the 2-cell embryo. Injection of xMD3-MO caused curvature of the neural axis towards the site of injection, which was not observed in Con-MO embryos (Figure 7.4). Co-injection of β-galactosidase enabled identification of the injected side.

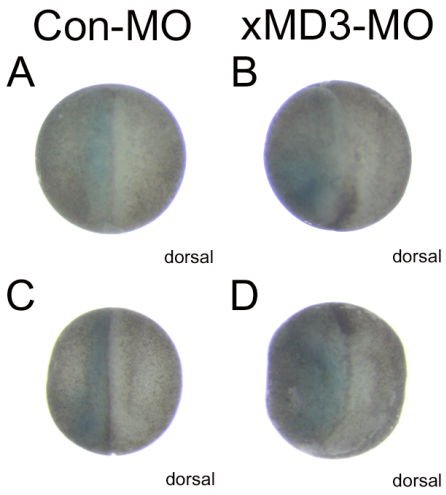

Figure 7.4 – xMarvelD3 morpholino injection results in curvature of the neural fold in stage 20 embryos. Control or xMarvelD3 morpholino (30ng) was injected in to a single cell at the 2-cell stage. Injected embryos were fixed at stage 20 and β-galactosidase staining allowed identification of the injection side. Unilateral injection of xMD3-MO resulted in curvature of the neural fold (B and D) when compared to control-injected embryos (A and C). Shown are representative embryos from three independent experiments.

Given the curvature observed at stage 20 following injection of xMD3-MO into a single cell at the 2-cell stage and the more apparent effect of bilateral xMD3-MO injection at later stages of development, the effect of unilateral xMD3-MO injection on the later stages of development was assessed. Unilaterally injected embryos were

allowed to develop until stage 35/36. Embryos injected with 5ng xMD3-MO were indistinguishable from Con-MO-injected embryos (Figure 7.5). Injection of 30ng xMD3-MO, however, caused a dramatic curvature of the embryo along the anterior-posterior axis towards the site of injection, which was not seen following injection of 30ng Con-MO (Figure 7.5). In addition, injection of xMD3-MO at this and an intermediate dose (20ng) resulted in a shortening of the length of the embryo. Quantification showed that both the shortening and curvature of the anterioposterior body axis increased in severity with increasing concentration of xMD3-MO. Bending of the body axis towards the xMD3-MO-injected side is consistent with the direction of curvature of the neural fold in stage 20 embryos following xMD3-MO injection. That these effects were not seen in Con-MO-injected embryos suggests this phenotype is a result of the disruption to MarvelD3 function following xMD3-MO injection.

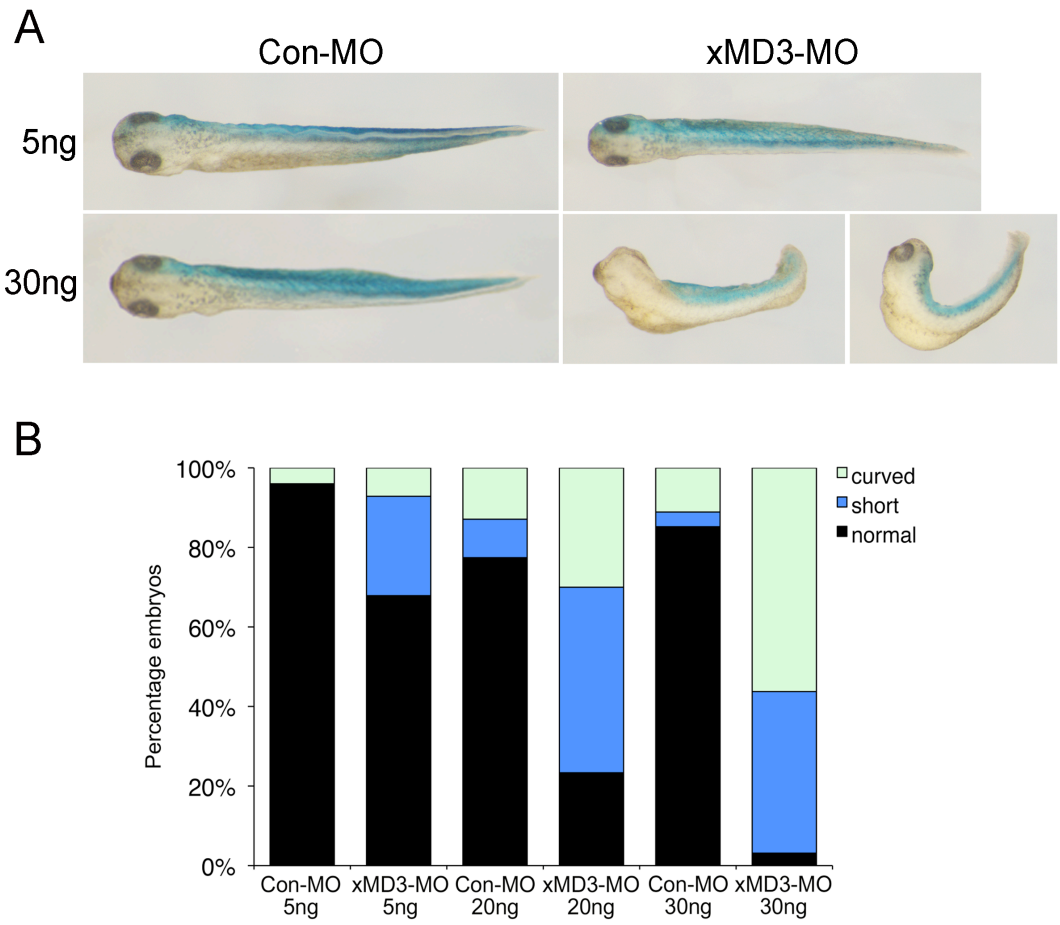

Figure 7.5 – Injection of xMD3-MO results in shortening and curvature of the anterioposterior body axis. (A) Con-MO and xMD3-MO-injected embryos were fixed at stage 35/36. Development of β-galactosidase staining was used to identify the side of injection. Embryos injected with 5ng xMD3-MO appear similar to controls. Embryos injected with 30ng xMD3-MO have reduced body length and curve towards the site of injection. Injection of 30ng Con-MO caused no observable defect in development. (B) Quantification of "curved", "short" and "normal" phenotypes correlates severity with increasing concentration of xMD3-MO. Between 25 and 30 embryos were counted for each treatment group across two independent experiments. Images are representative of two independent experiments.

Furthermore, in keeping with the observations made above, unilateral injection of xMD3-MO resulted in perturbed eye development when compared to the uninjected side of the embryo (Figure 7.6). The numbers of melanophores present on the

injected side were also reduced following xMD3-MO injection. These observations further suggest MarvelD3 may play a role in the regulation of the later stages of development, possibly beginning at neurulation.

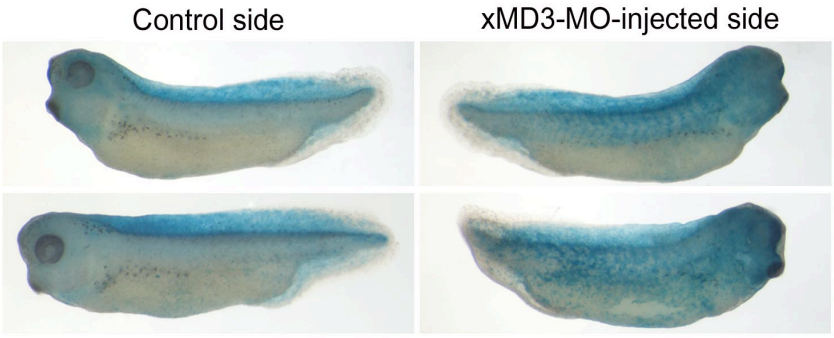

Figure 7.6 – Unilateral injection of xMD3-MO perturbs eye and melanophore development. Embryos injected with 30ng xMD3-MO into a single cell at the 2 cell stage were fixed at stage 35 and images taken of the control (uninjected) side and the xMD3-MO-injected side. Within the same embryo, xMD3-MO injection perturbs development of eye pigmentation and the number of melanophores on the lateral epidermis. β-galactosidase staining in blue enables the injected side to be identified. Images are representative of two independent experiments.

To confirm the phenotypes observed were due to depletion of xMD3, RNA encoding human MarvelD3 isoform 2 (hMD3_2) was generated for injection alongside the Con- or xMD3-MO. To confirm the human MarvelD3_2 was expressed following mRNA injection, hMD3_2 or GFP mRNA (control) was injected into both cells at the 2-cell stage and the embryos were lysed at stage 10 to determine protein expression. Immunoblotting with the antibody against human MarvelD3 detected a band of approximately 40kDa in the hMD3_2-injected embryos but not those injected with GFP or not injected (Figure 7.7), suggesting human MarvelD3 protein is expressed

following injection of its mRNA in *Xenopus* embryos. GFP protein could also be detected following injection of its mRNA, providing a control for subsequent experiments.

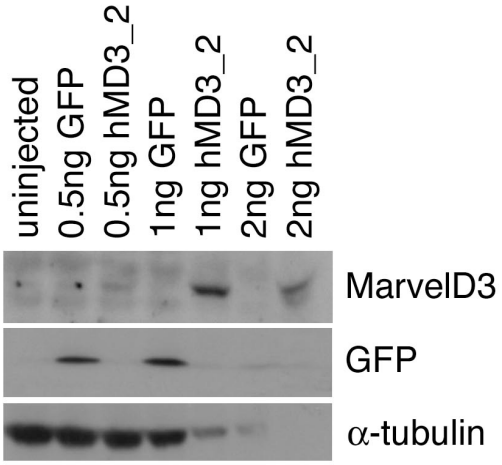

Figure 7.7 – Expression of human MarvelD3 isoform 2 and GFP following mRNA injection in *Xenopus laevis* embryos. Embryos were injected with mRNA encoding GFP or human MarvelD3 isoform 2 (hMD3_2) into both cells of the 2-cell embryo and allowed to develop until stage 10. Embryos were then lysed and protein expression analysed by immunoblotting. MarvelD3 protein is expressed following injection of 1ng and 2ng mRNA. GFP protein is detected following injection of 0.5ng and 1ng GFP. α-tubulin was used as a loading control. Immunoblotting is representative of two independent experiments.

Rescue experiments were designed in which hMD3_2 or GFP mRNA would be injected alongside Con- or xMD3-MO both unilaterally and bilaterally at the 2 cell stage, to see if hMD3_2 expression could rescue the phenotypes reported above. Unfortunately, however, those experiments performed to date have resulted in large amounts of embryo death leaving few embryos from which to base conclusions. Since the level of death was also high amongst uninjected embryos it is thought these

problems were due to poor quality eggs, rather than an effect of morpholino or mRNA injection. Thus these experiments need to be repeated in the future to confirm the phenotypes observed following xMD3-MO injection are specific to loss of xMD3 and perform additional gain-of-function experiments, to assess the effect of MarvelD3 overexpression during *Xenopus laevis* development.

Neural crest cells are a highly migratory cell population, which migrates out from the neural fold. Melanocytes and iris pigment cells are derived from neural crest cells and since disruption of xMD3 function appears to reduce their expression and has been shown to regulate migration in studies *in vitro*, the effect of xMD3-MO injection on neural crest cell migration was examined. To do this, embryos were injected unilaterally with xMD3-MO and fixed at stages 20 and 23 before being analysed by whole mount *in situ* hybridisation for the expression of the neural crest cell marker, *Twist* (Hopwood et al., 1989). β-galactosidase staining was used to identify the injected side of the embryo and the expression and positioning of neural crest cell markers could then be compared to that on the uninjected side of the embryo. *Twist* was unaffected by *xMD3* depletion at stage 20 but the staining as lost on the injected side at stage 23 (Figure 7.8).

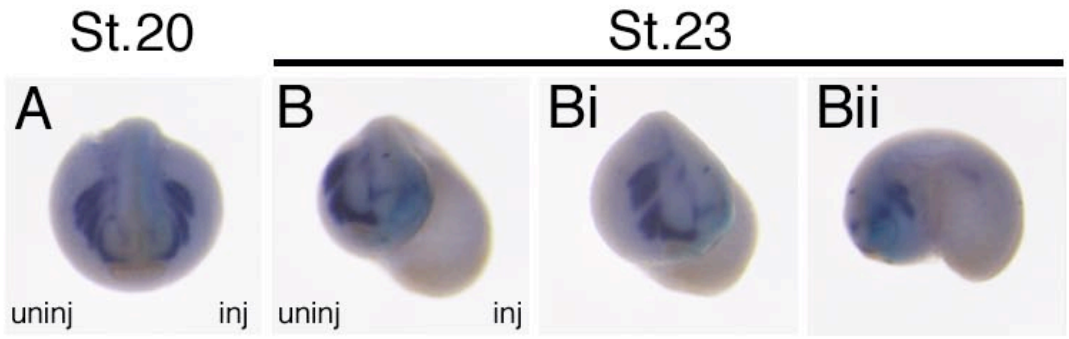

Figure 7.8 – Effect of xMD3-MO injection on *Twist* expression. Stage 20 and stage 23 embryos unilaterally injected with xMD3-MO were subjected to whole mount *in situ* hybridization to determine the effect of xMD3-MO injection on *Twist* expression, as a marker of the neural crest. (A) Injection of xMD3-MO does not affect *Twist* expression in stage 20 embryos. (B) Injection of xMD3-MO results in reduced *Twist* expression in stage 23 embryos. As the curvature of the embryo makes it difficult to appreciate the extent of lateral staining loss, (Bi) shows clearer orientation of the uninjected side and (Bii) shows the xMD3-MO-injected side of the embryo imaged in (B). β-galactosidase staining allows the injection side to be identifid. For clarity, embryos were imaged with the uninjected side on the left and the injected side on the right. All images are representative of two independent experiments.

Myoblasts are also a migratory cell type, ultimately differentiating in to muscle cells. The expression of the differentiated muscle marker *myosin heavy chain* (*MHC*;(Radice and Malacinski, 1989)) was reduced following xMD3-MO injection corresponding to curvature towards the injection side (Figure 7.9A). Staining for the differentiated primary neuron marker *neural β-tubulin* (*NBT*) was also reduced ventrally and dorsally on the side of xMD3-MO injection (Figure 7.9B). Thus morpholino-induced depletion of xMD3 appears to result in reduced expression of neural crest cell markers, reduced differentiation of muscle and primary neurons and repressed formation of neural crest cell derivatives (pigmented cells). The effect of

xMD3-MO injection on early myoblast markers, like *MyoD*, should also be assessed to further appreciate the temporal effects of loss of xMD3.

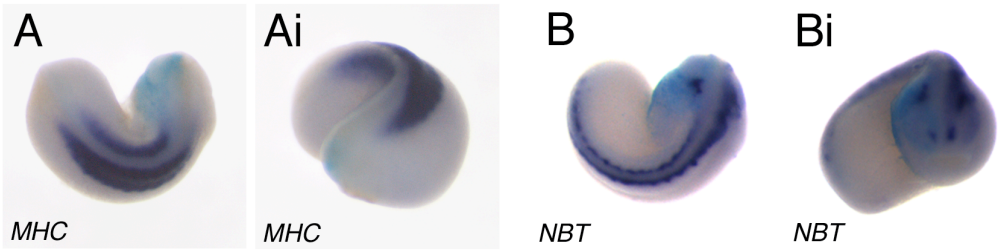

Figure 7.9 – Effect of xMD3-MO injection on *myosin heavy chain* and *neural b-tubulin* expression. Stage 23 embryos unilaterally injected with xMD3-MO were subjected to whole mount *in situ* hybridisation to determine the effect of xMD3-MO injection on expression of myosin heavy chain (*MHC*) and neural β-tubulin (*NBT*). β-galactosidase staining identifies the injected side of the embryo. Injection of xMD3-MO results in reduced *MHC* and *NBT* expression in stage 23 embryos. (A) is the dorsal view of the embryo shown in (Ai). (B) is the dorsal view of the embryo shown in (Bi). Images are representative of two independent experiments.

Discussion

The preliminary work described here indicates a role for MarvelD3 during development of *Xenopus laevis* embryos. Bilateral injection of xMD3-MO resulted in developmental delay after gastrulation and in reduced numbers of melanophores along the lateral epidermis and reduced iris pigmentation. Unilateral injection of xMD3-MO caused curvature of the neural fold and anterior-posterior (A-P) axis towards the side of injection. Reduced staining of neural crest cell marker *Twist* at stage 23 and of differentiated primary neuron marker, *neural β tubulin*, suggested these morphological phenotypes could be due to perturbed neural crest cell migration following loss of MarvelD3. Differentiated muscle marker *myosin heavy chain* was also reduced following injection of xMD3-MO. While further work is certainly required before a precise role for MarvelD3 in development can be fully ascribed, these results provide intriguing evidence that development is perturbed in the absence of MarvelD3.

Before further experiments are performed it is vital to first confirm the results presented above are due to MarvelD3. Rescue experiments using human MarvelD3 RNA to rescue the phenotypes of xMD3-MO injection have so far failed due to unfortunately high death rate in egg batches. These experiments should be repeated. While immunoblotting whole embryo lysates suggested hMD3 is expressed following injection its mRNA into *Xenopus laevis*, it may not be able to function or it may function differently to the *Xenopus* protein. Thus it would be beneficial to generate a morpholino-resistant RNA encoding the *Xenopus* sequence of MarvelD3 with which to repeat the rescue experiments previously described. Rescuing the phenotypes

observed by re-expressing xMD3 would confirm their specifity to MarvelD3. The phenotypes themselves should also be confirmed by designing a second morpholino targeting a different region of the *xMD3* promoter, thus reducing the possibility of off-target effects. Generation of an antibody specific for *Xenopus* MarvelD3 would also be a useful tool to analyse MarvelD3 expression during development and verify depletion of the protein following xMD3-MO injection.

RT-PCR performed at a number of developmental stages demonstrated that MarvelD3 is expressed in the maternal RNA and following the induction of embryonic transcription. RT-PCR of mRNA extracted from embryos at stage 10 and later produced a double-band. To confirm which band corresponds to xMD3 and identify the additional product, these RT-PCR products should be sequenced.

Understanding the spatial expression pattern of MarvelD3 during *Xenopus* development might further enhance our understanding of how MarvelD3 functions by concentrating on where it is expresssed. Attempts were made to synthesise probes specific for xMD3 for use in *in situ* hybridisation studies. Unfortunately however, these probes generated high levels of background staining preventing the spatial expression pattern of xMD3 from being observed. The high level of background staining may be due to the large size of the probes. Future studies should perhaps use a mix of probes specific for a number of regions in xMD3, which would hopefully maintain specificity and reduce background staining.

While keeping in mind their limitations, the results presented here suggest that MarvelD3 expression may play an important role in embryonic development after gastrulation. Until gastrulation (Stage 15), both unilaterally and bilaterally xMD3-MO-injected embryos developed in a manner indistinguishable from con-MO injected and uninjected embryos. The lack of effect of xMD3-MO injection on cleavage stages and the earliest stages of development suggests xMD3 is not necessary for tight junction formation in *Xenopus laevis*, which is necessary for formation of the blastula, and is consistent with the observations made in cell culture presented in chapter 3. At neurulation (Stage 20), however, unilaterally injected embryos presented a curved neural fold and at later stages displayed significant curvature of the anterioposterior body axis towards the side of injection. In bilaterally injected embryos, development of xMD3-MO-injected embryos proceeded more slowly than con-MO injected or uninjected counterparts. This developmental delay in response to xMD3-MO injection could explain the curvature in the unilaterally injected embryos, which are outgrown by their uninjected sides.

It also became apparent that the number of melanophores on the lateral epidermis was reduced following xMD3-MO, but not con-MO, injection. Similarly, iris pigmentation was also reduced in xMD3-MO-injected embryos when compared to controls. Interestingly, *in situ* hybridisation studies showed the neural crest cell marker *Twist* to be reduced by xMD3-MO injection in stage 23 embryos, but not at stage 20, suggesting induction of neural crest cells is not affected by loss of MarvelD3. This reduction in *Twist*-positive neural crest cells at stage 23, however, could explain the reduced neural crest cell derivatives at later embryonic stages.

The induction of neural crest cells and their subsequent transition to a migratory cell type involves regulation by a number of signals. At the gastrula stage, Wnt signalling is active and BMP signalling is inhibited inducing neural crest cells in the gastrula (Steventon et al., 2009). During neurulation, BMP signalling is activated alongside the already active Wnt signalling which together maintain the neural crest cell population (Steventon et al., 2009). BMP signalling is also responsible for the induction of neural crest cell delamination, which depends on the balance between BMP and noggin. As loss of MarvelD3 only appeared to affect *Twist* staining at later stages of neural crest migration, a simple hypothesis would be to propose that MarvelD3 regulates the migration of neural crest cells following their EMT, but does not regulate their induction, maintenance or delamination. This increased migration of neural crest cells may result in the reduced *Twist* staining observed as they have migrated more rapidly than the control side of the embryo and perhaps no longer express it, or they disperse across the embryo, which dilutes the signal and makes it appear reduced. Furthermore, by over-migrating through or beyond their target zones or by arriving too early, these neural crest cells may not receive the inductive signals necessary for differentiation. Thus neural crest cell derivatives, like primary neurons and pigmented cells, are reduced in xMD3-MO-injected embryos. This model is by no means complete and should be examined further by looking at more markers of neural crest cells and their derivatives, to confirm the effect of xMD3-MO injection to neural crest cells, and not just *Twist*-positive populations. Overexpression of the neural crest cell marker Slug, for example, has been shown to result in increased levels of neural crest cells and elevate the levels of melanocytes (LaBonne and Bronner-Fraser, 1998). As slug is a transcription factor implicated in the induction of EMT, it would be interesting to see the effect of MarvelD3 depletion on slug

expression during *Xenopus* development. If, like *Twist*, *Slug* is also reduced in response to loss of MarvelD3, this could provide a mechanism through which MarvelD3 reduces the abundance of melanocytes. Injection of Con-MO into a single cell of the 2 cell embryo should be performed to ensure the *in situ*s performed so far are specific to xMD3-MO rather than morpholino injection *per se*. Furthermore it will be important to determine whether the reduced staining is due to increased apoptosis in response to xMD3-MO injection by performing whole-mount TUNEL staining. Finally, it is important to note that loss of *Twist* staining could simply be due to inhibition of *Twist* transcription in the absence of MarvelD3. The effect of MarvelD3 expression on levels of twist protein should be assessed to examine this.

It has recently been shown that MarvelD3 is down-regulated in EMT induced by Snail in response to TGFβ (Kojima et al., 2011). If MarvelD3 were an inhibitor of migration, as the results presented in this thesis suggest, down-regulation of MarvelD3 would lift this inhibition and enable cells to migrate more rapidly. Concomitant down-regulation of adhesion proteins like E-cadherin during EMT may result in the more rapid migration of single cells rather than collective cell migration in the presence of cell-cell adhesion. The defects presented here concern loss of MarvelD3, and therefore suggest the presence of MarvelD3 must also be important. Perhaps, therefore, during neural crest cell migration, MarvelD3 expression initially serves to inhibit migration of neural crest cells in response to BMP. Eventually, BMP-induced activation of transcription factors like snail may then lead to downregulation of MarvelD3, which promotes migration. Complete loss of MarvelD3 in the morpholino scenario however may result in increased migration in

response to BMP at an earlier time and/or an elevated rate of migration. With this in mind, it would be useful to identify the specific cell types in which MarvelD3 is expressed, or absent, and how this expression changes during the developmental process. This could be achieved by isolating groups of cells and performing RT-PCR for *xMD3* to obtain a more detailed expression profile at various developmental stages. As an inhibitor of migration, the expression of MarvelD3 may be important to ensure some cells remain non-motile during development. To further examine the effect of MarvelD3 depletion on neural crest cell migration, neural crest cells can be isolated and their migration observed *ex vivo*. The effect of loss of MarvelD3 on protrusion formation, directional migration, collective or single-cell migration of the neural crest cells could all be assessed to begin to see whether the effects of MarvelD3 *ex vivo* are the same as those observed in cell culture.

Interestingly, TGFβ signalling induces the expression of AP1 transcription factor components cJun and cFos (Verrecchia et al., 2001a) and, furthermore, AP1 has been implicated in regulating the transcriptional response to TGFβ (Verrecchia et al., 2001b). Signalling by TGFβ family members, BMPs and activin, is incredibly abundant during development. MarvelD3 could therefore regulate the cellular response to TGFβ, or other family members, through its inhibition of AP1 signalling. In the absence of MarvelD3, loss of this inhibition would result in increased transcription of TGFβ target genes and promotion of cell migration. The effect of MarvelD3 expression on TGFβ-mediated alterations in gene expression should therefore be examined. For simplicity, this could first be studied in cell culture by applying TGFβ to control and MarvelD3-depleted Caco-2 cells and assessing the

effect on levels of cJun and cFos. Additional experiments to determine levels of *cJun* and *cFos* transcripts from *Xenopus laevis* embryos injected with Con- or xMD3-MO by RT-PCR would further confirm the regulation of AP1 signalling by MarvelD3.

To summarise, the results in this chapter suggest a role for MarvelD3 during the embryonic development of *Xenopus laevis*, providing a useful model system in which to address the function of MarvelD3 *in vivo*. Loss of MarvelD3 affected embryonic development after gastrulation stage and resulted in developmental delay, indicated by slower development of bilaterally injected embryos and curvature following unilateral injection of xMD3-MO. Reduced expression of *Twist* following xMD3-MO injection and reduced neural crest derivatives suggested MarvelD3 might regulate neural crest cell migration. After confirming the specificity of these effects to MarvelD3, future work should focus on investigating the role for MarvelD3 in regulation of TGFβ signalling and whether this is facilitated by the inhibitory action of MarvelD3 on AP1-mediated transcription.

Chapter 8:

Final Discussion

Final Discussion

At the beginning of this thesis, MarvelD3 was recognised as an occludin-like Marvel domain-containing protein of unknown function (Sanchez-Pulido et al., 2002). The aim of this thesis was to determine if, like occludin and tricellulin, MarvelD3 was a component of the tight junction and to examine the functional role of MarvelD3 in the cell. Results presented here identify MarvelD3 as a novel component of the tight junction and indicate its importance in the regulation of epithelial cell proliferation and migration, by impacting on intracellular signalling pathways that regulate gene expression and rearrangement of the actin cytoskeleton. Taken together, this suggests MarvelD3 serves more than a structural role at the tight junction and offers support to the developing hypothesis that tight junctions are important signalling centres in addition to providing a paracellular diffusion barrier. I will now discuss the relevance of these findings to our understanding of tight junction biology, in addition to future applications and studies. I will support the direction proposed for future studies by showing some preliminary data.

Identification of MarvelD3 and regulation of tight junction properties

MarvelD3 was identified as a novel component of the tight junction and showed a broad expression pattern in epithelial and endothelial cell lines and in many tissue types. MarvelD3 colocalised with occludin at the tight junction of epithelial cells and apically to E-cadherin at the adherens junction. Depletion of MarvelD3 by siRNA transfection demonstrated that MarvelD3 is not required for junction formation in Caco-2 cells, in contrast to studies performed by other groups (Kojima et al., 2011; Raleigh et al., 2010). Initial studies performed here in *Xenopus laevis* also suggest MarvelD3 is not necessary for junction formation during embryonic development.

While the experiments performed in *Xenopus laevis* did not address tight junction formation directly, the xMD3-MO-injected embryos developed beyond blastula stage, which was reported to fail in the absence of tight junction formation, due to the inability to seal off the internal cavity from the medium outside (Regen and Steinhardt, 1986). These considerations suggest that MarvelD3 is not necessary for the formation of the tight junction, but instead its expression and integration into the tight junction serves to alter their properties and regulate intracellular signalling pathways in the cytoplasm beneath. Detailing the recruitment of MarvelD3 during tight junction formation may provide further insight in to how the temporal regulation of MarvelD3 helps this to be achieved.

Though loss of MarvelD3 did not appear to affect the paracellular permeability properties of tight junctions, ion conductance was increased in the absence of MarvelD3. The ability of tight junctions to regulate these two permeability properties independently is intriguing. It is considered that by regulating the complement of claudins expressed tight junctions are able to regulate ion conductance based on charge. Thus MarvelD3, if not regulating charge directly, may affect the complement of claudin molecules expressed, subsequently resulting in increased epithelial resistance. The regulation of ion conductance by MarvelD3 could, however, be subtler, occurring at the protein level rather than the level of transcription. Recently presented data suggested that phosphorylation of occludin on serine residue 408 altered the dynamic properties of the tight junction, subsequently elevating transepithelial resistance (Raleigh et al., 2011). Post-translational modifications have not yet been identified for MarvelD3, but it would be interesting to investigate their

existence and, if so, how they may affect tight junction dynamics, as has been demonstrated for occludin. Such studies provide additional insight into the function of proteins that are easily missed in loss-of-function studies. Indeed, loss of MarvelD3 protein from the tight junction may itself affect protein dynamics and be responsible for the increased ion conductance observed.

In addition to ion conductance, the ability of tight junctions to regulate permeability based on size is currently proposed to proceed via the dynamic and constant remodelling of the tight junction strand network (Sasaki et al., 2003; Steed et al., 2010). In the present study no effect of MarvelD3 depletion was observed on paracellular permeability to large dextran tracers. The possibility of MarvelD3 and the importance of the Marvel domain in regulating strand dynamics, however, should not be ruled out. Analysis of the tight junction strand network in MarvelD3-expressing and MarvelD3-depleted cells by electron microscopy (EM) may provide a more comprehensive insight in to the role of MarvelD3 in strand formation that may have been missed at the level of confocal microscopy. Cryo-immuno EM should also be performed to confirm the localisation of MarvelD3 to the tight junction strands.

Regulation of cell proliferation and migration by MarvelD3

The main finding of this thesis is the regulation of epithelial proliferation and migration by MarvelD3. Reduced MarvelD3 expression in epithelial metastatic tumour cell lines prompted the examination of the role of MarvelD3 in tumourogenic-related processes. Increased proliferation and migration following MarvelD3

depletion from Caco-2 cells alluded to the significance of loss of MarvelD3 in metastatic tumour cell lines. Furthermore, expression of exogenous MarvelD3 in the pancreatic tumour cell line MiaPaCa confirmed the ability of MarvelD3 to inhibit proliferation and migration in epithelial cells. In keeping, initial studies performed in *Xenopus laevis* have suggested perturbations in neural crest cell migration following injection of morpholinos targeting the *Xenopus* sequence of MarvelD3. Together, these data provide convincing evidence for the ability of MarvelD3 to regulate cell proliferation and migration.

Identification of an interaction between MEKK1 and the N-terminus of MarvelD3 provided insight in to how this regulation may be achieved. MEKK1 is a MAPKKK activated in response to growth factor signalling and stresses that change cell shape or arrangement of the cytoskeleton (Yujiri et al., 1998; Zhang et al., 2003). Disruption of junctional MEKK1 staining in MarvelD3-depleted cells suggested the importance of the MarvelD3-MEKK1 interaction for the junctional localisation of MEKK1. Examination of MarvelD3 in response to hyperosmotic shock further confirmed the functional relevance of the interaction between MarvelD3 and MEKK1, with hyperosmotic shock-induced phosphorylation of MEKK1 being prolonged in MarvelD3-depleted cells, suggesting MarvelD3 regulates MEKK1 phosphorylation in response to certain stimuli. MEKK1 has been shown to activate transcription mediated by AP1 transcription factors by associating with and activating MAPKK with preference for downstream activation of JNK. Activation of JNK stimulates the expression of components of the AP1 transcription factor and further promotes their activity by activating phosphorylation. Levels of active JNK were reduced following

expression of MarvelD3 in MiaPaCa cells and MarvelD3 expression reduced AP1 promoter activity in both MiaPaCa and Caco-2 cells. These observations prompted the hypothesis that the association between MarvelD3 and MEKK1 may serve to inhibit MEKK1 activity, which, in turn, would perturb the downstream signalling pathways normally resulting in JNK activation and AP1-responsive promoter activity. Reduction of AP1 signalling affords a mechanism through which MarvelD3 expression may regulate gene expression; by regulating the expression of those genes with AP1 recognition sites in their promoters. One such gene is the EGFR, expression of which was shown to decrease following MarvelD3 expression and increase in its absence. In addition, expression of cyclinD1 is also regulated by AP1 signalling, and was reduced here following expression of MarvelD3. The detailed mechanism behind MarvelD3-mediated regulation of these promoters, however, requires further investigation. While depletion of MarvelD3 potentiated cyclinD1 promoter activity and protein levels, AP1 promoter activity was not increased by loss of MarvelD3 alone. This suggests MarvelD3 may regulate cyclinD1 promoter activity by a mechanism independent of AP1 and, further, that MarvelD3-mediated regulation of AP1 activity may require additional input before the effect of MarvelD3 loss is observed. MarvelD3-depletion in Caco-2 cells significantly increased AP1 promoter activity in response to EGF. This suggests expression of MarvelD3 inhibits activation of AP1 promoter activity induced by EGF. This could be mediated by reduced EGFR expression, and therefore reduced downstream signalling, caused by MarvelD3 expression, or a direct effect of MarvelD3 in inhibiting the EGFR signalling pathway. It is proposed that, by regulating MEKK1, MarvelD3 inhibits JNK and AP1 activity leading to reduced EGFR expression. The activation of MEKK1 and AP1 signalling by EGF-induced activation of the EGFR provides a

negative feedback loop whereby EGF-induced signalling is further reduced following MarvelD3 expression (Figure 8.1).

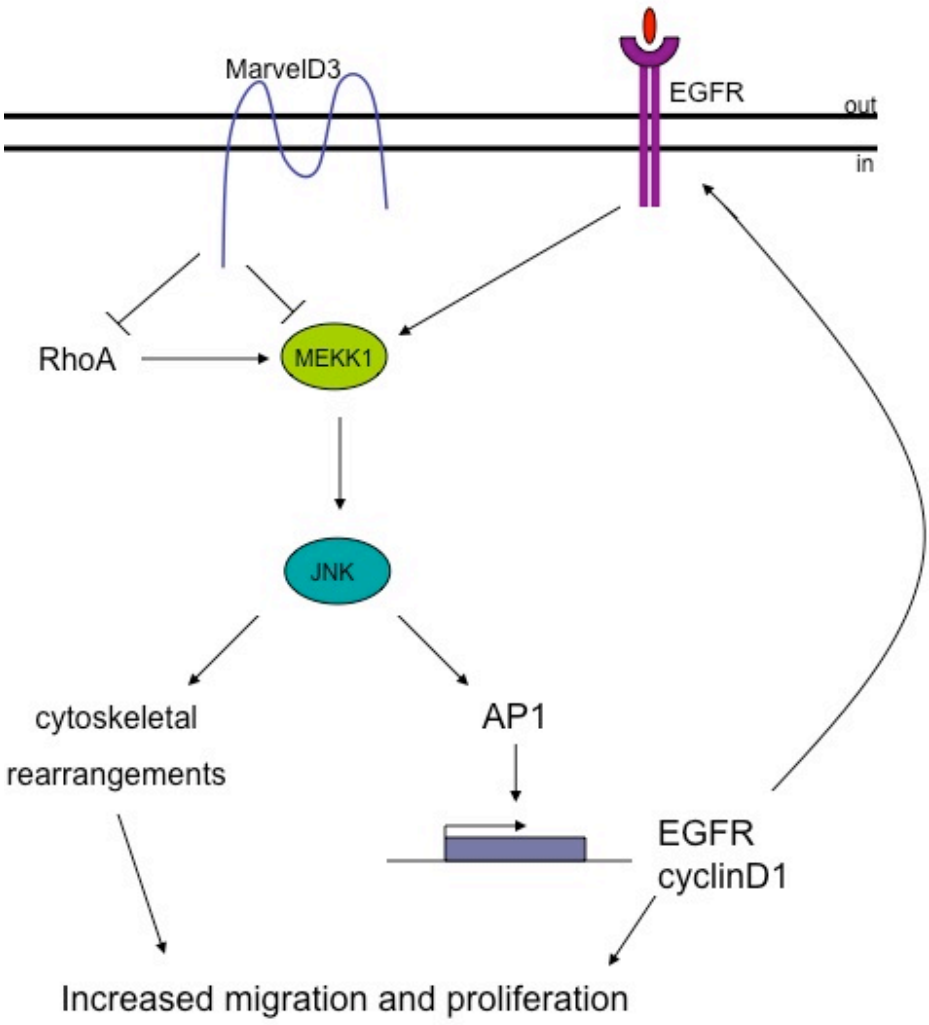

Figure 8.1 – Hypothetical model for the regulation of migration and proliferation by MarvelD3 in epithelial cells. As described in the text, interaction between MarvelD3 and MEKK1 at the tight junction inhibits MEKK1 activity and prevents activation of the JNK branch of the MAPK pathway. Subsequent reductions in AP1 promoter activity may result in reduced expression of AP1 target genes like the EGFR and cyclinD1, and reduced proliferation and migration. By regulating MEKK1 and JNK activity, MarvelD3 expression also perturbs cytoskeletal rearrangements necessary for productive migration. MarvelD3 also regulates the rearrangements of the cytoskeleton in response to hyperosmotic shock.

An important question to address in the near future is the mechanism behind the regulation of MEKK1 by MarvelD3. Interaction with the N-terminus of MarvelD3 has been suggested here to inhibit MEKK1 activity thus explaining the reduced JNK and AP1 activity in response to MarvelD3 expression. However, the activation state of MEKK1 in interaction with MarvelD3 has not yet been determined. To examine this further, antibodies specific to three phosphorylated forms of MEKK1 (MEKK1-S67, MEKK1-T1402 and MEKK1-S1455; kindly provided by Ewen Gallagher, Imperial College London) could be used to determine the phosphorylation state of MEKK1 interacting with MarvelD3. Initial studies in MiaPaCa cell lysates could also be performed to assess the effect of MarvelD3 expression on the levels of these phosphorylated forms of MEKK1. Phosphorylation of MEKK1 at serine 67 has been shown to inhibit the binding of JNK to MEKK1 and therefore prevents MEKK1-mediated JNK activation (Gallagher et al., 2002). Promoting phosphorylation of this site, therefore, would be a simple mechanism through which MarvelD3 may impact upon JNK activity via MEKK1. Alternatively, phosphorylation of T1402 within the kinase domain of MEKK1 is thought to be required for MEKK1 kinase activity towards JNK (Siow et al., 1997). Inhibition of T1402 phosphorylation could thus provide an alternative mechanism through which MarvelD3 impacts upon the JNK MAPK pathway. Like T1402, S1455 is also found in the kinase domain of MEKK1, but the significance of its phosphorylation has not yet been reported. In the current study, this site was phosphorylated in response to hyperosmotic shock and remained phosphorylated for longer when Caco-2 cells were depleted of MarvelD3. Attempts should be made, therefore, to determine the effect of S1455 phosphorylation on MEKK1 kinase activity towards JNK, by generating phosphomimetic mutants and mutants that cannot be phosphorylated for use in kinase assays.

When the identity of the phosphorylation state regulated by MarvelD3 has been identified it would be informative to discover the mechanism behind this regulation. RhoA can bind to MEKK1 and stimulate its kinase activity (Gallagher et al., 2004). Interestingly, levels of active RhoA are reduced following MarvelD3. Thus MarvelD3 may inhibit MEKK1 activity by inhibiting the activity of RhoA. The mechanism behind MarvelD3-mediated inhibition of RhoA, however, needs to be addressed. One mechanism by which MarvelD3 may be able to inhibit RhoA could be by cross-talk with adherens junction proteins involved in RhoA regulation, like p120-catenin.

p120-catenin localises to the adherens junction via interaction with E-cadherin and has been shown to locally inhibit RhoA activity, important for the stabilisation of adherens junctions (Anastasiadis et al., 2000). Preliminary immunofluroescent studies in MiaPaCa cells showed p120-catenin to be recruited to cell-cell contacts in MarvelD3-expressing MiaPaCa cells, but not in control MiaPaCa cells (Figure 8.2A). At the adherens junction, transient interaction of p190RhoGAP with p120-cadherin complex facilitates the inhibition of RhoA by p190RhoGAP (Wildenberg et al., 2006). In the absence of p120-catenin, p190RhoGAP fails to recruit to the plasma membrane and RhoA activity is significantly elevated alluding to the importance of this mechanism in the localised regulation of RhoA. Interestingly, p190RhoGAP was also recruited to cell-cell contacts in MarvelD3 expressing MiaPaCa cells (Figure 8.2A). In addition, pulldown assays identified a potential interaction between the N-terminus of MarvelD3 and both p120-catenin and p190RhoGAP (Figure 8.2B). Furthermore, depletion of MarvelD3 from Caco-2 cells altered p120-catenin

localisation (Figure 8.2C). In control cells, p120-catenin colocalised with MarvelD3 and some more basal staining could also be seen. In MarvelD3-depleted cells, p120-catenin demonstrated staining indicative of the adherens junction only, suggesting MarvelD3 may serve to localise the tight junctional pool of p120-catenin. Thus, in a similar manner to the cadherin-p120-catenin complex at the adherens junction, MarvelD3 may regulate RhoA activity at the tight junction by interacting with p120-catenin/p190RhoGAP, which may subsequently reduce the activity of RhoA. This hypothesis becomes more intriguing when considering the idea that Rac activation provides the stimulus for p190RhoGAP translocation from the cytoplasm to the membrane, preceding its interaction with p120-catenin and subsequent inhibition of RhoA (Wildenberg et al., 2006). Rac is activated in response to hyperosmotic shock. Thus, one may speculate that translocation of p190RhoGAP to the membrane in response to hyperosmotic shock-induced activation of Rac might enable p120/p190RhoGAP-mediated inhibition of RhoA at the level of the tight junction. In the absence of the proposed MarvelD3-p120-catenin complex, p190RhoGAP may fail to inhibit RhoA at the level of the tight junction resulting in elevated RhoA activity and increased phospho-MLC and increased dephosphorylation of cofilin in the cytoplasm, ultimately preventing the reorganisation of the actin cytoskeleton necessary for the osmoadaptive response. To investigate this hypothesis, the effect of hyperosmotic shock on p120-catenin and p190RhoGAP localisation should be tested. These studies may also help understand the spatial regulation of MarvelD3 in the membrane and cytoplasm, and its involvement in coordinating changes to intracellular signalling pathways with rearrangement of the cytoskeleton.

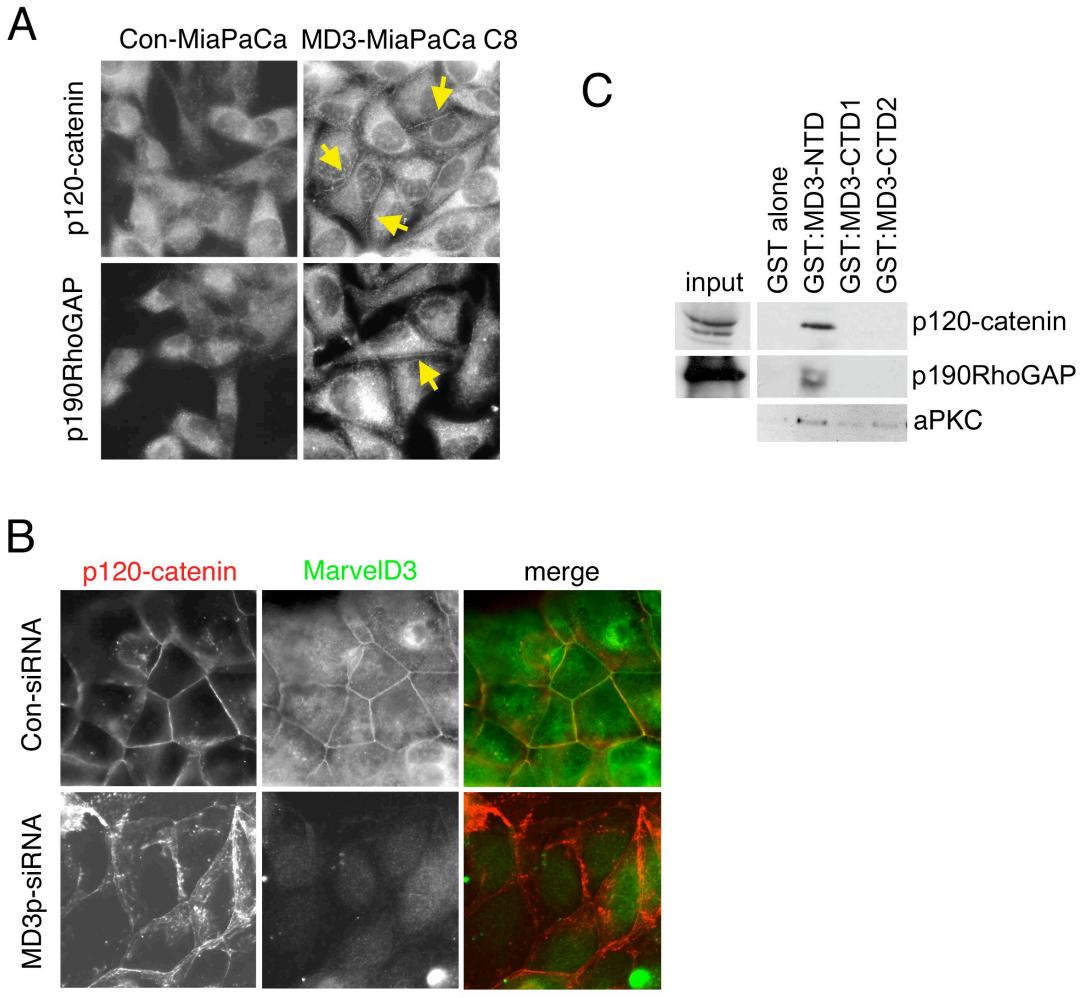

Figure 8.2 – Preliminary observations suggest the MarvelD3 may exist in a complex with p120-catenin and p190RhoGAP at the tight junction. (A) Immunofluorescence analysis of p120-catenin and p190RhoGAP shows their recruitment to points of cell-cell contact following expression of MarvelD3 in MiaPaCa cells. (B) p120-catenin colocalises with MarvelD3 in control Caco-2 cells. siRNA-mediated depletion of MarvelD3 in Caco-2 cells disrupts localisation of p120-catenin, which appears to localise more basally following loss of MarvelD3. (C) Immunoblotting cell lysates from pulldown assays suggests an interaction between the N-terminus of MarvelD3 and p120-catenin, p190RhoGAP and aPKC (see below). These are preliminary observations and require repetition. Immunofluorescence in (A) and (B) was performed by Sandra Hemkemeyer during a Masters project. I performed the pulldown assays in (C) and lysates were immunoblotted by Sandra Hemkemeyer.

Coexpression of conventional PKCβII with MEKK1 in insect cells demonstrated the ability of PKC to activate MEKK1 (Siow et al., 1997). Though no role for aPKC in MEKK1 phosphorylation has been shown, aPKC localises to the tight junction and preliminary results also indicate an interaction with MarvelD3 (Figure 8.2C). Using aPKC inhibitors it would be interesting to determine whether MEKK1 phosphorylation can be regulated by aPKC and, furthermore, whether MarvelD3 plays a role in bringing aPKC and MEKK1 together at the tight junction. If aPKC is capable of phosphorylating MEKK1 and this is regulated by MarvelD3, it could provide a mechanism by which MarvelD3 prevents JNK activation in migrating cells.

Regulation of the actin cytoskeleton by MarvelD3

MarvelD3 has been shown here to inhibit protrusion formation in migrating cells. Furthermore, reorganisation of the actin cytoskeleton in response to hyperosmotic shock is perturbed in the absence of MarvelD3 suggesting MarvelD3 also functions in coordinating remodelling of the actin cytoskeleton in response to hyperosmotic shock. The generation of cell protrusions is thought to require JNK activity (Altan and Fenteany, 2004). Inhibition of JNK, therefore, could also be the mechanism behind MarvelD3-mediated inhibition of protrusion formation. In response to hyperosmotic shock, the cytoskeleton fails to reorganise which may be due to elevated levels of active cofilin preventing the formation of long actin filaments from which bundles can be formed. Combined cofilin and Arp2/3 activity act together to drive lamellipodia extension at the leading edge (DesMarais et al., 2004; Pollard and Borisy, 2003). Defective regulation of cofilin, therefore, may also be involved in increased migration in MarvelD3-depleted cells. From the results obtained from

hyperosmotic shock and migration experiments, it seems MarvelD3 may function in stabilisation of the cytoskeleton. Cell migration requires dynamic remodelling of the actin cytoskeleton. In the absence of MarvelD3, these dynamic properties appear to be increased as cells migrate more rapidly and the generation of protrusive structures increases. MarvelD3 expression during migration, therefore, may serve to restrict migration speed by capping the speed with which the cytoskeleton remodels. Under hyperosmotic shock, the actin cytoskeleton reorganises to generate a rigid structure that enables the cell to physically resist the changes in the extracellular environment. This rigid actin network, however, is not achieved in the absence of MarvelD3, suggesting again that the actin cytoskeleton may be more dynamic following loss of MarvelD3, which, under conditions of hyperosmotic shock, is detrimental to the cell. The precise mechanism behind MarvelD3-mediated regulation of the cytoskeleton is not well understood though the data here suggests it may involve loss of MarvelD3-mediated RhoA inhibition and elevated levels of active cofilin. Analysis of active cofilin localisation in control and MarvelD3-depleted cells in response to hyperosmotic shock, however, needs to be determined.

MarvelD3 may also impact on the cytoskeleton via its interaction with MEKK1, which is required for stress fibre formation in response to TGFβ. Given the abundance of TGFβ during development and the potential role for MarvelD3 in regulating neural crest cell migration, regulating MEKK1 in response to TGFβ could be a significant function of MarvelD3. The effect of MarvelD3 on cytoskeletal reorganisation in response to TGFβ could easily be tested in control and MarvelD3-depleted cells. If MarvelD3 inhibits MEKK1, one would expect more stress fibres in

MarvelD3-depleted cells and little or none in MarvelD3 overexpressing cells. Regulation of TGFβ and EGFR signalling by MarvelD3 could be of significant physiological relevance.

EGF and TGFβ have been shown to cooperate in the induction of EMT. Experiments performed in pig thyrocytes, for example, have demonstrated that while individually EGF and TGFβ are ineffective at inducing EMT, together they can (Grande et al., 2002). Furthermore, this response to EGF and TGFβ is lost if EGFR kinase activity is inhibited (Grande et al., 2002). In addition, amplification of the EGFR gene and subsequent hyperactivity of Ras in breast cancer has been shown to increase their responsiveness to TGFβ (Yin et al., 1999). Therefore, by reducing expression of the EGFR, MarvelD3 may also reduce the responsiveness of cells to TGFβ signalling. Thus MarvelD3 expressing cells fail to increase their migration in response to TGFβ. This regulation of TGFβ-induced migration by MarvelD3 may prove significant during development where migration of some cell types is required while surrounding cells remain stationary. In tumours, loss of MarvelD3 may encourage metastasis by increasing EGFR expression levels and making cells more responsive to EGF and TGFβ. It would be interesting to determine if MarvelD3 affects expression of the TGFβ receptor. The TGFβ receptor 1 localises at the tight junction via an interaction with occludin (Barrios-Rodiles et al., 2005) and is therefore ideally situated for regulation by tight junction proteins. By inhibiting MEKK1, MarvelD3 may prevent EGF and TGFβ-induced activation of JNK and AP1 activity. The effect of MarvelD3 depletion on MEKK1, JNK and AP1 activation in response to TGFβ, EGF and TGFβ + EGF should be tested to further examine this hypothesis.

Relevance of MarvelD3 function at the epithelial cell tight junction

Results presented here demonstrate a role for MarvelD3 in the regulation of intracellular signalling pathways governing cell proliferation and migration. The localisation of MarvelD3 to the tight junction in epithelial cells thus implicates the tight junction in the regulation of these processes. So, why regulate proliferation and migration from the tight junction? The tight junction is a site at which epithelial cells contact their neighbours. In order for integrity across the monolayer to be maintained it makes sense that cellular processes potentially compromising this integrity be regulated from the sites where physical communication between neighbouring cells and with the extracellular space is permitted. In combination with the adherens junctions and desmosomes, tight junctions form part of the epithelial junctional complex. Together these junctions mediate cell-cell adhesion and intracellular signalling pathways. The differences in the properties of these junctions, however, must be important to the epithelial cells to necessitate the need for more than one type of junctional complex. Adhesion between neighbouring cells is necessary for epithelial cell function. In contrast to tight junctions, adherens junctions and desmosomes provide strong cell-cell adhesion between neighbouring epithelial cells. Thus, perhaps one may view tight junctions as an additional layer of junctional regulation building upon the adhesion provided by these basolateral junctional complexes. Thus the cell-cell adhesion mediated by tight junction proteins, like claudins in the strands, is sufficient to draw two already close plasma membranes closer together, generating the kissing points, but requires the adhesion already provided by the adherens junctions and desmosomes to do so. By relying on adhesion provided by other junctional complexes, therefore, cells may be able to alter the expression of transmembrane proteins in the tight junction without compromising

adhesion and, in so doing, exploit the signalling properties of their cytoplasmic domains. To consider MarvelD3, integration of this protein into claudin-based strands appears to inhibit proliferation and migration from the tight junction. When cells are at low density, lack of MarvelD3, which localises in a cell contact-dependent manner, means this inhibition is lifted and cells can proliferate and migrate in response to growth factor signalling, like EGF. By interacting with and inhibiting MEKK1 at the tight junction, MarvelD3 expression inhibits expression of the EGFR and subsequently reduces the output of its downstream signalling. Thus, by mediating cross-talk between the JNK MAPK pathway and the EGFR signalling pathway, MarvelD3 expression inhibits the proliferation and migration of epithelial cells. Regulating this from the tight junction may enable epithelial cells to regulate the expression of tight junction transmembrane proteins as required, without compromising cell-cell adhesion mediated by the adherens junctions. Depletion of MarvelD3 here did not appear to affect expression of adherens junction transmembrane proteins, thought alterations to the localisation of p120-catenin in the cytoplasm were observed.

This suggestion, however, is not to say that the expression of tight junction proteins within the membrane is not important for more than signalling purposes. The identification of the Marvel domain in proteins involved in membrane apposition events alludes to its importance at the tight junction and prompted the studies undertaken in this thesis. The relevance of the Marvel domain itself to the tight junction, however, has not been addressed here and is poorly understood. Depletion of occludin results in spreading of tricellulin along the bicellular contacts suggesting

there may be some redundancy between Marvel domain-containing proteins of the tight junction and that the Marvel domain itself may be of importance to the tight junction structure (Ikenouchi et al., 2008). To better understand this, studies utilising double and triple knockdowns of MarvelD3, occludin and tricellulin and the effect this has on junction formation, strand morphology and tight junction properties should be examined. In their study, Raleigh *et al*., (2010) observed a greater delay in junction formation following combined depletion of MarvelD3, occludin and tricellulin when compared to depletion of any protein alone. It would be interesting to repeat these studies in the system used here to begin to identify a role for the Marvel domain itself at the tight junction, away from the signalling properties contained in the cytoplasmic portions of these proteins. Perhaps the Marvel domain is necessary for efficient occlusion of the plasma membranes at the tight junction. Comparing the distance between outer leaflets of the plasma membrane of control cells and those depleted of the tight junction Marvel domain complement by EM may help to identify this. Differential expression of a complement of proteins with the same transmembrane domain, but different cytoplasmic domains, may enable complexes like the tight junction to take advantage of their different signalling properties (for example, the opposing roles of MarvelD3 and occludin in migration) while ensuring the Marvel domain is always present.

Final Conclusion

Experiments conducted in preparation of this thesis have identified MarvelD3 as a novel component of the epithelial cell tight junction. Presence of MarvelD3 in the tight junction serves to regulate the activation of intracellular signalling pathways promoting cell proliferation and migration in response to physiological levels of growth factors, like EGF. Thus MarvelD3 expression at the tight junction may function in maintaining homeostasis of the epithelial monolayer. Relief of this MarvelD3-mediated inhibition results in activation of the JNK MAPK pathway and AP1 signalling, facilitating cytoskeletal reorganisation and changes in gene expression promoting cell proliferation and migration. Identification of MarvelD3 and its role at the tight junction has furthered our appreciation of tight junction composition and developed our understanding of the role of these protein complexes as mediators of intracellular signalling pathways.

Acknowledgements

The writing of this thesis would not have been possible without the help and support of my two supervisors, Professors Karl Matter and Maria S. Balda. I am delighted to have been able to work in your lab and sincerely thank you for your guidance and encouragement throughout the last three years, and for showing faith in me when I needed it the most. I have learnt a great deal from both of you and I'm sure I will carry it with me wherever I go next.

I would like to extend my gratitude to Shin-Ichi Ohnuma and member's of the Ohnuma lab for being so welcoming, and a special thank you to Katerina and Wanzhou for giving their time and patience so generously to teach me the *Xenopus* techniques. Thank you to my thesis committee Drs Franck Pichaud, Tim Levine and Yasuyuki Fujita for helpful discussions. Thank you also to Dr Ewen Gallagher at Imperial College London for kindly providing phospho-MEKK1 antibodies.

I have met some wonderful people over the past three years and thank everyone at the Institute of Ophthalmology and MRC Laboratory for Molecular Cell Biology for making my time here so enjoyable. I feel privileged to have been able to work alongside such great people and meet many friends I hope I will know for a long time to come. I'd like to say an extra thank you to Jay, Jenny and Natalie for their friendship and encouragement over the last three years and especially while I've been writing.

Thank you to my family and friends for creating a happy life around me and helping any little blips quickly fade away. Especially Ella, Cait, Matt and Sam for your constant support throughout the years and giving me the knowledge that it will always be all right in the end. Thank you as well to Ami for sharing your time in London,

I'm so pleased we came here together. And of course, to Mark for your patience, for always being there to make things better and for giving me so many things to look forward to along the way.

Finally I would like to say a big thank you to my mum and dad and my brother, Edward. I couldn't have done any of this without your love and support behind me and I'll always be thankful. I hope you enjoy having a flick through – there'll be questions afterwards!

This PhD was funded by the Medical Research Council.

References

Altan, Z.M., and Fenteany, G. (2004). c-Jun N-terminal kinase regulates lamellipodial protrusion and cell sheet migration during epithelial wound closure by a gene expression-independent mechanism. Biochem Biophys Res Commun *322*, 56-67.

Amasheh, S., Meiri, N., Gitter, A.H., Schoneberg, T., Mankertz, J., Schulzke, J.D., and Fromm, M. (2002). Claudin-2 expression induces cation-selective channels in tight junctions of epithelial cells. J Cell Sci *115*, 4969-4976.

Anastasiadis, P.Z., Moon, S.Y., Thoreson, M.A., Mariner, D.J., Crawford, H.C., Zheng, Y., and Reynolds, A.B. (2000). Inhibition of RhoA by p120 catenin. Nat Cell Biol *2*, 637-644.

Angelow, S., Ahlstrom, R., and Yu, A.S. (2008). Biology of claudins. Am J Physiol Renal Physiol *295*, F867-876.

Balda, M.S., Garrett, M.D., and Matter, K. (2003). The ZO-1-associated Y-box factor ZONAB regulates epithelial cell proliferation and cell density. J Cell Biol *160*, 423-432.

Balda, M.S., and Matter, K. (2000). The tight junction protein ZO-1 and an interacting transcription factor regulate ErbB-2 expression. EMBO J *19*, 2024-2033.

Balda, M.S., and Matter, K. (2009). Tight junctions and the regulation of gene expression. Biochim Biophys Acta *1788*, 761-767.

Balda, M.S., Whitney, J.A., Flores, C., Gonzalez, S., Cereijido, M., and Matter, K. (1996). Functional dissociation of paracellular permeability and transepithelial electrical resistance and disruption of the apical-basolateral intramembrane diffusion barrier by expression of a mutant tight junction membrane protein. J Cell Biol *134*, 1031-1049.

Barrios-Rodiles, M., Brown, K.R., Ozdamar, B., Bose, R., Liu, Z., Donovan, R.S., Shinjo, F., Liu, Y., Dembowy, J., Taylor, I.W., *et al*. (2005). High-throughput mapping of a dynamic signalling network in mammalian cells. Science *307*, 1621-1625.

Basbaum, C.B., and Werb, Z. (1996). Focalized proteolysis: spatial and temporal regulation of extracellular matrix degradation at the cell surface. Curr Opin Cell Biol *8*, 731-738.

Basuroy, S., Seth, A., Elias, B., Naren, A.P., and Rao, R. (2006). MAPK interacts with occludin and mediates EGF-induced prevention of tight junction disruption by hydrogen peroxide. Biochem J *393*, 69-77.

Behrens, J., von Kries, J.P., Kuhl, M., Bruhn, L., Wedlich, D., Grosschedl, R., and Birchmeier, W. (1996). Functional interaction of beta-catenin with the transcription factor LEF-1. Nature *382*, 638-642.

Ben-Yosef, T., Belyantseva, I.A., Saunders, T.L., Hughes, E.D., Kawamoto, K., Van Itallie, C.M., Beyer, L.A., Halsey, K., Gardner, D.J., Wilcox, E.R., Rasmussen, J., Anderson, J.M., Dolan, D.F., Forge, A., Raphael, Y., Camper, S.A., Friedman, T.B. (2003). Claudin 14 knockout mice, a model for autosomal recessive deafness *DFNB29*, are deaf due to cochlear hair cell degeneration. Hum Mol Genet *12*, 2049-2061.

Benais-Pont, G., Punn, A.., Flores-Maldonado, C., Eckert, J., Raposo, G., Fleming, T.P., Cereijido, M., Balda, M.S., and Matter, K. (2003) Identification of a tight junction-associated guanine nucleotide exchange factor that activates Rho and regulates paracellular permeability. *J Cell Biol* 160, 729-740

Bell, L.M., Leong, M.L., Kim, B., Wang, E., Park, J., Hemmings, B.A., and Firestone, G.L. (2000). Hyperosmotic stress stimulates promoter activity and regulates cellular utilization of the serum- and glucocorticoid-inducible protein kinase (Sgk) by a p38 MAPK-dependent pathway. J Biol Chem *275*, 25262-25272.

Betanzos, A., Huerta, M., Lopez-Bayghen, E., Azuara, E., Amerena, J., and Gonzalez-Mariscal, L. (2004). The tight junction protein ZO-2 associates with Jun, Fos and C/EBP transcription factors in epithelial cells. Exp Cell Res *292*, 51-66.

Bjorklund, M., and Koivunen, E. (2005). Gelatinase-mediated migration and invasion of cancer cells. Biochim Biophys Acta *1755*, 37-69.

Brizuela, B.J., Wessely, O., and De Robertis, E.M. (2001). Overexpression of the Xenopus tight-junction protein claudin causes randomization of the left-right body axis. Dev Biol *230*, 217-229.

Buchwalter, G., Gross, C., and Wasylyk, B. (2004). Ets ternary complex transcription factors. Gene *324*, 1-14.

Bustamante, M., Roger, F., Bochaton-Piallat, M.L., Gabbiani, G., Martin, P.Y., and Feraille, E. (2003). Regulatory volume increase is associated with p38 kinase-dependent actin cytoskeleton remodeling in rat kidney MTAL. Am J Physiol Renal Physiol *285*, F336-347.

Campos, S.B., Ashworth, S.L., Wean, S., Hosford, M., Sandoval, R.M., Hallett, M.A., Atkinson, S.J., and Molitoris, B.A. (2009). Cytokine-induced F-actin reorganization in endothelial cells involves RhoA activation. Am J Physiol Renal Physiol *296*, F487-495.

Carlton, V.E.H., Harris, B.Z., Puffenberger, E.G., Batta, A.K., Knisely, A.S., Robinson, D.L., Strauss, K.A., Schneider, B.L., Lim, W.A., Salen, G., Morton, D.H.,

Bull, L.N. (2003). Complex inheritance of familial hypercholanemia with associated mutations in *TJP2* and *BAAT*. Nat Genetics *34*, 91-96.

Carmona-Fontaine, C., Matthews, H.K., Kuriyama, S., Moreno, M., Dunn, G.A., Parsons, M., Stern, C.D., and Mayor, R. (2008). Contact inhibition of locomotion in vivo controls neural crest directional migration. Nature *456*, 957-961.

Cereijido, M., Contreras, R.G., and Shoshani, L. (2004). Cell adhesion, polarity, and epithelia in the dawn of metazoans. Physiol Rev *84*, 1229-1262.

Chang, D.J., Hwang, Y.S., Cha, S.W., Chae, J.P., Hwang, S.H., Hahn, J.H., Bae, Y.C., Lee, H.S., and Park, M.J. (2010). Xclaudin 1 is required for the proper gastrulation in Xenopus laevis. Biochem Biophys Res Commun *397*, 75-81.

Chen, X., and Macara, I.G. (2005). Par-3 controls tight junction assembly through the Rac exchange factor Tiam1. Nat Cell Biol *7*, 262-269.

Cheng, H., Kartenbeck, J., Kabsch, K., Mao, X., Marques, M., and Alonso, A. (2002). Stress kinase p38 mediates EGFR transactivation by hyperosmolar concentrations of sorbitol. J Cell Physiol *192*, 234-243.

Christerson, L.B., Vanderbilt, C.A., and Cobb, M.H. (1999). MEKK1 interacts with alpha-actinin and localizes to stress fibers and focal adhesions. Cell Motil Cytoskeleton *43*, 186-198.

Colegio, O.R., Van Itallie, C.M., McCrea, H.J., Rahner, C., and Anderson, J.M. (2002). Claudins create charge-selective channels in the paracellular pathway between epithelial cells. Am J Physiol Cell Physiol *283*, C142-147.

Daro, E., van der Sluijs, P., Galli, T., and Mellman, I., (1996) Rab4 and cellubrevin define different early endosome populations on the pathway of transferrin receptor recycling. *Proc. Natl. Acad. Sci. USA* 93, 9559-9564

Daniels, M., Dhokia, V., Richard-Parpaillon, L., and Ohnuma, S. (2004). Identification of Xenopus cyclin-dependent kinase inhibitors, p16Xic2 and p17Xic3. Gene *342*, 41-47.

Deng, M., Chen, W.L., Takatori, A., Peng, Z., Zhang, L., Mongan, M., Parthasarathy, R., Sartor, M., Miller, M., Yang, J., *et al*. (2006). A role for the mitogen-activated protein kinase kinase kinase 1 in epithelial wound healing. Mol Biol Cell *17*, 3446-3455.

DesMarais, V., Macaluso, F., Condeelis, J., and Bailly, M. (2004). Synergistic interaction between the Arp2/3 complex and cofilin drives stimulated lamellipod extension. J Cell Sci *117*, 3499-3510.

Di Ciano, C., Nie, Z., Szaszi, K., Lewis, A., Uruno, T., Zhan, X., Rotstein, O.D., Mak, A., and Kapus, A. (2002). Osmotic stress-induced remodeling of the cortical cytoskeleton. Am J Physiol Cell Physiol *283*, C850-865.

Di Ciano-Oliveira, C., Sirokmany, G., Szaszi, K., Arthur, W.T., Masszi, A., Peterson, M., Rotstein, O.D., and Kapus, A. (2003). Hyperosmotic stress activates Rho: differential involvement in Rho kinase-dependent MLC phosphorylation and NKCC activation. Am J Physiol Cell Physiol *285*, C555-566.

Drees, F., Pokutta, S., Yamada, S., Nelson, W.J., and Weis, W.I. (2005). Alpha-catenin is a molecular switch that binds E-cadherin-beta-catenin and regulates actin-filament assembly. Cell *123*, 903-915.

Drubin, D.G., and Nelson, W.J. (1996). Origins of cell polarity. Cell *84*, 335-344.

Du, D., Xu, F., Yu, L., Zhang, C., Lu, X., Yuan, H., Huang, Q., Zhang, F., Bao, H., Jia, L., *et al*. (2010). The tight junction protein, occludin, regulates the directional migration of epithelial cells. Dev Cell *18*, 52-63.

Du, D., Xu, F., Yu, L., Zhang, C., Lu, X., Yuan, H., Huang, Q., Zhang, F., Bao, H., Jia, L., Wu, X., Zhu, X., Zhang, X., Chen, Z. (2010). The tight junction protein, occludin, regulates the directional migration of epithelial cells. Dev Cell *18*, 52-63.

Ebnet, K., Suzuki, A., Horikoshi, Y., Hirose, T., Meyer Zu Brickwedde, M.K., Ohno, S., and Vestweber, D. (2001). The cell polarity protein ASIP/PAR-3 directly associates with junctional adhesion molecule (JAM). EMBO J *20*, 3738-3748.

Etienne-Manneville, S., and Hall, A. (2001). Integrin-mediated activation of Cdc42 controls cell polarity in migrating astrocytes through PKCzeta. Cell *106*, 489-498.

Etienne-Manneville, S., and Hall, A. (2002). Rho GTPases in cell biology. Nature *420*, 629-635.

Fackler, O.T., and Grosse, R. (2008). Cell motility through plasma membrane blebbing. J Cell Biol *181*, 879-884.

Fanning, A.S., Jameson, B.J., Jesaitis, L.A., and Anderson, J.M. (1998). The tight junction protein ZO-1 establishes a link between the transmembrane protein occludin and the actin cytoskeleton. J Biol Chem *273*, 29745-29753.

Farquhar, M.G., and Palade, G.E. (1963). Junctional complexes in various epithelia. J Cell Biol *17*, 375-412.

Fesenko, I., Kurth, T., Sheth, B., Fleming, T.P., Citi, S., and Hausen, P. (2000). Tight junction biogenesis in the early Xenopus embryo. Mech Dev *96*, 51-65.

Fischer, O.M., Hart, S., Gschwind, A., Prenzel, N., and Ullrich, A. (2004). Oxidative and osmotic stress signalling in tumor cells is mediated by ADAM proteases and heparin-binding epidermal growth factor. Mol Cell Biol *24*, 5172-5183.

Friedl, P., and Wolf, K. (2010). Plasticity of cell migration: a multiscale tuning model. J Cell Biol *188*, 11-19.

Fujimoto, K. (1995). Freeze-fracture replica electron microscopy combined with SDS digestion for cytochemical labeling of intergral membrane proteins: aplication to the immunogold labeling of intercellular junctional complex. J Cell Sci *108*, 3443-3449.

Fujishiro, S.H., Tanimura, S., Mure, S., Kashimoto, Y., Watanabe, K., and Kohno, M. (2008). ERK1/2 phosphorylate GEF-H1 to enhance its guanine nucleotide exchange activity toward RhoA. Biochem Biophys Res Commun *368*, 162-167.

Furuse, M., Fujita, K., Hiiragi, T., Fujimoto, K., and Tsukita, S. (1998a). Claudin-1 and -2: novel integral membrane proteins localizing at tight junctions with no sequence similarity to occludin. J Cell Biol *141*, 1539-1550.

Furuse, M., Hirase, T., Itoh, M., Nagafuchi, A., Yonemura, S., and Tsukita, S. (1993). Occludin: a novel integral membrane protein localizing at tight junctions. J Cell Biol *123*, 1777-1788.

Furuse, M., Itoh, M., Hirase, T., Nagafuchi, A., Yonemura, S., Tsukita, S., and Tsukita, S. (1994). Direct association of occludin with ZO-1 and its possible involvement in the localization of occludin at tight junctions. J Cell Biol *127*, 1617-1626.

Furuse, M., Sasaki, H., Fujimoto, K., and Tsukita, S. (1998b). A single gene product, claudin-1 or -2, reconstitutes tight junction strands and recruits occludin in fibroblasts. J Cell Biol *143*, 391-401.

Furuse, M., Sasaki, H., and Tsukita, S. (1999). Manner of interaction of heterogeneous claudin species within and between tight junction strands. J Cell Biol *147*, 891-903.

Galcheva-Gargova, Z., Derijard, B., Wu, I.H., and Davis, R.J. (1994). An osmosensing signal transduction pathway in mammalian cells. Science *265*, 806-808.

Gallagher, E.D., Gutowski, S., Sternweis, P.C., and Cobb, M.H. (2004). RhoA binds to the amino terminus of MEKK1 and regulates its kinase activity. J Biol Chem *279*, 1872-1877.

Gallagher, E.D., Xu, S., Moomaw, C., Slaughter, C.A., and Cobb, M.H. (2002). Binding of JNK/SAPK to MEKK1 is regulated by phosphorylation. J Biol Chem *277*, 45785-45792.

Garrod, D., and Chidgey, M. (2008). Desmosome structure, composition and function. Biochim Biophys Acta *1778*, 572-587.

Garrod, D.R., Merritt, A.J., and Nie, Z. (2002). Desmosomal cadherins. Curr Opin Cell Biol *14*, 537-545.

Getsios, S., Huen, A.C., and Green, K.J. (2004). Working out the strength and flexibility of desmosomes. Nat Rev Mol Cell Biol *5*, 271-281.

Ghassemifar, M.R., Sheth, B., Papenbrock, T., Leese, H.J., Houghton, F.D., and Fleming, T.P. (2002). Occludin TM4(-): an isoform of the tight junction protein present in primates lacking the fourth transmembrane domain. J Cell Sci *115*, 3171-3180.

Giampieri, S., Manning, C., Hooper, S., Jones, L., Hill, C.S., and Sahai, E. (2009). Localized and reversible TGFbeta signalling switches breast cancer cells from cohesive to single cell motility. Nat Cell Biol *11*, 1287-1296.

Giannelli, G., Falk-Marzillier, J., Schiraldi, O., Stetler-Stevenson, W.G., and Quaranta, V. (1997). Induction of cell migration by matrix metalloprotease-2 cleavage of laminin-5. Science *277*, 225-228.

Gonzalez-Mariscal, L., Chavez de Ramirez, B., and Cereijido, M. (1985). Tight junction formation in cultured epithelial cells (MDCK). J Membr Biol *86*, 113-125.

Gow, A., Southwood, C.M., Li, J.S., Pariali, M., Riordan, G.P., Brodie, S.E., Danias, J., Bronstein, J.M., Kachar, B., Lazzarini, R.A., (1999). CNS myelin and sertoli cell tight junction strands are absent in Osp/claudin-11 null mice. Cell *99*, 649-659.

Grande, M., Franzen, A., Karlsson, J.O., Ericson, L.E., Heldin, N.E., and Nilsson, M. (2002). Transforming growth factor-beta and epidermal growth factor synergistically stimulate epithelial to mesenchymal transition (EMT) through a MEK-dependent mechanism in primary cultured pig thyrocytes. J Cell Sci *115*, 4227-4236.

Guillemot, L., Paschoud, S., Pulimeno, P., Foglia, A., and Citi, S. (2008). The cytoplasmic plaque of tight junctions: a scaffolding and signalling center. Biochim Biophys Acta *1778*, 601-613.

Haskins, J., Gu, L., Wittchen, E.S., Hibbard, J., and Stevenson, B.R. (1998). ZO-3, a novel member of the MAGUK protein family found at the tight junction, interacts with ZO-1 and occludin. J Cell Biol *141*, 199-208.

Henson, J.H. (1999). Relationships between the actin cytoskeleton and cell volume regulation. Microsc Res Tech *47*, 155-162.

Hirokawa, N., and Tilney, L.G. (1982). Interactions between actin filaments and between actin filaments and membranes in quick-frozen and deeply etched hair cells of the chick ear. J Cell Biol *95*, 249-261.

Hofmann, I., Mertens, C., Brettel, M., Nimmrich, V., Schnolzer, M., and Herrmann, H. (2000). Interaction of plakophilins with desmoplakin and intermediate filament proteins: an in vitro analysis. J Cell Sci *113 (Pt 13)*, 2471-2483.

Hoover, K.B., Liao, S.Y., and Bryant, P.J. (1998). Loss of the tight junction MAGUK ZO-1 in breast cancer: relationship to glandular differentiation and loss of heterozygosity. Am J Pathol *153*, 1767-1773.

Hopwood, N.D., Pluck, A., and Gurdon, J.B. (1989). A Xenopus mRNA related to Drosophila twist is expressed in response to induction in the mesoderm and the neural crest. Cell *59*, 893-903.

Horikoshi, Y., Suzuki, A., Yamanaka, T., Sasaki, K., Mizuno, K., Sawada, H., Yonemura, S., and Ohno, S. (2009). Interaction between PAR-3 and the aPKC-PAR-6 complex is indispensable for apical domain development of epithelial cells. J Cell Sci *122*, 1595-1606.

Huang, C., Rajfur, Z., Borchers, C., Schaller, M.D., and Jacobson, K. (2003). JNK phosphorylates paxillin and regulates cell migration. Nature *424*, 219-223.

Huang da, W., Sherman, B.T., and Lempicki, R.A. (2009). Systematic and integrative analysis of large gene lists using DAVID bioinformatics resources. Nat Protoc *4*, 44-57.

Huber, O., Korn, R., McLaughlin, J., Ohsugi, M., Herrmann, B.G., and Kemler, R. (1996). Nuclear localization of beta-catenin by interaction with transcription factor LEF-1. Mech Dev *59*, 3-10.

Huerta, M., Munoz, R., Tapia, R., Soto-Reyes, E., Ramirez, L., Recillas-Targa, F., Gonzalez-Mariscal, L., and Lopez-Bayghen, E. (2007). Cyclin D1 is transcriptionally down-regulated by ZO-2 via an E box and the transcription factor c-Myc. Mol Biol Cell *18*, 4826-4836.

Hurd, T.W., Gao, L., Roh, M.H., Macara, I.G., and Margolis, B. (2003). Direct interaction of two polarity complexes implicated in epithelial tight junction assembly. Nat Cell Biol *5*, 137-142.

Ikenouchi, J., Furuse, M., Furuse, K., Sasaki, H., and Tsukita, S. (2005). Tricellulin constitutes a novel barrier at tricellular contacts of epithelial cells. J Cell Biol *171*, 939-945.

Ikenouchi, J., Sasaki, H., Tsukita, S., and Furuse, M. (2008). Loss of occludin affects tricellular localization of tricellulin. Mol Biol Cell *19*, 4687-4693.
Ilina, O., and Friedl, P. (2009). Mechanisms of collective cell migration at a glance. J Cell Sci *122*, 3203-3208.

Irarrazabal, C.E., Williams, C.K., Ely, M.A., Birrer, M.J., Garcia-Perez, A., Burg, M.B., and Ferraris, J.D. (2008). Activator protein-1 contributes to high NaCl-induced increase in tonicity-responsive enhancer/osmotic response element-binding protein transactivating activity. J Biol Chem *283*, 2554-2563.

Ishiyama, N., Lee, S.H., Liu, S., Li, G.Y., Smith, M.J., Reichardt, L.F., and Ikura, M. (2010). Dynamic and static interactions between p120 catenin and E-cadherin regulate the stability of cell-cell adhesion. Cell *141*, 117-128.

Itoh, M., Furuse, M., Morita, K., Kubota, K., Saitou, M., and Tsukita, S. (1999a). Direct binding of three tight junction-associated MAGUKs, ZO-1, ZO-2, and ZO-3, with the COOH termini of claudins. J Cell Biol *147*, 1351-1363.

Itoh, M., Morita, K., and Tsukita, S. (1999b). Characterization of ZO-2 as a MAGUK family member associated with tight as well as adherens junctions with a binding affinity to occludin and alpha catenin. J Biol Chem *274*, 5981-5986.

Itoh, M., Sasaki, H., Furuse, M., Ozaki, H., Kita, T., and Tsukita, S. (2001). Junctional adhesion molecule (JAM) binds to PAR-3: a possible mechanism for the recruitment of PAR-3 to tight junctions. J Cell Biol *154*, 491-497.

Joshi, B., Strugnell, S.S., Goetz, J.G., Kojic, L.D., Cox, M.E., Griffith, O.L., Chan, S.K., Jones, S.J., Leung, S.P., Masoudi, H.*, et al*. (2008). Phosphorylated caveolin-1 regulates Rho/ROCK-dependent focal adhesion dynamics and tumor cell migration and invasion. Cancer Res *68*, 8210-8220.

Kaihara, T., Kusaka, T., Nishi, M., Kawamata, H., Imura, J., Kitajima, K., Itoh-Minami, R., Aoyama, N., Kasuga, M., Oda, Y.*, et al*. (2003). Dedifferentiation and

decreased expression of adhesion molecules, E-cadherin and ZO-1, in colorectal cancer are closely related to liver metastasis. J Exp Clin Cancer Res *22*, 117-123.

Kakiashvili, E., Dan, Q., Vandermeer, M., Zhang, Y., Waheed, F., Pham, M., and Szaszi, K. (2011). The epidermal growth factor receptor mediates tumor necrosis factor-alpha-induced activation of the ERK/GEF-H1/RhoA pathway in tubular epithelium. J Biol Chem *286*, 9268-9279.

Kalluri, R., and Weinberg, R.A. (2009). The basics of epithelial-mesenchymal transition. J Clin Invest *119*, 1420-1428.

Kamai, T., Tsujii, T., Arai, K., Takagi, K., Asami, H., Ito, Y., and Oshima, H. (2003). Significant association of Rho/ROCK pathway with invasion and metastasis of bladder cancer. Clin Cancer Res *9*, 2632-2641.

Karin, M., Takahashi, T., Kapahi, P., Delhase, M., Chen, Y., Makris, C., Rothwarf, D., Baud, V., Natoli, G., Guido, F., *et al*. (2001). Oxidative stress and gene expression: the AP-1 and NF-kappaB connections. Biofactors *15*, 87-89.

Kavurma, M.M., and Khachigian, L.M. (2003). ERK, JNK, and p38 MAP kinases differentially regulate proliferation and migration of phenotypically distinct smooth muscle cell subtypes. J Cell Biochem *89*, 289-300.

Keon, B.H., Schafer, S., Kuhn, C., Grund, C., and Franke, W.W. (1996). Symplekin, a novel type of tight junction plaque protein. J Cell Biol *134*, 1003-1018.

Kevil, C.G., Oshima, T., Alexander, B., Coe, L.L., and Alexander, J.S. (2000). H(2)O(2)-mediated permeability: role of MAPK and occludin. Am J Physiol Cell Physiol *279*, C21-30.

Kikuchi, A. (2000). Regulation of beta-catenin signalling in the Wnt pathway. Biochem Biophys Res Commun *268*, 243-248.

Klinger, M., Kudlacek, O., Seidel, M.G., Freissmuth, M., and Sexl, V. (2002). MAP kinase stimulation by cAMP does not require RAP1 but SRC family kinases. J Biol Chem *277*, 32490-32497.

Kojima, T., Takasawa, A., Kyuno, D., Ito, T., Yamaguchi, H., Hirata, K., Tsujiwaki, M., Murata, M., Tanaka, S., and Sawada, N. (2011). Downregulation of tight junction-associated MARVEL protein marvelD3 during epithelial-mesenchymal transition in human pancreatic cancer cells. Exp Cell Res.

Kolligs, F.T., Kolligs, B., Hajra, K.M., Hu, G., Tani, M., Cho, K.R., and Fearon, E.R. (2000). gamma-catenin is regulated by the APC tumor suppressor and its oncogenic activity is distinct from that of beta-catenin. Genes Dev *14*, 1319-1331.

Kong, L., Deng, Z., Shen, H., and Zhang, Y. (2011). Src family kinase inhibitor PP2 efficiently inhibits cervical cancer cell proliferation through down-regulating phospho-Src-Y416 and phospho-EGFR-Y1173. Mol Cell Biochem *348*, 11-19.

Koshikawa, N., Giannelli, G., Cirulli, V., Miyazaki, K., and Quaranta, V. (2000). Role of cell surface metalloprotease MT1-MMP in epithelial cell migration over laminin-5. J Cell Biol *148*, 615-624.

Kottke, M.D., Delva, E., and Kowalczyk, A.P. (2006). The desmosome: cell science lessons from human diseases. J Cell Sci *119*, 797-806.

Kouklis, P.D., Hutton, E., and Fuchs, E. (1994). Making a connection: direct binding between keratin intermediate filaments and desmosomal proteins. J Cell Biol *127*, 1049-1060.

Kovacs, E.M., Goodwin, M., Ali, R.G., Paterson, A.D., and Yap, A.S. (2002). Cadherin-directed actin assembly: E-cadherin physically associates with the Arp2/3 complex to direct actin assembly in nascent adhesive contacts. Curr Biol *12*, 379-382.

Koval, M. (2002). Sharing signals: connecting lung epithelial cells with gap junction channels. Am J Physiol Lung Cell Mol Physiol *283*, L875-893.

Kowalik, T.F., DeGregori, J., Schwarz, J.K., and Nevins, J.R. (1995). E2F1 overexpression in quiescent fibroblasts leads to induction of cellular DNA synthesis and apoptosis. J Virol *69*, 2491-2500.

Krause, G., Winkler, L., Mueller, S.L., Haseloff, R.F., Piontek, J., and Blasig, I.E. (2008). Structure and function of claudins. Biochim Biophys Acta *1778*, 631-645.

Kwon, H.M., and Handler, J.S. (1995). Cell volume regulated transporters of compatible osmolytes. Curr Opin Cell Biol *7*, 465-471.

Kreis, T.E. (1987) Microtubules containing detyrosinated tubulin are less dynamic. *EMBO J*. 6, 2597-2606

LaBonne, C., and Bronner-Fraser, M. (1998). Neural crest induction in Xenopus: evidence for a two-signal model. Development *125*, 2403-2414.

Lammermann, T., and Sixt, M. (2009). Mechanical modes of 'amoeboid' cell migration. Curr Opin Cell Biol *21*, 636-644.

Li, H., Ung, C.Y., Ma, X.H., Li, B.W., Low, B.C., Cao, Z.W., and Chen, Y.Z. (2009). Simulation of crosstalk between small GTPase RhoA and EGFR-ERK signalling pathway via MEKK1. Bioinformatics *25*, 358-364.

Liu, J., and Lin, A. (2005). Role of JNK activation in apoptosis: a double-edged sword. Cell Res *15*, 36-42.

Maciver, S.K., Wachsstock, D.H., Schwarz, W.H., and Pollard, T.D. (1991). The actin filament severing protein actophorin promotes the formation of rigid bundles of actin filaments crosslinked with alpha-actinin. J Cell Biol *115*, 1621-1628.

Maeda, O., Usami, N., Kondo, M., Takahashi, M., Goto, H., Shimokata, K., Kusugami, K., and Sekido, Y. (2004). Plakoglobin (gamma-catenin) has TCF/LEF family-dependent transcriptional activity in beta-catenin-deficient cell line. Oncogene *23*, 964-972.

Mandai, K., Nakanishi, H., Satoh, A., Obaishi, H., Wada, M., Nishioka, H., Itoh, M., Mizoguchi, A., Aoki, T., Fujimoto, T., *et al*. (1997). Afadin: A novel actin filament-binding protein with one PDZ domain localized at cadherin-based cell-to-cell adherens junction. J Cell Biol *139*, 517-528.

Matter, K., Aijaz, S., Tsapara, A., and Balda, M.S. (2005). Mammalian tight junctions in the regulation of epithelial differentiation and proliferation. Curr Opin Cell Biol *17*, 453-458.

Matter, K., and Balda, M.S. (2003a). Functional analysis of tight junctions. Methods *30*, 228-234.

Matter, K., and Balda, M.S. (2003b). Signalling to and from tight junctions. Nat Rev Mol Cell Biol *4*, 225-236.

Matter, K., and Balda, M.S. (2007). Epithelial tight junctions, gene expression and nucleo-junctional interplay. J Cell Sci *120*, 1505-1511.

Merzdorf, C.S., Chen, Y.H., and Goodenough, D.A. (1998). Formation of functional tight junctions in Xenopus embryos. Dev Biol *195*, 187-203.

Millan, J., Puertollano, R., Fan, L., Rancano, C., and Alonso, M.A. (1997). The MAL proteolipid is a component of the detergent-insoluble membrane subdomains of human T-lymphocytes. Biochem J *321 (Pt 1)*, 247-252.

Minden, A., Lin, A., Smeal, T., Derijard, B., Cobb, M., Davis, R., and Karin, M. (1994). c-Jun N-terminal phosphorylation correlates with activation of the JNK

subgroup but not the ERK subgroup of mitogen-activated protein kinases. Mol Cell Biol *14*, 6683-6688.

Miralles, F., Posern, G., Zaromytidou, A.I., and Treisman, R. (2003). Actin dynamics control SRF activity by regulation of its coactivator MAL. Cell *113*, 329-342.

Miranda, L., Carpentier, S., Platek, A., Hussain, N., Gueuning, M.A., Vertommen, D., Ozkan, Y., Sid, B., Hue, L., Courtoy, P.J., *et al*. (2010). AMP-activated protein kinase induces actin cytoskeleton reorganization in epithelial cells. Biochem Biophys Res Commun *396*, 656-661.

Miravet, S., Piedra, J., Miro, F., Itarte, E., Garcia de Herreros, A., and Dunach, M. (2002). The transcriptional factor Tcf-4 contains different binding sites for beta-catenin and plakoglobin. J Biol Chem *277*, 1884-1891.

Muresan, Z., Paul, D.L., and Goodenough, D.A. (2000). Occludin 1B, a variant of the tight junction protein occludin. Mol Biol Cell *11*, 627-634.

Nadkarni, V., Gabbay, K.H., Bohren, K.M., and Sheikh-Hamad, D. (1999). Osmotic response element enhancer activity. Regulation through p38 kinase and mitogen-activated extracellular signal-regulated kinase kinase. J Biol Chem *274*, 20185-20190.

Newport, J., and Kirschner, M. (1982a). A major developmental transition in early Xenopus embryos: I. characterization and timing of cellular changes at the midblastula stage. Cell *30*, 675-686.

Newport, J., and Kirschner, M. (1982b). A major developmental transition in early Xenopus embryos: II. Control of the onset of transcription. Cell *30*, 687-696.

Nie, M., Aijaz, S., Leefa Chong San, I.V., Balda, M.S., and Matter, K. (2009). The Y-box factor ZONAB/DbpA associates with GEF-H1/Lfc and mediates Rho-stimulated transcription. EMBO Rep *10*, 1125-1131.

Nobes, C.D., and Hall, A. (1995). Rho, rac, and cdc42 GTPases regulate the assembly of multimolecular focal complexes associated with actin stress fibers, lamellipodia, and filopodia. Cell *81*, 53-62.

Nusrat, A., Giry, M., Turner, J.R., Colgan, S.P., Parkos, C.A., Carnes, D., Lemichez, E., Boquet, P., and Madara, J.L. (1995). Rho protein regulates tight junctions and perijunctional actin organization in polarized epithelia. Proc Natl Acad Sci U S A *92*, 10629-10633.

Nusrat, A., Parkos, C.A., Verkade, P., Foley, C.S., Liang, T.W., Innis-Whitehouse, W., Eastburn, K.K., and Madara, J.L. (2000). Tight junctions are membrane microdomains. J Cell Sci *113 (Pt 10)*, 1771-1781.

Ozawa, M., Baribault, H., and Kemler, R. (1989). The cytoplasmic domain of the cell adhesion molecule uvomorulin associates with three independent proteins structurally related in different species. EMBO J *8*, 1711-1717.

Ozdamar, B., Bose, R., Barrios-Rodiles, M., Wang, H.R., Zhang, Y., and Wrana, J.L. (2005). Regulation of the polarity protein Par6 by TGFbeta receptors controls epithelial cell plasticity. Science *307*, 1603-1609.

Paris, J., Osborne, H.B., Couturier, A., Le Guellec, R., and Philippe, M. (1988). Changes in the polyadenylation of specific stable RNA during the early development of Xenopus laevis. Gene *72*, 169-176.

Pedersen, S.F., Hoffmann, E.K., and Mills, J.W. (2001). The cytoskeleton and cell volume regulation. Comp Biochem Physiol A Mol Integr Physiol *130*, 385-399.

Pedersen, S.F., Mills, J.W., and Hoffmann, E.K. (1999). Role of the F-actin cytoskeleton in the RVD and RVI processes in Ehrlich ascites tumor cells. Exp Cell Res *252*, 63-74.

Pollard, T.D., and Borisy, G.G. (2003). Cellular motility driven by assembly and disassembly of actin filaments. Cell *112*, 453-465.

Radice, G.P., and Malacinski, G.M. (1989). Expression of myosin heavy chain transcripts during Xenopus laevis development. Dev Biol *133*, 562-568.

Raleigh, D.R., Boe, D.M., Yu, D., Weber, C.R., Marchiando, A.M., Bradford, E.M., Wang, Y., Wu, L., Schneeberger, E.E., Shen, L., *et al*. (2011). Occludin S408 phosphorylation regulates tight junction protein interactions and barrier function. J Cell Biol *193*, 565-582.

Raleigh, D.R., Marchiando, A.M., Zhang, Y., Shen, L., Sasaki, H., Wang, Y., Long, M., and Turner, J.R. (2010). Tight junction-associated MARVEL proteins marveld3, tricellulin, and occludin have distinct but overlapping functions. Mol Biol Cell *21*, 1200-1213.

Razani, B., and Lisanti, M.P. (2001). Caveolin-deficient mice: insights into caveolar function human disease. J Clin Invest *108*, 1553-1561.

Regen, C.M., and Steinhardt, R.A. (1986) Global properties of the *Xenopus* blastula are mediated by a high-resistance epithelial seal. Dev Biol *113*, 147-154

Reyes, J.L., Lamas, M., Martin, D., del Carmen Namorado, M., Islas, S., Luna, J., Tauc, M., and Gonzalez-Mariscal, L. (2002). The renal segmental distribution of claudins changes with development. Kidney Int *62*, 476-487.

Riazuddin, S., Ahmed, Z.M., Fanning, A.S., Lagziel, A., Kitajiri, S., Ramzan, K., Khan, S.N., Chattaraj, P., Friedman, P.L., Anderson, J.M., *et al*. (2006). Tricellulin is a tight-junction protein necessary for hearing. Am J Hum Genet *79*, 1040-1051.

Ridley, A.J. (2001). Rho family proteins: coordinating cell responses. Trends Cell Biol *11*, 471-477.

Roh, M.H., Fan, S., Liu, C.J., and Margolis, B. (2003). The Crumbs3-Pals1 complex participates in the establishment of polarity in mammalian epithelial cells. J Cell Sci *116*, 2895-2906.

Rosenblatt, J., Raff, M.C., and Cramer, L.P. (2001). An epithelial cell destined for apoptosis signals its neighbors to extrude it by an actin- and myosin-dependent mechanism. Curr Biol *11*, 1847-1857.

Rosette, C., and Karin, M. (1996). Ultraviolet light and osmotic stress: activation of the JNK cascade through multiple growth factor and cytokine receptors. Science *274*, 1194-1197.

Rosse, C., Formstecher, E., Boeckeler, K., Zhao, Y., Kremerskothen, J., White, M.D., Camonis, J.H., and Parker, P.J. (2009). An aPKC-exocyst complex controls paxillin phosphorylation and migration through localised JNK1 activation. PLoS Biol *7*, e1000235.

Saitou, M., Fujimoto, K., Doi, Y., Itoh, M., Fujimoto, T., Furuse, M., Takano, H., Noda, T., and Tsukita, S. (1998). Occludin-deficient embryonic stem cells can differentiate into polarized epithelial cells bearing tight junctions. J Cell Biol *141*, 397-408.

Saitou, M., Furuse, M., Sasaki, H., Schulzke, J.D., Fromm, M., Takano, H., Noda, T., and Tsukita, S. (2000). Complex phenotype of mice lacking occludin, a component of tight junction strands. Mol Biol Cell *11*, 4131-4142.

Samak, G., Suzuki, T., Bhargava, A., and Rao, R.K. (2010). c-Jun NH2-terminal kinase-2 mediates osmotic stress-induced tight junction disruption in the intestinal epithelium. Am J Physiol Gastrointest Liver Physiol *299*, G572-584.

Sanchez-Pulido, L., Martin-Belmonte, F., Valencia, A., and Alonso, M.A. (2002). MARVEL: a conserved domain involved in membrane apposition events. Trends Biochem Sci *27*, 599-601.

Sasaki, H., Matsui, C., Furuse, K., Mimori-Kiyosue, Y., Furuse, M., and Tsukita, S. (2003). Dynamic behavior of paired claudin strands within apposing plasma membranes. Proc Natl Acad Sci U S A *100*, 3971-3976.

Schulzke, J.D., Gitter, A.H., Mankertz, J., Spiegel, S., Seidler, U., Amasheh, S., Saitou, M., Tsukita, S., and Fromm, M. (2005). Epithelial transport and barrier function in occludin-deficient mice. Biochim Biophys Acta *1669*, 34-42.

Schutze, S., Machleidt, T., Adam, D., Schwandner, R., Wiegmann, K., Kruse, M.L., Heinrich, M., Wickel, M., and Kronke, M. (1999). Inhibition of receptor internalization by monodansylcadaverine selectively blocks p55 tumor necrosis factor receptor death domain signalling. J Biol Chem *274*, 10203-10212.

Shaulian, E., and Karin, M. (2002). AP-1 as a regulator of cell life and death. Nat Cell Biol *4*, E131-136.

Shin, K., Fogg, V.C., and Margolis, B. (2006). Tight junctions and cell polarity. Annu Rev Cell Dev Biol *22*, 207-235.

Shin, K., Wang, Q., and Margolis, B. (2007). PATJ regulates directional migration of mammalian epithelial cells. EMBO Rep *8*, 158-164.

Sigismund, S., Argenzio, E., Tosoni, D., Cavallaro, E., Polo, S., and Di Fiore, P.P. (2008). Clathrin-mediated internalization is essential for sustained EGFR signalling but dispensable for degradation. Dev Cell *15*, 209-219.

Simon, D.B., Lu, Y., Choate, K.A., Velazquez, H., Al-Sabban, E., Praga, M., Casari, G., Bettinelli, A., Colussi, G., Rodriguez-Soriano, J., McCredie, D., Milford, D., Sanjad, S., Lifton, R.P., (1999). Paracellin-1, a renal tight junction protein required for paracellular Mg^{2+} resorption. Science *285*, 103-106.

Siow, Y.L., Kalmar, G.B., Sanghera, J.S., Tai, G., Oh, S.S., and Pelech, S.L. (1997). Identification of two essential phosphorylated threonine residues in the catalytic domain of Mekk1. Indirect activation by Pak3 and protein kinase C. J Biol Chem *272*, 7586-7594.

Smart, E.J., Graf, G.A., McNiven, M.A., Sessa, W.C., Engelman, J.A., Scherer, P.E., Okamoto, T., and Lisanti, M.P. (1999). Caveolins, liquid-ordered domains, and signal transduction. Mol Cell Biol *19*, 7289-7304.

Stappenbeck, T.S., and Green, K.J. (1992). The desmoplakin carboxyl terminus coaligns with and specifically disrupts intermediate filament networks when expressed in cultured cells. J Cell Biol *116*, 1197-1209.

Steed, E., Balda, M.S., and Matter, K. (2010). Dynamics and functions of tight junctions. Trends Cell Biol *20*, 142-149.

Steed, E., Rodrigues, N.T., Balda, M.S., and Matter, K. (2009). Identification of MarvelD3 as a tight junction-associated transmembrane protein of the occludin family. BMC Cell Biol *10*, 95.

Steventon, B., Araya, C., Linker, C., Kuriyama, S., and Mayor, R. (2009). Differential requirements of BMP and Wnt signalling during gastrulation and neurulation define two steps in neural crest induction. Development *136*, 771-779.

Straight, S.W., Shin, K., Fogg, V.C., Fan, S., Liu, C.J., Roh, M., and Margolis, B. (2004). Loss of PALS1 expression leads to tight junction and polarity defects. Mol Biol Cell *15*, 1981-1990.

Takagaki, Y., and Manley, J.L. (2000). Complex protein interactions within the human polyadenylation machinery identify a novel component. Mol Cell Biol *20*, 1515-1525.

Takai, Y., and Nakanishi, H. (2003). Nectin and afadin: novel organizers of intercellular junctions. J Cell Sci *116*, 17-27.

Tan, I., Yong, J., Dong, J.M., Lim, L., and Leung, T. (2008). A tripartite complex containing MRCK modulates lamellar actomyosin retrograde flow. Cell *135*, 123-136.

Tanos, T., Marinissen, M.J., Leskow, F.C., Hochbaum, D., Martinetto, H., Gutkind, J.S., and Coso, O.A. (2005). Phosphorylation of c-Fos by members of the p38 MAPK family. Role in the AP-1 response to UV light. J Biol Chem *280*, 18842-18852.

Thiele, C., Hannah, M.J., Fahrenholz, F., and Huttner, W.B. (2000). Cholesterol binds to synaptophysin and is required for biogenesis of synaptic vesicles. Nat Cell Biol *2*, 42-49.

Thirone, A.C., Speight, P., Zulys, M., Rotstein, O.D., Szaszi, K., Pedersen, S.F., and Kapus, A. (2009). Hyperosmotic stress induces Rho/Rho kinase/LIM kinase-mediated cofilin phosphorylation in tubular cells: key role in the osmotically triggered F-actin response. Am J Physiol Cell Physiol *296*, C463-475.

Thomason, H.A., Scothern, A., McHarg, S., and Garrod, D.R. (2010). Desmosomes: adhesive strength and signalling in health and disease. Biochem J *429*, 419-433.

Tournier, C., Hess, P., Yang, D.D., Xu, J., Turner, T.K., Nimnual, A., Bar-Sagi, D., Jones, S.N., Flavell, R.A., and Davis, R.J. (2000). Requirement of JNK for stress-induced activation of the cytochrome c-mediated death pathway. Science *288*, 870-874.

Traweger, A., Fuchs, R., Krizbai, I.A., Weiger, T.M., Bauer, H.C., and Bauer, H. (2003). The tight junction protein ZO-2 localizes to the nucleus and interacts with the heterogeneous nuclear ribonucleoprotein scaffold attachment factor-B. J Biol Chem *278*, 2692-2700.

Tricker, E., Arvand, A., Kwan, R., Chen, G.Y., Gallagher, E., and Cheng, G. (2011). Apoptosis induced by cytoskeletal disruption requires distinct domains of MEKK1. PLoS One *6*, e17310.

Tsukita, S., Furuse, M., and Itoh, M. (2001). Multifunctional strands in tight junctions. Nat Rev Mol Cell Biol *2*, 285-293.

Tuomi, S., Mai, A., Nevo, J., Laine, J.O., Vilkki, V., Ohman, T.J., Gahmberg, C.G., Parker, P.J., and Ivaska, J. (2009). PKCepsilon regulation of an alpha5 integrin-ZO-1 complex controls lamellae formation in migrating cancer cells. Sci Signal *2*, ra32.

Uhlik, M.T., Abell, A.N., Johnson, N.L., Sun, W., Cuevas, B.D., Lobel-Rice, K.E., Horne, E.A., Dell'Acqua, M.L., and Johnson, G.L. (2003). Rac-MEKK3-MKK3 scaffolding for p38 MAPK activation during hyperosmotic shock. Nat Cell Biol *5*, 1104-1110.

Van Itallie, C., Rahner, C., and Anderson, J.M. (2001). Regulated expression of claudin-4 decreases paracellular conductance through a selective decrease in sodium permeability. J Clin Invest *107*, 1319-1327.

Van Itallie, C.M., and Anderson, J.M. (2006). Claudins and epithelial paracellular transport. Annu Rev Physiol *68*, 403-429.

Van Itallie, C.M., Fanning, A.S., Holmes, J., and Anderson, J.M. (2010). Occludin is required for cytokine-induced regulation of tight junction barriers. J Cell Sci *123*, 2844-2852.

Ventura, J.J., Hubner, A., Zhang, C., Flavell, R.A., Shokat, K.M., and Davis, R.J. (2006). Chemical genetic analysis of the time course of signal transduction by JNK. Mol Cell *21*, 701-710.

Verma, S., Shewan, A.M., Scott, J.A., Helwani, F.M., den Elzen, N.R., Miki, H., Takenawa, T., and Yap, A.S. (2004). Arp2/3 activity is necessary for efficient formation of E-cadherin adhesive contacts. J Biol Chem *279*, 34062-34070.

Verrecchia, F., Tacheau, C., Schorpp-Kistner, M., Angel, P., and Mauviel, A. (2001a). Induction of the AP-1 members c-Jun and JunB by TGF-beta/Smad suppresses early Smad-driven gene activation. Oncogene *20*, 2205-2211.

Verrecchia, F., Vindevoghel, L., Lechleider, R.J., Uitto, J., Roberts, A.B., and Mauviel, A. (2001b). Smad3/AP-1 interactions control transcriptional responses to TGF-beta in a promoter-specific manner. Oncogene *20*, 3332-3340.

Volonte, D., Galbiati, F., Pestell, R.G., and Lisanti, M.P. (2001). Cellular stress induces the tyrosine phosphorylation of caveolin-1 (Tyr(14)) via activation of p38 mitogen-activated protein kinase and c-Src kinase. Evidence for caveolae, the actin cytoskeleton, and focal adhesions as mechanical sensors of osmotic stress. J Biol Chem *276*, 8094-8103.

Wakeling, A.E., Guy, S.P., Woodburn, J.R., Ashton, S.E., Curry, B.J., Barker, A.J., and Gibson, K.H. (2002). ZD1839 (Iressa): an orally active inhibitor of epidermal growth factor signalling with potential for cancer therapy. Cancer Res *62*, 5749-5754.

Welsh, C.F., Roovers, K., Villanueva, J., Liu, Y., Schwartz, M.A., and Assoian, R.K. (2001). Timing of cyclin D1 expression within G1 phase is controlled by Rho. Nat Cell Biol *3*, 950-957.

Whitmarsh, A.J., and Davis, R.J. (1996). Transcription factor AP-1 regulation by mitogen-activated protein kinase signal transduction pathways. J Mol Med (Berl) *74*, 589-607.

Wilcox, E.R., Burton, Q.L., Naz, S., Riazuddin, S., Smith, T.N., Ploplis, B., Belyantseva, I., Ben-Yosef, T., Liburd, N.A., Morell, R.J., *et al* (2001).Mutations in

the gene encoding tight junction claudin-14 cause autosomal recessive deafness DFNB29. Cell *104*, 165-172.

Wildenberg, G.A., Dohn, M.R., Carnahan, R.H., Davis, M.A., Lobdell, N.A., Settleman, J., and Reynolds, A.B. (2006). p120-catenin and p190RhoGAP regulate cell-cell adhesion by coordinating antagonism between Rac and Rho. Cell *127*, 1027-1039.

Williamson, L., Raess, N.A., Caldelari, R., Zakher, A., de Bruin, A., Posthaus, H., Bolli, R., Hunziker, T., Suter, M.M., and Muller, E.J. (2006). Pemphigus vulgaris identifies plakoglobin as key suppressor of c-Myc in the skin. EMBO J *25*, 3298-3309.

Winklbauer, R. (1990). Mesodermal cell migration during Xenopus gastrulation. Dev Biol *142*, 155-168.

Wittchen, E.S., Haskins, J., and Stevenson, B.R. (2003). NZO-3 expression causes global changes to actin cytoskeleton in Madin-Darby canine kidney cells: linking a tight junction protein to Rho GTPases. Mol Biol Cell *14*, 1757-1768.

Wolf, K., Mazo, I., Leung, H., Engelke, K., von Andrian, U.H., Deryugina, E.I., Strongin, A.Y., Brocker, E.B., and Friedl, P. (2003). Compensation mechanism in tumor cell migration: mesenchymal-amoeboid transition after blocking of pericellular proteolysis. J Cell Biol *160*, 267-277.

Xia, Y., Wang, J., Xu, S., Johnson, G.L., Hunter, T., and Lu, Z. (2007). MEKK1 mediates the ubiquitination and degradation of c-Jun in response to osmotic stress. Mol Cell Biol *27*, 510-517.

Xu, S., Robbins, D., Frost, J., Dang, A., Lange-Carter, C., and Cobb, M.H. (1995). MEKK1 phosphorylates MEK1 and MEK2 but does not cause activation of mitogen-activated protein kinase. Proc Natl Acad Sci U S A *92*, 6808-6812.

Yamada, S., Pokutta, S., Drees, F., Weis, W.I., and Nelson, W.J. (2005). Deconstructing the cadherin-catenin-actin complex. Cell *123*, 889-901.

Yang, J., and Weinberg, R.A. (2008). Epithelial-mesenchymal transition: at the crossroads of development and tumor metastasis. Dev Cell *14*, 818-829.

Yin, J.J., Selander, K., Chirgwin, J.M., Dallas, M., Grubbs, B.G., Wieser, R., Massague, J., Mundy, G.R., and Guise, T.A. (1999). TGF-beta signalling blockade inhibits PTHrP secretion by breast cancer cells and bone metastases development. J Clin Invest *103*, 197-206.

Yu, A.S., McCarthy, K.M., Francis, S.A., McCormack, J.M., Lai, J., Rogers, R.A., Lynch, R.D., and Schneeberger, E.E. (2005). Knockdown of occludin expression leads to diverse phenotypic alterations in epithelial cells. Am J Physiol Cell Physiol *288*, C1231-1241.

Yujiri, T., Fanger, G.R., Garrington, T.P., Schlesinger, T.K., Gibson, S., and Johnson, G.L. (1999). MEK kinase 1 (MEKK1) transduces c-Jun NH2-terminal kinase activation in response to changes in the microtubule cytoskeleton. J Biol Chem *274*, 12605-12610.

Yujiri, T., Sather, S., Fanger, G.R., and Johnson, G.L. (1998). Role of MEKK1 in cell survival and activation of JNK and ERK pathways defined by targeted gene disruption. Science *282*, 1911-1914.

Zhang, J., Betson, M., Erasmus, J., Zeikos, K., Bailly, M., Cramer, L.P., and Braga, V.M. (2005a). Actin at cell-cell junctions is composed of two dynamic and functional populations. J Cell Sci *118*, 5549-5562.

Zhang, L., Deng, M., Parthasarathy, R., Wang, L., Mongan, M., Molkentin, J.D., Zheng, Y., and Xia, Y. (2005b). MEKK1 transduces activin signals in keratinocytes to induce actin stress fiber formation and migration. Mol Cell Biol *25*, 60-65.

Zhang, L., Wang, W., Hayashi, Y., Jester, J.V., Birk, D.E., Gao, M., Liu, C.Y., Kao, W.W., Karin, M., and Xia, Y. (2003). A role for MEK kinase 1 in TGF-beta/activin-induced epithelium movement and embryonic eyelid closure. EMBO J *22*, 4443-4454.

Zhang, W., and Liu, H.T. (2002). MAPK signal pathways in the regulation of cell proliferation in mammalian cells. Cell Res *12*, 9-18.

Zhang, Y., Feng, X.H., and Derynck, R. (1998). Smad3 and Smad4 cooperate with c-Jun/c-Fos to mediate TGF-beta-induced transcription. Nature *394*, 909-913.

Zhurinsky, J., Shtutman, M., and Ben-Ze'ev, A. (2000). Differential mechanisms of LEF/TCF family-dependent transcriptional activation by beta-catenin and plakoglobin. Mol Cell Biol *20*, 4238-4252.